

# Sheffield Hallam University

*Residual strength of corroded reinforced concrete beams.*

HRISTOVA, Elena Hristova.

Available from the Sheffield Hallam University Research Archive (SHURA) at:

<http://shura.shu.ac.uk/19838/>

## A Sheffield Hallam University thesis

This thesis is protected by copyright which belongs to the author.

The content must not be changed in any way or sold commercially in any format or medium without the formal permission of the author.

When referring to this work, full bibliographic details including the author, title, awarding institution and date of the thesis must be given.

Please visit <http://shura.shu.ac.uk/19838/> and <http://shura.shu.ac.uk/information.html> for further details about copyright and re-use permissions.

25804

Adsetts Centre City Campus  
Sheffield S1 1WB

101 921 652 2



Sheffield Hallam University  
Learning and IT Services  
Adsetts Centre City Campus  
Sheffield S1 1WB

**REFERENCE**

ProQuest Number: 10697144

All rights reserved

INFORMATION TO ALL USERS

The quality of this reproduction is dependent upon the quality of the copy submitted.

In the unlikely event that the author did not send a complete manuscript and there are missing pages, these will be noted. Also, if material had to be removed, a note will indicate the deletion.



ProQuest 10697144

Published by ProQuest LLC (2017). Copyright of the Dissertation is held by the Author.

All rights reserved.

This work is protected against unauthorized copying under Title 17, United States Code  
Microform Edition © ProQuest LLC.

ProQuest LLC.  
789 East Eisenhower Parkway  
P.O. Box 1346  
Ann Arbor, MI 48106 – 1346

# **Residual Strength of Corroded Reinforced Concrete Beams**

**Elena Hristova Hristova**

A thesis submitted in partial fulfilment of the requirements of

Sheffield Hallam University

for the degree of Doctor of Philosophy

August 2006

Currently, much research is focused on the corrosion of reinforcement in concrete members. However, none addresses the problems associated with the residual strength of reinforced concrete beams exhibiting both main and shear reinforcement corrosion simultaneously. The aim of this research, therefore, was to determine the residual strength of corroded reinforced concrete beams where various degrees of reinforcement corrosion is present in both the main and shear reinforcement. This may provide a better understanding of the performance of deteriorated reinforced concrete beams in service.

One of the main causes of concrete deterioration is corrosion of the steel reinforcement and thus a reduction of the residual service life. In general, corrosion of reinforcement is believed to affect the structural performance of concrete elements in two ways. Firstly, by reducing the rebar cross sectional area, and secondly, by loss of bond strength between the concrete and steel reinforcement and resulting growth of cracks due to the formation of corrosion products at concrete/reinforcement interface.

The experimental programme was carried out to provide information on the loss of strength resulting from corrosion to the main and shear reinforcement. Corrosion was induced by means of external power supplies. The test programme was divided into three series. Series I was devised to determine the residual flexural strength of reinforced concrete beams where different diameters of main (high yield) reinforcement were subjected to varying degrees of accelerated corrosion (shear strength was provided by mild steel shear reinforcement which remained unaffected by corrosion). Series II was devised to determine the residual shear strength of reinforced concrete beams where the shear (mild steel) reinforcement was subjected to varying degrees of accelerated corrosion (flexural strength was provided by high yield steel which was protected from corrosion). Finally, Series III was devised to determine the residual strength of reinforced concrete beams where both the main (high yield) and shear (mild steel) reinforcement were simultaneously corroded and the effect of this on the performance of the beam was determined. In total, 116 beams were subjected to accelerated corrosion using an impressed current imposed on the reinforcement. Each beam was loaded to failure to determine the strength loss. Four degrees of corrosion were targeted, ranging from 0% (control) to 15%, in increments of 5%.

The results of the laboratory tests determined the significance of both main and shear reinforcement corrosion on the performance of deteriorated reinforced concrete beams. In addition, simplified analytical equations were developed which may assist the engineer in assessing the residual strength of corroded reinforced concrete beams.

## *Declaration*

---

I hereby declare that no portion of the work referred to in this thesis has been submitted in support of an application for another degree or qualification of this or any other University or other institution of learning. All sources of information have been made duly acknowledged.

Elena Hristova Hristova

August 2006

# *Acknowledgements*

---

The author would like to express her sincere gratitude to Dr Finbarr J. O'Flaherty of the Centre for Infrastructure Management, Sheffield Hallam University, for his guidance, support and patience throughout this research project.

The author also gratefully acknowledges the contributions, sincere assistance, guidance and supervision of Professor Pritpal S. Mangat of the Centre for Infrastructure Management, Sheffield Hallam University.

The author wishes to express her gratitude to the Sheffield Hallam University for funding this research project.

The author gratefully acknowledge Dr Paul Lambert of the Centre for Infrastructure Management, Sheffield Hallam University for his important contributions to the research.

The support provided in the laboratory by the technical staff, especially Mr. Robert Skelton, Mr. Geoff Harwood, Mr. John Bickers, and Mr. Pete Lonsborough, of the Construction Materials Laboratories, Sheffield Hallam University is also appreciated.

Finally, I pay my heartfelt feeling of acknowledgement to Andrew Browne for his priceless forbearance and peerless endurance throughout the writing-up of this research.

# *Table of Contents*

---

<b>Abstract.....</b>	<b>ii</b>
<b>Declaration.....</b>	<b>iv</b>
<b>Acknowledgements.....</b>	<b>v</b>
<b>Notation.....</b>	<b>xv</b>
<b>Glossary.....</b>	<b>xviii</b>
<b>List of Figures.....</b>	<b>xxvii</b>
<b>List of Tables.....</b>	<b>xxxv</b>
<b>Chapter 1 Introduction.....</b>	<b>1</b>
1.1 Introduction.....	1
1.2 Scope of research.....	2
1.3 Scope of present investigation.....	5
1.4 Thesis layout.....	6
<b>Chapter 2 Literature Review.....</b>	<b>9</b>
2.1 Introduction.....	9
2.2 History of concrete.....	10
2.3 Properties of reinforced concrete.....	10
2.4 Mechanism of concrete deterioration.....	11
2.5 Principles of corrosion.....	12

2.5.1	Introduction .....	12
2.5.2	Chemical and electrochemical reactions .....	12
2.5.3	General condition of corrosion, immunity and passivity .....	14
2.6	Corrosion initiation due to chloride attack .....	19
2.7	Corrosion initiation due to carbonation of concrete .....	21
2.8	Bond between steel and concrete .....	23
2.9	Reinforced concrete beams damaged by corrosion of tensile reinforcement .....	29
2.9.1	Previous experimental work .....	29
2.9.2	Corrosion simulation by the use of electrolysis .....	29
2.9.3	Model of steel corrosion .....	34
2.10	Previous theoretical work .....	36
2.11	Reinforced concrete beams damaged by corrosion of shear reinforcement .....	37
2.12	Conclusion .....	38
<b>Chapter 3 Optimisation of the Corrosion Process .....</b>		<b>40</b>
3.1	Introduction .....	40
3.2	Accelerated corrosion .....	40
3.2.1	Introduction .....	40
3.2.2	Laboratory simulation .....	41
3.3	Methods of accelerated corrosion .....	45
3.4	Validation of accelerated corrosion method .....	47

3.4.1	Corrosion of reinforcing bars in saline solution.....	47
3.4.2	Corrosion of reinforcing bars in concrete .....	51
3.5	Design of test beams using stainless steel.....	52
3.5.1	Preliminary beams details .....	52
3.5.2	Preliminary Series I.....	53
3.5.3	Performance of preliminary Series I .....	58
3.6	Discussions of the preliminary results .....	59
3.7	Further experimental work.....	60
3.7.1	Method I.....	61
3.7.2	Method II.....	62
3.7.3	Method III .....	62
3.8	Concluding remarks .....	63
<b>Chapter 4 Detailed Experimental Programme.....</b>		<b>64</b>
4.1	Introduction.....	64
4.2	Objectives of investigation.....	64
4.3	Details of experimental programme.....	65
4.4	Materials.....	69
4.4.1	Cement .....	69
4.4.2	Aggregates.....	69
4.4.3	Di – hydrate Calcium chloride .....	73

4.4.4	Steel reinforcement .....	74
4.5	Potential inspection technique for steel in concrete .....	74
4.5.1	Reference electrode .....	75
4.5.2	Digital voltmeter (ISO–TECH IDM97/97RMS) .....	76
4.5.3	Power supply .....	77
4.6	Instrumentation .....	78
4.6.1	Load measurement .....	78
4.6.2	Deflection measurement.....	78
<b>Chapter 5</b>	<b>Influence of Main Steel Corrosion on Structural Performance</b>	
	<b>(Series I) .....</b>	<b>79</b>
5.1	Introduction.....	79
5.2	Objectives of test programme .....	80
5.3	Experimental programme.....	80
5.3.1	General .....	80
5.3.2	Beam specimens.....	83
5.3.3	Process of accelerated corrosion .....	86
5.3.4	Test configuration and procedure.....	89
5.4	Influence of corrosion on the main steel reinforcement on the flexural performance.....	91
5.4.1	Beams reinforced with 2T8 main steel.....	96
5.4.2	Beams reinforced with 2T10 main steel.....	97

5.4.3	Beams reinforced with 2T12 main steel.....	102
5.5	Conclusions.....	104
5.5.1	Conclusions from accelerated corrosions tests .....	104
5.5.2	Conclusions from load tests .....	104
5.5.3	Conclusions from cover variations.....	105
5.5.4	Conclusions from diameter variations .....	105
<b>Chapter 6</b>	<b>Influence of Shear Reinforcement Corrosion on Structural Performance (Series II).....</b>	<b>107</b>
6.1	Introduction.....	107
6.2	Objectives of test programme .....	108
6.3	Experimental programme.....	108
6.3.1	Beam specimens.....	108
6.3.2	Process of accelerated corrosion.....	112
6.3.3	Test configuration and instrumentation .....	113
6.4	Test results and discussion.....	115
6.5	Conclusions.....	119
<b>Chapter 7</b>	<b>Influence of Main and Shear Reinforcement Corrosion on Structural Performance (Series III).....</b>	<b>120</b>
7.1	Introduction.....	120
7.2	Objectives of test programme .....	120
7.3	Experimental programme.....	121

7.3.1	Beam specimens.....	121
7.3.2	Material properties .....	121
7.3.3	Instrumentation .....	123
7.3.4	Test configuration and procedure.....	123
7.3.5	Process of accelerated corrosion .....	124
7.4	Influence of corrosion on the flexural performance.....	128
<b>Chapter 8 Experimental Results and Discussion – Series I .....</b>		
<b>(Main reinforcement corrosion).....</b>		<b>135</b>
8.1	Introduction.....	135
8.2	Aim.....	135
8.3	Critical overview of the test methodology .....	136
8.4	Structural performance of corrosion damaged beams under four point bending test .....	138
8.4.1	Beam Series I reinforced with 2T8 main steel reinforcement.....	139
8.4.1.1	Load / Deflection.....	139
8.4.1.2	Residual flexural strength .....	145
8.4.2	Beam Series I reinforced with 2T10 main steel reinforcement.....	155
8.4.2.1	Load / Deflection.....	155
8.4.2.2	Residual strength.....	164
8.4.3	Beam Series I reinforced with 2T12 main steel reinforcement.....	169
8.4.3.1	Load / Deflection.....	170

8.4.3.2	Flexural strength.....	170
8.5	Conclusions.....	175
8.5.1	General.....	175
8.5.2	Flexure.....	176
8.5.3	Load – Deflection.....	177
8.5.4	Further discussion .....	177
<b>Chapter 9</b>	<b>Experimental Results and Discussion – Series II.....</b>	
	<b>(Shear reinforcement corrosion).....</b>	<b>179</b>
9.1	Introduction.....	179
9.2	Aim.....	179
9.3	Structural performance of beams exhibiting shear reinforcement corrosion ....	179
9.3.1	Beam Series II reinforced with 2T8 main steel reinforcement .....	184
9.3.1.1	Load – central deflection relationships .....	184
9.3.1.2	Residual flexural strength .....	184
9.3.2	Beam Series II reinforced with 2T12 main steel reinforcement .....	187
9.3.2.1	Load – central deflection relationships .....	187
9.3.2.2	Residual flexural strength .....	189
9.4	Final remarks.....	193
<b>Chapter 10</b>	<b>Experimental Results and Discussion – Series III .....</b>	
	<b>(Main and shear reinforcement corrosion).....</b>	<b>195</b>
10.1	Introduction.....	195

10.2	Aim.....	195
10.3	Flexural testing.....	196
10.3.1	Load – deflection curves .....	198
10.3.2	Flexural strength.....	202
10.4	Final remarks.....	208
<b>Chapter 11 Analytical Modelling of Experimental Data.....</b>		<b>209</b>
11.1	Introduction .....	209
11.2	Current method of residual life prediction .....	210
11.3	British code BS 8110 and design of concrete structures EC2.....	212
11.4	Analysis of a doubly reinforced rectangular section.....	214
11.4.1	Design for moment of resistance .....	214
11.4.2	Design for shear resistance.....	216
11.5	Characteristics of reinforced concrete beams .....	219
11.6	Effect of corrosion on the flexural capacity of reinforced concrete beams .....	220
11.6.1	Characteristics of beam Series I.....	220
11.6.2	$M_{t(t)}/M_c$ relationship for various degrees of corrosion .....	220
11.6.3	Designing for durability .....	236
11.6.4	Residual tensile moment of resistance .....	241
11.7	Conclusions.....	242

<b>Chapter 12</b>	<b>Conclusions and Recommendations.....</b>	<b>245</b>
12.1	Introduction.....	245
12.2	Conclusions.....	245
12.2.1	Conclusions from experimental design.....	245
12.2.2	Conclusions from accelerated corrosion tests.....	246
12.2.3	Conclusions from load tests.....	247
12.2.4	Performance of corroded reinforced concrete beams.....	248
12.2.5	Practical implications.....	248
12.3	Recommendations.....	250
12.4	Final remarks.....	250
<b>Chapter 13</b>	<b>References.....</b>	<b>252</b>
<b>Appendix A.....</b>		<b>272</b>
<b>Appendix B.....</b>		<b>295</b>

## *Notation*

---

The great majority of the symbols listed below are essentially those used in the current British Design Practice. Less frequently used symbols and symbols which have different meanings in different contexts are defined where they are used.

$A$	atomic weight of iron
$A_c$	cross sectional area of concrete
$A_s$	cross sectional area of tensile reinforcement
$A_s'$	cross sectional area of hanger bars
$A_{sv}$	total cross sectional area of shear reinforcement
$\alpha$	slope of $M_{I(\text{Corr})}/M_c$ against percent of corrosion
$b$	width of beam
$b_w$	breadth of section
$\beta$	intercept (or $M_{I(\text{Corr})}/M_c$ ratio)
$c$	cover to main steel reinforcement
CSA	cross sectional area
$d$	effective depth
$d'$	depth from compression face to centroid of compression reinforcement
$D$	diameter of the main steel reinforcement

$E^{\circ}$	electrode potential under standard conditions
$E_c$	modulus of elasticity of concrete
$E_s$	modulus of elasticity of steel
$E_{\text{pitting}}$	pitting potential
$\varepsilon_{cu}$	maximum strain in concrete
$\varepsilon_s$	strain in reinforcement
$f_c$	concrete strength in compression
$f_{cu}$	cube compressive strength of concrete
$f_s$	tensile stress in steel reinforcement
$f_y$	yield stress in tensile reinforcement
$f_y'$	yield stress in compression reinforcement
$f_{yv}$	characteristic strength of the shear reinforcement
F	Faraday's constant
$F_{cc}$	force in the concrete in compression
$F_{sc}$	force in the steel in compression
$\phi'$	diameter of the compressive steel reinforcement
$i$	current density
$I$	corrosion current
$M_c$	maximum moment of resistance of the compression zone
$M_{t(0)}$	moment of resistance of the control beam in the tensile zone

$M_{I(Corr)}$	moment of resistance of the corroded beam in the tensile zone
$M$	design ultimate moment
$P_{con}$	average failure load of control specimens in the laboratory
$P_{ult}$	ultimate failure load from laboratory beam tests
$P$	design shear force due to ultimate loads
$R$	corrosion rate
$\rho$	steel ratio
$s_v$	centre to centre of spacing of shear reinforcement
$s$	depth of idealised compressive stress block
$T$	time
$2RT/D \%$	degree of corrosion
$\phi$	nominal perimeter of the steel bar
$v$	design shear stress at a cross section
$v_c$	design concrete shear stress
$V$	ultimate shear force
$x$	depth to neutral axis
$z$	lever arm

These definitions are not full, accurate scientific or dictionary definitions and may be incomplete if used outside the context of the subject of corrosion of steel in concrete.

## **Acid**

A solution that (among other things) attacks steel and other metals and reacts with alkalis forming a neutral product and water.

## **Alkali**

A solution that (among other things) protects steel and other metals from corrosion and reacts with acids forming a neutral product and water.

## **Anode**

The site of corrosion in an aqueous corrosion cell (a combination of anodes and cathodes).

An external component introduced into a cathodic protection system to be the site of oxidation reaction and prevent corrosion of the metal object to be protected.

**Carbonation**

The process by which carbon dioxide (CO<sub>2</sub>) in the atmosphere reacts with water in concrete pores to form carbonic acid which then react with the alkalis in the pores, neutralising them. This can then lead to the corrosion of the reinforcing steel.

**Cathode**

The site of a charge balancing reaction in a corrosion cell.

The protected metal structure in a cathodic protection system.

**Cathodic protection**

A process of protecting a metal object or structure from corrosion by the installation of sacrificial anode or impressed current system that makes the protected object a cathode and thus resistant to corrosion.

**Cathodic protection anode**

A cathodic protection anode for steel in concrete can be a conductive paint or other conductive material that will adhere to concrete, or a metal mesh or other conductive material that can be embedded in a concrete overlay on the surface of the structure to be protected. Anodes may be impressed current or sacrificial.

**Cement (paste)**

Portland cement is a mixture of alumina, silica, lime, iron oxide and magnesia ground to a fine powder, burned in a kiln and ground again. Cement paste is the binding agent for mortar and (Portland cement) concrete after hydration.

**Chloride**

The negative ion in salt, found in sea salt, de-icing salt and calcium chloride admixture for concrete. Chloride ions promote corrosion of steel in concrete but are not used up by the process so they can concentrate and accelerate corrosion.

**Chloroaluminates**

Chemical compounds formed in concrete when chlorides combine with the  $C_3A$  in the hardened cement paste. These chlorides are no longer available to cause corrosion. Sulphate resisting cements have a low  $C_3A$  content and are more prone to chloride induced corrosion than normal Portland cement based concretes.

**Concrete**

Portland cement concrete is a mixture of cement, fine and coarse aggregates and water. The water reacts with the cement to bind the aggregates together.

**Corrosion**

The process by which a refined metal reverts back to its natural state by an oxidation reaction with the non-metallic environment (e.g. oxygen and water).

**Galvanic corrosion**

The difference in electrochemical potential between two or more dissimilar metals in electrical contact and in the same electrolyte causes electron flow between them. Attack of the more noble metal or metals usually decreased, and corrosion of the more active metal is usually increased.

**Half cell**

Usually a pure metal in a solution of (fixed) concentration. The half reaction of the metal ions dissolving and reprecipitating creates a steady potential when linked to another half cell. Two half cells make an electrochemical cell that can be a model for corrosion. Reference half cells are connected to reinforcing steel to measure 'corrosion potentials' that show the corrosion condition of the steel in concrete.

**Impressed current cathodic protection**

A method of cathodic protection that uses a power supply and an inert (or controlled consumption) anode to protect a metallic object by making it cathode.

**Incipient anode**

An area of steel in a corroding structure that was originally cathodic due to the action of local anode. When the local anode is treated by patch repairing, the incipient anode is no longer protected and starts to corrode.

**Ion**

An atom or molecule with electrons added or subtracted. Ionic compounds like salt (calcium chloride) are composed of balanced ions ( $\text{CaCl}_2 = \text{Ca}^{2+} + 2\text{Cl}^-$ ). Some ions are soluble (e.g.  $\text{Ca}^{2+}$ ,  $\text{Cl}^-$ ,  $\text{Fe}^{2+}$ ) which can be important for transport through concrete.

**Ionic current**

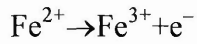
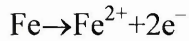
An electric current that flows as ions through an aqueous medium (e. g. concrete pore water), as opposed to an electronic flow of electrons through a metal conductor.

**iR drop**

Electrical current passing through a solution of finite resistance generates a voltage. This is superimposed on the half cell potential and must be subtracted to get accurate readings in linear polarisation and in cathodic protection. This is most easily done by 'instant off' measurements of potentials taken within a few seconds of switching off the current.

## Oxidation

The process of removing electrons from an atom or ion. The process:



is the oxidation of iron to its ferric ( $\text{Fe}^{2+}$ ) and ferric ( $\text{Fe}^{3+}$ ) oxidation state. Oxidation is done by an oxidising agent, of which oxygen is only one of many.

## Passivation

The process by which steel in concrete is protected from corrosion by the formation of a passive layer due to the highly alkaline environment created by the pore water. The passive layer is a thin  $10 \times 10^{-10}$  m, dense layer of iron oxides and hydroxides with some mineral content, that is initially formed as bare steel is exposed to oxygen and water, but then protects the steel from further corrosion as it is too dense to allow the water and oxygen to reach the steel and continue the oxidation process.

## pH

A measure of acidity and alkalinity based on the fact that the concentration of hydrogen ions  $[\text{H}^{+}]$  (acidity) times hydroxyl ions  $[\text{OH}^{-}]$  (alkalinity) is  $10^{-14}$  moles/l in aqueous solutions:

$$[\text{H}^{+}] [\text{OH}^{-}] = 1 \times 10^{-14}$$

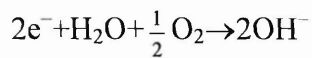
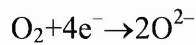
$$\text{pH} = -\log[\text{H}^{+}]$$

$$\text{pH} + \text{pOH} = 14$$

i.e. a strong acid has pH=1 (or less), a strong alkali has pH=14 (or more), a neutral solution has pH=7. Concrete has a pH of 12 to 13. Steel corrodes at pH 10 to 11.

### **Reduction**

Chemically this is the reverse of oxidation. The incorporation of electrons into a non-metal oxidising agent when a metal is oxidised. When oxygen (O<sub>2</sub>) oxidised iron (Fe) to Fe<sup>2+</sup> it receives the electrons that the iron gives up and is itself reduced:



are reduction reactions.

### **Pore (water)**

Concrete contains microscopic pores. These contain alkaline oxides and hydroxides of sodium, potassium and calcium. Water will move in and out of the concrete saturating, part filling and drying out the pores according to the external environments. The alkaline pore water sustains the passive layer if not attacked by carbonation or chlorides.

### **Reference electrode**

An alternative name for a half cell.

**Reinforced concrete**

Concrete containing a network of reinforcing steel bars to make a composite material that is strong in tension as well as in compression. Smaller volumes of material can therefore be used to make beams, bridge spans, etc. compared with unreinforced concrete, brick or masonry.

**Rust**

The corrosion product of iron and steel in normal atmospheric conditions. Chemically it is hydrated ferric oxide  $\text{Fe}_2\text{O}_3 \cdot \text{H}_2\text{O}$ . It has a volume several times that of the iron that was consumed to produce it.

**Sacrificial anode cathodic protection**

A system of cathodic protection that uses a more easily corroded metal such as zinc, aluminium or magnesium to protect a steel from corrosion. No power supply is required, but the anode is consumed.

**Steel**

An alloy of iron with up to 1.7% carbon to enhance its physical properties.

**Titanium mesh anode**

A type of impressed current anode consisting of an expanded titanium mesh coated by a corrosion resistant film of mixed metal oxides. After being fixed to the concrete surface the mesh is covered with concrete or mortar.

## *List of Figures*

---

Figure 1.1	The collapse of the Berlin Congress Hall, 1980 .....	3
Figure 1.2	Collapse of a salt damaged parking garage in Minnesota, 1984.....	3
Figure 1.3	Collapse of a car park in Wolverhampton, UK, in 1997.....	4
Figure 1.4	Collapse of a footbridge in North Carolina, USA, in 2000.....	4
Figure 2.1	Electrochemical equilibria of the iron – water system .....	14
Figure 2.2	Cartoon diagram for iron from Christmas message from Pourbaix <sup>42</sup> ....	16
Figure 3.1	Accelerated corrosion apparatus .....	41
Figure 3.2	Reinforcement bars under corrosion .....	48
Figure 3.3	Corrosion of the reinforcement in small concrete prisms .....	52
Figure 3.4	Preliminary Series I: a.) elevation; b.) cross section X–X.....	54
Figure 3.5	Accelerated corrosion of reinforcing steel in the laboratory.....	56
Figure 3.6	Preliminary beam under test.....	57
Figure 3.7	Schematic drawing for preliminary beam test .....	58

Figure 3.8	Stainless steel stirrups exhibiting pitting corrosion .....	61
Figure 4.1	Grading curve for fine aggregate .....	71
Figure 4.2	Grading curve for coarse aggregate .....	72
Figure 4.3	Monitoring of the accelerating corrosion technique .....	75
Figure 4.4	Standard Calomel reference electrode .....	76
Figure 4.5	Digital voltmeter .....	77
Figure 5.1	Geometry of the beam Series I used for the design .....	84
Figure 5.2	Reinforced concrete beams undergoing main reinforcement corrosion .....	87
Figure 5.3	Iron oxide formation on the beams after corrosion.....	88
Figure 5.4	Loading configuration and instrumentation of a test beam.....	90
Figure 5.5	Reinforcement cage after corrosion .....	90
Figure 5.6	Beam specimens electrically connected in series.....	95
Figure 6.1	Geometry of the beam Series II used for the design .....	109
Figure 6.2	Electrical connections between the shear reinforcement and the power supply .....	110

Figure 6.3	Reinforcing cage used for beam Series II .....	111
Figure 6.4	Shear reinforcement corrosion .....	113
Figure 6.5	Beam in the loading rig during testing .....	114
Figure 7.1	Geometry of the beam Series III used for the design.....	122
Figure 7.2	Exposed main and shear reinforcement .....	124
Figure 7.3	Transformer Rectifier (TR) .....	126
Figure 7.4	Precision linear power supplies.....	127
Figure 7.5	Deteriorated reinforced concrete beam exhibiting both main and shear reinforcement corrosion under test .....	129
Figure 7.6	Deteriorated main reinforcement bars after corrosion .....	130
Figure 7.7	Shear reinforcement with most severe corrosion .....	131
Figure 8.1	Average load – deflection curves of corroded reinforced concrete beams of Series I under four point bending test.....	140
Figure 8.2	Average load – deflection curves of corroded reinforced concrete beams of Series I under four point bending test.....	141
Figure 8.3	Average load – deflection curves of corroded reinforced concrete beams of Series I under four point bending test.....	142

Figure 8.4	Relationship between stiffness and degree of corrosion for beam designed with 2T8 .....	146
Figure 8.5	Relationship between $P_{ult} / P_{con}$ and degree of corrosion for beam designed with 2T8 and 26 mm cover to main steel.....	148
Figure 8.6	Relationship between $P_{ult} / P_{con}$ and degree of corrosion for beam designed with 2T8 and 36 mm cover to main steel.....	149
Figure 8.7	Relationship between $P_{ult} / P_{con}$ and degree of corrosion for beam designed with 2T8 and 56 mm cover to main steel.....	150
Figure 8.8 (a)	Control beam crack pattern at ultimate load .....	152
Figure 8.8 (b)	Beam 2T8/18.45+10D6/0/20 crack pattern at ultimate load level ....	152
Figure 8.8 (c)	Beam 2T8/17.76+10D6/0/30 crack pattern at ultimate load level ....	153
Figure 8.8 (d)	Beam 2T8/16.35+12D6/0/50 crack pattern at ultimate load level....	153
Figure 8.9	Average load – deflection curves of corroded reinforced concrete beams of Series I under four point bending test.....	156
Figure 8.10	Average load – deflection curves of corroded reinforced concrete beams of Series I under four point bending test.....	157
Figure 8.11	Average load – deflection curves of corroded reinforced concrete beams of Series I under four point bending test.....	158

Figure 8.12	Relationship between stiffness and degree of corrosion for beam designed with 2T10 .....	161
Figure 8.13 (a)	Beam 2T10/7.5+10D6/0/20 crack pattern at ultimate load level .....	162
Figure 8.13 (b)	Beam 2T10/6.7+10D6/0/30 crack pattern at ultimate load level ..	163
Figure 8.13 (c)	Beam 2T10/6.1+12D6/0/50 crack pattern at ultimate load level .....	163
Figure 8.14	Relationship between $P_{ult} / P_{con}$ and degree of corrosion for beam designed with 2T10 and 26 mm cover to main steel.....	165
Figure 8.15	Relationship between $P_{ult} / P_{con}$ and degree of corrosion for beam designed with 2T10 and 36 mm cover to main steel.....	166
Figure 8.16	Relationship between $P_{ult} / P_{con}$ and degree of corrosion for beam designed with 2T10 and 56 mm cover to main steel.....	167
Figure 8.17	Beam 2T12/5.9/50 crack pattern at ultimate load level .....	169
Figure 8.18	Average load – deflection curves of corroded reinforced concrete beams of Series I under four point bending test.....	171
Figure 8.19	Relationship between stiffness and degree of corrosion for beam designed with 2T12.....	172
Figure 8.20	Relationship between $P_{ult} / P_{con}$ and degree of corrosion for beam designed with 2T12 and 56 mm cover to main steel.....	174

Figure 9.1	Beam 2T8/0+12D6/23.2/50 crack pattern at ultimate load level .....	182
Figure 9.2	Beam 2T12/0+12D6/6.1/50 crack pattern at ultimate load level .....	183
Figure 9.3	Load – deflection curves of corroded concrete beams of Series II under four point bending test .....	185
Figure 9.4	Relationship between stiffness and shear reinforcement corrosion .....	186
Figure 9.5	Relationship between $P_{ult} / P_{con}$ and degree of corrosion.....	188
Figure 9.6	Load – deflection curves of corroded concrete beams of Series II under four point bending test .....	190
Figure 9.7	Relationship between stiffness and shear reinforcement corrosion .....	191
Figure 9.8	Relationship between $P_{ult} / P_{con}$ and degree of corrosion for beam designed with 2T12 and 50 mm cover .....	192
Figure 10.1	Load – deflection curves of corroded concrete beams of Series III under four point bending test .....	199
Figure 10.2	Relationship between stiffness and main reinforcement corrosion .....	200
Figure 10.3	Relationship between stiffness and shear reinforcement corrosion .....	201
Figure 10.4	Relationship between stiffness and simultaneous main and shear reinforcement corrosion .....	203

Figure 10.5	Beam 2T8/8.8/50+12D6/9.1 crack pattern at ultimate load level .....	204
Figure 10.6	Beam 2T8/25.7/50+12D6/27.6 crack pattern at ultimate load level .....	204
Figure 10.7	The effect of corrosion degree on the flexural load capacity of corrosion damaged reinforced concrete beams .....	205
Figure 10.8	The effect of corrosion degree on the flexural load capacity of corrosion damaged reinforced concrete beams .....	206
Figure 11.1 (a)	EC2 stress block <sup>148</sup> .....	213
Figure 11.1 (b)	BS 8110 stress block <sup>148, 149</sup> .....	213
Figure 11.2	Cross sectional area of reinforced concrete beams used in the analysis .....	215
Figure 11.3	Schematic representation of stress due to external loading .....	218
Figure 11.4	Effect of corrosion on the $M_{U(Corr)}/M_c$ ratio for 2T8/Corr%+10D6/0/20 beams.....	224
Figure 11.5	Effect of corrosion on the $M_{U(Corr)}/M_c$ ratio for 2T8/Corr%+10D6/0/30 beams.....	225
Figure 11.6	Effect of corrosion on the $M_{U(Corr)}/M_c$ ratio for 2T8/Corr%+12D6/0/50 beams.....	226

Figure 11.7	Effect of corrosion on the $M_{I(Corr)}/M_c$ ratio for 2T10/Corr%+10D6/0/20 beams.....	227
Figure 11.8	Effect of corrosion on the $M_{I(Corr)}/M_c$ ratio for 2T10/Corr%+10D6/0/30 beams.....	228
Figure 11.9	Effect of corrosion on the $M_{I(Corr)}/M_c$ ratio for 2T10/Corr%+12D6/0/50 beams.....	229
Figure 11.10	Effect of corrosion on the $M_{I(Corr)}/M_c$ ratio for 2T12/Corr%+24D6/0/50 beams.....	230
Figure 11.11	Summary of the effect of corrosion on the $M_{I(Corr)}/M_c$ ratio for beam Series I.....	231
Figure 11.12	Effect of corrosion on the $M_{I(Corr)}/M_c$ ratio for 2T8/Corr%+12D6/Corr%/50 (beam Series III shear reinforcement corrosion $\leq 5\%$ ).....	232
Figure 11.13	Comparison with other researchers .....	234
Figure 11.14	Effect of $\alpha$ on the $M_{I(0)}/M_c$ ratio .....	237
Figure 11.15	Effect of % Reinforcement on the $M_{I(0)}/M_c$ ratio .....	239
Figure 11.16	Effect of Cover on the $M_{I(0)}/M_c$ ratio .....	240

## *List of Tables*

---

Table 2.1	Summary of experimental tests on corroded beams <sup>83</sup> .....	33
Table 3.1	Active and passive condition of steel rebar .....	46
Table 3.2	Reduction in reinforcing bar diameter .....	49
Table 3.3	Preliminary test programme .....	55
Table 3.4	Experimental program for preliminary beam Series I.....	59
Table 4.1	Experimental Programme.....	66
Table 4.2	Concrete mix design form .....	68
Table 4.3	Chemical composition of Portland cement by Castle Cement Ltd. ....	70
Table 5.1	Beam Series I – Corrosion details and load behaviour of beams with main reinforcement (2T8) corrosion .....	92
Table 5.2	Beam Series I – Corrosion details and load behaviour of beams with main reinforcement (2T10) corrosion .....	98
Table 5.3	Beam Series I – Corrosion details and load behaviour of beams with main reinforcement (2T12) corrosion .....	103

Table 6.1	Beam Series II – Corrosion details and load behaviour of beams with shear reinforcement corrosion (2T8).....	116
Table 6.2	Beam Series II – Corrosion details and load behaviour of beams with shear reinforcement corrosion (2T12).....	117
Table 7.1	Beam Series III – Corrosion details and load behaviour of beams with main and shear reinforcement corrosion.....	132
Table 8.1	Beam Series I (2T8/Corr%) test results .....	143
Table 8.2	Comparison of residual strength at different covers and degrees of corrosion.....	151
Table 8.3	Beam Series I (2T10/Corr%) test results .....	159
Table 8.4	Comparison of residual strength at different covers and degrees of corrosion.....	168
Table 8.5	Beam Series I (2T12/Corr%) test results .....	173
Table 9.1	Beam Series II (2T8/0+12D6/Corr%/50) test results.....	181
Table 9.2	Beam Series II (2T12/0+12D6/Corr%/50) test results.....	181
Table 10.1	Beam Series III (2T8/Corr %+12D6/Corr %/50) test results.....	197
Table 11.1	Variables in test programme. ....	221

Table 11.2	Beams properties .....	222
Table 11.3	Results of regression analysis .....	233
Table 11.4	Overall comparisons.....	236

## ***Introduction***

### **1.1 Introduction**

The development of reinforced concrete by French engineers in the middle of the 19<sup>th</sup> century was one of the major advances in the history of construction <sup>1</sup>. Most of today's concrete construction relies on the composite interaction of concrete and steel, which is aided by the near equivalence of their thermal expansion characteristics. In general, reinforced concrete has proved to be a highly successful material in terms of structural performance. However, there have been numerous examples of the durability problems arising from the corrosion of reinforcement in concrete structures, mostly due to poor quality concrete, poor design and workmanship, inadequate cover to reinforcement, chlorides in the concrete or combinations of these. These have led to various forms of corrosion induced damage such as cracking and spalling, resulting in reductions in structural capacity.

When steel reinforcement corrodes, corrosion products generate tensile stresses in the concrete. Concrete is very strong in compression but weak in tension, the tensile strength <sup>2</sup> being only about 10 percent of the compressive strength. Therefore tensile cracks are readily nucleated and propagated as a result <sup>3</sup>. The development of corrosion products along the bar surface may affect the failure mode and ultimate strength of flexural members due to two causes: firstly, due to a reduction in the degree of bar

confinement caused by an opening of longitudinal cracks along the reinforcement and, secondly, due to significant changes at the steel–concrete interface caused by changes in the surface conditions of the reinforcing steel. The changes in the surface conditions due to corrosion are characterised initially by changes in the roughness of the surface, then, by development of less firm adherent interstitial layers of corrosion products between concrete and steel and, eventually, by local damage in terms of heavy pitting and degradation in the profile of the bar ribs <sup>4</sup>.

## 1.2 Scope of research

Reinforcement corrosion in concrete structures is the biggest durability problem facing the UK at present. In the press release, the Building Research Establishment estimated the direct cost of reinforcement corrosion to the UK economy to be around £550M per year <sup>5</sup> since repair and maintenance is required to increase the service life of the structure <sup>6,7,8,9</sup>.

Corrosion of reinforcing bars is one of the main causes which induces deterioration of concrete beams, thus reducing their residual service life. For example, the collapse of the Berlin Congress Hall in 1980 (Figure 1.1) <sup>10</sup> and a parking garage in Minnesota, USA in 1984 (Figure 1.2) <sup>10</sup> are examples of spectacular failures due to a reduction in residual strength due to corrosion of the steel reinforcement.

Furthermore, the sudden collapse of part of a car park in Wolverhampton, UK in 1997, which was built using the American developed lift slab technique, Figure 1.3 <sup>11</sup> and a footbridge in North Carolina, USA in 2000, Figure 1.4, are also examples of problems associated with reinforcement corrosion. Upon inspection of the footbridge in

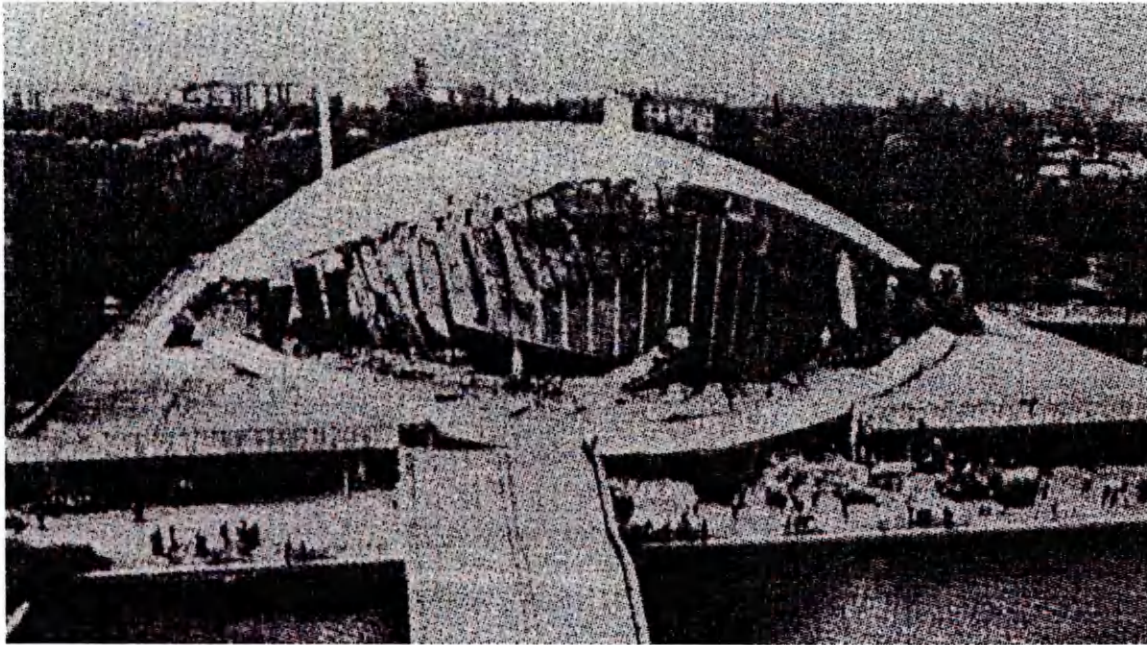


Figure 1.1 The collapse of the Berlin Congress Hall, 1980

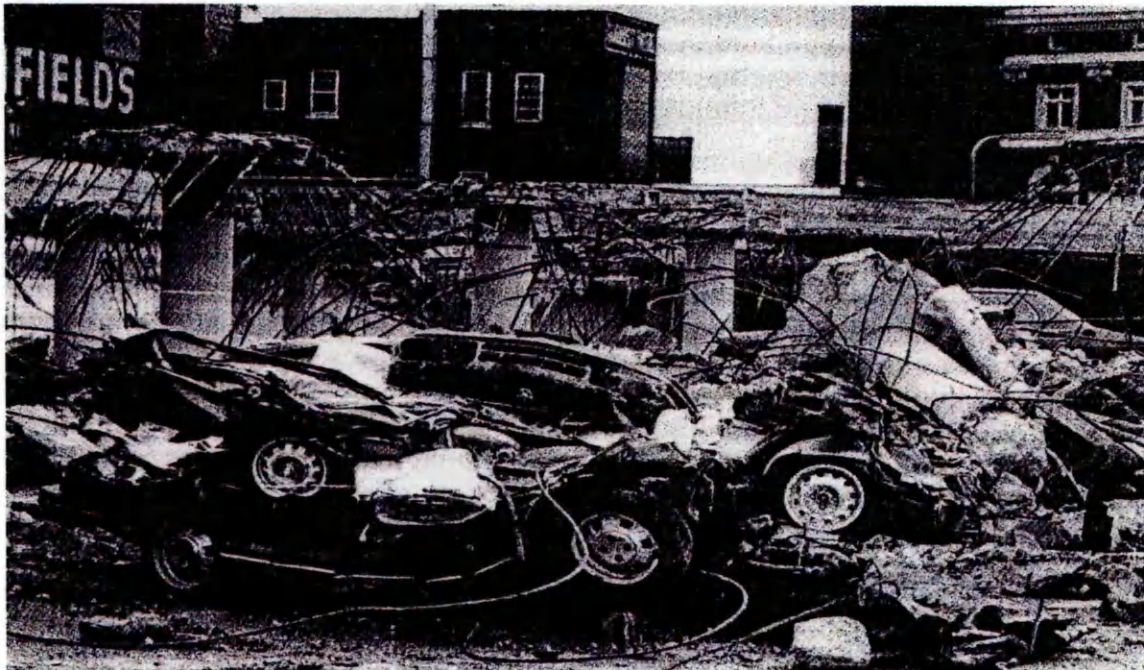


Figure 1.2 Collapse of a salt damaged parking garage in Minnesota, 1984

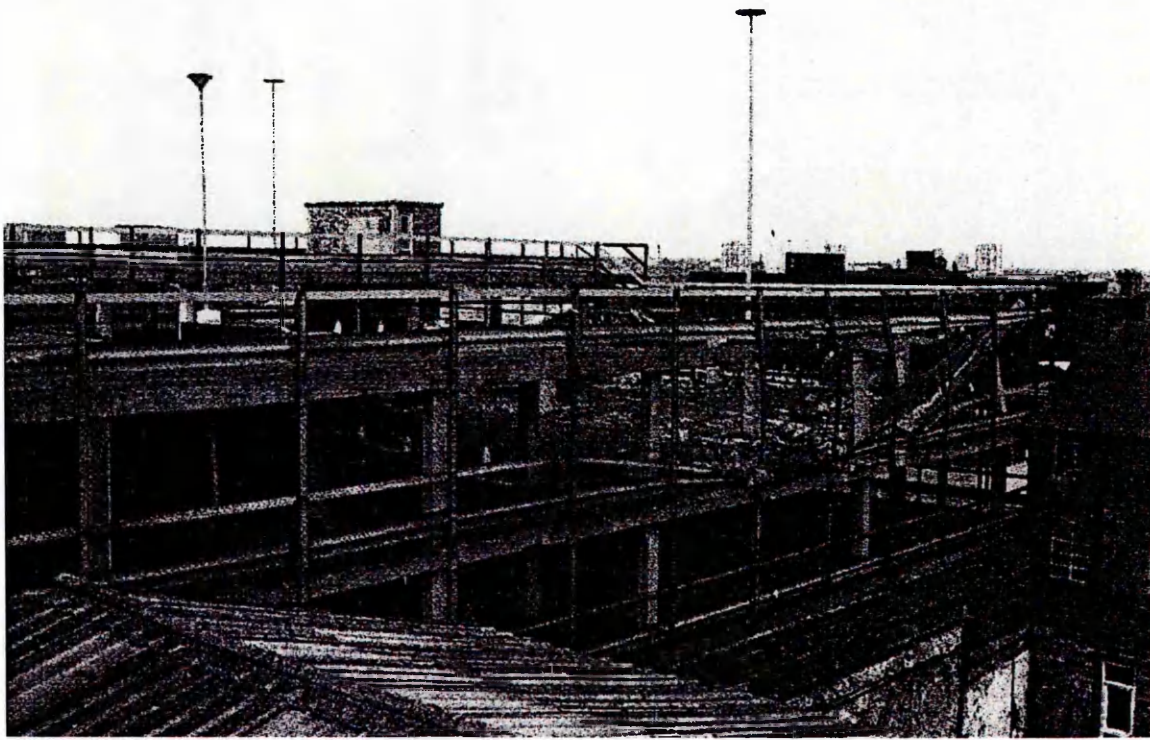


Figure 1.3 Collapse of a car park in Wolverhampton, UK, in 1997

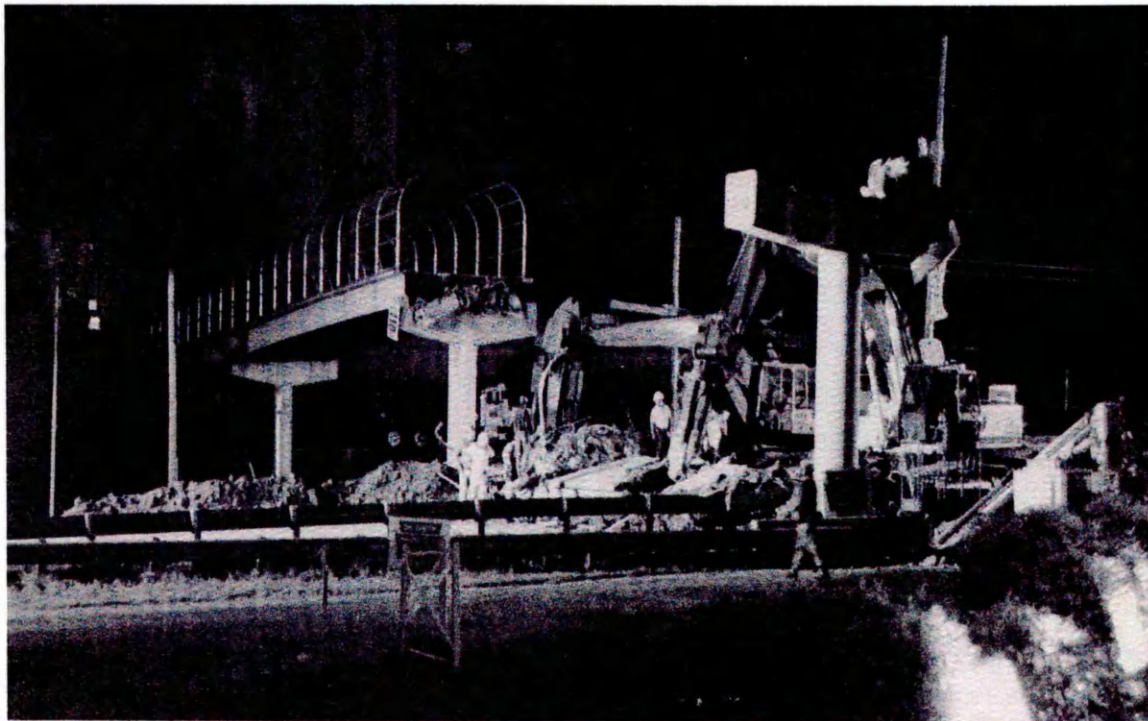


Figure 1.4 Collapse of a footbridge in North Carolina, USA, in 2000

Figure 1.4 after collapse, high levels of calcium chloride were found in grout used in the construction<sup>12</sup>.

Clearly, corrosion of the reinforcing bars is one of the main causes of deterioration of reinforced concrete beams. Corrosion affects both the main and shear reinforcement, therefore it is important to know the effect this will have on the residual strength of the member. Consequently, catastrophic failure such as those mentioned earlier can be controlled through better knowledge of the flexural and shear capacities of deteriorating members.

### **1.3 Scope of present investigation**

This study contributes to understanding the effect of reinforcement corrosion on the behaviour of reinforced concrete structures. Currently, much research is focused on corrosion in reinforced concrete members. However, the problems associated with the residual strength of corroded reinforced concrete beams have not been fully addressed. To date extensive research has been undertaken to assess flexural strength of corroded reinforced concrete beams, but to date, there is no evidence of research being conducted on the shear strength. Furthermore, the influence of both main and shear reinforcement corrosion occurring concurrently also needs to be investigated to determine its effect on the performance of the member. Therefore, the aim of this research was to determine the residual strength of corroded reinforced concrete beams when the main and shear reinforcement are subjected to varying degrees of corrosion. Analytical models are developed to predict the behaviour of deteriorated reinforced concrete elements. This will provide a better understanding of the performance of such beams in practice.

In order to fulfil the aim of the present investigation, the overall objectives, were to:

- investigate the chemical processes involved in corrosion of steel reinforcement;
- determine the techniques involved in accelerating corrosion in reinforced concrete members in the laboratory;
- investigate the residual strength of reinforced concrete beams subjected to different percentages of main steel corrosion;
- investigate the residual strength of reinforced concrete beams subjected to different percentages of shear reinforcement corrosion;
- investigate the residual strength of reinforced concrete beams subjected to different percentages of both main and shear reinforcement corrosion;
- develop analytical models to predict the behaviour of deteriorated reinforced concrete beams on the basis of the laboratory experiments.

#### **1.4 Thesis layout**

The thesis attempts to bring together results which will be used to assist the bridge engineer in the assessment of reinforced concrete structures exhibiting reinforcement corrosion.

This thesis is divided into thirteen chapters. An introduction to the thesis is given in Chapter 1.

Chapter 2 includes a brief discussion of the principles of metallic corrosion and the basic deterioration mechanisms in reinforced concrete structures. Chapter 3, presents the optimisation of the corrosion process.

The detailed experimental programme, including materials used and experimental procedures and techniques, is described in Chapter 4.

Chapter 5 presents experimental results obtained from the first test series. Included is research on the influence of corrosion on the main reinforcement of simply supported beams (shear strength was provided by mild steel links which remained unaffected by corrosion). The degree of under reinforcement was varied (8, 10 and 12 mm diameter main steel was used) and each was subjected to differing percentage of corrosion (0 – 15% in 5% increments).

Chapter 6 presents results on the second test series. The shear reinforcement was subjected to varying percentage of corrosion (0 – 15% in 5% increments) in order to determine its affect on the shear capacity. The main steel remained unaffected throughout.

In Chapter 7, the experimental results obtained from the third test series are presented. The residual strength of reinforced concrete beams is determined when the main and shear reinforcement are simultaneously subjected to varying degrees of reinforcement corrosion (0 – 15% in 5% increments).

Chapters 8, 9 and 10 presents the experimental results obtained from three series (Series I, Series II and Series III respectively) of tests, the analysis of test data, interpretation and discussion on the results.

Analytical models are derived in Chapter 11 which predict the residual strength of corroded reinforced concrete beams.

Chapter 12 presents the main conclusions from the study and recommendations are given for future research. References used in the thesis are listed in Chapter 13.

Appendix A summarises the design data. The publications to date arising from the results of this research are given in Appendix B.

### *Literature Review*

#### **2.1 Introduction**

The increase in the scale of the problem of deterioration of reinforced concrete members can be illustrated by the number of publications concerned with the science of reinforced concrete decay and its mechanism. However, it is not the intention of the present study to deal with causes, remedies or mechanisms of corrosion of the embedded reinforcing steel or the subsequent deterioration of the concrete. The main aim is to determine the structural performance of these deteriorated members.

In the light of the objectives stated in Chapter 1, the survey of previous research and related documents and reports presented herein has been confined to the specific area of structural integrity assessment of corrosion damaged, flexural members. In the present chapter, two areas of previous research work relevant to the present study are examined and discussed. These comprise:

- Theoretical, numerical and experimental work done specifically on the assessment of strength and characteristic behaviour of reinforced concrete beams damaged by the corrosion of tensile reinforcement;
- Similar work done on reinforced concrete beams where the tensile reinforcement is completely debonded from the adjoining concrete and shear reinforcement is not provided.

## 2.2 History of concrete

The development of concrete as a construction material dates back several thousand years to the days of ancient Egyptians, the Greeks and the Romans. These early concrete compositions were based on lime, although the Romans are known for their development of pozzolanic cement and lightweight concrete <sup>13</sup>. Apart from brief revivals over the years, there was little further development until the eighteenth century when the industrial revolution evolved. Later in the nineteenth century, the technique of reinforced concrete was introduced. The credit for introduction of steel as a requirement is variously attributed to Joseph Aspdin 1824, William Wilkinson 1854, Lambot in 1855 for ferrocement boats, to Monier in 1867 and to Hennebique in 1897 who built the first reinforced concrete frame building in Britain at Weaver's Mill, Swansea. Notable steps forward in this century have been introduction of prestressed concrete by Freyssinet in the 1940s, the extensive use of reinforced concrete during World War II, the rapid post-war concrete building expansion prompted by shortages of steel, the motorway building boom of the 1960s involving concrete pavements and bridges, and most recently, the contribution of structural concrete to modern offshore structures <sup>14</sup>.

## 2.3 Properties of reinforced concrete

Concrete may be described as a graded range of stone aggregate particles bound together by a hardened cement paste <sup>15</sup>. The main chemical constituents of Portland cements are lime (CaO), which composes 60% – 67% of the total, silica (SiO<sub>2</sub>), which forms 17% – 25% and alumina (Al<sub>2</sub>O<sub>3</sub>), which may constitute 3% – 8%. The rest are

iron oxide ( $\text{Fe}_2\text{O}_3$ ), magnesia ( $\text{MgO}$ ), sulphur trioxide ( $\text{SO}_3$ ) and sodium ( $\text{Na}_2\text{O}$ ) and potassium ( $\text{K}_2\text{O}$ ) oxides<sup>16</sup>. Concrete strength is derived from the hydration of the cement by water. The cement constituents progressively crystallize to form a gel or paste which surrounds the aggregate particles and binds them together. For any given condition of test, the strength of a workable concrete mix is dependent on a number of parameters, mainly the cement content and the water/cement ratio.

The tensile strength of concrete is only about 10 percent of the compressive strength<sup>13</sup>. Therefore, reinforcement is designed to carry these tensile forces, which are transferred by bond between the interfaces of the two materials<sup>17, 18, 19</sup>.

Reinforced concrete is a strong durable building material that can be formed into many varied shapes and sizes. Its utility and versatility is achieved by combining the best of features of concrete and steel. The materials are more or less complimentary; the steel is able to provide the tensile strength and probably some of the shear strength while the concrete, strong in compression, protects the steel to give durability and fire resistance<sup>14</sup>.

#### **2.4 Mechanism of concrete deterioration**

Deterioration of the concrete is rarely due to one isolated cause, and concrete can suffer from various mechanisms of deterioration<sup>13</sup>. Environmental processes may cause salts, oxygen, moisture or carbon dioxide to penetrate the concrete cover and eventually lead to corrosion of embedded steel reinforcement<sup>20, 21, 22, 23, 24</sup>. As the steel corrodes, apart from the resulting loss in its cross sectional area, the corrosion products expand in volume causing cracking<sup>25, 26, 27, 28, 29</sup>, rust staining and spalling of the concrete cover<sup>3, 4</sup>. The detrimental role that corrosion of embedded steel rebars plays in the

service life of reinforced concrete is well documented <sup>10</sup>, costing the UK an estimated £550m per annum. The problem is also widespread in overseas, i.e. it has been reported that corrosion costs in the USA alone are estimated to be close to \$300 billion a year, or approximately 3.2% of the USA gross domestic product <sup>30</sup>. Over the past 25 years, a number of methods for assessing the state of corrosion of reinforcing steel have been under development, but to date difficulties in accuracy and reliability are still present <sup>31</sup>. Consequently a reliable and accurate corrosion tool that can be used to survey reinforced concrete structures is required.

## **2.5 Principles of corrosion**

### **2.5.1 Introduction**

The word corrosion means the destruction of a material under the chemical or electrochemical action of the surrounding environment <sup>32, 33, 34</sup>. It is well known that iron, unless adequately protected, corrodes easily and is transformed into rust. Corrosion phenomena are very complex <sup>35, 36</sup>. Corrosion obeys the thermodynamic laws; metals tend to return to the state in which they are found in nature. Metals gradually destroy under the action of water, air and other atmospheric agents. They corrode and transform themselves into substances similar to the mineral ores from which they were originally extracted <sup>22, 37</sup>.

### **2.5.2 Chemical and electrochemical reactions**

The lack of success in applying chemical thermodynamics to corrosion is principally due to the fact that the phenomena of metallic corrosion in aqueous solutions are not

only chemical but also electrochemical, in which the moist concrete forms the electrolyte, the possible electrochemical reactions taking place on embedded steel<sup>38, 39</sup>.

A chemical reaction is a reaction in which only chemical bodies participate (neutral molecules or positively and negatively charged ions).

dissolution of water vapour  $2\text{H}_2\text{O} = 2\text{H}_2 + \text{O}_2$

electrolytic dissolution of liquid water  $\text{H}_2\text{O} = \text{H}^+ + \text{OH}^-$

precipitation of ferrous hydroxide  $\text{Fe}^{++} + 2\text{OH}^- = \text{Fe}(\text{OH})_2$

corrosion of iron with evolution of hydrogen  $\text{Fe} + 2\text{H}^+ = \text{Fe}^{++} + \text{H}_2$

An electrochemical reaction is a reaction in which both chemical and free electric charges take part (e.g. negative electrons dissolved in metallic electrode). Such reactions are oxidations if they proceed in the direction which corresponds to the liberation of negative charge; they are reductions if they proceed in the direction corresponding to the absorption of negative charge.

oxidation of hydrogen gas into hydrogen ions  $\text{H}_2 \rightarrow 2\text{H}^+ + 2\text{e}^-$

reduction of oxygen gas into hydroxide ions  $\text{O}_2 + 4\text{H}_2\text{O} + 4\text{e}^- \rightarrow 4\text{OH}^-$

oxidation of iron to ferrous ions  $\text{Fe} \rightarrow \text{Fe}^{++} + 2\text{e}^-$

oxidation of ferrous ions to ferric ions  $\text{Fe}^{++} \rightarrow \text{Fe}^{+++} + \text{e}^-$

When emphasizing the dependence of pH and potential, it is useful to write the equilibrium of precipitation of ferrous hydroxide as  $\text{Fe}^{++} + 2\text{H}_2\text{O} = \text{Fe}(\text{OH})_2 + 2\text{H}^+$ , where pH measures the effect of  $\text{H}^+$  ions, the electrode potential measures the effect of charge<sup>40, 41</sup>.

### 2.5.3 General condition of corrosion, immunity and passivity

It is convenient to use a graphical means to study such a complex phenomena (see Figure 2.1), thermodynamically represented by a simplified Pourboux diagram. Then

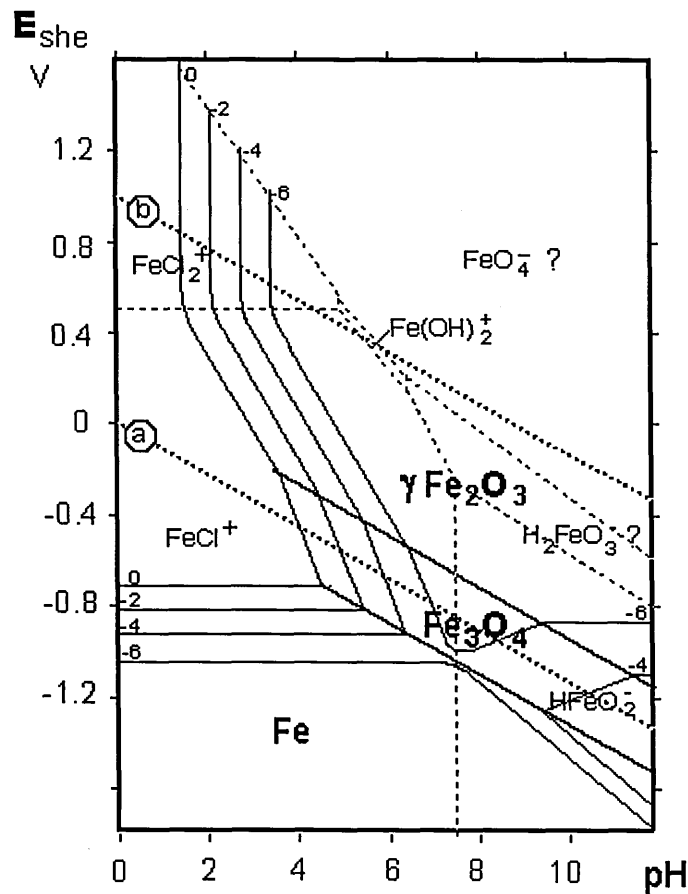


Figure 2.1 Electrochemical equilibria of the iron – water system <sup>42</sup>

all the competing and simultaneous reactions, both chemical and electrochemical, can be studied. It has been possible to establish one such graphical method with the use of diagrams of electrochemical equilibria, drawn as a function of pH (abscissa) and electrode potential (ordinate). The left portion of these diagrams represents acid media and the right portion alkaline media; the top portion represents oxidizing media and the bottom reducing media. The region below the dotted line (a) represents the

circumstances under which the water may be reduced with the evolution of hydrogen under pressure of 1 atmosphere; the region above the dotted line (b) represents the circumstances under which water may be oxidized with evolution of oxygen; and the region between the two lines (a) and (b) represents the circumstances in which both this reduction and oxidation are impossible. Water then is thermodynamically stable and this region represents the region of thermodynamic stability of water under 1 atm pressure.

Depending on the actual conditions of the pH and electrode potential, Figure 2.1 shows that the oxidation of iron may give rise to soluble products – green ferrous ions,  $\text{Fe}^{++}$ , yellow ferric ions,  $\text{Fe}^{+++}$ , and green dihypoferrite ions,  $\text{FeO}_2\text{H}^-$  – or to insoluble products – white ferrous hydroxide  $\text{Fe}(\text{OH})_2$  (unstable relative to black magnetite,  $\text{Fe}_3\text{O}_4$ ) and brown ferric oxide  $\text{Fe}_2\text{O}_3$ , which may be variously hydrated and is the main constituent of rust. Iron is corroding in the presence of an iron free solution when the quantity of iron that this solution may dissolve is greater than a given low value (e.g.,  $10^{-6}$  g-atoms / liter or 0.056 ppm), and conversely iron may be rendered passive if it becomes covered by a protective insoluble oxide of hydroxide (e.g.,  $\text{Fe}_2\text{O}_3$ ). Then the lines which are drawn in Figure 2.1 corresponding to a solubility of metal and its oxide equal to  $10^{-6}$  delineate various regions or areas. There are two areas where corrosion is possible (areas of corrosion), and area where corrosion is impossible (area of immunity or cathodic protection), and an area where passivation is possible (area of passivation), Figure 2.2. This assumes that the insoluble products,  $\text{Fe}_2\text{O}_3$  and  $\text{Fe}_3\text{O}_4$ , are sufficiently adherent and impermeable that corrosion of the underlying metal is essentially stifled and the metal is then “passive”.

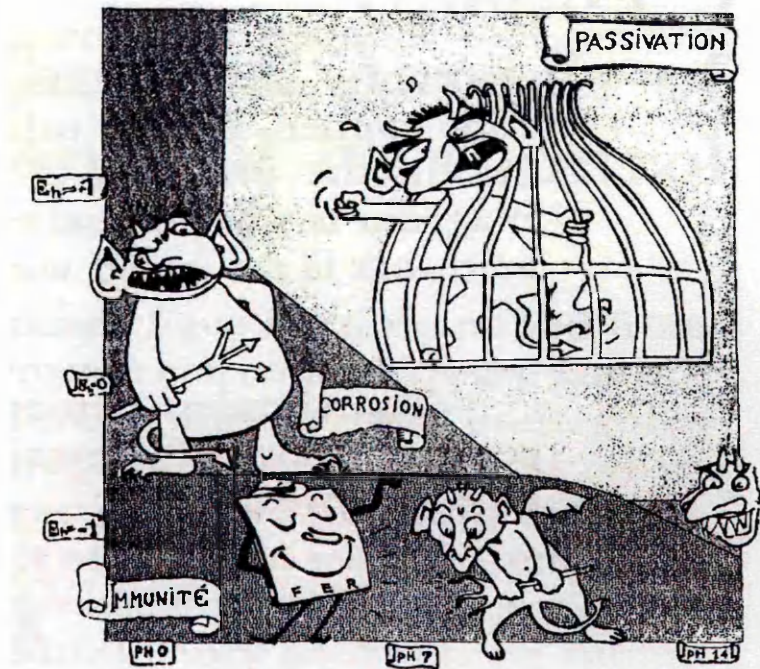
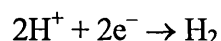
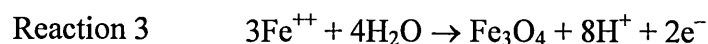
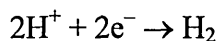


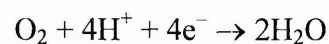
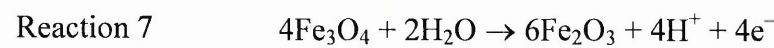
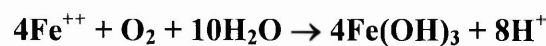
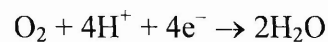
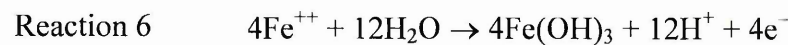
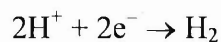
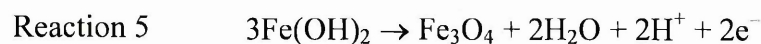
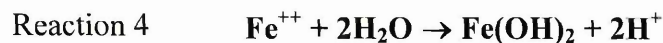
Figure 2.2 Cartoon diagram for iron from Christmas message from Pourbaix<sup>42</sup>

Diagram of electrochemical equilibria of the iron – water system at 25°C may be deduced by assuming that passivation results either from the formation of a film of  $\text{Fe}_2\text{O}_3$  or from the formation of a films of  $\text{Fe}_2\text{O}_3$  and  $\text{Fe}_3\text{O}_4$ <sup>10, 43</sup>. The region of stability of iron is entirely below the region of stability of water under atmospheric pressure.

In other words, regardless of the pH of the solution, metallic iron and water are not simultaneously thermodynamically stable at 25°C under a pressure of 1 atm. The simultaneous stability of iron in the presence of water at 25°C is only attained at pressures high enough to depress the equilibrium potential of the  $\text{H}_2\text{O} - \text{H}_2$  system (represented for 1 atm by line (a), in Figure 2.1) below the equilibrium potential of the  $\text{Fe} - \text{Fe}_3\text{O}_4$  system. This stability is attained only at pH values between 10 and 12 for

pressures greater or equal to 750 atm. At lower pressure iron always tends, if it is not passivated, to be corroded with reduction of water and evolution of hydrogen. This corrosion of iron gives rise to the dissolution of metal mainly with the formation of green ferrous ions  $\text{Fe}^{++}$  (reaction 1) or dihypoferrite ions  $\text{FeO}_2\text{H}^-$  (reaction 2) which are also green, depending on whether the pH is greater or less than 10.6. At values of pH below about 6 to 7, these ions may change to black magnetic iron oxide, or magnetite  $\text{Fe}_3\text{O}_4$  (reaction 3) or into white ferrous hydroxide  $\text{Fe}(\text{OH})_2$  (reaction 4). Because area of stability of magnetite,  $\text{Fe}_3\text{O}_4$ ,  $\text{Fe}(\text{OH})_2$  will be thermodynamically unstable with respect to  $\text{Fe}_3\text{O}_4$  and will tend to transform to this substance (reaction 5). In the presence of oxygen ferrous ions and magnetite may be oxidized to ferric oxide  $\text{Fe}_2\text{O}_3$  (or ferric hydroxide  $\text{Fe}(\text{OH})_3$  (reaction 6 and 7).





Corrosion of iron is possible in two regions, roughly triangular in shape, which correspond to the dissolution of metal with the formation of ferrous and dihydroferrite ions, respectively. Such corrosion by dissolution will affect the entire metal surface and so will be of a general nature.

The metal may be protected against this corrosion by lowering its electrode potential to the region of immunity (in which case there will be cathodic protection, obtainable by intervention of a reducing action) or by raising its electrode potential into the region of passivation (in which case there will be protection by passivation, obtained by intervention of an oxidizing action).

In the case of protection by immunity, the metal will be thermodynamically stable and, as a result, will not corrode; it will possess a truly metallic surface. Since water is not stable under the conditions of electrode potential and pH corresponding to this state of immunity, this protection will only be achieved by continuous consumption of external energy which causes hydrogen evolution on the iron.

Passivity is defined as a state of metal in which the rate of ionization in a given condition is much less than the rate at a less oxidizing condition. The mechanism of the passive film formation and its growth on the steel in concrete is not exactly the same as that of the steel directly in alkaline solution. However, the appreciation of the passivity of steel directly in an alkaline solution is important for understanding the passivity of steel in concrete which has highly alkaline pore solution. In this case of protection by passivation the metal itself will not be stable, but will be covered by a stable oxide film ( $\text{Fe}_3\text{O}_4$  or  $\text{Fe}_2\text{O}_3$  according to the conditions of potential or pH). The protection will be perfect or imperfect depending on whether or not this film perfectly shields the metal from contact with the solution. In the case of imperfect position, corrosion only affects the weak points of the passive film and therefore has a localized character. Water being stable under the conditions of electrode potential and pH which correspond to the state of passivation<sup>10</sup>, this state will be attained without consumption of external energy; the solution needs only be sufficiently oxidizing for the electrode potential of the metal to be maintained permanently in the passivation region.

## 2.6 Corrosion initiation due to chloride attack

It is well documented that the intrusion of chloride ions in reinforced concrete can cause corrosion if oxygen and moisture are present<sup>3, 44, 45, 46, 47, 48, 49, 50, 51, 52, 53, 54, 55, 56</sup>.

Chloride ions may be introduced into concrete in a variety of ways, such as during manufacturing as intentional or accidental intrusion or by penetration from an external source. In concrete, chloride ions may be present in various forms such as:

- Free chloride ions in pore solution;
- Chloride loosely bonded to hydrates of calcium silicate;
- Chloride strongly bonded to hydrates of calcium aluminates.

It is principally only the free chloride ions that influence the corrosion process. There is, however, a general lack of information about the level of chloride likely to remain un-combined for a long period in the solution phase.

The concept of critical chloride level or corrosion threshold for steel in concrete has been suggested by a number of investigators using variety of experimental techniques. There is some evidence that the hydroxyl ion concentration of concrete has an influence on the critical chloride level <sup>57, 58, 59</sup>. The Building Research Establishment categorise the chloride ion content (% by weight of cement) in terms of corrosion risk as follows:

- Less than 0.4% – low risk;
- Between 0.4 – 1.0% – medium risk;
- More than 1% – high risk.

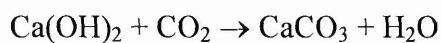
It is highly recognised that chloride has negligible influence on the pH of concrete. The enhancement of the  $C_3A$  content reduces the chloride content within the cement but the optimum level has not been established. The chloride complex with  $C_3A$ , however, becomes unstable when carbonation occurs which tends to liberate chloride ions. On the other hand, the diffusion kinetics of chloride ions in hardened concrete is a decisive

factor in relation to corrosion risk. Investigations have confirmed that diffusion is strongly influenced by cement type and fineness, the ion exchange capacity of the system, and the curing of the concrete surface. The effect of water/cement ratio is only limited to a surface layer of the concrete and to short duration of chloride exposure. It was reported<sup>60</sup> that the high cement content and low water/cement ratio of the mixes do not present a barrier to the penetration of chlorides into concrete.

The precise mechanism by which depassivation occurs is still a subject of contention. Either the chloride ions convert the insoluble iron oxides to soluble ion chlorides which diffuse away and destroy the passive film or ions are absorbed on the metal surface and promote the hydration and dissolution of metal ions.

## **2.7 Corrosion initiation due to carbonation of concrete**

Carbonation is the process whereby concrete is attacked by atmospheric carbon dioxide. More specifically, carbonation is a chemical reaction between one of the main hydration products of cement in concrete, calcium hydroxide, and carbon dioxide from the atmosphere. A simplified equation for the reaction can be given as:



Essentially, carbonation begins at the outer surface of a concrete element and progresses inwards. The rate of progress of this carbonation front is affected by many factors, some of which are external to the concrete and some internal.

Although the reaction in the carbonation process is a chemical one, the rate at which this reaction takes place depends on physical factors, and the process is considered to be one

of diffusion of carbon dioxide into any concrete pores which afford a continuous passage from the external atmosphere.

In pure air, carbon dioxide makes up approximately 0.03% by volume compared with about 20.5% by volume of oxygen. Since carbonation is a diffusion controlled process, it may be assumed that the rate of carbonation will vary in direct proportion to the approximate square root of the concentration of carbon dioxide in the air.

The mechanism which relates the relative humidity in the atmosphere to the rate of carbonation is not clear. It is, however, generally accepted that at very high relative humidity, the rate of carbonation decreases significantly<sup>61</sup>. The mechanism put forward for this decrease is the blocking of pores in the concrete by water which has condensed within them. It may be thought that the dry atmosphere would allow the rapid evaporation of water produced by the carbonation reaction, thereby promoting rapid carbonation. However, this evaporation would depend on the temperature. An increase in the ambient temperature will allow the reaction rate of the carbonation process to increase and will also increase the rate of diffusion of the carbon dioxide through the concrete.

Diffusion is the process by which matter is transported from one part of a system to another as a result of random molecular motions leading to a more uniform concentration of those molecules. The diffusion of carbon dioxide into concrete depends on the diffusion properties of the concrete, i.e. the diffusivity. The diffusivity will depend on the capillary pores and continuity of such pores in the concrete. A measure of these capillary pores and their continuity can be obtained from the permeability of concrete to the gas concerned. For good quality naturally occurring aggregates, the porosity is generally reasonably low and therefore the porosity of the

concrete is more dependent on the porosity of the hardened cement paste which surrounds the aggregate particles.

An increase in the cement content in the concrete directly slows the rate of carbonation.

As was stated earlier the porosity of the hardened cement paste is the main factor that contributed to the diffusivity of the concrete and this porosity depends on the compaction of the concrete and water/cement ratio of the concrete <sup>62</sup>.

## **2.8 Bond between steel and concrete**

The development of corrosion products along the bar surface affects the ultimate strength of flexural members through a significant loss of bond between steel and concrete <sup>20, 63, 64, 65, 66, 67, 68, 69, 70</sup>. The mechanical pressure due to volume of expansion of corrosion products causes cracking along the reinforcing bar called longitudinal cracking. The crack starts from the surface of reinforcement and expands in width as it proceeds to the concrete surface. When the crack reaches the concrete surface, the width at the reinforcement has become wide enough to introduce oxygen and water to accelerate corrosion. Cracking of concrete cover and reduction of reinforcement-concrete bond due to reinforcement corrosion cause concern about the performance and serviceability of structures <sup>66</sup>.

An investigation programme on an existing structure was carried out <sup>20</sup>. The age of the reinforced concrete building was about nine years, and a considerable amount of degradation due to corrosion of steel such as cover concrete cracking and spalling along the reinforcing steel and exudation of rust juice was observed especially at the eaves. It was found that the ribbed bars did not show much change in bond strength with corrosion. It was concluded from this investigation that the most important structural

properties such as yield strength and ultimate tensile strength which are required for the reinforcing steel, remained unchanged unless cover concrete cracking due to the corrosion was found. The detrimental effects started at the stage when the concrete cover cracked. The occurrence of the cover concrete cracking accelerated very rapidly the corrosion of the reinforcing steel thereafter, and was a direct cause of the degradation of the structural and the functional properties of the reinforced concrete structure.

Furthermore, the bond strength was measured after an embedded bar was corroded electrolytically<sup>19</sup>. Cylindrical concrete specimens with ribbed bars of 9, 19, and 25 mm diameter were used. The concrete contained different amounts of calcium chloride of 0.5, 1.0 and 5.0% by weight of cement. These specimens were exposed to a direct current to simulate the corrosion on the surface of the reinforcing steel. It was clear that the bond strength increases with increase in the amount of corrosion and the bond strength of a corroded specimen becomes two to three times larger than that of an uncorroded specimen. The ratio of the bond strength decreases after the amount of corrosion reaches level at which the concrete cover cracks but most of the specimens still sustain strength ratios well above 100. It was suggested that the corrosion had a rather favourable effect on the bond strength until the amount reaches the cracking level. It was concluded that the ratio of bond strengths was high with greater cover thickness. It was also concluded that the rate of corrosion was increased in proportion to the chloride content and with decrease of bar diameter. The influence of water/cement ratio and the cover thickness was not remarkable.

Similar laboratory studies were carried out<sup>4</sup>, where the specimens used were 150 mm cube with 10, 14 and 20 mm diameter bars embedded centrally to give cover/diameter

(c/d) ratio of 7.5, 5.36 and 3.75 respectively. A constant current density of  $2 \text{ mA/cm}^2$  was used in order to simulate corrosion. The bond behaviour relative to the four stages of corrosion: non-corrosion, corrosion corresponding to pre-cracking, cracking and post-cracking levels, was studied. The bond strength in the case of pullout tests increased with the increase of corrosion up to about 1.0%. With the further increase of corrosion, the bond strength declined consistently and become negligible at, for example, 8.5% post-cracking corrosion for 10 mm bar. It was concluded that cover to diameter is a very definitive corrosion protection factor because about 4% and 1% corrosion was needed to crack the reinforced concrete members with c/d values of 7 and 3, respectively. It was finally concluded that the amount of corrosion which causes the cracking of the cover concrete was a very important measure to judge the life and soundness of reinforced concrete structures.

Furthermore, it was reported <sup>71</sup> that the bond strength went up to 1.2 times that of non-corroded control specimen when the corrosion was simulated by impressing the voltage of 3 volts versus a saturated calomel electrode. The bond strength in pullout specimens was significantly affected by the level of corrosion, while the reduction in bond strength in the case of beams was much less than that in the pullout specimens. Pullout specimens showed about 10% decrease in bond strength at the cracking stage which occurred at 2.2% corrosion. In the post-cracking stage, the bond strength was reported to be reduced to 24% of that of non-corroded control specimen at 12% corrosion. Corrosion caused a significant increase in the value of mid-span deflection of beams.

Using the same galvanostatic technique <sup>72</sup>, deterioration mechanism of concrete structures was investigated. The test specimens were reinforced concrete beams with the dimensions of 10 x 10 x 40 cm and 10 x 10 x 70 cm and the corrosion was induced

by applying a direct current of 167 mA. It was found that the bond between a bar and concrete failed as a result of corrosion and cracks were formed from the boundary of the bars and concrete. The rate of corrosion increased when these cracks reached the surface forming the longitudinal crack along the bar. After the formation of the longitudinal crack, the bond between the bar and concrete was reduced, but there was no indication of the value of the bond strength corresponding to the cracking stage. It was concluded that the effect of corrosion of reinforcing steel bars on the load carrying capacity of concrete members was quite large compared to the strength reduction of the bar itself.

Investigation on the deterioration of flexural bond in reinforced concrete structures under combined effects of exposure to marine environments under heavy sustained loads was carried out<sup>73</sup>. The reinforced concrete beams with dimensions of 76 x 152 x 914 mm were loaded to develop specific crack widths, and loadings were then maintained to simulate service condition. Corrosion was accelerated electrochemically by applying a constant current density of 5 and 10 mA/cm<sup>2</sup>. It was reported that the time of initiation of crack was three times more for the beams with 5 mA/cm<sup>2</sup> in comparison with beams with 10 mA/cm<sup>2</sup>. The reduction of the ultimate strength was only about 12% for the beams subjected to 5 mA/cm<sup>2</sup> current, while the reduction of ultimate strength was about 50% for beams with 10 mA/cm<sup>2</sup>. When the flexural cracks remain open during the entire corrosion process, there was practically no effect on corrosion rate with different crack widths.

Another study<sup>74</sup> where conversion of corrosion rate values to loss of load carrying capacity suggested that aspects such as bond, steel mechanical properties and presence

of cracks should be elucidate in order to assess the damage due to corrosion of a structure.

Further <sup>18</sup>, the appreciable reduction in load carrying capacity of concrete members on account of corrosion can not be explained by the reduction of the tensile strength of the bars alone, but cracks formed due to corrosion play an important role in changing the load carrying mechanism.

Tests on debonded beams with very long lengths of debonded tensile reinforcement showed the increased demand on the bond of the remaining short embedded lengths, resulting in the ultimate anchorage failure of the damaged beams. Large gaps between debonded tensile reinforcement and adjacent concrete have also shown to influence and subsequently reduce ultimate load capacity, even in cases where the debond length is completely confined within a constant moment region. This is due to differential deformation of the debonded steel strain at ultimate load.

A new strain compatibility criteria was used in the analysis <sup>75</sup> of damaged reinforced concrete beams with debonded tensile reinforcement, based on concrete and steel deformations along the entire length of debonded reinforcement. Reduction in ultimate load capacity of debonded beams result as a consequence to switch from under reinforced failure of the sound beams to an over reinforced failure of the damaged beam, due to the reduced debonded steel strain at ultimate load. It was described by the authors that the load capacity reduction of the damaged reinforced concrete beams depends on percentage of reinforcement, the length and position of the delamination and the moment distribution along the member.

The loss of bond strength was caused by the opening of longitudinal cracks along the reinforcement due to radial tensile stress induced at the steel–concrete interface by the

expansive products of corrosion. Bond strength of corroding reinforcement was shown to increase with increasing degree of corrosion. A maximum increase of 25% occurs at 0.4% corrosion. Beyond 0.4% degree of corrosion, bond strength decreases sharply<sup>4, 66, 71, 76, 77</sup>.

A reduction of 10 – 25% in rebar cross section has been suggested to cause serviceability failure. The value of the reduction of the cross section remains between 10% and 35% for corrosion ranging from 5% to 20%. The loss of bonding with concrete due to the formation of expansive corrosion products has been identified as the primary cause of flexural strength loss of corroding beams<sup>78, 79, 80</sup>.

The interactive corrosion cracking bond relationship tends to become all the more relevant with reinforcing bar corrosion becoming a predominant global deterioration factor in concrete structures. This sort of problem is becoming more prevalent with the use of ultimate strength design in order to utilize the full capacity of reinforcement in concrete and thus, results in structures with smaller quantities of steel.

It can be seen from the above that the limited data available on the effects of corrosion on bond strength are conflicting. The author is of the opinion that these conflicts arise from different bond test techniques and different rates of corrosion. The lateral is considered to be highly important as the available data has been obtained at different rates of corrosion varying from those which cause cracking in a few hours to long term field test.

## **2.9 Reinforced concrete beams damaged by corrosion of tensile reinforcement**

### **2.9.1 Previous experimental work**

Previous research concerned with the experimental investigation of the strength assessment and general characteristics of corrosion damaged reinforced concrete beams have dealt with the simulation of reinforcement corrosion in two distinct ways:

- Controlled corrosion of reinforcing bars by the use of electrolysis (exposing the reinforced concrete beams to chloride solution while applying direct current to the steel bars, thereby accelerating the corrosion process);
- Including the consequences of tensile steel corrosion as a feature of the manufacture of the reinforced concrete beams, leaving specific lengths of tensile reinforcing steel exposed and without cover, simulating the degradation of bond between concrete and steel and spalling concrete cover, but without loss in steel cross sectional area.

### **2.9.2 Corrosion simulation by the use of electrolysis**

A series of tests were conducted<sup>73</sup> on 14 reinforced concrete beams, using electrolysis to investigate the deterioration of flexural bond in reinforced concrete structures under combined effects of exposure to marine environment and heavy sustained load. Of the 14 rectangular beams tested, 8 of the beams were reinforced with a single 16 mm diameter steel bar continuously over the entire span; and the remaining six, were divided into three pairs reinforced with a single 16 mm diameter steel bar having 100 mm, 150 mm or 200 mm overlapping at mid-span respectively. Shear reinforcement was not provided in either of the beams. The tests involved:

- Loading reinforced concrete beams to develop specific crack widths and maintaining the loads to simulate service conditions (loading arrangements: single point load at mid-span);
- Exposing the loaded beams to sea water;
- Using electrolysis to accelerate the corrosion of reinforcements, for an 8 day period, with impressed currents of  $5 \text{ mA/cm}^2$  and  $10 \text{ mA/cm}^2$ .

For the beams designed with continuous reinforcement, a reduction in moment capacity was observed due to longitudinal cracking. The average percentage decrease in moment capacity was 12% and 50%, for the beams subjected to  $5 \text{ mA/cm}^2$  and  $10 \text{ mA/cm}^2$  impressed current respectively. Beams with  $5 \text{ mA/cm}^2$  impressed current failed in flexure with the formation of two cracks near mid-span. Beams with  $10 \text{ mA/cm}^2$  impressed current failed by shear bond with the formation of a single crack.

For the beams designed with a lapped splice, ultimate moment capacity was a function of the magnitude of tension developed at the overlap, which in turn, depends on the capacity of the ultimate bond stress. In the case of reinforcement corrosion, the ultimate bond stresses depend on the level of deterioration due to longitudinal crack. The test results of these beams, which all failed in shear bond, indicated a 32 – 36% reduction of moment capacity mainly due to the deterioration of flexural bond in the corroded specimens. This study formed <sup>73</sup> only a preliminary study into finding the strength of a structure after it is damaged by the development of corrosion cracks. Experimental results demonstrated clearly the potential problems of stray current corrosion in the reinforced concrete structures, placing emphasis on the effect of a longitudinal crack on the flexural bond strength, resulting in potential reductions in ultimate load capacity.

Further, investigation into the influence of longitudinal cracking due to reinforcement corrosion on characteristics of rectangular reinforced concrete members was reported<sup>81</sup>. Beams with spans of 140 cm, 120 cm and 100 cm (shear span/depth ratios of 3.43, 2.89 and 2.29 respectively) were tested under two point loading. Electrolysis in conjunction with spraying with chloride solution was used to induce longitudinal cracking. It was observed that in the corroded beams, the flexural cracks occurred concentrically in the pure moment span and the number of flexural cracks in the shear span was less than that of the sound beam. The yield strengths of the corroded beams with potential longitudinal cracks were scarcely reduced in comparison with sound control beams and only reduced by 4% at ultimate load. Further, a somewhat rapid reduction in strength of corroded beams was observed in comparison with the uncorroded equivalents, when subjected to reverse cyclic flexure in the post yield stage.

The development of corrosion products along the reinforcing bar surface and the associated opening of longitudinal cracks affects the failure mode and ultimate strength of flexural members through a significant loss of bond between concrete and reinforcement<sup>4</sup>. It also reiterated the fact that little has been done to evaluate the effect of bar surface changes due to corrosion, on ultimate strength of flexural members. Twelve beam specimens, designed originally to fail in flexure, with differing degrees of even spread corrosion (measured as the loss of metal relative to the original bar weight) along the length of reinforcement were tested as simply supported beams under a two point loading with a total span of 900 mm and shear spans of 300 mm. All corroded beams failed in flexure, with yielding of tensile reinforcement prior to final crushing of concrete; the same mode of failure as their non corroded counterparts. A 12% reduction in ultimate load capacity was measured for the most highly corroded beam tested,

attributed possibly to the reduction in bar cross sectional area. The stiffness of the beams was shown by the tests to reduce with the increasing corrosion intensity.

It was reported elsewhere<sup>82</sup> on the mechanical behaviour and the failure mechanisms of reinforced concrete beams damaged by corrosion of reinforcement. Experimental loading and bond tests were performed on reinforced concrete specimens damaged with an accelerated galvanostatic method, causing uniform corrosion of the whole body of tensile reinforcement. The degree of corrosion was recorded as the number of days, an electric current density of  $0.5 \text{ mA/cm}^2$  was applied to the reinforcements. No shear reinforcement was provided. Reductions in stiffness, load carrying capacity and flexural cracking were observed in the damaged reinforced concrete beams compared to the non-corroded. Changes in the properties and behaviour of the corroded reinforcing bars were confirmed by pullout tests which demonstrated the deterioration of bond strength, and by punching shear tests which verified the inadequate transmission of stresses between reinforcing steel and surrounding concrete, due to cracking in the axial direction to the bar cross sections, caused by swelling of the corrosion products which generate internal stresses, manifesting as longitudinal cracks along the side of the corroded reinforced concrete beams.

More recently, a further study<sup>83</sup> was conducted aimed at evaluating the influence of rebars corrosion on the collapse mechanism of reinforced concrete beams. Nine beams have been designed, constructed, artificially corroded and tested. Four point bending tests were performed with the loading span appropriately selected to display transfer from bending to shear failure. The obtained experimental results were compared with the analytical ones, accounting for a number of parameters potentially affected by corrosion such as, besides the steel diameter, the stress and elongation of longitudinal

and transverse reinforcement, cover delamination, etc. The good agreement with similar specimens reported in the technical literature pointed out by the comparisons allows validating the analytical procedure.

The studies in Table 2.1 show the various methods and degrees of corrosion stimulation of tensile reinforcement adopted by researchers in their investigation of the behaviour of the corrosion damaged reinforced concrete beams.

Table 2.1 Summary of experimental tests on corroded beams<sup>83</sup>

Authors	b (cm)	h (cm)	L (cm)	tensile bars	corrosion (loss %)*	capacity (loss %)
Umoto et al. <sup>84</sup>	100	200	2100	2Ø16	2 <sub>w</sub>	17
Tachibana et al. <sup>82</sup>	150	200	2000	2Ø16	5 <sub>w</sub>	–
Cabrera et al. <sup>71</sup>	125	160	1000	2Ø12	9 <sub>a</sub>	20
Rodriguez et al. <sup>85</sup>	150	200	2300	2Ø10	14 <sub>d</sub>	33
Rodriguez et al. <sup>85</sup>	150	200	2300	4Ø12	10 <sub>d</sub>	25
Mangat et al. <sup>86</sup>	100	150	910	2Ø10	10 <sub>d</sub>	25
Castel et al. <sup>79</sup>	150	280	3000	2Ø12	10 <sub>a</sub>	20

\* <sub>w</sub> = weight loss, <sub>a</sub> = bar area loss, <sub>d</sub> = bar diameter loss

Bond properties in each of the studies are therefore subject to considerable scatter and subsequently, constructive quantitative conclusions cannot be made. However, the studies are unified in their description of the behavioural characteristics of corrosion damaged beams as compared to their fully bonded equivalents, comprising: possibility of reduction in ultimate load capacity, reduction in flexural stiffness and reduction in flexural cracking, with fewer but wider cracks.

However, in order to enable practical quantitative conclusions to be made concerning strength assessment of corrosion damaged beams, a unified approach needs to be adopted for the corrosion process and period. In addition, the remaining bond strengths of corroded reinforcement need to be determined and associated with the possible reductions in load capacity. Unfortunately, at present, non destructive techniques for the calculation of the extent of the degradation of bond and cross sectional area are not available. In some cases <sup>75</sup>, it has already been suggested that the engineer would be wise to assume the complete loss of bonding and subsequent shear stress transfer between steel and concrete.

### **2.9.3 Model of steel corrosion**

Investigations on the structural effects of loss of cover to the main steel of 7 reinforced concrete beams was carried out <sup>87</sup>. In addition, a control, fully bonded beam was also tested. The simulation of spalling of concrete cover to main bars was conducted by casting beams with the bars half embedded and others in which “the bars barely contacted the concrete”, implying as fully exposed. All beams were cast in an upside down position, either pouring fresh concrete just below the level of main tensile bars or to the level of the bar centres. The length of the half or “more or less fully” exposed bars (three 16 mm bars of high yield, deformed steel) extended over the whole of a clear span, but were fully covered for a length of approximately 200 mm beyond each support (anchorage length). Static loading tests were conducted on the 3.0 m long beams (cross sectional dimensions 150 x 300 mm with 30 mm cover to main steel, if present), simply supported on spans of approximately 2.7 m and subjected to concentrated load at mid-span. Compression and shear reinforcement of 6 mm high yield steel were also provided. The loss of structural performance, in case of beams with half embedded

main steel was very slight, failing in the same flexural tension mode (tensile yielding of the main reinforcement prior to the crushing of the concrete at mid-span) as the control beam full length and depth of cover concrete, with similar stiffness and crack patterns. Of the remaining four beams with no cover to tensile steel, only one failed in flexural compression mode, surprisingly, with no loss of load carrying capacity. Although the authors report that no apparent yielding of the tensile reinforcement was detected prior to concrete compression failure in this beam, the fact that the beam suffered no loss in load capacity indicates that yielding must have been imminent. The remaining 3 damaged beams were reported to have collapsed as a result of anchorage failure, with reductions in strength ranging from 12% to 44%, reduced stiffness and much reduced flexural cracking. The authors failed to draw quantitative conclusions due to insufficient data available and more importantly, due to considerable scatter of the reinforcement bond properties of the damaged test beams. However, they made the following statements concerning the effects of a reduction of bond along tensile reinforcement in damaged reinforced concrete beams as compared to normal fully bonded equivalent: the number of cracks formed is limited partly because the force transferred to the concrete between early cracks is insufficient to produce new cracks between them and partly due to the increased depth of compression zone at sections toward the support (tied arch behaviour); the formation of shear cracks is inhibited as the teeth of concrete between flexural cracks are subjected to reduced bond forces; the increased main steel forces and the loss of tension suffered by the concrete cause increased deflection; the greater elongation also reduced the depth of the compression zone at the section of maximum moment; the reduced bond leads to an increase in the main steel force to be anchored at supports or beyond section of zero moment. The benefit of reduced or total absent of shear cracks along shear spans was recognised in

special cases of inadequate provision of shear reinforcement. More importantly, the effects of reduced concrete compression depth at the section of maximum moment and the increased demand on reinforcement bond along the anchorage lengths were highlighted for their tendency to reduce ultimate strength of the damaged members by producing premature flexural compression or anchorage failures. A test programme<sup>88</sup> was carried out at The Queen's University of Belfast with the aim of developing a more comprehensive explanation of the relationship between ultimate capacity and anchorage length.

Further, research investigated the effectiveness of different repair materials<sup>6, 89</sup> and surface preparation with simulated faults caused by corrosion of main steel. In the cases where debonded tensile reinforcement are in contact with adjacent concrete, the effectiveness of any debond length within a region of constant moment is negligible, since strains in the steel and adjacent concrete at any section within the constant moment region are identical, as in the case of an undamaged, fully bonded beams. Thus, such damaged beams suffer from reduction in load capacity. Therefore, the position and length of debond relative to the loading pattern and the presence of any gap between debonded tensile reinforcement and the adjacent concrete are therefore important parameters which require consideration in the strength assessment of debonded beams.

## **2.10 Previous theoretical work**

A fairly simple theory is presented which provides means of predicting certain characteristics of simply supported reinforced concrete beams that experience two point loading with their main reinforcement fully exposed in a symmetrical fashion about the

mid-span<sup>90</sup>. Such an analysis is relevant when, in the course of the patch repair process, the concrete cover and steel-concrete bond are removed prior to application of the patch repair materials. Encouraging correlations have been found between the theoretical predictions and some previously reported large scale test data for ultimate loads of reinforced concrete beams. The final numerical results throw some light on the perhaps initially puzzling experimental observation previously reported that the ultimate loads of beams with exposed main reinforcement can increase significantly if nominal top steel (in the form of, for example 2 x 6 mm diameter bars), such as is invariably used for holding stirrups in place, is used. Representative results provided identified the relative influence of changes in various design parameters such as concrete cube strength, depth of removal of concrete, and the length of exposed main reinforcement on the flexural strength of reinforced concrete beams with fully exposed main reinforcement over part of their span.

### **2.11 Reinforced concrete beams damaged by corrosion of shear reinforcement**

The shear stress at failure is far from being constant even in the case of the same concrete, cross section, and reinforcement<sup>91</sup>. The transformation of a reinforced concrete beam into a tied arch may occur suddenly or may develop gradually<sup>92</sup>. The transformation of the reinforced concrete beam into a tied arch certainly weakens the comb-like structure. However, this does not mean that the remaining arch collapses immediately when the loading exceeds the capacity of the concrete. Because the strength of the concrete is lowest in tension, the cracks are always normal to the direction of principal tensile stresses. Good bond creates closely spaced cracks, while poor or non-existent bond results in only a few cracks or no cracks at all in the part

where shear force exists. Enhanced bond means lower diagonal load carrying capacity<sup>93</sup>.

There is a possibility that members with corroded shear reinforcement will not achieve their full flexural capacity due to premature shear failure. Corrosion can reduce the shear load carrying capacity earlier and, sometimes, at a faster rate than it reduces the flexural load carrying capacity. In real structures, shear links have lower cover than flexural reinforcement and will start to corrode first. It has been reported elsewhere<sup>5</sup> that the effects of corrosion on the shear strength are not straightforward, but nevertheless, this will be investigated in the current study.

There is a relationship between corrosion and bond deterioration. It has been confirmed that the presence of uncorroded stirrups have a significant influence on the residual bond strength of main steel when it is subjected to high corrosion levels<sup>21</sup>. However, the research<sup>21</sup> did not determine the bond strength of the main steel when the shear reinforcement was also subjected to corrosion, hence this will be investigated in the current investigation.

## **2.12 Conclusion**

From the review of literature concerning the laboratory and field testing of corroded reinforced concrete beams, quantitative conclusions have not been possible due to the extent of scatter in the bond properties of the damaged beams. However, the tests have clearly shown the effect of tensile reinforcement bond degradation on the behaviour of reinforced concrete beams, resulting in:

- possible reduction in load capacity;

- reduction in flexural stiffness;
- reduction in flexural cracking, with fewer but wider cracks.

As reviewed in the above, very little work has been done to evaluate the effect of reinforcement steel corrosion on the strength of flexural members. The literature is found to be contradictory on some points. Confusion arises about the influence of thickness of concrete cover on the rate of corrosion.

### ***Optimisation of the Corrosion Process***

#### **3.1 Introduction**

A short programme of preliminary tests was devised and conducted to validate the accelerated corrosion method in the laboratory and to determine the actual percentage of corrosion on the steel reinforcement.

Preliminary design and testing was conducted on reinforced concrete beams with main reinforcement of high yield steel, top hanger bars made of mild steel and stirrups made of stainless steel as described in Section 3.5 of this chapter.

After necessary modifications and adjustments, final tests on corroded and control reinforced concrete beams were subsequently performed (Chapters 5 to 7).

#### **3.2 Accelerated corrosion**

##### **3.2.1 Introduction**

In order for the corrosion process to take place, there must be differences in potential; anodic and cathodic surface zones of the steel must be connected electrically and electrolytically, i.e. a flow of electrons and ions between them must be possible. The electrolytic connection is represented by the concrete. Anodic dissolution of iron must be possible due to depassivation of the steel surface, sufficient oxygen must be available at the cathode resulting from continuous diffusion of oxygen from the surface of the

concrete to the steel surface acting as the cathode. The measurement of the potential between the anodes, or the reinforcement, and the noble cathode gives further information on the onset of corrosion.

### 3.2.2 Laboratory simulation

After the curing process, the beam specimens were immersed in artificial seawater in a plastic tank. A 3.5%  $\text{CaCl}_2$  solution (see Chapter 4) was used as the electrolyte. The direction of the current was arranged so that the reinforcing steel served as the anode while a copper plate counter electrode was positioned in the tank to act as a cathode. The schematic drawing of the arrangement is shown in Figure 3.1.

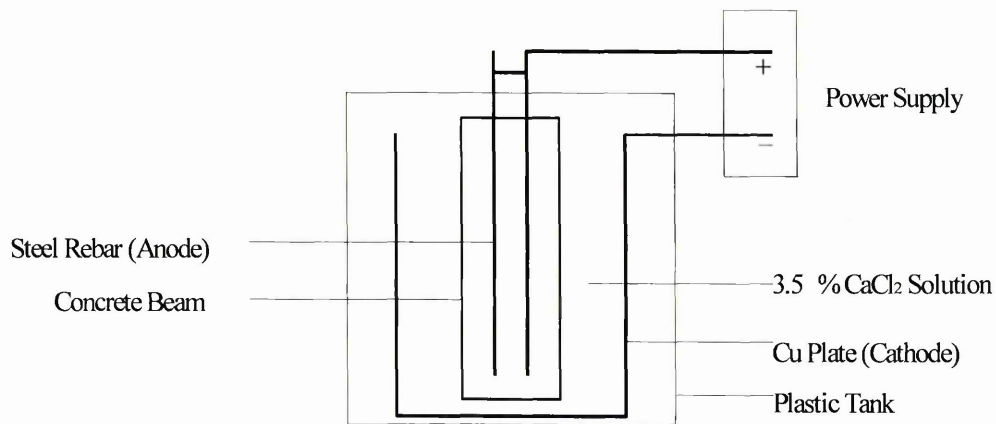


Figure 3.1 Accelerated corrosion apparatus

A constant current density of  $1 \text{ mA/cm}^2$  was passed over the reinforcement surface and the total impressed current was adjusted for each specimen to maintain this current density for bars of different diameters. The current density of  $1 \text{ mA/cm}^2$  was adopted on the basis of pilot tests to provide desired levels of corrosion in a reasonable time.

The current supplied to each specimen was checked on a daily basis and any drift was corrected.

The relationship between corrosion current density and the weight of metal lost due to corrosion was determined by applying Faraday's Law (Equation 3.1):

$$\Delta\omega = \frac{A \times I \times t}{Z \times F} \quad \text{Equation 3.1}$$

where:

$\Delta\omega$  = weight loss due to corrosion in (g),

$A$  = atomic weight of iron (56 g),

$I$  = electrical current in (A),

$t$  = time in (sec.),

$Z$  = valence of iron which is 2,

$F$  = Faraday's constant (96 500 coulombs).

The metal weight loss due to corrosion can also be expressed as:

$$\Delta\omega = a \times \delta \times \gamma \quad \text{Equation 3.2}$$

where:

$a$  = rebar surface area before corrosion ( $\text{cm}^2$ ),

$\delta$  = material loss (cm),

$\gamma$  = density of material ( $7.86 \text{ g/cm}^3$ ).

The corrosion current can be expressed as:

$$I = (i) \times (a) \quad \text{Equation 3.3}$$

where:

$i$  = corrosion current density ( $\text{Amp/cm}^2$ ).

Therefore, combining Equations 3.1, 3.2 and 3.3 gives:

$$a \times \delta \times \gamma = \frac{A \times I \times t}{Z \times F} = \frac{A \times i \times a \times t}{Z \times F} \quad \text{Equation 3.4}$$

Substituting known values into Equation 3.4. gives:

$$\delta = \frac{A \times i \times t}{\gamma \times Z \times F} = \frac{56 \times i \times 365 \times 24 \times 60 \times 60}{7.86 \times 2 \times 96500} = 1165 \times i \quad (\text{cm/year})$$

$$\text{Equation 3.5}$$

Rewriting Equation 3.5, where  $R$  is defined as the material loss per year (cm/year), gives:

$$R = 1165 \times i \text{ (cm/year)} \quad \text{Equation 3.6}$$

As an example, for a corrosion rate,  $i$ , of 1 (mA/cm<sup>2</sup>),  $R$ , equals 1.165 (cm/year) (from equation 3.6).

If, in a reinforced concrete structure, the period of corrosion after initiation is  $T$  years, then

$$\text{Metal loss after } T \text{ years} = R \times T \text{ (cm)} \quad \text{Equation 3.7}$$

Therefore

$$\% \text{ reduction in rebar diameter in } T \text{ years} = \frac{2 \times R \times T}{D} \times 100 \quad \text{Equation 3.8}$$

The expression  $[2 \times R \times (T/D)]\%$ , which represents reduction in rebar diameter due to corrosion over  $T$  years, is also defined as the degree of reinforcement corrosion.

The corrosion rate adopted in these investigations was 1 (mA/cm<sup>2</sup>). The target degree of corrosion,  $[2 \times R \times (T/D)]\%$ , ranged between 0% (control) and 20% in increments of 5%.

### 3.3 Methods of accelerated corrosion

When the specimen is subsequently immersed in CaCl<sub>2</sub> solution, the chloride ions will penetrate the mortar very rapidly together with the water as it is drawn in by capillary suction. The unhydrated cement can then begin to react and will be affected by the presence of the Cl<sup>-</sup> ions which will have a greater chance of being chemically bound than if they penetrated fully hardened cement paste and may also have an accelerating effect on the hydration. The longer the period of moist curing, the slower will be the penetration of chlorides, but the degree of chemical binding can also be expected to be lower. The initiation time for corrosion increases approximately linearly with an increasing period of moist curing. On the other hand, any increase in chemical binding is not reflected in higher critical chloride concentration for corrosion and, in fact, the tendency is the opposite.

There are several methods available to study the accelerated corrosion of steel reinforcement in the laboratory. The galvanostatic method was used in this study to simulate the field conditions. The method involves passing a direct current through the reinforcement to accelerate corrosion. The galvanostatic corrosion is carried out whilst the beam is unloaded, which is quite different from the corrosion in actual structures. The corrosion by galvanostatic method is general, whereas actual structures have some specific areas that are more prone to corrosion. Thus in the latter case, there is always the possibility of pitting corrosion whereas the cross sectional area of the reinforcing

bars could be significantly reduced, thereby reducing the tensile strength of the reinforcing bars. However, to ensure consistency of results in this investigation, the steel reinforcement was subjected to general corrosion only, which allows easier repeatability compared to pitting corrosion.

According to standard corrosion theory, steel embedded in concrete is largely in a protected state because of the alkalinity of the matrix. The corrosion rate depends on the ratio of the cathodic area to the anodic area<sup>94, 95, 96, 97</sup>. In this investigation, the potential was measured every day to ensure that the steel was corroding. The potential cannot be measured directly, as the available measuring devices can measure only a difference in potential. To overcome this limitation, a Saturated Calomel Electrode (SCE) was added to the system by means of a suitable salt bridge. The potential of the SCE is (by arbitrary definition) zero. The potential for the concrete beams in this study ranged between  $-340$  mV and  $-300$  mV which represents the active state (see Table 3.1).

Table 3.1 Active and passive condition of steel rebar

E (mV vs SCE)	Condition of rebars
$> -220$	Passive
Between $-220$ and $-270$	Active or Passive
$< -270$	Active

where E is the rebar potential (mV),

SCE is Saturated Calomel Electrode (reference electrode).

### 3.4 Validation of accelerated corrosion method

Preliminary tests were carried out before commencing the formal research programme to confirm the reliability of the accelerated corrosion technique.

The aim of this was to determine the actual percentage reductions in reinforcing bar diameter and compare these with the calculated percentage reductions. The degree of corrosion (as a percentage of reduction in reinforcing bar diameter) is defined by the expression  $2RT/D$  percent, where R is the rate of corrosion in mm/year, D is the reinforcing bar diameter in mm, and T is the time in years after corrosion initiation (see Section 3.2.2).

#### 3.4.1 Corrosion of reinforcing bars in saline solution

Figure 3.2 show reinforcement bars undergoing accelerated corrosion using specialist equipment in the laboratory in order to verify the corrosion model. In this situation, the bars were anodic and therefore corroded while the copper plate was cathodic. Electrolyte was a 3.5%  $\text{CaCl}_2$  solution. Since there was no protective layer, there was no initiation time, i.e. corrosion occurred immediately after the current flow.

The degree of corrosion was measured both as gravimetric weight loss and reduction in the diameter of the reinforcing bars. With regards to the gravimetric weight loss method, the steel reinforcement was weighted before the specimens were corroded. A predefined corrosion rate was applied to the reinforcing bars over a specified period of time. Upon completion of the corrosion period, the reinforcing bars were removed from the solution, cleaned with a wire brush and re-weighted. The percentage loss in weight was subsequently calculated.

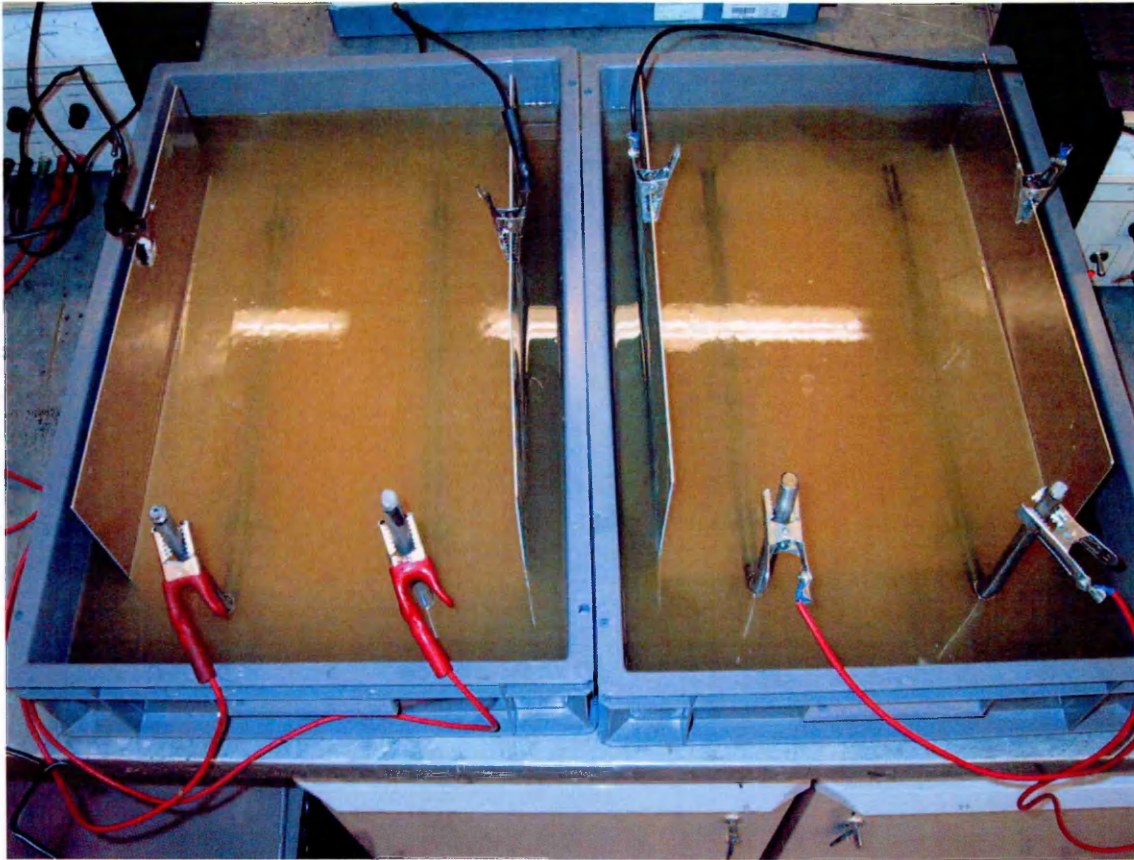


Figure 3.2 Reinforcement bars under corrosion

The second method to determine the percentage corrosion was similarly performed, except that the average rebar diameter both before and after corrosion was measured and the loss was determined from a reduction in the diameter.

Referring to Table 3.2, four degrees of corrosion were investigated at this stage, i.e., 1.0, 1.5 (twice), 5.0 (twice) and 10.0 percent reduction in bar diameter (see column 1, Table 3.2). The length of reinforcing bar was varied between 350 mm and 650 mm (column 2, Table 3.2). Two reference methods were chosen to monitor the accelerated corrosion process. Method I involved measuring the reduction in reinforcing bar diameter.

Table 3.2 Reduction in reinforcing bar diameter

Degree of corrosion	Method I Reduction in bar diameter						Method II Gravimetric weight loss					
	L (mm)	D (mm)	D' (mm)	$\delta$ (mm)	$\delta t$ (mm)	% difference	W (g)	W' (g)	$\omega$ (g)	$\omega t$ (g)	% difference	
(1)	(2)	(3)	(4)	(5)	(6)	(7)	(8)	(9)	(10)	(11)	(12)	
1.0%	350.5	12.09	11.93	0.16	0.12	33%	314.53	306.33	16.40	12.73	28.83%	
1.5%	400.0	12.01	11.74	0.27	0.18	50%	358.63	347.65	21.96	21.35	2.86%	
1.5%	400.0	12.00	11.73	0.27	0.18	50%	356.88	345.83	22.10	21.33	3.61%	
5.0%	650.0	12.09	11.39	0.70	0.62	12.90%	584.33	533.03	102.60	118.44	13.37%	
5.0%	598.0	12.04	11.14	0.90	1.22	26.23%	534.40	480.60	107.60	108.59	0.91%	
10.0%	400.2	12.06	9.82	2.24	1.22	83.61%	359.95	284.70	150.50	144.15	4.41%	
						AV=42.6%						AV=9%

Key:

- (1) target degree of corrosion,
- (2) measured length of reinforcing bar (mm),
- (3) measured diameter of reinforcing bar before corrosion (mm),
- (4) measured diameter of reinforcing bar after corrosion (mm),
- (5) actual material loss (mm),
- (6) theoretical material loss (mm),
- (7) percent error in diameter reduction,
- (8) measured weight of reinforcing bar before corrosion (g),
- (9) measured weight of reinforcing bar after corrosion (g),
- (10) measured weight loss of reinforcing bar (g),
- (11) calculated weight loss of reinforcing bar (g),
- (12) percent error in weight loss.

Hence, the diameter of the reinforcing bar was measured before corrosion acceleration at 10 locations along the bar and the average diameter was calculated (column 3, Table 3.2). After the accelerated corrosion period, the bars were removed from the concrete and cleaned with a wire brush and the diameter was re-measured as before and the average diameter was determined (column 4, Table 3.2). The actual loss in bar diameter is given in column 5. Column 6, Table 3.2 shows the theoretical loss in diameter as calculated in Section 3.2.2. Column 7 in Method I (Table 3.2) shows the percentage difference between the measured and actual loss in diameter for the reinforcing bars.

Method II (Table 3.2) takes into account the gravimetric weight loss in the bar after corrosion. The weight of reinforcing bar was measured before acceleration of corrosion (column 8, Table 3.2), whereas the weight of the bar after corrosion is recorded in column 9. The actual metal weight loss due to corrosion is given in column 10. The theoretical metal weight loss, as calculated in Section 3.2.2 is given in column 11. The difference between actual weight loss in the reinforcing bar and the theoretical weight loss is given as a percentage in column 12.

The results showed that Method I (reduction in bar diameter) is not a reliable method, as shown by the significant error ( $A_v=42.6\%$ , column 7) between the calculated reduction in the reinforcing bar diameters and the measured reduction in reinforcing bar diameters at the end of the corrosion inducing period.

This is due to the fact that it is difficult to measure accurately the diameter of the reinforcing bars both before, and especially after, the corrosion period. Also, the diameter of the steel bars is not perfectly circular hence this exaggerates the error even more. Furthermore, the presence of ribs also makes it difficult to measure the diameter

accurately. Method II (Gravimetric weight loss) is a reliable method since the error is substantially less ( $A_v=9\%$ , column 12, table 3.2) between the theoretical weight loss and the measured weight loss after the corrosion inducing period (although the percentage difference for the 1% test is higher at 28.83%). Therefore, in this research, the gravimetric weight loss method was employed as a means of monitoring the actual loss in the reinforcing bar diameters.

### **3.4.2 Corrosion of reinforcing bars in concrete**

Further, in order to model the corrosion process in reinforcement bars in concrete, small specimens were cast prior to the preliminary test in order to verify the model and to establish the necessary time to break the protective passive layer. Figure 3.3 show reinforced concrete specimens undergoing accelerated corrosion using specialised equipment in the laboratory.

The aim of this investigation was to establish the additional time to the onset of corrosion. The time required to induce a specified loss in bar diameter was calculated from Equation 3.8. It was estimated that the additional time required to establish the onset of corrosion was between four to ten days. Therefore, once the time required for corrosion to occur had elapsed, an additional four days was initially added to the duration. The steel was then broken out for examination and re-weighed. This process was repeated with an additional day for the onset of corrosion being added to the duration. It was established from this trial and error method that an additional seven days was required for the onset of corrosion to occur.

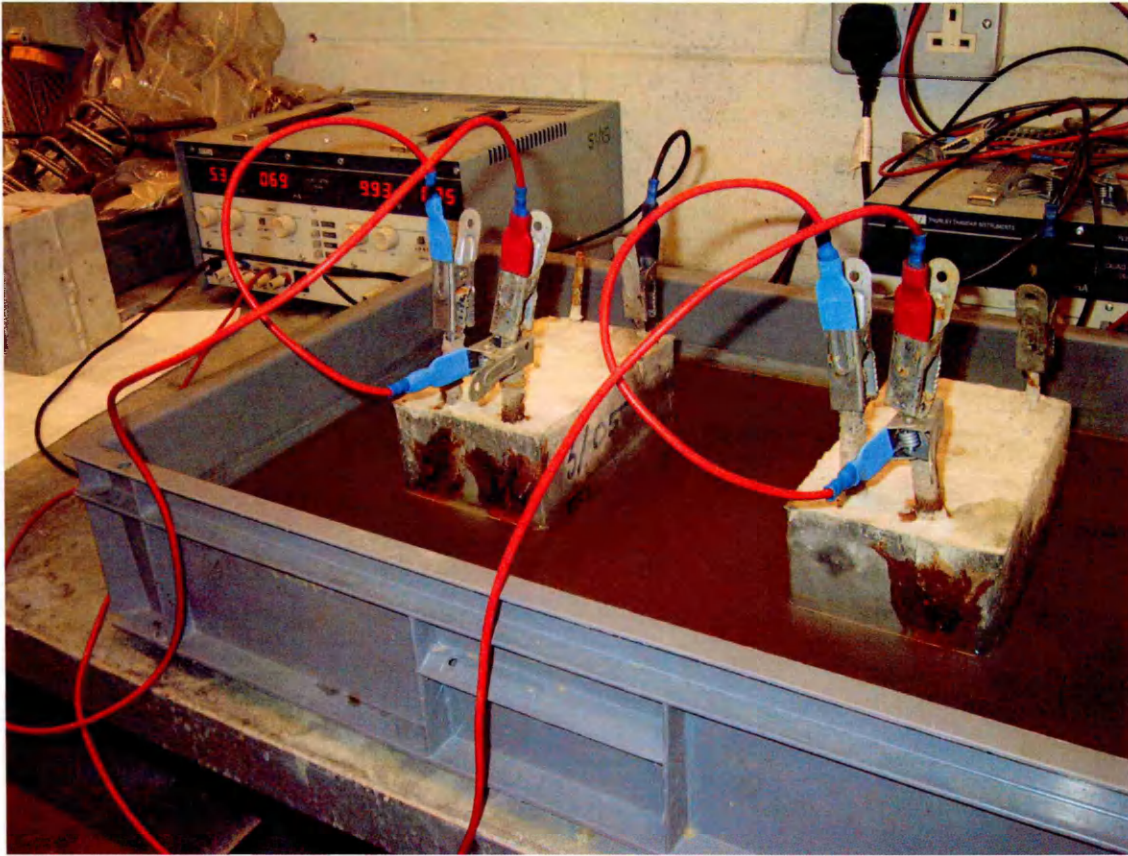


Figure 3.3 Corrosion of the reinforcement in small concrete prisms

### 3.5 Design of test beams using stainless steel

A combination of stainless and carbon steel was used to study the behaviour of corroded reinforced concrete beams. The aim was to employ stainless steel<sup>98</sup> as reinforcement where the steel was to remain uncorroded. Carbon steel was used where the reinforcement was subjected to the accelerated corrosion technique.

#### 3.5.1 Preliminary beams details

Preliminary investigations were conducted on beam specimens following the completion of the trials described in Sections 3.4.1 and 3.4.2. The Construction

Materials laboratory at Sheffield Hallam University was used to cast and test the beams. Reinforced concrete beams of 500 mm length with a cross section of 100 mm deep and 100 mm wide were used. Beams were cast using standard cast iron prism moulds. Preliminary Series I was used to determine the influence of corrosion on the main steel only and therefore, determine if the procedure is successful. A concrete mix was designed to give 28 day cube strength of 50 N/mm<sup>2</sup> and a slump 30 – 60 mm. After casting, the samples were kept for 24 hrs at 20°C in 95% ± 5% relative humidity (RH) before demolding. The specimens were then stored at 20°C in 100% RH (water tank) for an additional 27 days and, thereafter, in the laboratory atmosphere at approximately 50% RH for the duration of corrosion acceleration.

### **3.5.2 Preliminary Series I**

Preliminary Series I was used to study the effect of main steel corrosion on the flexural strength of the beam. The main steel was subjected to different degrees of accelerated corrosion whereas the shear reinforcement (stainless steel) was to remain free from corrosion. The stainless steel used was type 304 (18–8) austenitic steel. A detailed X-Ray analysis was performed by the Materials & Engineering Research Institute at Sheffield Hallam University, to determine the chromium and nickel content.

In total, 10 beam specimens, measuring 100 x 100 mm in cross section and 500 mm in length were cast and tested in Preliminary Series I<sup>99</sup> (see Figure 3.4 and Table 3.3). Beam specimens were cast from a 0.44 water/cement ratio concrete having an average tested compressive strength of 68 MPa. Beams were reinforced with either 2T8 (4 specimens), 2T10 (4 specimens) or 2T12 (2 specimens) main steel in the tensile zone and 8 mm stainless steel<sup>100, 101</sup> shear reinforcement at 50 mm or 55 mm centres

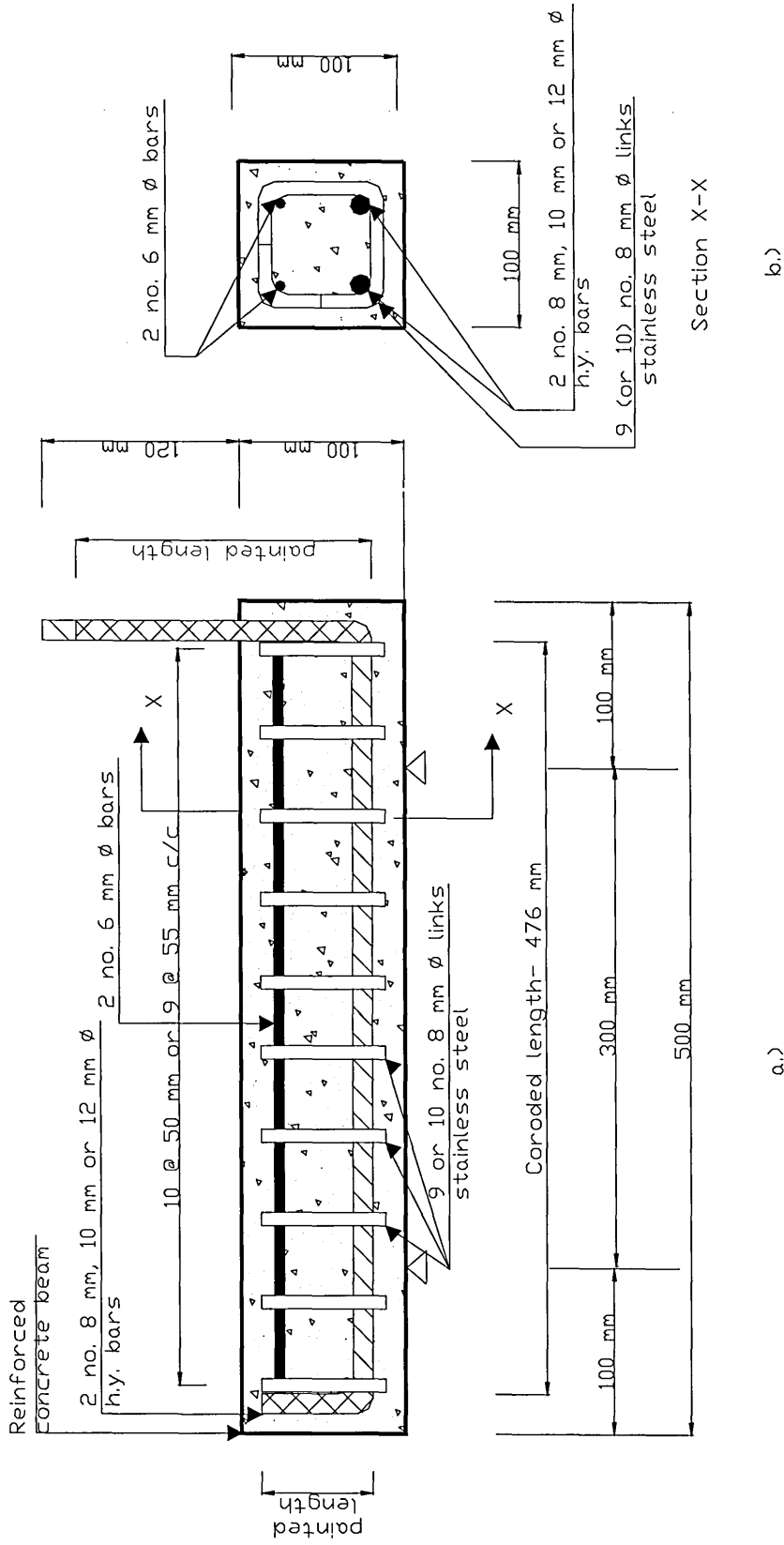


Figure 3.4 Preliminary Series I: a.) elevation; b.) cross section X-X

Table 3.3 Preliminary test programme

		Number of Preliminary Specimens		
		Preliminary Series I		
		Shear Reinforcement: 8 mm Stainless Steel (Uncorroded)		
		Main Reinforcement: 8, 10, 12 mm High Yield Steel (Corroded)		
		8 mm	10 mm	12 mm
Target % Corrosion	0 %	2	2	2
	5 %	2	2	—
Totals		4	4	2
		10		

(see Figure 3.4). The target corrosion was either 0% (control) or 5%. Two 6 mm plain mild steel hanger bars were used in the compression zone to support the shear reinforcement.

Corrosion to the main steel reinforcement was induced through a galvanostatic electrolyte corrosion technique (see Figure 3.5) as described in Section 3.3.

This ensured that the diameter of the main steel was reduced by up to 5% (Table 3.3).

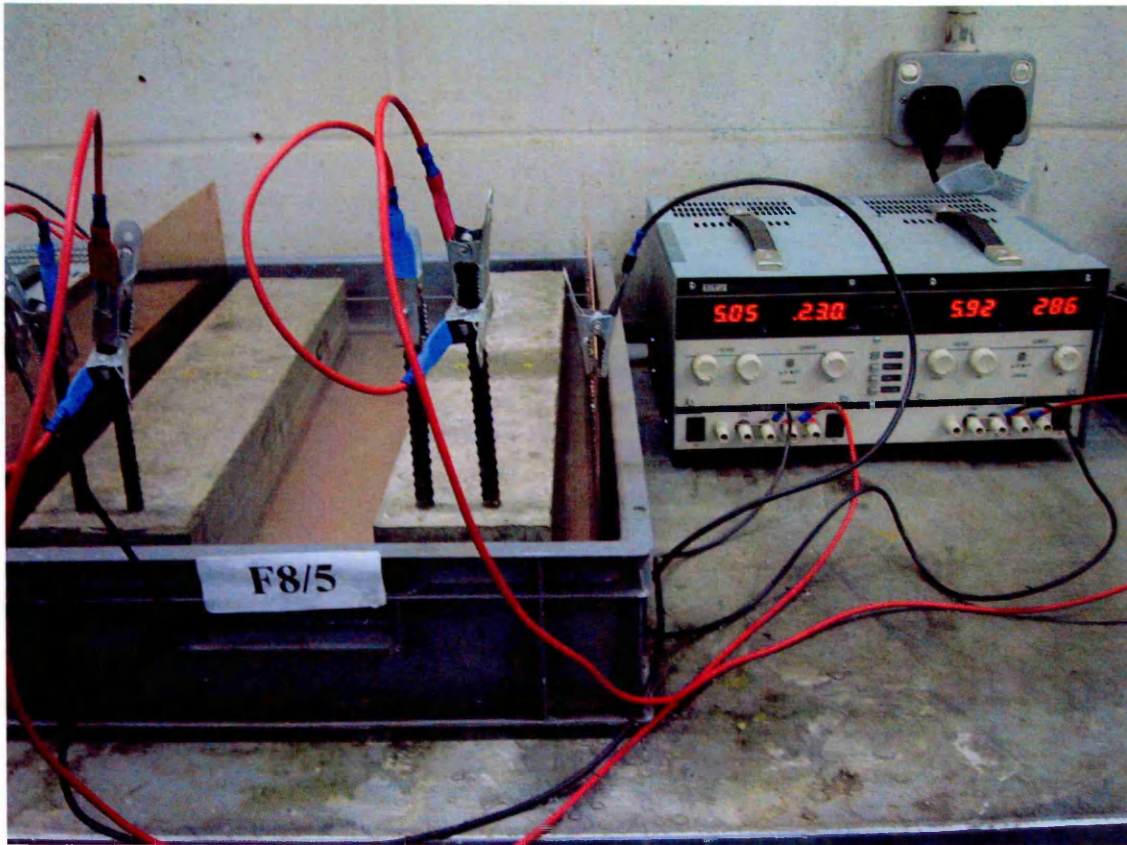


Figure 3.5 Accelerated corrosion of reinforcing steel in the laboratory

When the circuit is completed between two electrodes, the main bars behave as anodic and dissolve while the external copper plate behave as cathodic and is subject to plating out. The process was monitored on a daily basis to ensure that there was no short circuit. When the cell is short circuited, both electrodes have the same potential and there will be an associated limiting corrosion current. The relative areas of main bars and copper plate were carefully chosen. The principle that the large cathode to anode area ratio can be disastrous, while a small cathode to anode area ratio of a potentially damaging couple can, at times, be tolerated.

Chapter 3  
Optimisation of the Corrosion Process

After applying a predetermined amount of current to the beams to cause corrosion, the structural behaviour was examined by loading to failure. The specimens were tested as simply supported beams under four point bending with a total span of 500 mm and shear span of 100 mm as shown in Figure 3.6 and Figure 3.7. The loading rate of the testing machine was 12 kN/min.

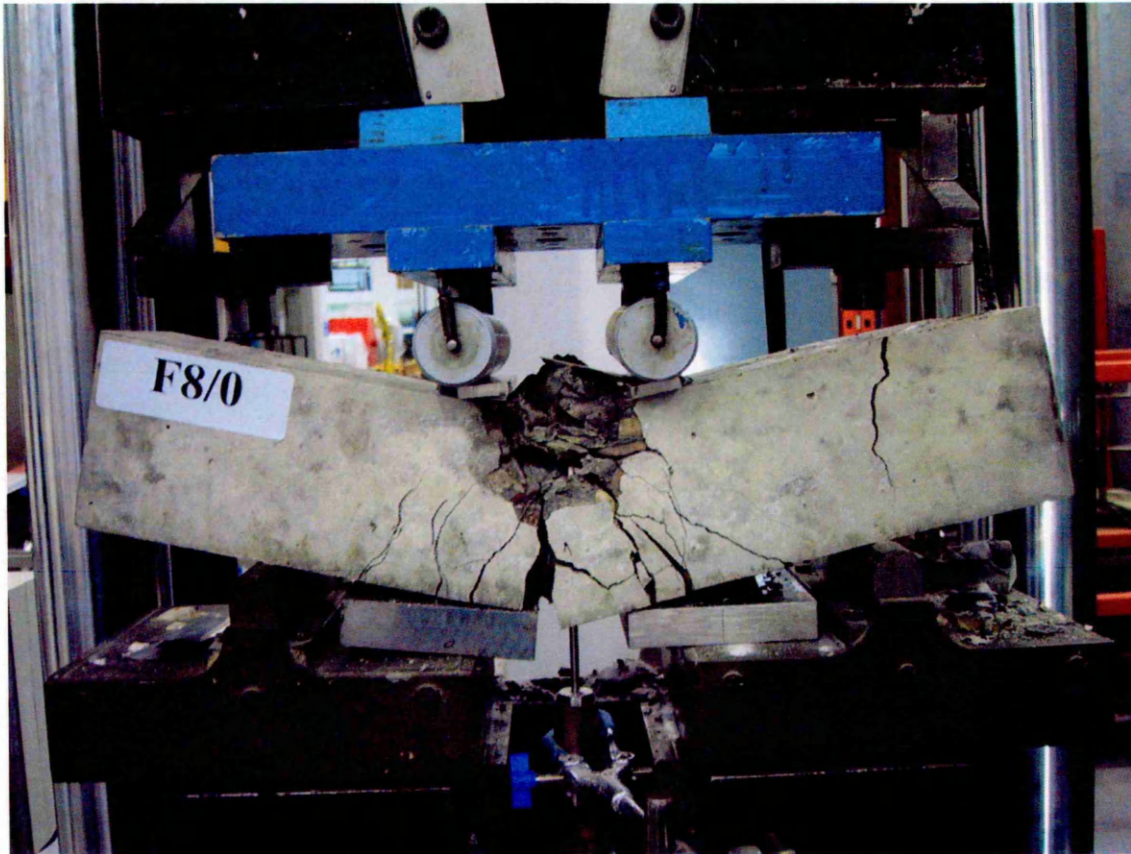


Figure 3.6 Preliminary beam under test

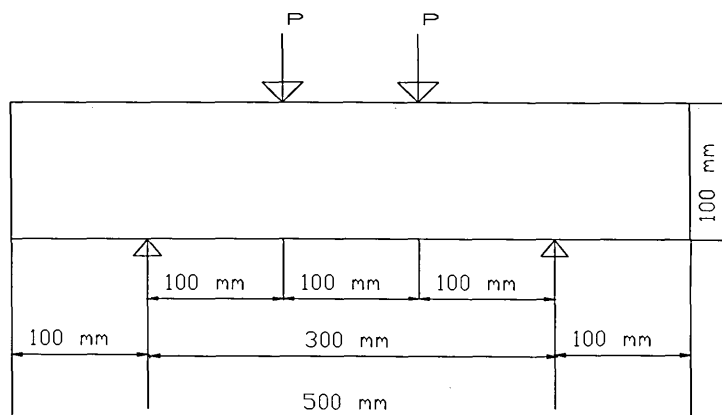


Figure 3.7 Schematic drawing for preliminary beam test

### 3.5.3 Performance of preliminary Series I

One degree of corrosion (5%) was applied (column 1, Table 3.4) to two different beam types (column 2, Table 3.4) and the resulting performance was compared with the control specimens not exposed to any corrosion. The designation used in column 2 of Table 3.4 fully identifies each beam. The first part gives the number, type and diameter of main reinforcement (2T8, 2T10 or 2T12) followed by the target degree of corrosion in percentage. The second part represents the number of shear reinforcement and diameter, percentage corrosion (in this case 0%) and cover in mm, e.g. 9D8/0/20.

Two specimens were cast of each beam type (column 3, Table 3.4). A corrosion rate of  $1 \text{ mA/cm}^2$  was applied to the corroded specimens (column 4). The corrosion duration in hours, which is the time taken to complete the corrosion of the reinforcement to the desired degree, is given in column 5.

Table 3.4 Experimental program for preliminary beam Series I

Degree of corrosion %	Beam number	No. of specimens	Corrosion Rate (mA/cm <sup>2</sup> )	Corrosion duration* (hrs)
(1)	(2)	(3)	(4)	(5)
0% (Control)	2T8/0+9D8/0/20	2	–	–
	2T10/0+9D8/0/20	2	–	–
	2T12/0+10D8/0/20	2	–	–
5%	2T8/5+9D8/0/20	2	1	318.4
	2T10/5+9D8/0/20	2	1	356.0

\* includes initiation time

At 28 days after casting, the beams with 0% corrosion (control) were tested under four point bending to determine their load – deflection curves and their ultimate flexural strength. The corroded specimens were tested at 42 days and 45 days for 2T8 and 2T10 respectively, in order to achieve the desire level of corrosion. Average load – deflection relationships for the beam specimens were obtained by averaging the results of two specimens tested.

### 3.6 Discussions of the preliminary results

Ten reinforced concrete beams were designed, constructed, artificially corroded and tested. The beams were of the same geometry, however, the tensile rebars diameter and the corrosion level <sup>84, 85</sup> were varied. As the intention was corrosion on main reinforcement only, the specimens were designed with main reinforcement made of high yield carbon steel and stirrups made from stainless steel which remained uncorroded.

After the test were performed the steel bars were taken out for examination. This was done by removing the concrete manually where extra care was taken so no mechanical damage was done to the steel and the cage was then re-assembled. It was evident that since the connection between the main bars and the stirrups was not protected, the current was spread between the anode (main deformed bars) and the rest of the reinforcement cage at a degree which could not be determined experimentally. Corrosion percentage in the shear reinforcement could not be calculated from mass losses as it could be misleading when deterioration was highly localized, (i.e. heavy pitting corrosion). The weight loss for the main bars was determined as degree of corrosion. Due to the pitting corrosion, an insignificant portion of the current went through the main steel, therefore, the target corrosion was not achieved. Figure 3.8 shows the severe pitting that occurred at the stainless steel shear reinforcement.

Since the aim of this work was to corrode only the main reinforcement, this method of using stainless steel shear reinforcement was discarded for the main series of beams due to susceptibility to pitting corrosion of the stainless steel.

### **3.7 Further experimental work**

Further to the results in the previous section, it was decided that the cathodic area is to be reduced and the connection between main reinforcement and stirrups improved, so that the current is passed only through the main reinforcement and therefore, leaving the shear reinforcement in a protected state.

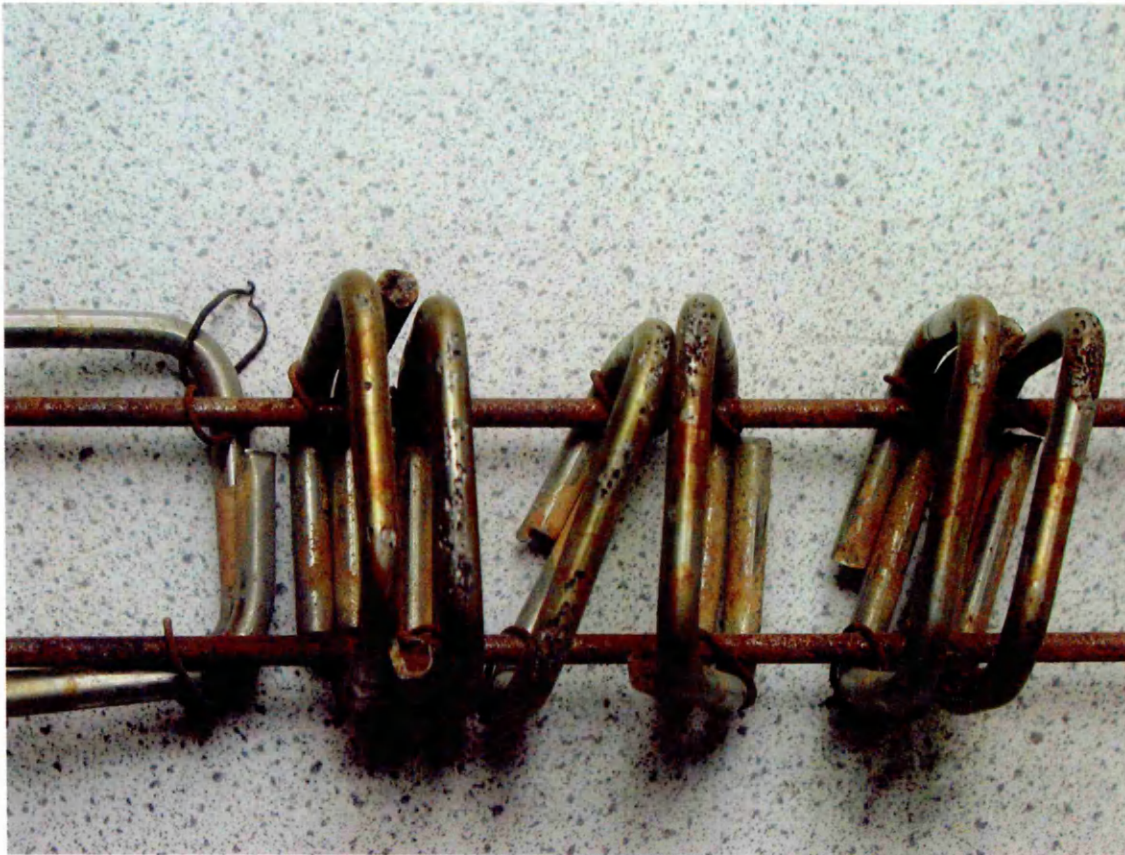


Figure 3.8 Stainless steel stirrups exhibiting pitting corrosion

### 3.7.1 Method I

Investigations were done using epoxy paint. The paint was used at the points of contact between the main and shear reinforcement. Two beams were cast and cured as described in Section 3.5.1. Corrosion was accelerated as before and the main reinforcement was broken out and examined. However, this method was disregarded as the paint was not sufficient to provide the desired protection. The shear reinforcement was corroded at a rate which was not possible to establish.

### 3.7.2 Method II

A Sika Latex, which is a modified styrene butadiene emulsion, was also tried as a means of protecting the shear reinforcement from corrosion. It was applied at the points of contact as described in Section 3.7.1 (Method 1). Due to its polymeric action, mortars containing Sika Latex have superior adhesion, good compressive strengths and considerably improved flexural and tensile strengths. In addition, Sika Latex mortar has greatly reduced water permeability, improved resistance to chemicals and to abrasion; are non-toxic and non-corrosive. Before application, it was ensured that the surface was sound, clean and free from oils. All loose material was removed using a mechanical abrasion. The following composition was used: Sika Latex one part, water one part, cement one part, washed fine sand one part. Further two beams were cast, corroded and tested to verify this model. After the steel bars were removed from the concrete and visually examined, it was evident that it did not provide sufficient protection when high constant current was passed. Therefore, Sika Latex was also disregarded from the experiments.

### 3.7.3 Method III

A sealed electrical connection was provided by heat sealable shrinkage plastic tubing (with an integrally bonded adhesive inner lining, designed to provide a permanent encapsulation for protection against moisture). Shrink wrap was applied at the points of contact between the main bars and the shear reinforcement as well as the bent-up portion of the main reinforcement. Manufactured from an irradiated polyolefin material, the sleeving has a specially formulated adhesive inner wall which melts when heated and is forced into steel interstices by the shrinking action of the outer wall. When cooled, the sleeving becomes a semi-flexible, tough homogenous encapsulate

with a controlled wall thickness. The sleeving will shrink to 33% of its supplied diameter when heated above 125°C. It contains high mechanical and electrical strength and resistance to water. Also, when used as a cap, it ensures that the steel ends are waterproof and permit long term storage without risk of moisture penetration. It is a medium wall moulded cap internally coated with an adhesive sealant. Installation is simple, the cap is centred over the end of the steel and on application of heat the cap shrinks to form a reliable seal.

A further two beams were cast, cured, corroded and tested in a similar manner to those described in Section 3.5.1. When current was applied, the circuit was completed between the two electrodes, the main bars behaved as an anode and dissolved whilst the cage behaved as a cathode and was subject to plating out. This method was verified by examining the steel after testing as described previously. In this instance, the main bars corroded to the desired levels, whereas the shear reinforcement remained protected and uncorroded.

### **3.8 Concluding remarks**

Based on the preliminary investigations described in this chapter, the final test beams for the main programme were designed using only carbon steel with the use of shrink wrap at the points of contact between the main and shear reinforcement. The time to the onset of corrosion was also established. Full details of the main test beams are given in Chapters 5, 6 and 7.

### ***Detailed Experimental Programme***

#### **4.1 Introduction**

Reinforced concrete structures that are properly designed generally exhibit excellent durability throughout their lifetime. However, there are numerous examples where problems have occurred due to the corrosion of the steel reinforcement in the structures due to poor design and workmanship, in addition to exposure to aggressive environments such as motorway bridges, car parks and marine structures. These structures have required premature and costly repair, remediation or even replacement.

The aim of this research, therefore was to determine the residual strength of corroded reinforced concrete beams when both the main and shear reinforcement is subjected to varying degrees of corrosion.

#### **4.2 Objectives of investigation**

The principle objectives of the experimental work were to:

- 1) investigate the influence of concrete cover in corrosion damaged reinforced concrete beams;
- 2) study the influence of various degrees of main reinforcement corrosion on the structural performance of reinforced concrete beams;

- 3) study the influence of various degrees of shear reinforcement corrosion on the structural performance of reinforced concrete beams;
- 4) study the effect of both main and shear reinforcement corrosion on the structural performance of corroded reinforced concrete beams;
- 5) develop analytical models to predict the residual strength of corrosion damaged beams.

### **4.3 Details of experimental programme**

The Construction Materials laboratory at Sheffield Hallam University was used to carry out the investigations. Three series of beam were tested to fulfil the objectives of the project. Series I determined the influence of corrosion on the main steel only (74 beams were tested, Table 4.1), Series II investigated the influence of corrosion on the shear reinforcement only (8 beams, Table 4.1), whereas Series III investigated the performance of reinforced concrete beams which exhibited both main and shear reinforcement corrosion (34 beams, Table 4.1). A total of 116 beams (Table 4.1) were tested.

Under reinforced concrete beams of 910 mm length with a cross section of 150 mm deep and 100 mm wide were used in the investigation. Beams were cast using standard cast iron prism moulds. Each beam was reinforced with two high yield steel bars of either 8 mm, 10 mm or 12 mm diameter. Shear reinforcement consisted of 6 mm diameter mild steel stirrups. The stirrups were supported by 6 mm diameter mild steel hanger bars in the compression zone.

Table 4.1 Experimental Programme

Series I			Series II			Series III			
Main Reinforcement: 8, 10, 12 mm High Yield Steel (Corroded)			Main Reinforcement: 12 mm High Yield Steel (Uncorroded)			Main Steel Reinforcement: 8 mm High Yield Steel (Corroded)			
Shear Reinforcement: 6 mm Mild Steel (Uncorroded)			Shear Reinforcement: 6 mm Mild Steel (Corroded)			Shear Reinforcement: 6 mm Mild Steel (Corroded)			
Main Steel Diameter	8 mm	10 mm	12 mm	Cover to Links = 50 mm	Cover to Links = 50 mm	Cover to Links = 50 mm	% of Links Corrosion		
Cover to Main Steel	26 mm	36 mm	56 mm				0 %	5 %	10 %
% of Main Bars Corrosion	0 %	2	2	8	7	2	2	2	
	5 %	4	4	4	2	4	2	2	
	10 %	2	2	2	2	2	2	2	
	15 %	2	2	2	2	2	2	2	
Total	10	10	10	14	14	8	8	8	
	30			36			8		
	74			8			34		
Total	116			116			116		

The concrete mix design, in accordance with British Cement Association (BCA) methods is given in the standard form in Table 4.2. The concrete mix proportions by weight were 1 : 1.49 : 2.88 (cement, fine aggregates, coarse aggregates). The water/cement ratio was 0.44.

Fine and coarse aggregates were oven dried at 100°C for 24 hours to eliminate the free water content and then maintained dry prior to their use (normally three days after drying). Di-hydrate Calcium Chloride ( $\text{CaCl}_2$ ) was added to the mix (3% by weight of cement, adopted from a previous research) in order to promote corrosion of the steel reinforcement. The aggregates and cement were dry mixed in a mechanical mixer for one minute. The water was then added gradually. As  $\text{CaCl}_2$  was used it was necessary for it to be dissolved in the mixing water prior to pouring into the mixer. This wet mix was then stirred for a further 2.5 minutes. In order to incorporate any dry material a further hand stirring of the wet mix was necessary. The mix was then placed in steel moulds in three layers, each layer being carefully compacted on a vibrating table. The specimens were then placed in the mist curing room (20°C and 95%  $\pm$  5% RH)<sup>102</sup> for 24 hours. The samples were demolded after 1 day and cured in water at 20°C for a further 27 days (28 days in total) and, thereafter, under laboratory conditions (approximately 50%  $\pm$  5% RH, 20°C) whilst awaiting exposure to the accelerated corrosion technique.

Two specimens were prepared and tested for each investigation. The transfer of samples from 100% RH to the laboratory atmosphere results in a drying out of the mortar. Thus, the samples were stored at 100% RH for one day prior being subjected to accelerated corrosion.

Table 4.2 Concrete mix design form

Table 1 Concrete mix design form

Job title: *Research Experimental Programme*

Stage	Item	Reference or calculation				
1	1.1 Characteristic strength	Specified	{ $\frac{50}{\text{Proportion defective}}$	N/mm <sup>2</sup> at $\frac{28}{\text{days}}$		
	1.2 Standard deviation	Fig 3		N/mm <sup>2</sup> or no data	-	
	1.3 Margin	C1 or Specified	(k = - )	x - = -	N/mm <sup>2</sup>	
	1.4 Target mean strength	C2	- + - = -		N/mm <sup>2</sup>	
	1.5 Cement type	Specified	<i>OPC/SRPC/RHPC</i>			
	1.6 Aggregate type: coarse		<i>Crushed / uncrushed</i>			
	1.6 Aggregate type: fine		<i>Crushed / uncrushed</i>			
	1.7 Free-water / cement ratio	Table 2, Fig 4	$\frac{0.44}{\text{Specified}}$	}		
1.8 <i>Maximum free-water / cement ratio</i>	Specified	$\frac{0.45}{\text{Use the lower value}}$			<b>0.44</b>	
2	2.1 Slump or Vebe time	Specified	Slump $\frac{30-60}{\text{mm or Vebe time}}$		$\frac{3-6}{\text{s}}$	
	2.2 Maximum aggregate size	Specified	$\frac{20-5 \text{ mm graded}}{\text{mm}}$		$\frac{20}{\text{mm}}$	
	2.3 Free-water content	Table 3			<b>180 kg/m<sup>3</sup></b>	
3	3.1 Cement content	C3	$\frac{180}{\text{Specified}}$ / $\frac{0.44}{\text{Specified}}$	=	$\frac{409.1}{\text{kg/m}^3}$	
	3.2 <i>Maximum cement content</i>	Specified	-		kg/m <sup>3</sup>	
	3.3 <i>Minimum cement content</i>	Specified	$\frac{400}{\text{use 3.1 if } \leq 3.2}$		kg/m <sup>3</sup>	
			$\frac{400}{\text{use 3.3 if } > 3.1}$		<b>409.1 kg/m<sup>3</sup></b>	
3.4 Modified free-water/cement ratio					<b>0.44</b>	
4	4.1 Relative density of aggregate (SSD)		$\frac{2.60}{\text{known/assumed}}$			
	4.2 Concrete density	Fig 5		=	$\frac{2376.9}{\text{kg/m}^3}$	
	4.3 Total aggregate content	C4	$\frac{2377.9}{\text{kg/m}^3}$ - $\frac{409.1}{\text{kg/m}^3}$ - $\frac{180}{\text{kg/m}^3}$	=	$\frac{1787.8}{\text{kg/m}^3}$	
5			Percentage passing 600 µm sieve			
	5.1 Grading of fine aggregate			$\frac{70}{\text{}}\%$		
	5.2 Proportion of fine aggregate	Fig 6	$\frac{34}{\text{}}\%$			
	5.3 Fine aggregate content	C5	{ $\frac{1788}{\text{}} \times \frac{0.34}{\text{}}$	=	$\frac{607.9}{\text{kg/m}^3}$	
	5.4 Coarse aggregate content		$\frac{1788}{\text{}} - \frac{607.9}{\text{}}$	=	$\frac{1179.9}{\text{kg/m}^3}$	

Quantities	Cement	Water	Fine aggregate	Coarse aggregate (kg)		
	(kg)	(kg or L)	(kg)	10mm	20mm	40mm
per m <sup>3</sup> (to nearest 5 kg)	410	180	605	-	1180	-
per trial mix of 5x10 <sup>-3</sup> m <sup>3</sup>	2	0.9	3	-	5.9	-

Items in italics are optional limiting values that may be specified (see Section 7)

1 N/mm<sup>2</sup> = 1 MN/m<sup>2</sup> = 1 Mpa (see footnote to Section 3).

For each mix, six cube specimens (100 mm × 100 mm × 100 mm) were cast and tested in compression at 28 days in accordance with BS 1881: Part 116: 1983. Each mix represents the average of the three cubes tested at the age of 28 days and the average of the three cubes tested on the day of the beam test.

## **4.4 Materials**

### **4.4.1 Cement**

Portland cement was supplied by Castle Cement Ltd., Stamford, Lincolnshire.

The chemical composition of the cement, tested in accordance with BS 12<sup>103</sup> by Castle Cement Ltd. is given in Table 4.3.

### **4.4.2 Aggregates**

The aggregates used in the investigation were supplied by Tarmac Roadstone Ltd., Nottingham. Coarse aggregates consisted of 20 – 5 mm graded quartzite whereas the fine aggregate consisted of medium grade sand. Grading curves of the aggregates are given in Figures 4.1 and 4.2. These were determined in accordance with BS 882<sup>104</sup>.

The density of fully compacted concrete is depending upon free water content and relative density of the combined aggregate in saturated surface condition (SSC)<sup>105</sup>. When no information is available an approximation can be made by assuming a value of 2.6 for uncrushed aggregates. Also the water absorption is relatively low and therefore was not taken into account.

Table 4.3 Chemical composition of Portland cement by Castle Cement Ltd.

<i>Compound</i>	<i>%</i>
CaO	64.92
SiO <sub>2</sub>	21.07
Al <sub>2</sub> O <sub>3</sub>	5.05
Fe <sub>2</sub> O <sub>3</sub>	3.03
SO <sub>3</sub>	2.85
MgO	1.09
K <sub>2</sub> O	0.76
Na <sub>2</sub> O	0.14
Cl	0.02
Loss on ignition	0.60
Non detected	0.47
	<b>Total 100.00</b>
 <i>Cement compounds</i>	
Tricalcium Silicate (C <sub>3</sub> S)	54.40
Dicalcium Silicate (C <sub>2</sub> S)	20.10
Tetracalcium Aluminoferrite (C <sub>4</sub> AF)	6.20
Tricalcium Aluminate (C <sub>3</sub> A)	9.80

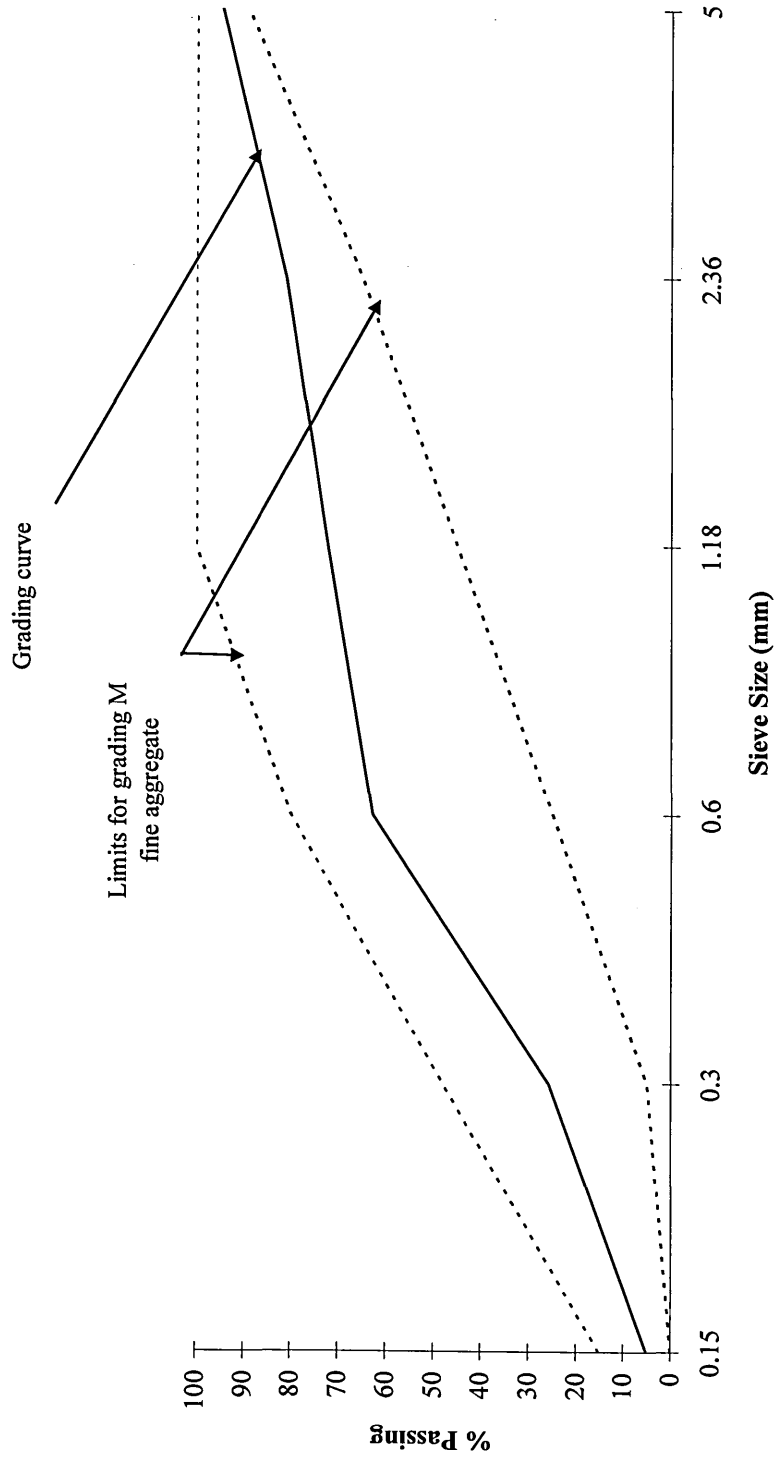


Figure 4.1 Grading curve for fine aggregate

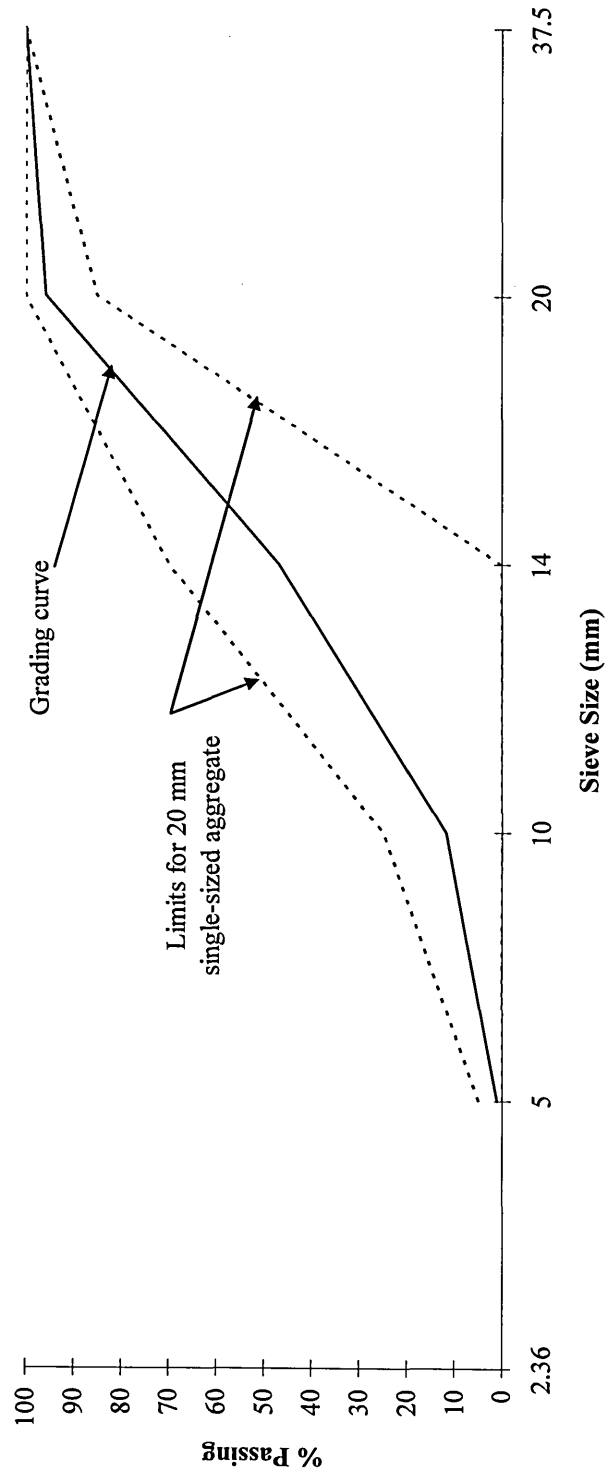


Figure 4.2 Grading curve for coarse aggregate

#### 4.4.3 Di – hydrate Calcium chloride

Portland cement concrete normally provides both a very good chemical and physical protection to all embedded steel. The chemical protection is primarily provided by the high alkaline nature of the pore water (pH 13.0 – 13.5), where the steel becomes electrochemically passivated. In addition, a physical protection is provided by the concrete, either by retarding or preventing the penetration of aggressive species like chlorides or carbon dioxide to the steel–concrete interface.

When chlorides penetrate concrete, some of it is bound either in the form of Friedel's salt ( $3\text{CaO} \cdot \text{Al}_2\text{O}_3 \cdot \text{CaCl}_2 \cdot 10\text{H}_2\text{O}$ ) or physically adsorbed to the amorphous calcium silicate hydrates (CSH). Thus, it is only the remaining free chlorides that represent a risk depassivation and corrosion of the steel.

For accelerated corrosion testing on embedded steel in concrete, chlorides are often added to the fresh concrete mixture. In addition to breaking down the passive film on embedded steel, the level of chloride content in concrete also influences the electrical resistivity of the concrete and, hence, the kinetics of the reinforcement corrosion, as long as the corrosion process is under resistance control. While there is a general agreement in the literature that the binding of chlorides in concrete is higher when  $\text{CaCl}_2$  is added to the fresh concrete, in comparison with  $\text{NaCl}$ , the effect of different chloride sources on the concrete resistivity is not well known. Friedel's salt is formed from calcium aluminate hydrate and a soluble chloride source after:  $\text{CaCl}_2(\text{aq}) + 3\text{CaO} \cdot \text{Al}_2\text{O}_3 \cdot 6\text{H}_2\text{O}(\text{s}) + 4\text{H}_2\text{O} \rightarrow 3\text{CaO} \cdot \text{Al}_2\text{O}_3 \cdot \text{CaCl}_2 \cdot 10\text{H}_2\text{O}(\text{s})$ .

The addition of sodium chloride to the fresh concrete will increase the pH, and this effect is well documented in the literature. It is also well documented that an increased

alkalinity will activate the cement hydration and will give a more dense paste structure with smaller pores compared with that of non-activated cements.

In order to lessen the electrical resistance of concrete and to control the rate of corrosion, 3% calcium chloride by weight of cement was chosen in all the series of tests. As reported in the literature when  $\text{CaCl}_2$  was added to the fresh mortar, the amount of dissolved hydroxyl ions or pH level was reduced. The acid capacity for  $\text{Ca}(\text{OH})_2$  or amount of  $\text{Ca}(\text{OH})_2$  was decreased and the acid capacity for CSH and/or Friedel's Salt was increased<sup>106</sup>.

Calcium chloride used in the investigation was in flake form supplied by J. Preston Ltd., Sheffield, England.

#### **4.4.4 Steel reinforcement**

Deformed high yield steel bars of grade 460 with 8, 10 and 12 mm diameter were used as main reinforcement in the experimental investigation described in Chapters 5, 6 and 7. Hanger bars and stirrups were standard 6 mm mild steel bars, grade 250. The steel was supplied by Derim Steels Ltd., Chesterfield, Derbyshire.

#### **4.5 Potential inspection technique for steel in concrete**

The accelerated corrosion technique was tested by making an electrical connection between the voltmeter and the exposed steel reinforcement (Figure 4.3). A flat surface was filed on the reinforcing bar and the electrical cable was attached to the steel reinforcement with self tapping screws, making sure that an electrical circuit was formed between the voltmeter and steel reinforcement (tested with a DC resistivity

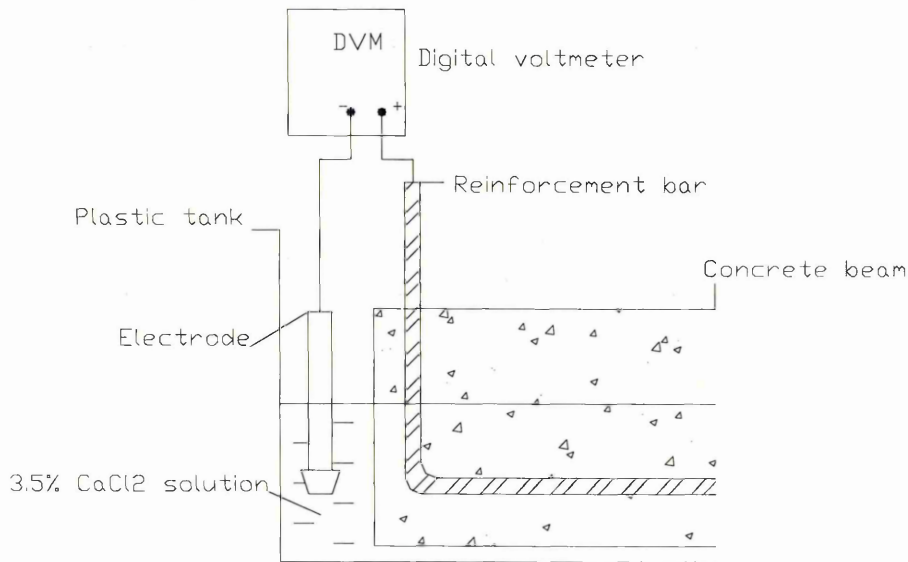


Figure 4.3 Monitoring of the accelerating corrosion technique

meter between two points on the reinforcement cage). Measurements were made in both a forward and reverse direction (i.e. with the connections reversed). A resistance of less than  $1\Omega$  indicated that the steel circuit is continuous. Connecting the reference electrode to the negative terminal of the voltmeter and the reinforcing steel to the positive terminal gives a potential indication and therefore indicates that accelerated corrosion is possible.

#### 4.5.1 Reference electrode

The reference electrode was a Saturated Mercury / Mercury Chloride (Calomel) Electrode (see Figure 4.4). The reference electrode was calibrated against another



Figure 4.4 Standard Calomel reference electrode

saturated calomel electrode to ensure that a stable reading of potential difference is obtained before use. The test verified that the potential difference was not greater than 20 mV.

#### 4.5.2 Digital voltmeter (ISO-TECH IDM97/97RMS)

The digital voltmeter (DVM) used in the investigation (see Figure 4.5) has high input impedance so that current flowing through the reference electrode does not cause disturbance or affect its potential. The voltmeter has a resolution  $\pm 1$  V, although values



Figure 4.5 Digital voltmeter

can be recorded to the nearest 5 V. The potential drop along the cable from the reinforcing steel to the voltmeter was less than 0.1 mV when measured between two previously calibrated reference electrodes.

### 4.5.3 Power supply

To accelerate the corrosion process, direct current was impressed on the steel bars embedded in beam specimens using an integrated system incorporating power supply

with a built in ammeter to monitor the current (PL 330 QMD), and a potentiometer to control the current intensity.

## **4.6 Instrumentation**

The following section describes the use of instrumentation implemented during experimental testing of the beams, to measure the magnitude of applied load and deflection.

The electrical measuring instruments were switched on an hour prior to testing to attain a true balance.

### **4.6.1 Load measurement**

Load measurements were taken by 3000 kN load cell connected to amplifier with low pass filter which in turn connected to a load cell power supply and digital balancing and monitoring unit. The amplifier was calibrated to ensure a direct reading of the applied load on the digital monitoring unit, with an accuracy of 0.1 kN.

### **4.6.2 Deflection measurement**

Deflections were measured at mid-span for all beams via data loggers with an accuracy of 0.01 mm.

### *Influence of Main Steel Corrosion on Structural Performance (Series I)*

#### **5.1 Introduction**

Reinforced concrete is widely used in construction due to its versatility and durability when properly designed and placed. In general, the environment provided by concrete protects the reinforcing steel. This is due to the high pH environment present in Portland cement pore solution which passivates the steel<sup>10</sup>. Corrosion of the steel reinforcement will not occur unless an external agent changes the normal passive state of the steel in this alkaline environment. When this occurs, corrosion becomes a subject of technical and scientific interest as well as of economic interest. It was reported that over £550 million is spent annually in the UK on refurbishment as the tendency is to repair a structure to increase its design life rather than demolish and replace<sup>107</sup>.

The expansive products of reinforcement corrosion cause cracking, rust staining and spalling of the cover zone which can lead to serviceability failure of structures during their design life<sup>78</sup>. Additionally, corrosion results in a loss of reinforcement cross sectional area and bond, and therefore, a loss in load carrying capacity of the structural element. A survey of bridge stock in the UK revealed that 75% is contaminated with chlorides which in time will cause reinforcement corrosion<sup>108,109</sup>. In such cases, repair is necessary to increase the service life of the member<sup>6,110</sup>.

## **5.2 Objectives of test programme**

The literature review carried out suggested that there is insufficient information available to enable a realistic assessment of deteriorated structural elements in concrete bridges. In many instances, data is available in the literature, but it is either conflicting or in a form which is not readily usable in assessment. There is a particular need for systematic analysis of the various ways of investigating corrosion to determine which methods realistically predict the process of corrosion in real structures.

It is recognised that the corrosion of steel in reinforced concrete can cause serious loss of structural performance. In particular, loss of bond between the steel and concrete can cause catastrophic failure. The series of beam tests described in this chapter were devised to determine the flexural strength of reinforced concrete beams in which the bond between the reinforcement and the concrete was impaired as a result of corrosion to the reinforcement. The test programme was designed to provide information on the influence of corrosion on the structural performance of deteriorated beams. Therefore, the aim of this series of tests is to establish the residual strength of under reinforced beams exhibiting main reinforcement corrosion.

## **5.3 Experimental programme**

### **5.3.1 General**

The mechanism of corrosion of steel in concrete is well documented in the literature and the factors which contribute to the initiation and subsequent rate of corrosion are well understood. Similarly, procedures for detection and repair of corroded structures are well established. However, the structural effects of corrosion have not received the

same degree of attention and there is very little guidance available to bridge assessors to enable the load capacity of deteriorated structures to be determined. Where serious deterioration is present, the methods of incorporating the resulting structural effects, such as use of estimated section loss or the application of condition factors, are very crude. It is to be expected that, in general, a deteriorated bridge will not be allowed to remain in poor condition indefinitely. It is, however, necessary to be able to take account of deterioration in strength calculations in order to assess the immediate need for traffic restrictions or temporary strengthening.

Previous research reported in the literature suggests that loss in strength due to general corrosion can be estimated by allowing for a loss of cross section of the steel reinforcement<sup>76, 86</sup>. However, for the reinforced concrete to behave as a composite member, adequate bond between the concrete and reinforcement must be maintained. The presence of steel corrosion can be detrimental to this bond as well as the possible disruption of the concrete surrounding the bar arising from the expansiveness of the corrosion products. The loss of bond can reduce the effectiveness of the member in both flexure and shear. The general conclusion of the literature review is that, while small amounts of corrosion can have a beneficial effect, the eventual cracking of the concrete cover can have a significant detrimental effect on the bond and can, in extreme cases, lead to catastrophic failure.

For deformed bars, the main component of the bond is the interlock between the deformations and the surrounding concrete. When cover is low and where no transverse steel is present, failure occurs by splitting of the concrete and the bond strength depends on the tensile strength of the concrete. Where splitting of the concrete is prevented, either by adequate cover or the provision of transverse steel, the concrete between the

Chapter 5  
*Influence of Main Steel Corrosion on Structural Performance (Series 1)*

ribs shears from the surrounding concrete. In this case, the bond strength is a function of the strength of the concrete in direct shear. This pullout type of failure occurs for plain bars irrespective of cover as it is loss of adhesion bond which leads to failure <sup>111, 112, 113, 114, 115</sup>.

The effects of corrosion on the bond between the steel and concrete has been examined by various authors using widely different techniques, ranging from the mechanical blocking out of concrete to simulate loss of cover and/or bond, to the use of impressed current as well as the addition of salt to the mix water of concrete. In most cases, the experimental tests were pullout tests, where a length of reinforcement was imbedded in concrete and measurements made of the tensile force required to pull the bar from the concrete. A limited number of beam tests have been carried out, mostly with mechanical simulation of loss of cover and/or bond <sup>116, 117, 118</sup>.

The structural consequences are very dependent on the cover provided to the concrete. It should be noted that the degree of cracking and spalling associated with loss of bond may be sufficient to render the structure unserviceable before strength is seriously affected. Knowledge of residual strengths would still be required, however, in order to decide on immediate action, e.g., weight restrictions, as well as future maintenance strategy <sup>119, 120, 121</sup>.

In this investigation, the main steel in reinforced concrete beams was subjected to an accelerated corrosion technique in the laboratory using one of the several methods available. The galvanostatic method was used in this study to simulate the field conditions. The method involves passing a direct current through the reinforcement to accelerate corrosion. The galvanostatic corrosion is carried out whilst the beam is unloaded, which is different from the corrosion in actual structures. The corrosion by

galvanostatic method is general, whereas actual structures have some specific areas that are more prone to corrosion. Thus, in the latter case, there is always the possibility of pitting corrosion whereby the cross sectional area of the reinforcing bars could be significantly reduced, thus reducing the tensile strength of the reinforcing bars. However, to ensure consistency of results in this investigation, the steel reinforcement was subjected to general corrosion only, which allows easier repeatability compared to pitting corrosion.

According to standard corrosion theory, steel embedded in concrete is largely in a protected state because of the alkalinity of the matrix. The corrosion rate depends on the ratio of the cathodic area to the anodic area. In this investigation, the potential was measured every day to ensure that the steel was corroding. The potential cannot be measured directly, as the available measuring devices can measure only a difference in potential. To overcome this limitation, a Saturated Calomel Electrode (SCE) was added to the system by means of a suitable salt bridge. The potential for the steel reinforcement in this study ranged between  $-750$  mV and  $-500$  mV which represent the active state of corrosion process.

### **5.3.2 Beam specimens**

A total of seventy four reinforced concrete beams were tested to examine the influence of main steel diameter and reinforcement cover on the flexural behaviour of deteriorated beams. Details of test specimens are given in Figure 5.1. Beams were 910 mm long with a cross section of 100 mm wide and 150 mm deep. All specimens were detailed for flexural failure; sufficient shear reinforcement were provided to ensure adequate shear capacity at the anticipated maximum load of the corroded beam. Each beam was

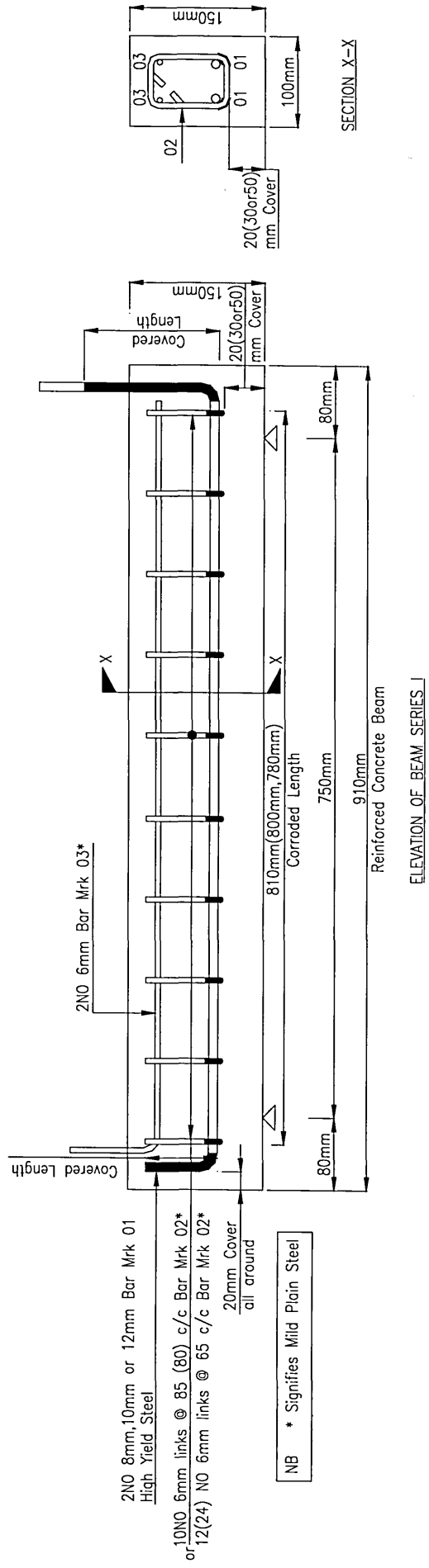


Figure 5.1 Geometry of the beam Series I used for the design

reinforced with either two 8 mm, 10 mm or 12 mm diameter reinforcing bars, with cover to the stirrups either 20 mm, 30 mm or 50 mm (26 mm, 36 mm or 56 mm to the main steel).

Main reinforcement consisted of high yield (ribbed) bars with a nominal characteristic strength of  $460 \text{ N/mm}^2$ . Shear reinforcement was 6 mm diameter plain round mild steel bars with yield strength of  $250 \text{ N/mm}^2$  at either 85 mm, 80 mm or 65 mm spacing for 20 mm, 30 mm and 50 mm cover respectively. Hanger top bars for all beams consisted of two 6 mm diameter plain round mild steel bars with a yield strength of  $250 \text{ N/mm}^2$ . Electrical continuity between the reinforcing bars was ensured by connecting the bars at the end.

In all, 74 beams were cast, cured corroded and tested. The designation used in this thesis to describe each beam is of the form 2T8/0+10D6/0/30. The first part describes the main steel (e.g. 2T8/0) and the second part the shear reinforcement (e.g. 10D6/0/30). Regarding the main steel, the number, type and diameter of the main bar, ("T" for high tensile steel) is given, followed by the target corrosion, where "0" indicates no corrosion (or control beams). The second part identifies the shear reinforcement where in this example, ten number, 6 mm diameter mild steel shear reinforcement are used with 0% corrosion and 30 mm cover.

The following parameters were examined:

- Influence of corrosion level (up to 20% loss of steel cross section) on structural performance;
- Effect of different bar diameters (8 mm, 10 mm and 12 mm);

- Influence of cover (26 mm, 36 mm and 56 mm to the main steel) on structural performance of deteriorated members due to corrosion.

Through the testing care was taken to ensure that all the beams in the series contained concrete of similar quality and strength. This was done by following the same procedures of drying aggregates, mixing, casting and curing each time. Cubes were taken at the same time of casting from all mixes used and tested to determine the concrete strength at the time of testing. In all, 444 cubes were tested, with strengths in the range 42.8 – 66.6 N/mm<sup>2</sup>. The mean steel strength was found from tensile tests on uncorroded samples (see Appendix A).

### 5.3.3 Process of accelerated corrosion

In order to determine the effect of reinforcement corrosion on the flexural capacity of reinforced concrete beams, corrosion was accelerated by applying a current to the reinforcement and immersing partially the beam in a salt bath containing a 3.5% salt solution of CaCl<sub>2</sub>. The saline solution was maintained in the tank to a depth of 130 mm, Figure 5.2, (volume: 10 litres) and was replaced weekly as, after that time, the chloride ion concentration became significantly reduced. In general, a current of 406 mA, 494 mA and 596 mA was applied for beams reinforced with 2T8, 2T10 and 2T12 respectively, representing a current density of about 1 mA/cm<sup>2</sup>. This current density was adopted on the basis of pilot tests to provide desired levels of corrosion in a reasonable time. The current density was kept low (1 mA/cm<sup>2</sup>) in order to simulate general behaviour of structures with naturally occurring corrosion. The results from such tests are conservative, due mainly to the more uniform distribution of corrosion at the critical section. Natural corrosion would tend to be less uniform, thus reducing the



Figure 5.2 Reinforced concrete beams undergoing main reinforcement corrosion

likelihood of loss of bond occurring along the entire anchorage length. The method, however, does offer the significant advantage of repeatability and control to the experimental process.

The current supplied to each specimen was checked on a daily basis and any drift was corrected. To complete the circuit, the direction of the current was selected so that the main reinforcing steel served as the anode and the hanger bars and the stirrups acted as the cathode.

The beams were corroded as described in above, except for the twenty five beams which were left uncorroded and tested as control specimens. The progress of each beam was monitored as the corrosion process proceeded. Longitudinal cracking of the cover concrete occurred at various times, depending on the type of bar and depth of concrete cover.

The first sign of corrosion was rust staining on the surface of the concrete which first appeared after a few of days. Cracking was first observed on the low cover beams (2T8/5/20, 2T10/5/20, 2T12/5/20) after 5 days. Once the beams had cracked, lumps of iron oxide formed on the beam, (see Figure 5.3).



Figure 5.3 Iron oxide formation on the beams after corrosion

It was found after removing the specimens from the tank that all beams had some longitudinal cracking to various degrees.

#### 5.3.4 Test configuration and procedure

Before the application of load, the test beams were inspected carefully for any cracks due to shrinkage or corrosion and then transferred to the testing rig.

The beams were placed on simple supports, spanning 750 mm, with four point bending with load applied at a shear span of 250 mm. Figure 5.4 shows the loading configuration and instrumentation used for the load tests. The load was applied with a hydraulic pump and jack reacting against a cross head which was tied down using two Macalloy bars. A 3000 kN load cell was placed in line with the loading jack to measure the applied load. The loading rig had a maximum capacity of about 150 kN.

As the test was in load control (i.e. 5 kN/min) it was possible to record the exact failure load and central deflection.

The behaviour of the beam was monitored using a Celesco displacement gauge placed under the beam. The displacement gauge and load cell readings were powered and monitored using a data logging system.

The reinforcement was then taken out by removing the concrete manually where extra care was taken so no mechanical damage was done to the steel.

Recovery of the reinforcement for examination revealed that the corrosion occurred between the cathodic shear reinforcement placed throughout the length of the beams (see Figure 5.5). In general, the steel section was lost from the bottom of the bars, with no pitting taking place.

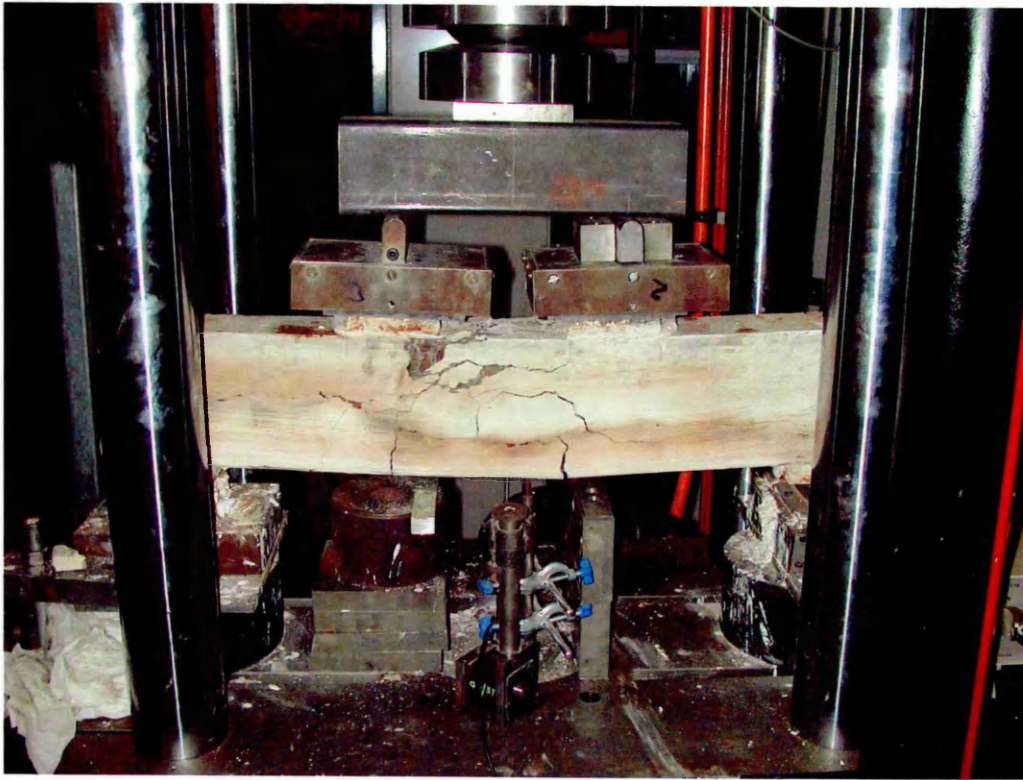


Figure 5.4 Loading configuration and instrumentation of a test beam

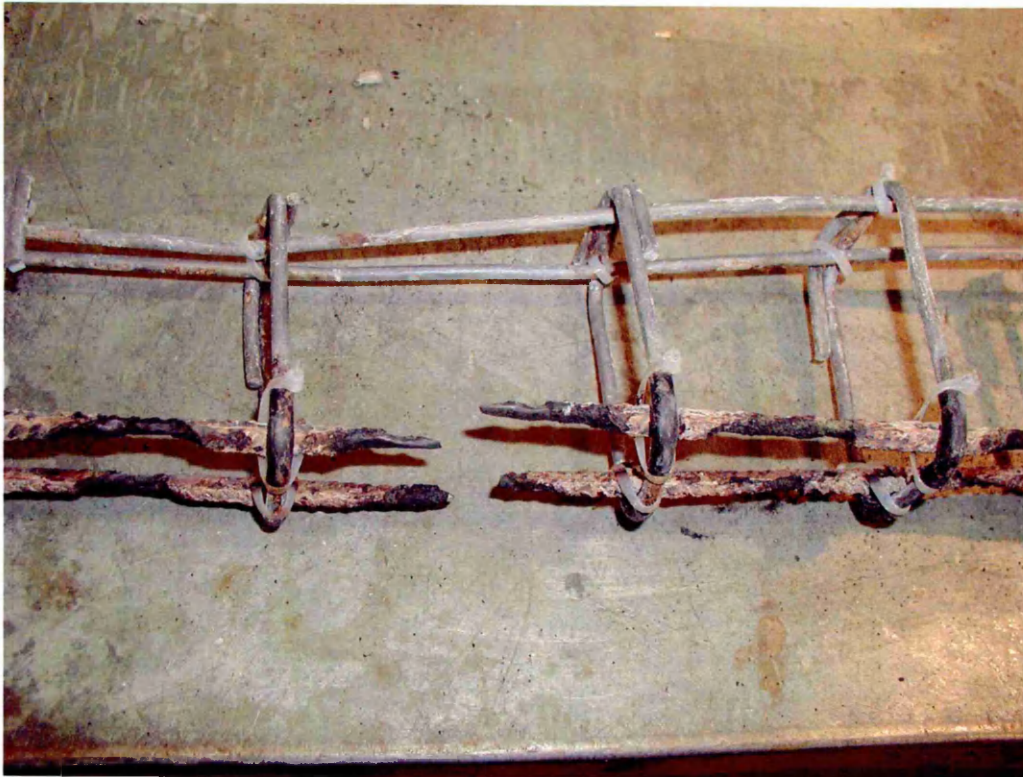


Figure 5.5 Reinforcement cage after corrosion

#### 5.4 Influence of corrosion on the main steel reinforcement on the flexural performance

Control specimens, with no corrosion, were tested for comparison. Four degrees of main steel corrosion only were targeted, namely 0%, 5%, 10% and 15% loss of section by weight, based on a combination of Faraday's law and the experience of previous research. These nominal degrees of corrosion were approximate and were used in the designation of the beam number, for example, see column 1, Table 5.1 (and also reinforcement was cleaned prior to casting with Diammonium hydrogen citrate (which is citric acid diammonium salt, 1,2,3 – Propanetricarboxylic acid, 2 – hydroxyl–, diammonium salt; gas No.: 3012–65–5 with molecular weight; 226.19 and chemical formula:  $(\text{NH}_4)_2\text{HC}_6\text{H}_5\text{O}_7$ ) for about 20 minutes at room temperature and then rinsed with acetone and stored in a desiccator. The main steel reinforcement was wire brushed and the initial weight was recorded (column 2, Tables 5.1 to 5.3). Subsequent to the load tests, the beams were demolished and the reinforcement was recovered for visual examination and evaluation of the weight loss resulting from the corrosion process (column 3, Tables 5.1 to 5.3). The weight loss recorded in Tables 5.1 to 5.3 (column 4) was determined by taking 810 mm, 800 mm and 780 mm of corroded lengths of bar for 2T8, 2T10 and 2T12 respectively and de-scaling it to remove the corrosion products. The choice of sample was made by taking the whole length of heavily corroded bar from the beam specimens being tested, so that the recorded weight loss represents the overall section loss in the reinforcement. The great scatter in the measured weight loss figure results from the non uniformity of the corrosion and the uncertainty of the corrosion process.

Table 5.1 Beam Series I – Corrosion details and load behaviour of beams with main reinforcement (2T8) corrosion

Beam number	Corrosion details				Load behaviour		
	Weight of main reinforcement before corrosion gr (2)	Weight of main reinforcement after corrosion gr (3)	Weight loss gr (4)	Actual corrosion % (5)	$P_{ult}$ kN (6)	$P_{ult} / P_{con}^*$ % (7)	Mode of failure (8)
(1)							
2T8/0+10D6/0/20	–	–	0	0	57.40	103.0	Flexure
2T8/0+10D6/0/20	–	–	0	0	54.10	97.0	Flexure
2T8/5+10D6/0/20	883.4	871.3	12.1	1.0	52.75	94.6	Flexure
2T8/5+10D6/0/20	883.0	865.6	17.4	1.4	54.70	98.1	Flexure
2T8/5+10D6/0/20	883.3	854.5	28.8	2.3	43.78	78.5	Flexure
2T8/10+10D6/0/20	882.4	839.7	42.7	3.4	50.12	89.9	Flexure
2T8/10+10D6/0/20	887.7	775.1	112.6	8.9	41.10	73.7	Flexure
2T8/15+10D6/0/20	883.6	756.5	127.1	10.0	34.98	62.7	Flexure
2T8/15+10D6/0/20	881.8	685.0	196.8	15.5	19.23	34.5	Flexure
2T8/15+10D6/0/20	886.2	652.0	234.2	18.5	20.57	36.9	Flexure

\* $P_{con}$  is the average of the ultimate loads for the control (0% corrosion beams)

Table 5.1 Beam Series I – Corrosion details and load behaviour of beams with main reinforcement (2T8) corrosion (Continued...)

Beam number	Corrosion details				Load behaviour		
	Weight of main reinforcement before corrosion gr (2)	Weight of main reinforcement after corrosion gr (3)	Weight loss gr (4)	Actual corrosion % (5)	$P_{ult}$ kN (6)	$P_{ult} / P_{con}^*$ % (7)	Mode of failure (8)
(1)							
2T8/0+10D6/0/30	–	–	0	0	50.40	95.5	Flexure
2T8/0+10D6/0/30	–	–	0	0	55.20	104.6	Flexure
2T8/5+10D6/0/30	856.0	845.5	10.5	0.8	56.80	107.6	Flexure
2T8/5+10D6/0/30	864.4	853.5	10.9	0.9	52.10	98.7	Flexure
2T8/5+10D6/0/30	866.3	848.1	18.2	1.4	45.03	85.3	Flexure
2T8/5+10D6/0/30	871.5	812.8	58.7	4.6	44.60	84.5	Flexure
2T8/10+10D6/0/30	875.6	767.8	107.8	8.5	34.70	65.7	Flexure
2T8/10+10D6/0/30	865.2	743.5	121.7	9.6	34.20	64.8	Flexure
2T8/15+10D6/0/30	859.2	668.8	190.4	15.0	24.57	46.5	Flexure
2T8/15+10D6/0/30	868.2	642.7	225.5	17.8	20.90	39.6	Flexure

\* $P_{con}$  is the average of the ultimate loads for the control (0% corrosion beams)

Table 5.1 Beam Series I – Corrosion details and load behaviour of beams with main reinforcement (2T8) corrosion (Continued...)

Beam number	Corrosion details				Load behaviour		
	Weight of main reinforcement before corrosion gr (2)	Weight of main reinforcement after corrosion gr (3)	Weight loss gr (4)	Actual corrosion % (5)	$P_{ult}$ kN (6)	$P_{ult} / P_{con}^*$ % (7)	Mode of failure (8)
(1)							
2T8/0+12D6/0/50	–	–	0	0	40.00	96.7	Flexure
2T8/0+12D6/0/50	–	–	0	0	42.70	103.3	Flexure
2T8/5+12D6/0/50	852.5	818.9	33.6	2.7	42.91	103.8	Flexure
2T8/5+12D6/0/50	852.5	807.6	44.9	3.5	39.24	94.9	Flexure
2T8/5+12D6/0/50	853.8	787.0	66.8	5.3	33.26	80.4	Flexure
2T8/5+12D6/0/50	856.7	769.0	87.7	6.9	34.58	83.6	Flexure
2T8/10+12D6/0/50	855.1	757.0	98.1	7.7	33.48	81.0	Flexure
2T8/10+12D6/0/50	858.0	745.2	112.8	8.9	26.34	63.7	Flexure
2T8/15+12D6/0/50	857.9	666.8	191.1	15.1	17.08	41.3	Flexure
2T8/15+12D6/0/50	852.8	645.2	207.6	16.4	10.10	24.4	Flexure

\* $P_{con}$  is the average of the ultimate loads for the control (0% corrosion beams)

The accelerated corrosion set up meant that the current flow through the test beams per series was affected by the length of the current path (beam specimens undergoing accelerated corrosion were electrically connected in series), see Figure 5.6.

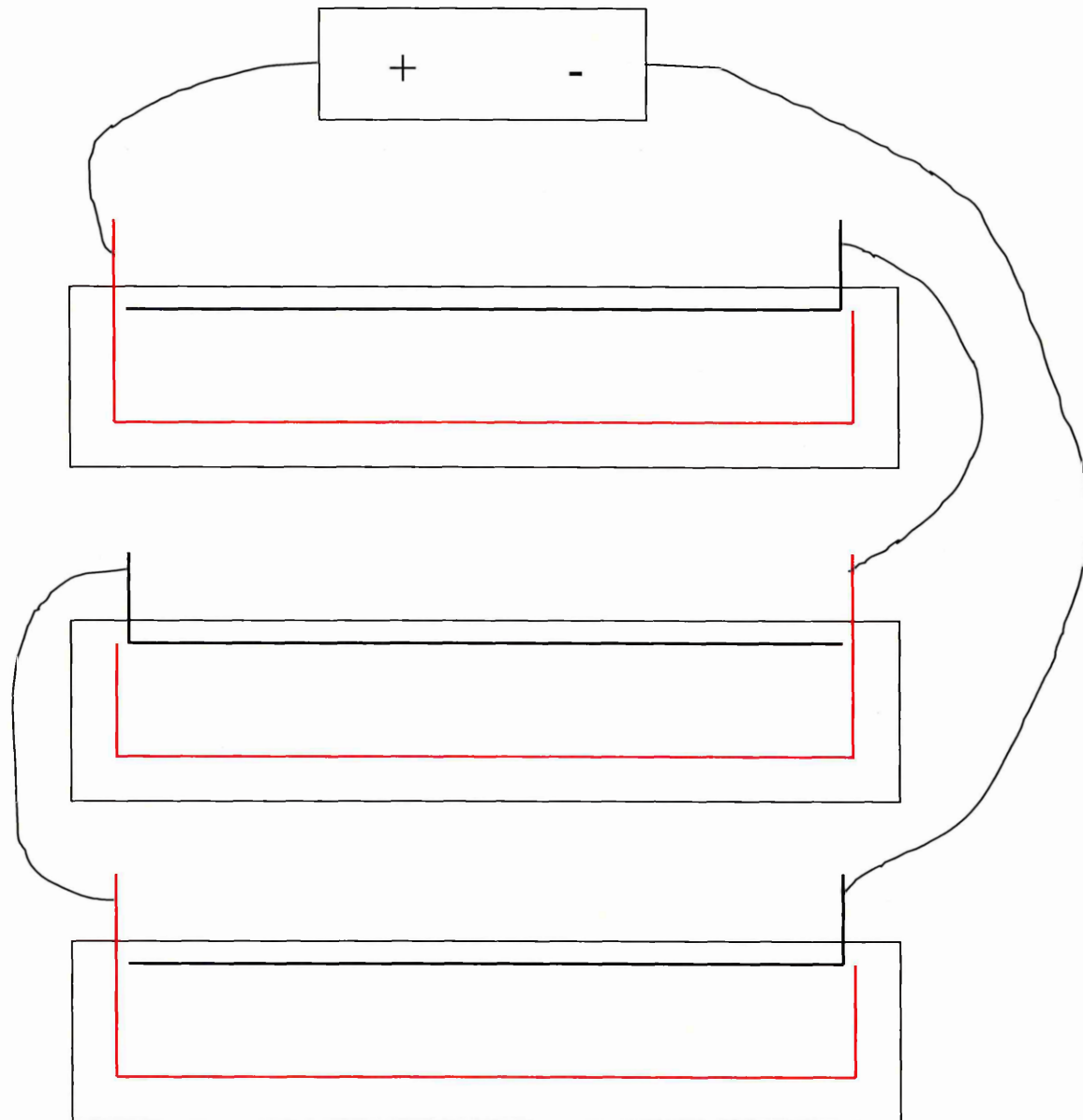


Figure 5.6 Beam specimens electrically connected in series

#### 5.4.1 Beams reinforced with 2T8 main steel

The control specimens (zero percent corrosion) were tested at the age of 28 days but the deteriorated beams were tested at 42, 48 and 54 days for the 5, 10 and 15% target corrosion respectively due to the time taken to reach the desired levels of corrosion. All specimens were tested under four point bending as shown in Figure 5.5, to determine the ultimate flexural strength. Premature shear failure was prevented by sufficient shear reinforcement.

The first load tests were carried out on the control specimens and these behaved as expected and in accordance with the design procedures of BS 8110 (British Standards Institutions). Failure of all 30 beams was in flexure; no shear failure occurred.

Upon completion of the corrosion period and flexural testing, the reinforcing bars were removed from the concrete as shown in Figure 5.4, cleaned and re-weighed. The percentage loss in weight was subsequently calculated. The resulting degree of corrosion in this investigation,  $2RT/D$  %, ranged between 0% (control) and 18.5 % (column 5, Table 5.1). The corrosion damage was generally spread along the length of the bars. For the purpose of calculations, general rather than pitting corrosion was assumed.

The actual corrosion calculated as described in Chapter 3 is also given along with the ultimate load at failure. It is clear from the ultimate loads given in Table 5.1 (column 6) that the strength of the beams decrease with increasing main steel corrosion (compare the control load of beam 2T8/0+10D6/0/20 with that of 2T8/15+10D6/0/20, with actual corrosion to the main steel of 18.5% the ultimate load decreases from 57.40 kN to 20.57 kN). This is also applicable to the other two categories (36 and 56 mm cover to the main steel, Table 5.1) which also show significant reductions in ultimate strength due to

corrosion. Column 8 in Table 5.1 also shows that the failure of each beam in the three categories (26, 36 and 56 mm cover to the main steel) was flexural.

In all cases, the actual percentage of corrosion was used in the analysis of data as opposed to the target corrosion. This led to a better correlation between flexural performance and degree of corrosion as there was some variation between target and actual values (Table 5.1). Detailed analysis of this Series is presented in Chapter 8.

#### **5.4.2 Beams reinforced with 2T10 main steel**

The control specimens (zero percent corrosion) were also tested at the age of 28 days but the deteriorated beams were tested at 43, 51 and 59 days for the 5, 10 and 15% main steel target corrosion respectively due to the time taken to reach the desired levels of corrosion. All specimens were tested under four point bending as described in section 5.4.1, shown in Figure 5.5, to determine the ultimate flexural strength. Premature shear failure was also prevented by sufficient shear reinforcement.

The first load tests were carried out on the control specimens and these behaved as expected and in accordance with the design procedures of BS 8110 (British Standards Institutions). Failure of all 36 beams was in flexure; no shear failure occurred.

Upon completion of the corrosion period and flexural testing, the reinforcing bars were also removed from the concrete, cleaned and re-weighted. The percentage loss in weight was subsequently calculated. The resulting degree of corrosion in this investigation,  $2RT/D$  %, ranged between 0% (control) and 14.4% (column 5, Table 5.2).

The corrosion damage was generally spread along the length of the bars. For the purpose of calculations general rather than pitting corrosion was assumed.

Table 5.2 Beam Series I – Corrosion details and load behaviour of beams with main reinforcement (2T10) corrosion

Beam number	Corrosion details				Load behaviour		
	Weight of main reinforcement before corrosion gr (2)	Weight of main reinforcement after corrosion gr (3)	Weight loss gr (4)	Actual corrosion % (5)	$P_{ult}$ kN (6)	$P_{ult} / P_{con}^*$ % (7)	Mode of failure (8)
(1)							
2T10/0+10D6/0/20	–	–	0	0	84.63	97.2	Flexure
2T10/0+10D6/0/20	–	–	0	0	89.40	102.7	Flexure
2T10/0+10D6/0/20	–	–	0	0	87.45	100.4	Flexure
2T10/0+10D6/0/20	–	–	0	0	88.80	102.0	Flexure
2T10/0+10D6/0/20	–	–	0	0	96.50	110.8	Flexure
2T10/0+10D6/0/20	–	–	0	0	86.50	99.3	Flexure
2T10/0+10D6/0/20	–	–	0	0	85.02	97.6	Flexure
2T10/0+10D6/0/20	–	–	0	0	78.40	90.0	Flexure
2T10/5+10D6/0/20	1377.3	1326.7	50.6	2.6	68.50	78.7	Flexure
2T10/5+10D6/0/20	1372.3	1294.8	77.5	4.0	65.30	75.0	Flexure

\* $P_{con}$  is the average of the ultimate loads for the control (0% corrosion beams)

Table 5.2 Beam Series I – Corrosion details and load behaviour of beams with main reinforcement (2T10) corrosion (Continued...)

Beam number	Corrosion details				Load behaviour		
	Weight of main reinforcement before corrosion gr (2)	Weight of main reinforcement after corrosion gr (3)	Weight loss gr (4)	Actual corrosion % (5)	$P_{ult}$ kN (6)	$P_{ult} / P_{con}^*$ % (7)	Mode of failure (8)
(1)							
2T10/10+10D6/0/20	1372.1	1290.4	81.5	4.2	86.98	99.9	Flexure
2T10/10+10D6/0/20	1368.9	1281.4	87.5	4.5	82.50	94.7	Flexure
2T10/15+10D6/0/20	1395.3	1269.5	125.8	6.5	64.48	74.0	Flexure
2T10/15+10D6/0/20	1375.4	1229.4	146	7.5	62.70	72.0	Flexure
2T10/0+10D6/0/30	–	–	0	0	75.65	99.6	Flexure
2T10/0+10D6/0/30	–	–	0	0	73.30	96.5	Flexure
2T10/0+10D6/0/30	–	–	0	0	76.30	100.4	Flexure
2T10/0+10D6/0/30	–	–	0	0	74.30	97.8	Flexure
2T10/0+10D6/0/30	–	–	0	0	79.70	104.9	Flexure
2T10/0+10D6/0/30	–	–	0	0	77.90	102.5	Flexure

\* $P_{con}$  is the average of the ultimate loads for the control (0% corrosion beams)

Table 5.2 Beam Series I – Corrosion details and load behaviour of beams with main reinforcement (2T10) corrosion (Continued...)

Beam number	Corrosion details				Load behaviour		
	Weight of main reinforcement before corrosion gr (2)	Weight of main reinforcement after corrosion gr (3)	Weight loss gr (4)	Actual corrosion % (5)	$P_{ult}$ kN (6)	$P_{ult} / P_{con}^*$ % (7)	Mode of failure (8)
(1)							
2T10/0+10D6/0/30	–	–	0	0	74.80	98.4	Flexure
2T10/5+10D6/0/30	1379.5	1335.1	44.4	2.3	70.49	92.8	Flexure
2T10/5+10D6/0/30	1368.4	1320.1	48.3	2.5	69.42	91.4	Flexure
2T10/5+10D6/0/30	1373.6	1309.1	64.5	3.3	70.66	93.0	Flexure
2T10/10+10D6/0/30	1338.2	1272.5	65.7	3.4	90.35	118.9	Flexure
2T10/10+10D6/0/30	1370.7	1239.9	130.8	6.7	57.66	75.9	Flexure
2T10/15+10D6/0/30	1346.5	1184.6	161.9	8.3	55.24	72.7	Flexure
2T10/15+10D6/0/30	1366.3	1186.5	179.8	9.2	53.99	71.1	Flexure

\* $P_{con}$  is the average of the ultimate loads for the control (0% corrosion beams)

Table 5.2 Beam Series I – Corrosion details and load behaviour of beams with main reinforcement (2T10) corrosion (Continued...)

Beam number	Corrosion details				Load behaviour		
	Weight of main reinforcement before corrosion gr (2)	Weight of main reinforcement after corrosion gr (3)	Weight loss gr (4)	Actual corrosion % (5)	$P_{ult}$ kN (6)	$P_{ult} / P_{con}^*$ % (7)	Mode of failure (8)
(1)							
2T10/0+12D6/0/50	–	–	0	0	61.42	98.5	Flexure
2T10/0+12D6/0/50	–	–	0	0	63.30	101.5	Flexure
2T10/5+12D6/0/50	1377.3	1266.5	110.8	5.7	63.00	101.0	Flexure
2T10/5+12D6/0/50	1370.1	1251.1	119.0	6.1	55.00	88.2	Flexure
2T10/10+12D6/0/50	1361.5	1211.5	150.0	7.7	47.70	76.5	Flexure
2T10/10+12D6/0/50	1372.1	1187.0	185.1	9.5	50.30	80.7	Flexure
2T10/15+12D6/0/50	1374.1	1174.5	199.6	10.2	42.80	68.6	Flexure
2T10/15+12D6/0/50	1371.3	1090.8	280.5	14.4	39.90	64.0	Flexure

\* $P_{con}$  is the average of the ultimate loads for the control (0% corrosion beams)

It is clear from the ultimate loads given in Table 5.2 that the strength of the beams decrease with increasing main steel corrosion (compare the control load of beam 2T10/0+12D6/0/50 with that of 2T10/14.4+12D6/0/50, the ultimate load decreases from 62.36 kN to 39.90 kN). This is also applicable to the other two categories (26 and 36 mm cover to the main steel, Table 5.2) which also show significant reductions in ultimate strength due to corrosion.

In all cases, the actual percentage of corrosion was used in the analysis of data as opposed to the target corrosion as there was some variation between target and actual values (Table 5.2). Detailed analysis is presented in Chapter 8.

#### **5.4.3 Beams reinforced with 2T12 main steel**

In this group of eight beams, the control specimens (zero percent corrosion) were tested at the age of 28 days but the deteriorated beams were tested at 44, 54 and 63 days for the 5, 10 and 15% target main steel corrosion respectively due to the time taken to reach the desired levels of corrosion after the initiation period. All specimens were tested under four point bending as shown in Figure 5.5, to determine the ultimate flexural strength. Premature shear failure was prevented by sufficient shear reinforcement which in this case consisted of 24 links.

The first load tests were carried out on the control specimens and these behaved as expected and in accordance with the design procedures of BS 8110 (British Standards Institutions). Failure of all 8 beams was in flexure; no shear failure occurred.

The resulting degree of corrosion in this investigation,  $2RT/D$  %, ranged between 0% (control) and 5.9% (column 5, Table 5.3). The corrosion damage was generally spread along the length of the bars mainly due to the low percentages of corrosion.

Table 5.3 Beam Series I – Corrosion details and load behaviour of beams with main reinforcement (2T12) corrosion

Beam number	Corrosion details				Load behaviour		
	Weight of main reinforcement before corrosion gr (2)	Weight of main reinforcement after corrosion gr (3)	Weight loss gr (4)	Actual corrosion % (5)	$P_{ult}$ kN (6)	$P_{ult} / P_{con}^*$ % (7)	Mode of failure (8)
(1)							
2T12/0+24D6/0/50	–	–	0	0	76.98	97.0	Flexure
2T12/0+24D6/0/50	–	–	0	0	81.68	103.0	Flexure
2T12/5+24D6/0/50	1946.4	1910.1	36.3	1.3	73.80	93.0	Flexure
2T12/5+24D6/0/50	1941.7	1895.4	46.3	1.7	70.80	89.3	Flexure
2T12/10+24D6/0/50	1961.9	1893.4	68.5	2.5	63.60	80.2	Flexure
2T12/10+24D6/0/50	1947.4	1860.5	86.9	3.1	57.30	72.2	Flexure
2T12/15+24D6/0/50	1976.2	1861.0	115.2	4.2	61.70	77.8	Flexure
2T12/15+24D6/0/50	1956.0	1791.9	164.1	5.9	50.70	63.9	Flexure

\* $P_{con}$  is the average of the ultimate loads for the control (0% corrosion beams)

It is clear from the ultimate loads given in Table 5.3 that the strength of the beams decrease with increasing main steel corrosion (compare the control load of beam 2T12/0+24D6/0/50 with that of 2T12/5.9+24D6/0/50, the ultimate load decreases from 79.33 kN, the average between the two control beams, to 50.7 kN).

The actual percentage of corrosion was also used in the further analysis of data (Chapter 8) as opposed to the target corrosion.

## **5.5 Conclusions**

### **5.5.1 Conclusions from accelerated corrosions tests**

The use of impressed current was a practical and convenient method of producing corroded specimens for examining the structural effects of reinforcement corrosion. The first sign of corrosion was rust staining on the concrete surface, followed by longitudinal cracking in the concrete cover.

The corrosion tended to occur along the whole length of the main steel. The damage was generally spread along the bottom of the bars, with variable section loss along the bar. General corrosion was evident rather than localised pitting corrosion. The weight loss obtained was approximately as expected.

The time to first cracking depended, as expected, on cover and type of bar. There was no evidence to suggest that deformed bars are more susceptible to corrosion.

### **5.5.2 Conclusions from load tests**

The presence of longitudinal cracking resulting from the corrosion of reinforcement does not necessarily mean loss of strength. The beams with target corrosion of 5%

suffered negligible strength loss, even where longitudinal cracking was present over the length of beam. Failure was ductile and in flexure. There was no evidence of bond failure. The strength of these beams could have been accurately assessed by making due allowance for section loss in the evaluation of moment capacity.

First evidence of bond failure occurred in the beams with target corrosion of 10%. This evidence consisted of horizontal cracking of the beam along the line of the reinforcement both bottom and side, as the load test proceeded, suggesting local bond failure. Failure was ductile and in flexure.

The series of beams with the highest corrosion suffered significant strength loss. In these tests, the beams collapsed as a result of bond failure. Further beams failed as a result of fracture of the reinforcing bars at a location of heavy section loss.

### **5.5.3 Conclusions from cover variations**

The main conclusions from the results reported in this chapter are as follows:

- the cracking in the cover concrete was more severe at 56 mm cover to the main steel compared to 26 mm cover to the main steel at similar levels of main steel reinforcement corrosion;
- deteriorated reinforced concrete beams suffer the most reduction in flexural strength when the beams are designed with high reinforcement cover and are subjected to high levels of main steel corrosion.

### **5.5.4 Conclusions from diameter variations**

The main conclusions from the results reported in this chapter are as follows:

- reinforced concrete beams show a loss in residual flexural strength with increasing corrosion of the main steel reinforcement;
- beams reinforced with larger diameter main steel experience a higher reduction in flexural strength than beams designed with smaller diameter main steel at similar degrees of corrosion;
- the cracking in the cover concrete was more severe in beams reinforced with 2T12 mm compared to those reinforced with 2T8 mm even at lower levels of main steel reinforcement corrosion.

### *Influence of Shear Reinforcement Corrosion on Structural Performance (Series II)*

#### **6.1 Introduction**

There is a possibility that members with corroded shear reinforcement will not achieve their full flexural capacity due to premature shear failure. Corrosion can reduce the shear load carrying capacity earlier and, sometimes, at a faster rate than it reduces the flexural load carrying capacity. In real structures, shear reinforcement has lower cover than flexural reinforcement and will start to corrode first. Good bond creates closely spaced cracks, while poor or non-existent bond results in only a few cracks or no cracks at all in the part where shear force exists. It has been reported elsewhere<sup>5, 93</sup> that the effects of corrosion on the shear strength are not straightforward, but nevertheless, this will be investigated in the current study.

Corrosion of reinforcing steel can, therefore, cause serious loss of structural performance and can lead to catastrophic failure. This series of beam tests were developed to determine the influence of shear reinforcement corrosion on the structural performance of reinforced concrete beams. In these beams, the structural performance was not only affected, by loss of steel cross section, but also by impairment of the bond between the reinforcement and the concrete.

## **6.2 Objectives of test programme**

This series of beam tests (test Series II) was developed to determine the influence of shear reinforcement corrosion on the flexural performance of reinforced concrete beams. The test programme was designed to provide information on the influence of corrosion on the structural performance of deteriorated beams. Therefore, the aim of this series of tests is to establish the residual strength of under reinforced beams exhibiting shear reinforcement corrosion only.

## **6.3 Experimental programme**

### **6.3.1 Beam specimens**

Details of the beams used in the experimental programme are given in Figure 6.1. The beams measured 910 mm in length with a 100 mm x 150 mm cross section. Each beam was reinforced longitudinally with either two 8 mm or two 12 mm diameter deformed reinforcing bars, which remained uncorroded, with 50 mm cover to the shear reinforcement. Shear reinforcement were 6 mm diameter plain bars at 65 mm spacing. Electrical continuity between the reinforcing bars was ensured by connecting the exposed bars with screw connectors (see Figure 6.2). The shear reinforcement were connected to the main and hanger bars in a manner that ensured the electrical circuit between the corroded links and uncorroded reinforcement was broken. This was done by using plastic tie wire and shrink wrap over the uncorroded bars at the points of contact with the shear reinforcement as described in Section 3.7.3 and shown in Figure 6.3.

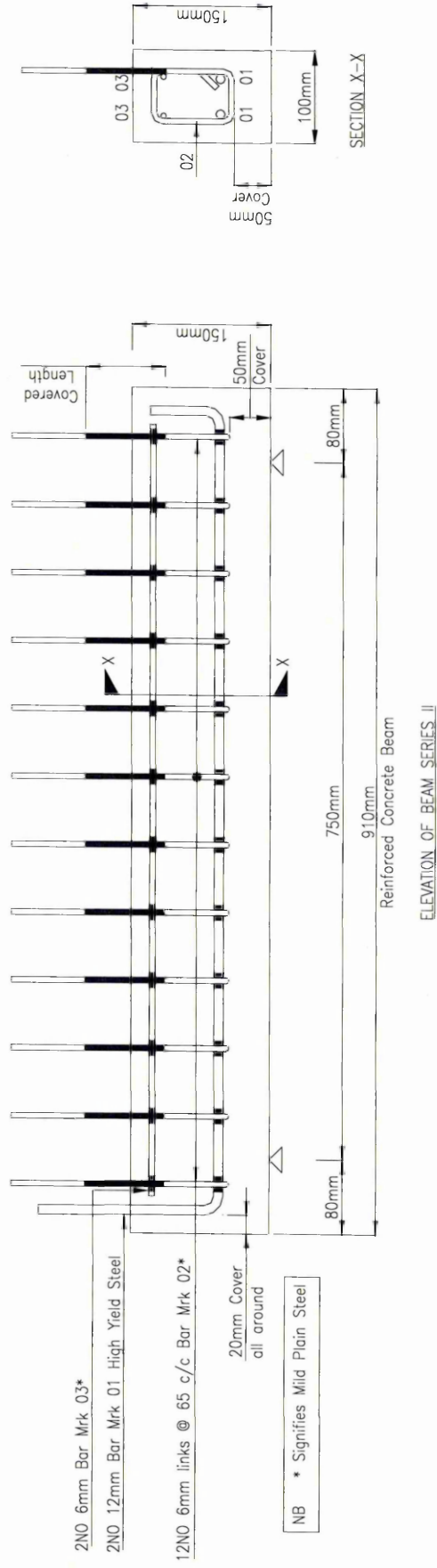


Figure 6.1 Geometry of the beam Series II used for the design

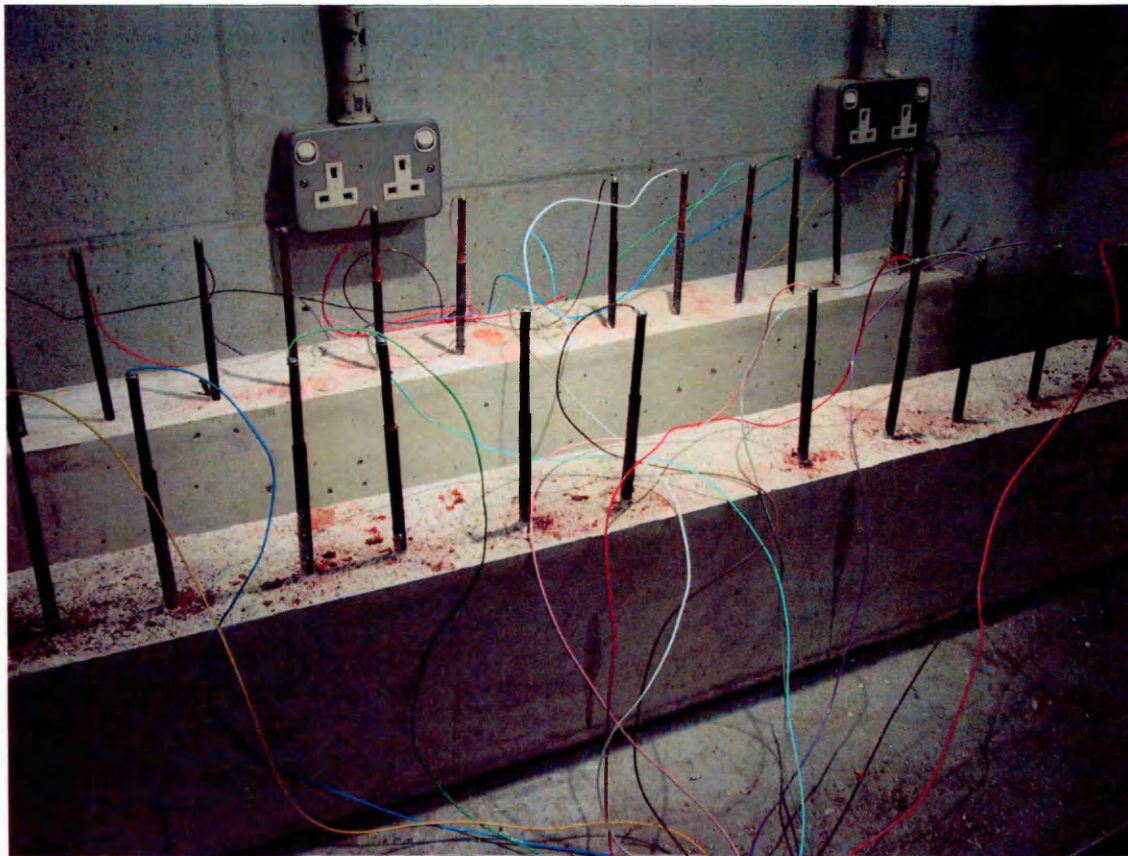


Figure 6.2 Electrical connections between the shear reinforcement and the power supply

The extended length of the shear reinforcement was also covered with shrink wrap in order to prevent severe section loss in this area.

There were two different beam types (uncorroded main reinforcement of either 2T8 or 2T12 and corroded 12D6 shear reinforcement) and four different degrees of corrosion. In all, sixteen beams were tested.

The following parameters were examined:

- Influence of corrosion (up to 15% loss of reinforcing steel cross section) on the structural performance;



Figure 6.3 Reinforcing cage used for beam Series II

- Effect of different main steel diameters.

By following the same pattern of mixing, casting and curing, care was taken to ensure that all the beams in the series contained concrete of the same quality. Cubes were taken at the time of casting from all mixes and tested to determine the concrete strength at the time of testing the beams. In all, 96 cubes were tested. The concrete strength used in the analysis was, therefore, the actual strength at the time of testing and not the 28 day design value.

### 6.3.2 Process of accelerated corrosion

The process of corrosion was accelerated by immersing the beam in a salt bath and applying a small current to the shear reinforcement. A current of 480 mA, representing a current density of about  $1 \text{ mA/cm}^2$ , was employed, to simulate naturally occurring corrosion in the field. The conclusion in the literature is that results from such tests are conservative, due mainly to the more uniform distribution of the corrosion at the critical section (see Figure 6.4). Natural corrosion would tend to be less uniform, thus reducing the likelihood of loss of bond occurring along the entire anchorage length. The method does offer the significant advantage of repeatability and control to the experimental process. The current was applied directly to the shear reinforcement. The cathode consisted of the two main bars, placed along the full length of the beam. To complete the circuit, the beam was fully immersed in a tank containing a 3.5%  $\text{CaCl}_2$  solution. The saline solution was maintained in the tank to a depth of 150 mm so that the shear reinforcement were fully submerged.

Four degrees of corrosion were targeted 0% (control), 5%, 10% and 15% loss of cross section by weight, based on a combination of Faraday's Law (see section 3.2.2) and the experience of previous research (Chapter 3). These nominal degrees of corrosion were approximate and are used in the designation of the beam. Once the first set of corroded beams were tested and demolished, the time and current required to deteriorate subsequent beam specimens was reviewed. This was to ensure that steel reinforcement was sufficiently corroded to produce a level of corrosion as close as possible to the target corrosion.

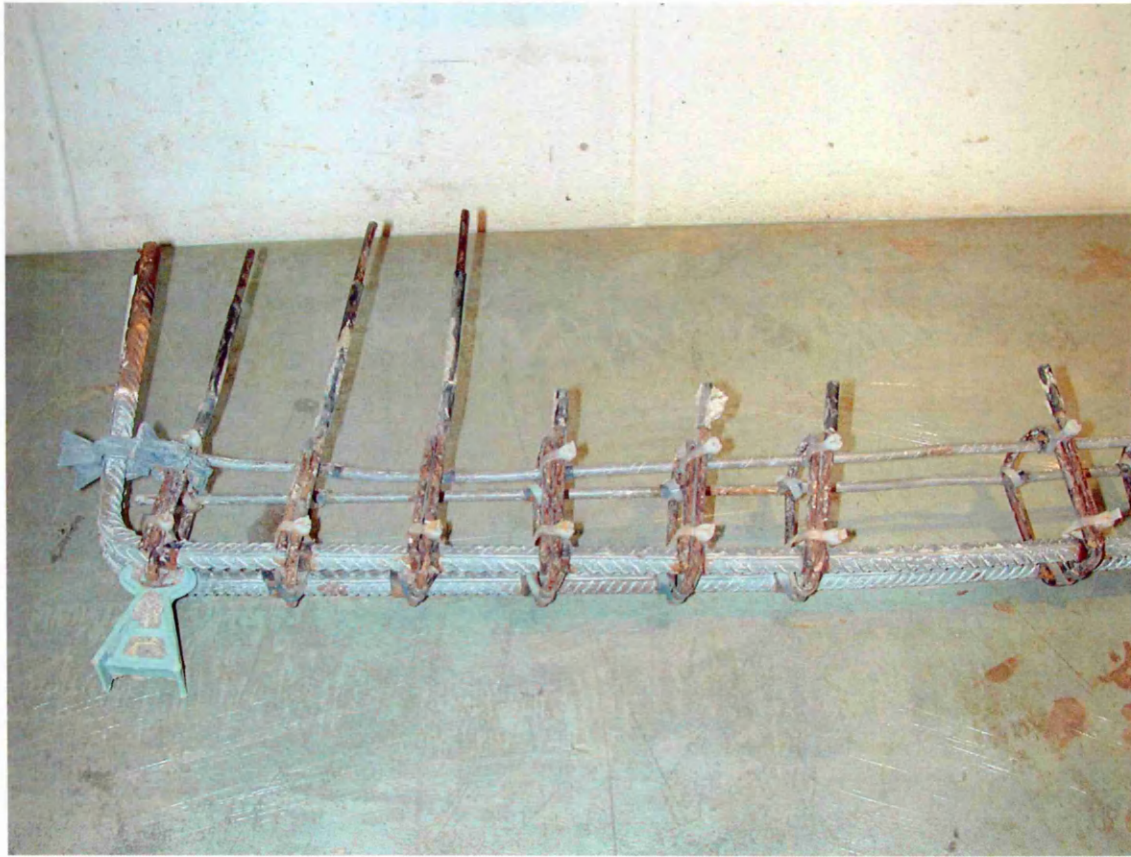


Figure 6.4 Shear reinforcement corrosion

### 6.3.3 Test configuration and instrumentation

The control specimens (zero percent corrosion) were tested at the age of 28 days but the deteriorated beams were tested at 42, 48 and 54 days for the 5, 10 and 15% target corrosion respectively due to the time taken to reach the desired levels of corrosion.

The loading configuration was devised to investigate the structural behaviour of beams with corroded shear reinforcement and was generally similar to the previously reported tests for flexure (Chapter 5). The beams were placed on a simple supports, spanning 750 mm, with four point bending (see Figure 6.5).

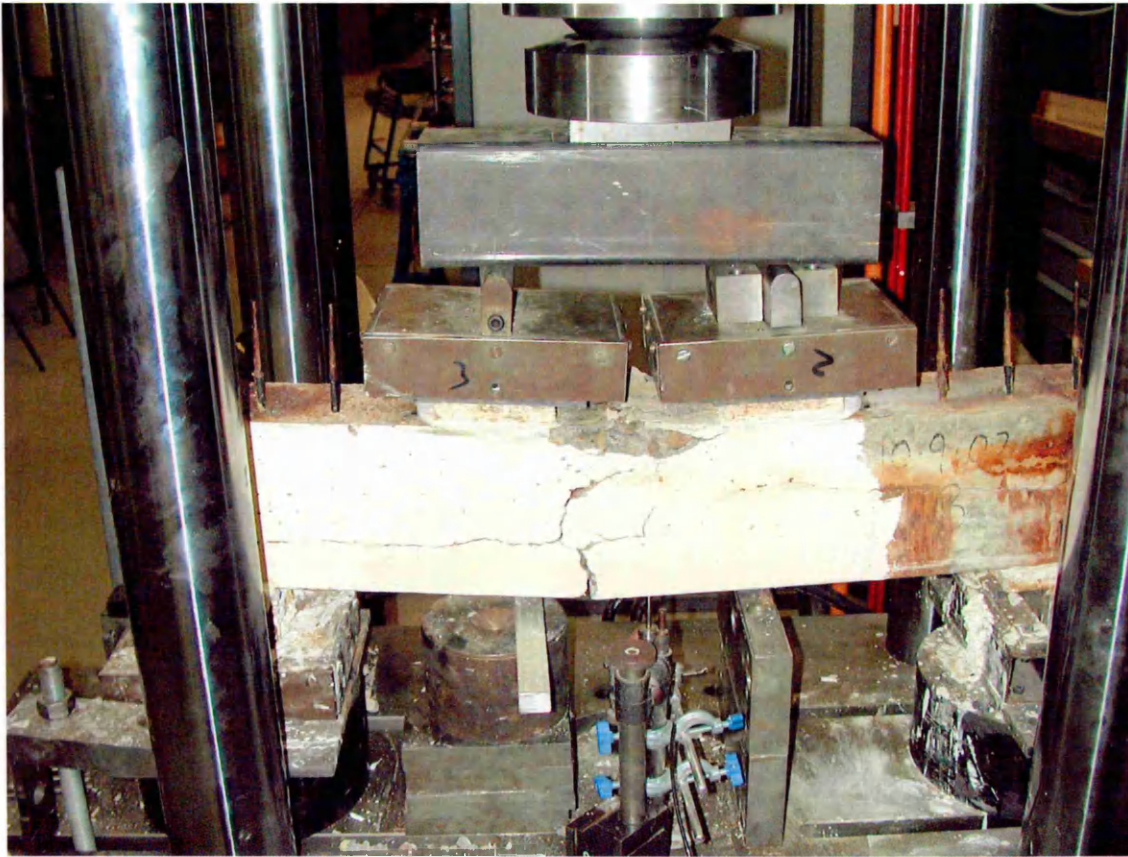


Figure 6.5 Beam in the loading rig during testing

The load was applied with a hydraulic pump and jack reacting against a cross head which was tied down using two Macalloy bars. A 3000 kN capacity load cell was placed in line with the loading jack to measure the applied load. The loading rig had a maximum capacity of about 150 kN.

The behaviour of the beam was monitored using a Celesco displacement gauge placed under the beam. The load cell and the displacement gauge were powered and monitored using an Orion data logging system. Figure 6.5 shows the loading configuration and instrumentation used for the load tests.

For the first set of eight beams (2T8 longitudinal reinforcement), the position of the load was applied 250 mm from the support (i.e. a shear span of 250 mm). The second set of eight beams (with 2T12 longitudinal reinforcement) were tested at the same shear span (250 mm). This shear span was chosen so that the theoretical failure mode was flexure. These tests were used to determine whether the mode of failure changed from flexure to shear as the level of corrosion in the shear reinforcement increases.

#### **6.4 Test results and discussion**

All the beams were corroded as described in Section 6.3.2. The beams were corroded in series of six, each series containing two beams of the same target corrosion. Details of the overall effect of the corrosion are given in Tables 6.1 and 6.2. The designation used in this thesis to describe each beam is of the form 2T8/0+12D6/0/50 or 2T12/0+12D6/0/50, as given in column 1 in Table 6.1 and 6.2. The first part refers to the number, type and diameter of main steel e.g. 2T8 or 2T12 (deformed bars) with no corrosion and hence /0, whereas in the second part of the identification, 12D6 is the number type and diameter (plain rolled mild steel) of the shear reinforcement. The target corrosion of the shear reinforcement was 0%, 5%, 10% and 15%, based on weight loss and this is indicated in the identity e.g. 12D6/0 (i.e. 0% corrosion or control). The cover to the shear reinforcement is 50 mm for all beams.

Subsequent to the load tests, the beams were demolished and the reinforcement was recovered for visual examination and evaluation of the weight loss resulting from the corrosion process. The weight loss recorded in Tables 6.1 and 6.2 was determined by taking 350 mm of corroded lengths of the shear reinforcement and de-scaling them

Table 6.1 Beam Series II – Corrosion details and load behaviour of beams with shear reinforcement corrosion (2T8)

Beam number	Corrosion details				Load behaviour		
	Weight of shear reinforcement before corrosion gr (2)	Weight of shear reinforcement after corrosion gr (3)	Weight loss gr (4)	Actual corrosion % (5)	$P_{ult}$ kN (6)	$P_{ult} / P_{con}^*$ % (7)	Mode of failure (8)
(1)							
2T8/0+12D6/0/50	–	–	–	0	40.00	96.7	Flexure
2T8/0+12D6/0/50	–	–	–	0	42.70	103.3	Flexure
2T8/0+12D6/5/50	982.0	920.9	61.1	4.9	41.11	99.4	Flexure
2T8/0+12D6/5/50	987.5	872.2	115.3	9.2	40.59	98.2	Flexure
2T8/0+12D6/10/50	990.2	872.6	117.6	9.4	39.09	94.5	Flexure
2T8/0+12D6/10/50	981.7	859.5	122.2	9.8	39.71	96.0	Flexure
2T8/0+12D6/15/50	980.4	746.0	234.4	18.7	35.07	84.8	Shear
2T8/0+12D6/15/50	981.6	691.3	290.3	23.2	34.44	83.3	Shear

\* $P_{con}$  is the average of the ultimate loads for the control (0% corrosion beams)

Table 6.2 Beam Series II – Corrosion details and load behaviour of beams with shear reinforcement corrosion (2T12)

Beam number	Corrosion details				Load behaviour		
	Weight of shear reinforcement before corrosion gr (2)	Weight of shear reinforcement after corrosion gr (3)	Weight loss gr (4)	Actual corrosion % (5)	$P_{ult}$ kN (6)	$P_{ult} / P_{con}^*$ % (7)	Mode of failure (8)
(1)							
2T12/0+12D6/0/50	1025.1	–	–	0	78.30	95.8	Flexure
2T12/0+12D6/0/50	1029.6	–	–	0	84.14	103.0	Flexure
2T12/0+12D6/5/50	1021.5	–	–	0	82.70	101.2	Flexure
2T12/0+12D6/5/50	1024.2	1013.7	10.5	0.66	79.70	97.5	Flexure
2T12/0+12D6/10/50	1032.2	1014.4	17.8	1.11	81.50	99.7	Flexure
2T12/0+12D6/10/50	1022.3	994.0	28.3	1.77	76.50	93.6	Flexure
2T12/0+12D6/15/50	1020.0	978.8	41.2	2.58	69.40	84.9	Flexure
2T12/0+12D6/15/50	1029.3	931.5	97.8	6.12	55.80	68.3	Flexure

\* $P_{con}$  is the average of the ultimate loads for the control (0% corrosion beams)

using Clark's solution to remove the corrosion products. The recorded weight loss represents the overall section loss in the shear reinforcement. The resulting degree of corrosion in this investigation,  $2RT/D$  %, ranged between 0% (control) and 23.2% (column 5, Table 6.1 and 6.2). The scatter in the measured weight loss figures results from the accelerated corrosion set up as described in Section 5.4 and shown in Figure 5.6.

The corrosion of each beam was monitored as the corrosion process proceeded. Longitudinal and vertical cracking of the cover concrete occurred, depending on the degree of corrosion of the shear reinforcement. It was difficult to observe the development of cracks due to the corrosion products in the salt bath obscuring the view. Nevertheless, it was possible to determine when rust staining first appeared and when significant corrosion cracking developed. It was then possible to relate the visual evidence of corrosion to the estimated section loss which was calculated on the basis of linear section loss during the corrosion process. The following conclusions were made:

- First visual signs of corrosion were the formation of rust spots on the concrete corresponding to positions of the links; this occurred at 0.5% to 3.5% section loss;
- Whilst some minor pitting occurred, the corrosion was generally uniform, with the steel section generally lost on the side of the bars closest to the cathode.

The corrosion damage was generally spread along the length of the bars. Where serious section loss occurred, it was in the form of localized pitting corrosion rather than general corrosion. This mainly occurred at higher percentages of corrosion. For the purpose of calculations general rather than pitting corrosion was assumed. The ultimate load at failure is given in column 6, Table 6.1 and 6.2. Column 7 in Table 6.1 and 6.2 shows  $P_{ult} / P_{con}$ , where  $P_{ult}$  is the ultimate load obtained from testing the beams in the

laboratory (those exhibiting shear reinforcement corrosion) and  $P_{con}$  is the average failure load of control specimens (0% corrosion to the shear reinforcement). Column 8 in Table 6.1 and 6.2 indicate the failure mode. Further analysis of the results will be given in Chapter 9.

## 6.5 Conclusions

These conclusions were drawn from the tests reported in this chapter.

- For shear reinforcement corrosion, staining first occurred at about 1% corrosion, with cracking occurring at about 3%;
- Shear reinforcement was very susceptible to corrosion at bends. For the majority of corroded specimens, there were a few links which suffered 100% local section loss in these areas as the bends have been work hardened and therefore more susceptible to corrosion;
- The beams with the most severe corrosion suffered significant strength loss. In most of the cases of severe strength loss, failure was precipitated as a result of local section loss;
- The presence of shear reinforcement helped maintain integrity of the beam even when they were severely corroded;
- Shear reinforcement with the least cover were more susceptible to loss of bond due to corrosion. The possibility of bond failure can be identified by the presence of serious corrosion cracking.

### ***Influence of Main and Shear Reinforcement Corrosion on Structural Performance (Series III)***

#### **7.1 Introduction**

In the beams subjected to corrosion, an account has been given to the possible changes of the failure mechanisms. In fact, as highlighted by some of experimental tests<sup>85</sup>, beams designed to obtain bending failure can show shear collapse for certain levels of the rebars and stirrups corrosion. Similarly, a ductility base design can be destroyed by brittle failure when corrosion attack induces strain localisation in the rebars<sup>122</sup>. Consequently a preliminary investigation has been carried out aiming to highlight the failure mechanism when varying the geometrical factors and percentage of corrosion. In agreement with the results of the literature, the following effects of corrosion have been considered: variation of the diameter of the steel rebars, diameter reduction of the main and shear reinforcement due to corrosion and concrete cover variation.

#### **7.2 Objectives of test programme**

This series of beam tests (test Series III) was developed to determine the influence of both main and shear reinforcement corrosion on the structural performance of reinforced concrete beams. In these beams, the structural performance was affected not only by loss of steel cross section, but also by impairment of the bond between the reinforcement and the concrete.

### **7.3 Experimental programme**

The work in this chapter reports an experimental study aimed at evaluating the influence of rebar corrosion on the collapse mechanism of reinforced concrete beams. Eighteen additional (to those already tested in Series I and II) beams were designed, constructed, artificially corroded and tested. Four point bending tests were performed with the loading span appropriately selected to display transfer from flexure to shear failure. The comparisons allow evaluating the combined role of corrosion of main and shear reinforcement corrosion in reducing the structural capacity in view of suggesting appropriate calibration of conventional design formulas for corroded structures.

#### **7.3.1 Beam specimens**

Details of the beams used in the experimental programme are given in Figure 7.1. Three groups of corroded beams were chosen as test specimens for the final programme of testing. These comprised of 2T8/0 (5, 10, 15%) and either 12D6/5/50, 12D6/10/50 or 12D6/15/50. Concerning beam size, span, loading conditions and reinforcement detailing, all beams in the final testing programme followed precisely those tested in Series I and Series II stages. The important exceptions, were that each beam was reinforced longitudinally with two 8 mm diameter deformed reinforcing bars, which were corroded in increments of 5% (i.e. 0%, 5%, 10% and 15%) and the shear reinforcement were 6 mm diameter plain bars at 65 mm spacing, which were also corroded to the same degree as the main bars.

#### **7.3.2 Material properties**

The concrete mix proportions used in the construction of Series III test beams is given

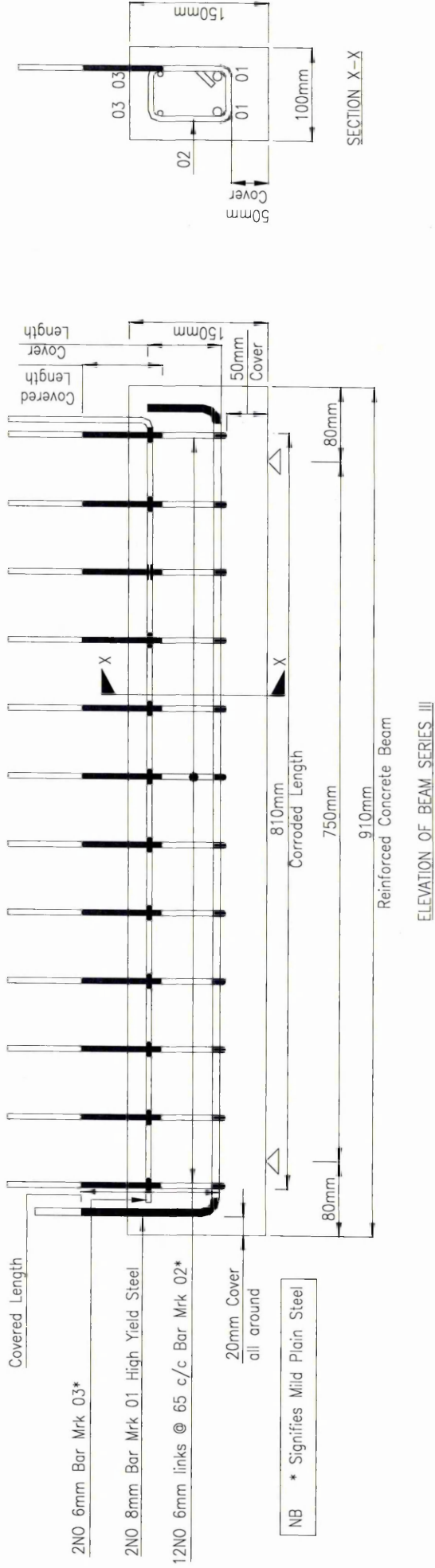


Figure 7.1 Geometry of the beam Series III used for the design

in Chapter 4. Also, the reinforcement used in Series III was found to exhibit a slightly different strength to those used during the test Series I and II, shown in Appendix A. In order to eliminate an over reinforced failure, the concrete mix proportions were chosen in order to ensure an under reinforced failure.

Care was taken to ensure that all beams in the series contained concrete of the same quality. Cubes were taken at the time of casting from all mixes and tested to determine the concrete strength at the time of testing the beams. In all, 108 cubes were tested. The concrete strength used in the analysis was, therefore, the actual strength at the time of testing and not the 28 day design value.

### **7.3.3 Instrumentation**

The use of instrumentation and the range of measurements made during Series III testing were similar to those of the Series I and II test beams as described below:

- For all beams, only the applied load and the mid-span deflections were recorded;
- Deflections were measured at mid-span for all beams with the use of a single potentiometer displacement transducer connected to a displacement transducer power supply and conditioning unit connected to the automatic data logger.

### **7.3.4 Test configuration and procedure**

Thick steel plates of 50 mm width were stuck to the upper and underside of the beam at the positions of load and support with a layer of quick hardening Plaster of Paris, for the stable bedding of the beam hinged supports.

Load was applied at a rate 5 kN/min. The deflection readings were taken constantly as the load increased. The appearance of the first crack was carefully observed and the

load was recorded. The possible appearance and propagation of all cracks were marked on the surface of the beam and recorded against the load. At onset of failure, the hydraulic jack was pumped at a uniform rate. Load and central deflection measurements at the failure were then recorded automatically.

### 7.3.5 Process of accelerated corrosion

The main bars and the shear reinforcement served as the anode and the hanger bars with an additional external copper plate served as a cathode. Electrical continuity between the reinforcing bars was ensured by connecting the exposed bars with screw connectors (see Figure 7.2).



Figure 7.2 Exposed main and shear reinforcement

The shear reinforcement were connected to the main bars using plastic cable ties. The electrical circuit between the corroded shear reinforcement and corroded main reinforcement was broken. This was ensured by using adhesive lined heat shrinkable tubing over the shear reinforcement at the points of contact with the main bars (see Figure 7.1 and 7.2). In order to investigate the corrosion of the links, the part of contact of the shear reinforcement with the top hanger bars was also covered with adhesive lined heat shrinkable tubing, so that the electrical circuit was also broken. As the anode area was greater (main and shear reinforcement) than the cathode (top hanger bars), an additional cathodic area which consisted of a copper plate was also provided.

As the level of electrolyte, in this case 3.5% CaCl<sub>2</sub> solution, was maintained at 150 mm, precaution was taken to sleeve part of the stirrups to avoid a short circuit and also prevent intensive corrosion on the border of the different environment, which was created where the bars exited the concrete.

Specimens were cured for 28 days under water, before galvanostatic corrosion was performed using equipment as shown in Figure 7.3 in combination with a linear power supply shown in Figure 7.4. Hence, the main bars and the shear reinforcement were corroded independently of each other.

The current was kept at a constant value of 406 mA for the main bars and 48 mA for the shear reinforcement. The current was passed for a period of 7, 14 and 21 days for the main bars and 5, 10 and 16 days for the shear reinforcement, in addition to the seven day initiation period (Chapter 3).

A similar schedule of accelerated corrosion was applied as in Series I and II as four degrees of corrosion were targeted 0% (control), 5%, 10% and 15% loss of cross section

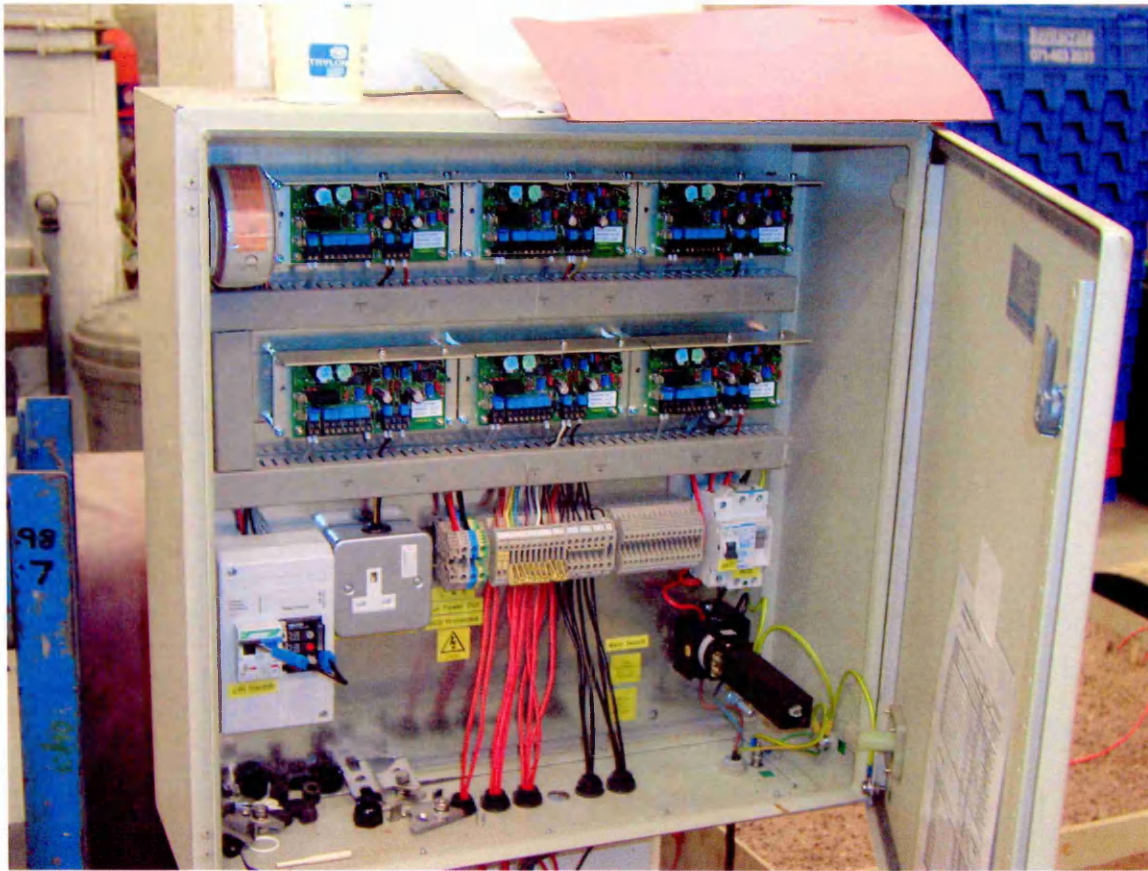


Figure 7.3 Transformer Rectifier (TR)

by weight, based on a combination of Faraday's Law and the experience of earlier investigations. Once the first set of corroded beams were tested and demolished, the time and current required to deteriorate subsequent beam specimens was reviewed. This was to ensure that steel reinforcement was sufficiently corroded to produce a level of corrosion as close as possible to the target corrosion.

Subsequent specimens were then removed from the corrosion tank and tested. After all tests had been completed, the reinforcing bars were removed from the specimens, and

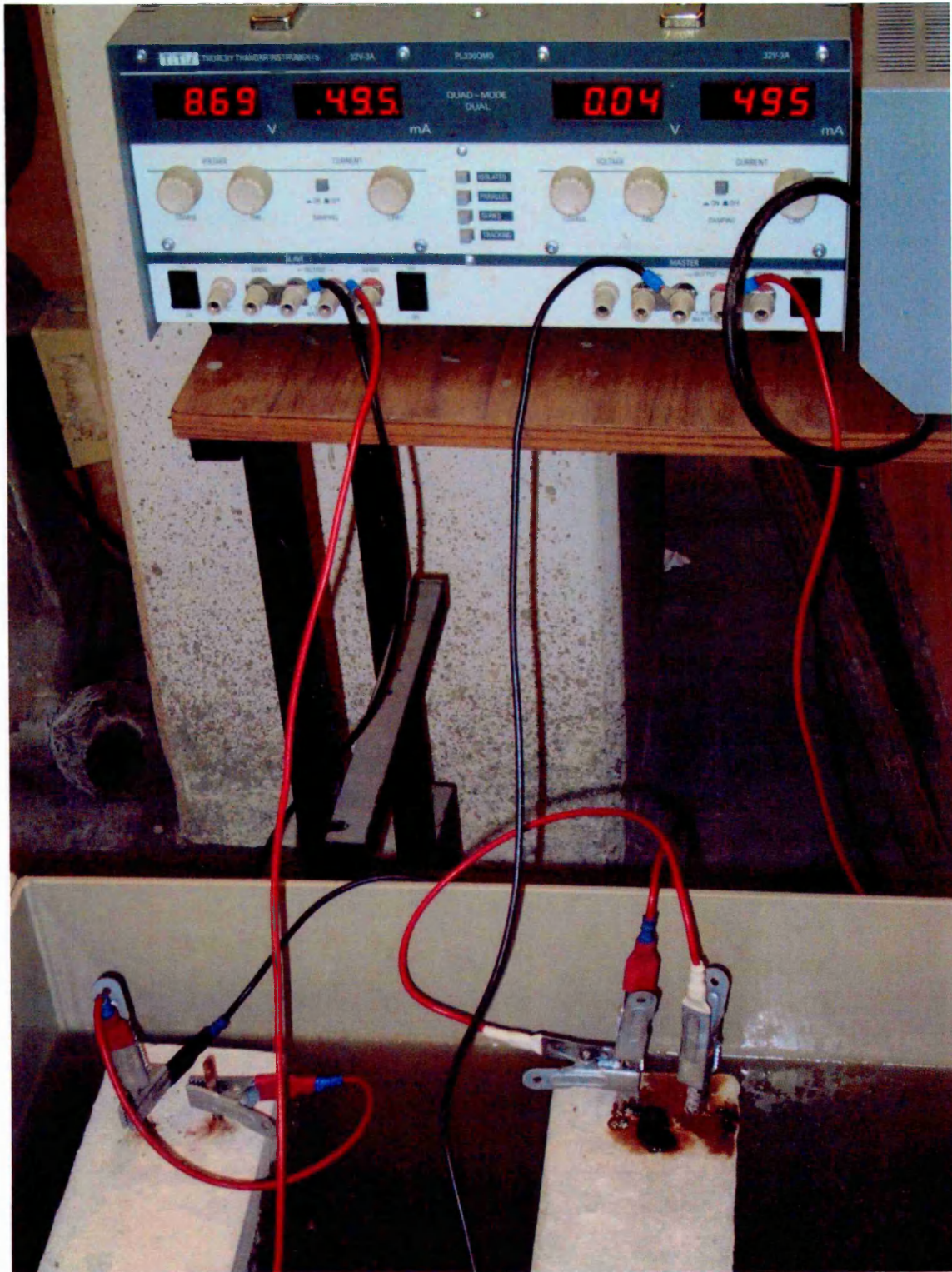


Figure 7.4 Precision linear power supplies

the main bars were wire brushed and the shear reinforcement chemically cleaned with diammonium hydrogen citrate and the weight loss due to corrosion was measured.

#### **7.4 Influence of corrosion on the flexural performance**

The effect of corroded main steel reinforcement (2T8) and influence of shear links reinforcement corrosion (12D6) on the residual capacity were examined in this test series.

Figure 7.5 shows the cracks that are formed in the beams as a result of the galvanostatic corrosion process. A similar behaviour was observed during the corrosion of the all test Series III beams. The cracks were first formed along the stirrups and then along the main reinforcing bars.

Subsequent to the load tests, the beams were demolished and the reinforcement was recovered for visual examination and evaluation of the weight loss resulting from the corrosion process (Figures 7.6 and 7.7). Table 7.1 show the results from testing 18 beams in flexure in the laboratory. These nominal degrees of corrosion were approximate and are used in the designation of the beam identification listed in Table 7.1. Weight loss was determined by de-scaling the reinforcement, weighing the clean bars and comparing with the uncorroded steel cage (column 3 and 7, Table 7.1). This method gave the average section loss over the length of the specimen rather than the localised section loss (column 4 and 8, Table 7.1).

The corrosion of each beam was monitored using a digital voltmeter and a standard Calomel reference electrode and any drift was adjusted on a daily basis as the corrosion process proceeded. Longitudinal and vertical cracking of the cover concrete occurred

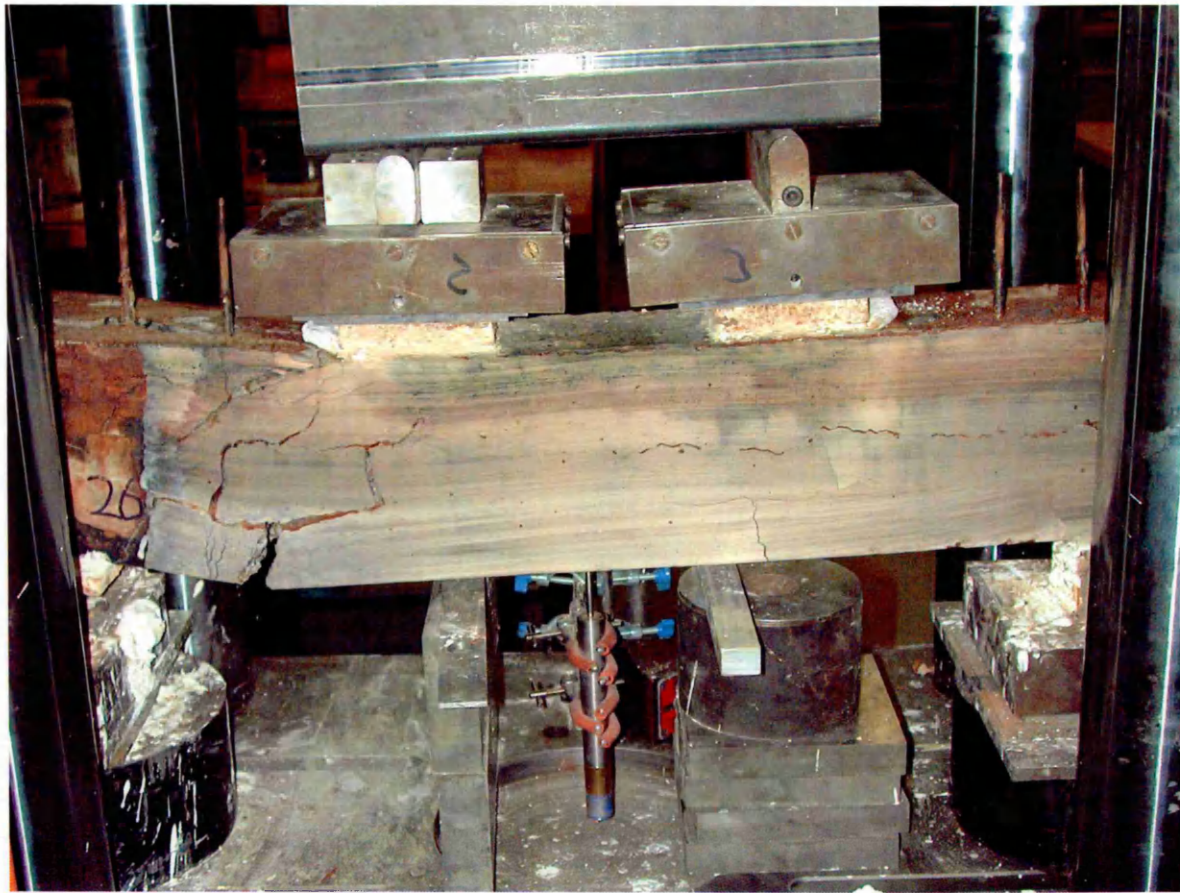


Figure 7.5 Deteriorated reinforced concrete beam exhibiting both main and shear reinforcement corrosion under test

and was dependant on the degree of corrosion of the main and shear reinforcement. It was difficult to observe the development of cracks due to the corrosion products in the salt bath obscuring the view. Nevertheless, it was possible to determine when rust staining first appeared and when significant corrosion cracking developed.

First visual signs of corrosion were the formation of rust spots on the concrete corresponding to positions of the shear reinforcement; this occurred at 0.5% to 3.5% section loss.



Figure 7.6 Deteriorated main reinforcement bars after corrosion

The reason for the early cracking in this series can be attributed to the smaller overall cover to the shear reinforcement.

Whilst some minor pitting occurred, the corrosion was generally uniform, with the steel section generally lost on the side of the bars closest to the cathode.

All beams had longitudinal cracking along the main reinforcement. Where shear reinforcement corrosion was present, vertical cracking also occurred to various degrees. The weight loss recorded in Table 7.1, columns 4 and 8 was determined by taking 810 and 350 mm of corroded lengths of the main and shear reinforcement respectively and



Figure 7.7 Shear reinforcement with most severe corrosion

de-scaling them using wire brush and Clark's solution to remove the corrosion products. The recorded weight loss represents the overall section loss in the main and shear reinforcement. The resulting degree of corrosion in this investigation,  $2RT/D$  %, ranged between 0% (control) and 25.7% for the main reinforcement and between 0% and 27.6% for the shear reinforcement (column 5 and 9 respectively, Table 7.1). The scatter in the measured weight loss figures results from the non uniformity of the corrosion, the uncertainty of the corrosion process and set up of the accelerated corrosion technique as described in Chapter 5, Section 5.4.

Table 7.1 Beam Series III – Corrosion details and load behaviour of beams with main and shear reinforcement corrosion

Beam number	Corrosion details								Load behaviour		
	Weight of main bars before corrosion gr (2)	Weight of main bars after corrosion gr (3)	Weight loss of main bars gr (4)	Actual corrosion of main bars % (5)	Weight of links before corrosion gr (6)	Weight of links after corrosion gr (7)	Weight loss of links gr (8)	Actual corrosion of links % (9)	$P_{ult}$ (10)	$P_{ult} / P_{con}^*$ (11)	Mode of failure (12)
(1)											
2T8/5+12D6/5/50	872.1	789.2	82.9	6.5	990.3	936.9	53.4	4.3	33.64	81.4	F
2T8/5+12D6/5/50	871.5	834.7	36.8	2.9	986.1	948.3	37.8	3.0	40.27	97.4	F
2T8/10+12D6/5/50	881.7	816.6	65.1	4.8	987.5	917.1	70.4	5.6	33.69	81.5	F
2T8/10+12D6/5/50	880.5	813.0	67.5	5.3	987.2	906.2	81.0	6.5	31.86	77.0	F
2T8/15+12D6/5/50	875.7	549.6	326.1	25.7	987.7	678.7	309.0	24.7	11.07	26.8	S
2T8/15+12D6/5/50	875.7	548.8	326.9	25.7	989.5	643.7	345.8	27.6	8.96	21.7	S
2T8/5+12D6/10/50	848.2	743.0	105.2	8.3	988.8	909.4	79.4	6.3	33.32	80.6	F
2T8/5+12D6/10/50	848.0	808.4	39.6	3.1	980.9	932.8	48.1	3.8	36.29	87.8	F
2T8/10+12D6/10/50	851.9	799.5	52.4	4.1	985.6	937.0	48.6	3.9	33.44	80.9	F

\* $P_{con}$  is the average of the ultimate loads for the control (0% corrosion beams)

Table 7.1 Beam Series III – Corrosion details and load behaviour of beams with main and shear reinforcement corrosion

(Continued...)

Beam number	Corrosion details						Load behaviour				
	Weight of main bars before corrosion gr (2)	Weight of main bars after corrosion gr (3)	Weight loss of main bars gr (4)	Actual corrosion of main bars % (5)	Weight of links before corrosion gr (6)	Weight of links after corrosion gr (7)	Weight loss of links gr (8)	Actual corrosion of links % (9)	$P_{ult}$ kN (10)	$P_{ult} / P_{con}^*$ % (11)	Mode of failure (12)
(1)											
2T8/10+12D6/10/50	843.6	784.0	59.6	4.7	983.9	881.1	102.8	8.2	32.65	79.0	F
2T8/15+12D6/10/50	848.6	750.0	98.6	7.8	983.3	927.5	55.8	4.5	26.69	64.5	F
2T8/15+12D6/10/50	851.6	740.2	111.4	8.8	981.6	867.4	114.2	9.1	27.25	65.9	F
2T8/5+12D6/15/50	859.5	723.9	135.6	10.7	986.5	836.0	150.5	12.0	25.32	61.2	F
2T8/5+12D6/15/50	850.5	700.8	149.7	11.8	985.8	808.1	177.7	14.2	26.56	64.2	F
2T8/10+12D6/15/50	863.8	778.6	85.2	6.7	986.3	868.1	118.2	9.4	44.04	106.5	F
2T8/10+12D6/15/50	852.4	752.3	100.1	7.9	985.3	883.2	102.1	8.2	27.54	66.6	F
2T8/15+12D6/15/50	847.6	759.9	87.7	6.9	981.8	889.6	92.2	7.4	30.54	73.9	F
2T8/15+12D6/15/50	845.7	758.1	87.6	6.9	987.2	937.6	49.6	4.0	32.11	77.7	F

\* $P_{con}$  is the average of the ultimate loads for the control (0% corrosion beams)

The corrosion damage was generally spread along the length of the bars. Where serious section loss occurred, it was in the form of localized pitting corrosion rather than general corrosion. This mainly occurred at higher percentages of corrosion. For the purpose of calculations general rather than pitting corrosion was assumed. The actual corrosion calculated as described in Chapter 4 is also given along with the ultimate load at failure (column 10, Table 7.1). Column 11 in Table 7.1 shows  $P_{ult} / P_{con}$ , where  $P_{ult}$  is the ultimate load obtained from testing the beams in the laboratory (those exhibiting main and shear reinforcement corrosion) and  $P_{con}$  is the average failure load of control specimens (0% corrosion to the main and shear reinforcement), in this case the results obtained in Chapter 5 were used. Column 12 in Table 7.1 indicates the failure mode. Further analysis of the results and failure mode will be given in Chapter 10.

### *Experimental Results and Discussion – Series I*

#### *(Main reinforcement corrosion)*

##### **8.1 Introduction**

In present day reinforced concrete design, the structure is more likely to be subjected to loads closer to the design loads, as indicated by reducing the reinforcement factor of safety from 1.15 to 1.05. It was found that, in the case of general corrosion, investigated in this study by the gravimetric method, there could be substantial reduction in the load carrying capacity and the ductility of the beams, even though the tensile strength of the bars may not be greatly affected.

Most of the papers published so far deal with the mechanism of the corrosion process, protection of structures and field survey of deteriorated concrete structures<sup>123, 124, 125, 126, 127, 128, 129</sup>. The available literature on the structural implications of corrosion on parameters like the load carrying capacity, etc. is rather limited. The results presented in this chapter will contribute to determining the influence of main steel corrosion on the residual strength of reinforced concrete beams.

##### **8.2 Aim**

The main objectives of the laboratory work in the test series were to evaluate the influence of main bar diameter subjected to different degrees of corrosion on the residual strength. This chapter includes experimental results and analytical

*(Main reinforcement corrosion)*

considerations of different parameters such as cover, uniform corrosion and different main steel diameters.

### 8.3 Critical overview of the test methodology

The set up described in Chapter 3 for inducing corrosion in reinforcement, which was employed throughout the experimental programme of this thesis, may be referred to as a driven corrosion cell, whereas a natural corrosion cell is present in the environmentally induced corrosion cell<sup>130, 131</sup> in the field. There are some differences in the mechanisms by which each of the two corrosion cells proceed. One difference is that, in a natural cell, the anodic and the cathodic reactions take place at the reinforcement surface (anodic and cathodic sites are adjacent to each other), whereas, in a driven cell, the reinforcing steel serves as the anode<sup>132</sup>. Further, in a natural corrosion cell, oxygen reduction is likely to be the predominant cathodic reaction whereas hydrogen evolution reaction is likely to be the predominant cathodic reaction in the driven corrosion cell<sup>132</sup>.

These differences in the mechanisms by which the two corrosion cells proceed can lead to significant differences in the mechanics of the corrosion product formation process. In the case of a natural corrosion cell,  $\text{Fe}^{2+}$  from reinforcement corrosion will combine with  $\text{OH}^-$  from the cathodic reaction of oxygen reduction and the corrosion products will form only at the steel–concrete interface; the surrounding concrete is to crack when the pressure build up due to the accumulation of corrosion products exceeds a critical value. On the other hand in the case of a driven corrosion cell,  $\text{Fe}^{2+}$  from reinforcement corrosion will combine with free  $\text{OH}^-$  from the immediate concrete pore solution to form the corrosion product  $\text{Fe}(\text{OH})_2$ , which will cause the pH of the pore solution to drop accordingly<sup>132</sup>. When all the free hydroxyl ions,  $\text{OH}^-$ , from the pore solution at

*(Main reinforcement corrosion)*

the steel–concrete interface are combined with  $\text{Fe}^{2+}$  to form  $\text{Fe}(\text{OH})_2$ , ferric ions,  $\text{Fe}^{2+}$ , from further corrosion at the steel surface, will travel to a distance into the concrete cover zone to combine with free  $\text{OH}^-$  at another alkaline rich location. So on and so forth, at each distance, when all of the free  $\text{OH}^-$  in the pore solution are consumed in the formation of  $\text{Fe}(\text{OH})_2$ ,  $\text{Fe}^{2+}$  from further reinforcement corrosion will travel further into the concrete cover zone in search of alkaline rich sites to combine with free  $\text{OH}^-$  to form  $\text{Fe}(\text{OH})_2$ . As a result, the formation of the corrosion product  $\text{Fe}(\text{OH})_2$  tends to move as a front in the outwards direction (away from the reinforcement–concrete interface and towards the electrolyte in the corrosion apparatus). Therefore, rust stains appear on the concrete surface after a relatively shorter period of time compared to that in the case of natural corrosion cell, and is not necessarily an indication of severe corrosion<sup>132</sup>. The rapidly changed colour of the electrolyte ( $\text{CaCl}_2$ ) in the corrosion apparatus from colourless to brownish red, which was always observed during inducing corrosion in reinforcement of all test specimens, supports the hypothesis of outward front like movement of  $\text{Fe}(\text{OH})_2$  formation.

The structural performance of corrosion damage concrete members may differ significantly depending on which type of corrosion cell is involved in the process of inducing corrosion in reinforcement. For example, in the case of a driven corrosion cell, the formation of corrosion products is not confined only to the reinforcement–concrete interface but, in fact, as described earlier, it can be occur at locations at different sites of high stress intensity due to the accumulation of corrosion products may exist. The presence of these sites of high stress intensity in the concrete cover zone can lead to possible initiation of cracks away from the reinforcement–concrete interface, and can also affect the mechanics of crack propagation in a way that the result will be more

(Main reinforcement corrosion)

severe crack patterns in the cover zone and poorer mechanical performance of the concrete member.

It may be concluded, therefore, that for the same level of reinforcement corrosion, deterioration of the concrete cover zone associated with driven corrosion cell are likely to be more severe than associated with the natural corrosion cell. Furthermore, the structural reliability of reinforced concrete beams determined on the basis of driven cells may be an under estimate of natural performance, and therefore, will be on the safe side.

It was assumed uniformity of corrosion along length of corroded bars, because the current was applied through the cage (main bars were anodic and stirrups and hanger bars were cathodic) covering the entire length of the corroding bars, it can be expected that the corrosion will be uniform along the entire embedded lengths. However, the presence of deformation and variation in permeability due to cracking resulted in some non-uniformity. It was assumed that the variation is acceptable considering the number of variables, such as non-uniformity of concrete, deformations in steel bars, and cracking of concrete.

#### **8.4 Structural performance of corrosion damaged beams under four point bending test**

Reinforced concrete beams were design and constructed as described in Chapter 5 and the results of the design are attached at the end of this thesis (see Appendix A, Tables A.1.1 to A.1.3).

*(Main reinforcement corrosion)*

The following sections describe the behaviour under load of the 910 mm beam specimens and the effect of the induced corrosion to the main reinforcement only. Strengths are related to the ultimate capacity of control (uncorroded) beams for flexure and shear. For direct comparison with the test results, mean values of strength as obtained from concrete cube and steel tensile tests were used in this analysis. For corroded beams, account was taken only of the section loss in steel cross section and for the purposes of this analysis the nominal actual section loss was used.

**8.4.1 Beam Series I reinforced with 2T8 main steel reinforcement****8.4.1.1 Load / Deflection**

Average load – deflection relationships for the beam specimens of Series I, reinforced with 2T8 tensile reinforcement are shown in Figures 8.1 to 8.3. These beams were subjected to different degrees of corrosion and were tested under four point bending. Each degree of corrosion was selected to provide a predefined percentage reduction in the rebar diameter within a short time scale. Each curve in regards to the control specimens represents the average of two beam specimens.

The load – deflection relationships for the beam specimens of Series I (2T8/Corr%) were obtained and the results are given Table 8.1. Table 8.1 shows the results from testing 30 beams in flexure in the laboratory. The cover to the main steel used in this test series was varied from 26, 36 and 56 mm (column 1). Each beam is identified by the amount of main steel, target corrosion and cover, e.g 2T8/5+12D6/0/50 indicates that the main steel is 2T8 with 5% target corrosion whereas the shear reinforcement is 12D6, remained uncorroded and the cover is 50 mm, column 2. The actual corrosion

(Main reinforcement corrosion)

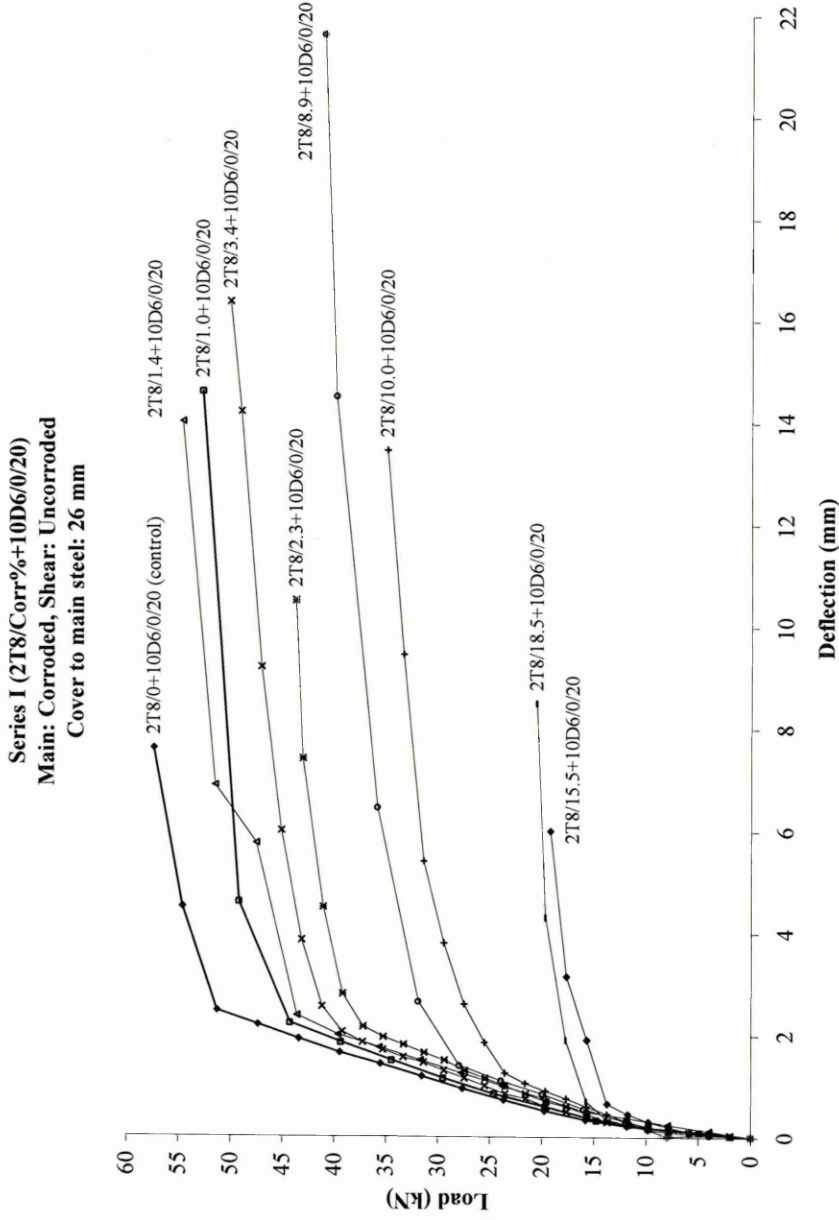


Figure 8.1 Average load – deflection curves of corroded reinforced concrete beams of Series I under four point bending test

(Main reinforcement corrosion)

Series I (2T8/Corr%+10D6/0/30)  
 Main: Corroded, Shear: Uncorroded  
 Cover to main steel: 36 mm

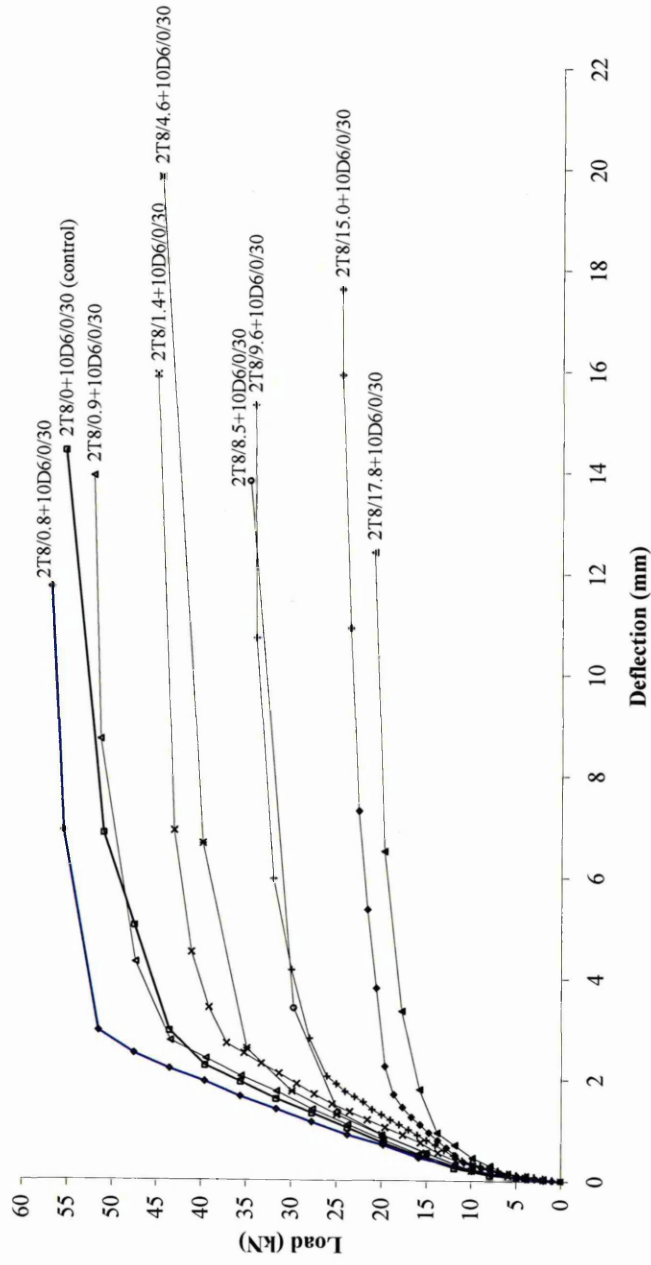


Figure 8.2 Average load – deflection curves of corroded reinforced concrete beams of Series I under four point bending test

(Main reinforcement corrosion)

Series I (2T8/Corr%+12D6(0/50))  
 Main: Corroded, Shear: Uncorroded  
 Cover to main steel: 56 mm

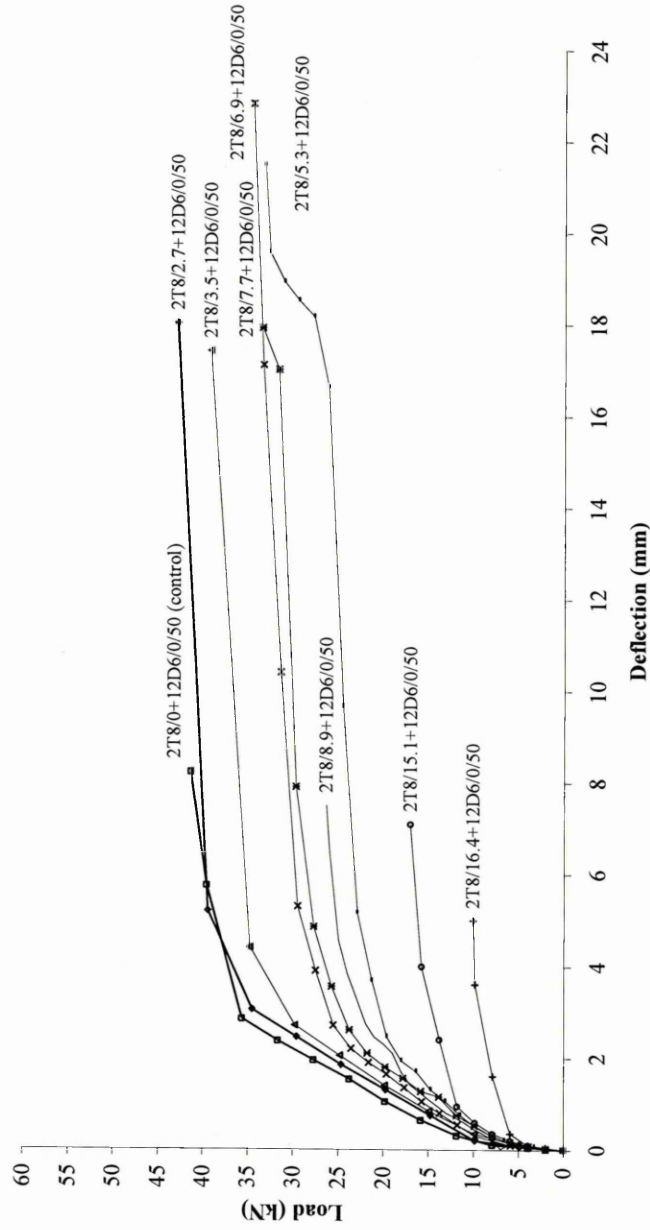


Figure 8.3 Average load – deflection curves of corroded reinforced concrete beams of Series I under four point bending test

(Main reinforcement corrosion)

Table 8.1 Beam Series I (2T8/Corr%) test results

Cover mm	Beam Identification	Actual	Stiffness	Ultimate	Failure Mode
		Main bars Corrosion		Load	
(1)	(2)	(3)	(4)	(5)	(6)
26 mm cover to main steel	2T8/0+10D6/0/20	0	17.8	57.40	Flexure
	2T8/0+10D6/0/20	0	16.5	54.10	Flexure
	2T8/5+10D6/0/20	1.0	15.5	52.75	Flexure
	2T8/5+10D6/0/20	1.4	14.8	54.70	Flexure
	2T8/5+10D6/0/20	2.3	13.1	43.78	Flexure
	2T8/10+10D6/0/20	3.4	15.2	50.12	Flexure
	2T8/10+10D6/0/20	8.9	13.7	41.10	Flexure
	2T8/15+10D6/0/20	10.0	13.1	34.98	Flexure
	2T8/15+10D6/0/20	15.5	11.2	19.23	Flexure
	2T8/15+10D6/0/20	18.5	5.6	20.57	Flexure
36 mm cover to main steel	2T8/0+10D6/0/30	0	13.9	50.40	Flexure
	2T8/0+10D6/0/30	0	13.7	55.20	Flexure
	2T8/5+10D6/0/30	0.8	14.9	56.80	Flexure
	2T8/5+10D6/0/30	0.9	12.9	52.10	Flexure
	2T8/5+10D6/0/30	1.4	11.1	45.03	Flexure
	2T8/5+10D6/0/30	4.6	12.9	44.60	Flexure
	2T8/10+10D6/0/30	8.5	12.9	34.70	Flexure
	2T8/10+10D6/0/30	9.6	10.3	34.20	Flexure
	2T8/15+10D6/0/30	15.0	8.0	24.57	Flexure
	2T8/15+10D6/0/30	17.8	5.9	20.90	Flexure

(Main reinforcement corrosion)

Table 8.1 Beam Series I (2T8/Corr%) test results (Continued...)

Cover mm	Beam Identification	Actual	Stiffness	Ultimate	Failure Mode
		Main bars Corrosion		Load	
(1)	(2)	(3)	(4)	(5)	(6)
56 mm cover to main steel	2T8/0+12D6/0/50	0	9.6	40.00	Flexure
	2T8/0+12D6/0/50	0	9.0	42.70	Flexure
	2T8/5+12D6/0/50	2.7	8.7	42.91	Flexure
	2T8/5+12D6/0/50	3.5	8.5	39.24	Flexure
	2T8/5+12D6/0/50	5.3	6.3	33.23	Flexure
	2T8/10+12D6/0/50	6.9	6.6	34.58	Flexure
	2T8/10+12D6/0/50	7.7	6.7	33.48	Flexure
	2T8/10+12D6/0/50	8.9	5.9	26.34	Flexure
	2T8/15+12D6/0/50	15.1	1.2	17.08	Flexure
	2T8/15+12D6/0/50	16.4	1.2	10.10	Flexure

(calculated as described in Chapter 3) is also given in column 3 along with the ultimate load at failure, column 5. The stiffness calculated from the slopes of the load – deflection curves (Figures 8.1 to 8.3) is shown in column 4. Column 6 in Table 8.1 shows that the failure of each beam was flexural.

The load – deflection curves of the corroded beams show that the reinforcement corrosion tends to reduce the stiffness of the concrete beam and this trend is more pronounced at higher degrees of reinforcement corrosion. For example, referring to Figure 8.1 and Table 8.1, beam 2T8/18.5+10D6/0/20 exhibits the lowest stiffness of 5.6 kN/mm, whereas the controls 2T8/0+10D6/0/20 has a stiffness of 17.75 kN/mm.

*(Main reinforcement corrosion)*

It is clear from Figures 8.1 to 8.3 that, as the degree of reinforcement increase, the average deflection at failure decreases. For example the deflection of the control 2T8/0+12D6/0/50 was 8.2 mm, whereas 2T8/16.4+12D6/0/50 was 5 mm. An explanation to this behaviour may be that the formation of micro cracks in the concrete due to reinforcement corrosion alters the mechanical behaviour of the concrete beam to an extent that causes the beam to fail before the concrete is able to develop its full plastic deformation.

The effect of corrosion degree on the overall stiffness of corroded flexural member is illustrate in Figure 8.4, which presents stiffness of corroded beams damaged by different degrees of corrosion, induced to 2T8 at different covers to the main reinforcement. Figure 8.4 clearly indicate that, for the whole range of corrosion levels employed in the investigation, the reduction in the beam stiffness due to reinforcement corrosion decreased with increasing degree of main reinforcement corrosion.

**8.4.1.2 Residual flexural strength**

It is clear from the ultimate loads given in Table 8.1 that the strength of the beams decrease with increasing main steel corrosion (compare the control load of beam 2T8/0+10D6/0/20 with that of 2T8/18.5+10D6/0/20, the ultimate load decreases from 57.40 kN to 20.57 kN). This is also applicable to the other two categories (36 and 56 mm cover to main steel, Table 8.1) which also show significant reductions in ultimate strength due to corrosion.

To gain a better understanding of the influence of corrosion on the flexural strength

(Main reinforcement corrosion)

Series I (2T8/Corr%)  
Main: Corroded, Shear: Uncorroded

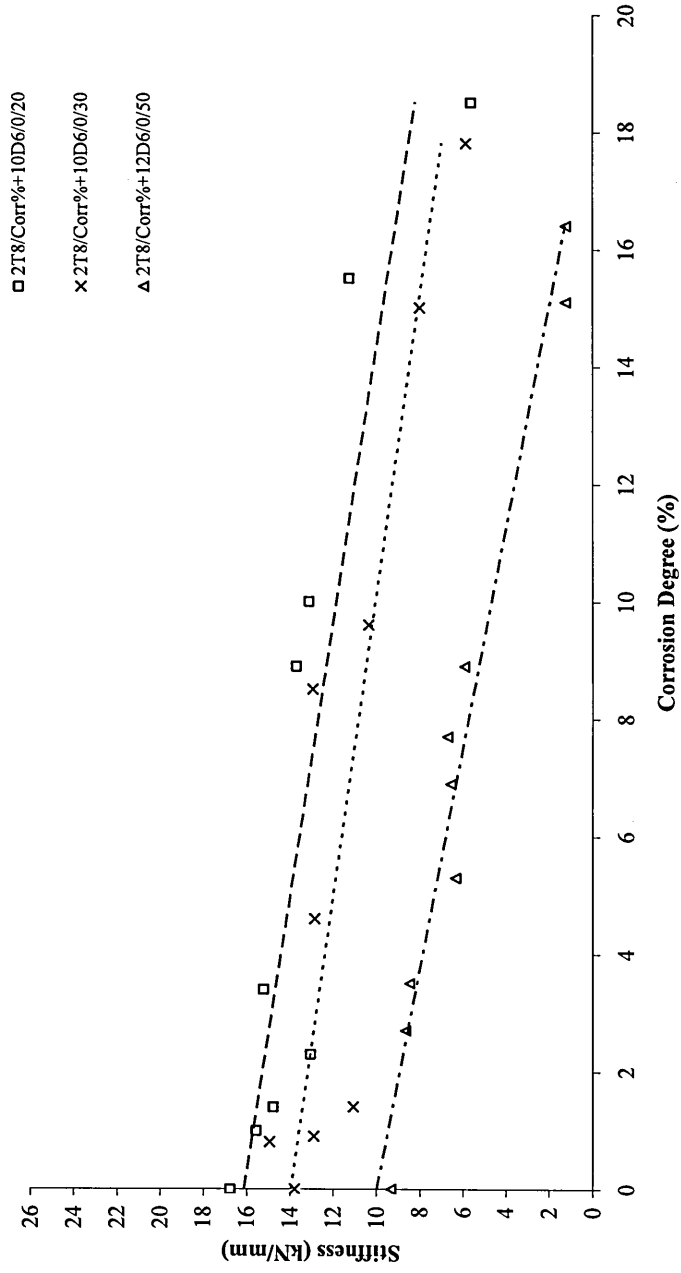


Figure 8.4 Relationship between stiffness and degree of corrosion for beam designed with 2T8

*(Main reinforcement corrosion)*

of the deteriorated beams, Figures 8.5 to 8.7 show the relationship between  $P_{ult} / P_{con}$  and the degree of corrosion to the main steel reinforcement.  $P_{ult}$  is the ultimate load obtained from testing the beams in the laboratory (those exhibiting main steel corrosion) and  $P_{con}$  is the average failure load of the control specimens (0% corrosion to the main steel reinforcement). In all cases, the actual percentage of corrosion was used in the analysis of data as opposed to the target corrosion. This led to a better correlation between flexural performance and degree of corrosion as there was some variation between target and actual values (Table 8.1). Referring to Table 8.2, comparisons are made between  $P_{ult} / P_{con}$  and the degree of corrosion at arbitrary values of 4, 10 and 16% corrosion (calculated from the best fit equations in Figures 8.5 to 8.7). It is evident from Table 8.2 that the variation of the cover results in only a small difference in residual strength at 4 and 10% for beam categories 26, 36 and 56 mm cover to the main steel (84, 86 and 90% at 4% corrosion and 63, 65 and 62% at 10% corrosion respectively). However, at 16% corrosion, the beams with 26 and 36 mm cover exhibit a residual strength of 41 and 43% respectively whereas the beam with 56 mm exhibits a lower residual strength of only 33%. Therefore, based on these results, it appears that beams designed with high reinforcement cover suffer a higher reduction in flexural strength when exposed to significant reinforcement corrosion (up to 15% loss of cross section). However, further analysis is carried out in Chapter 11 and it is shown that cover has only a secondary influence on performance when considered against other characteristics such as moments of resistance in tension and compression and percent of reinforcement.

(Main reinforcement corrosion)

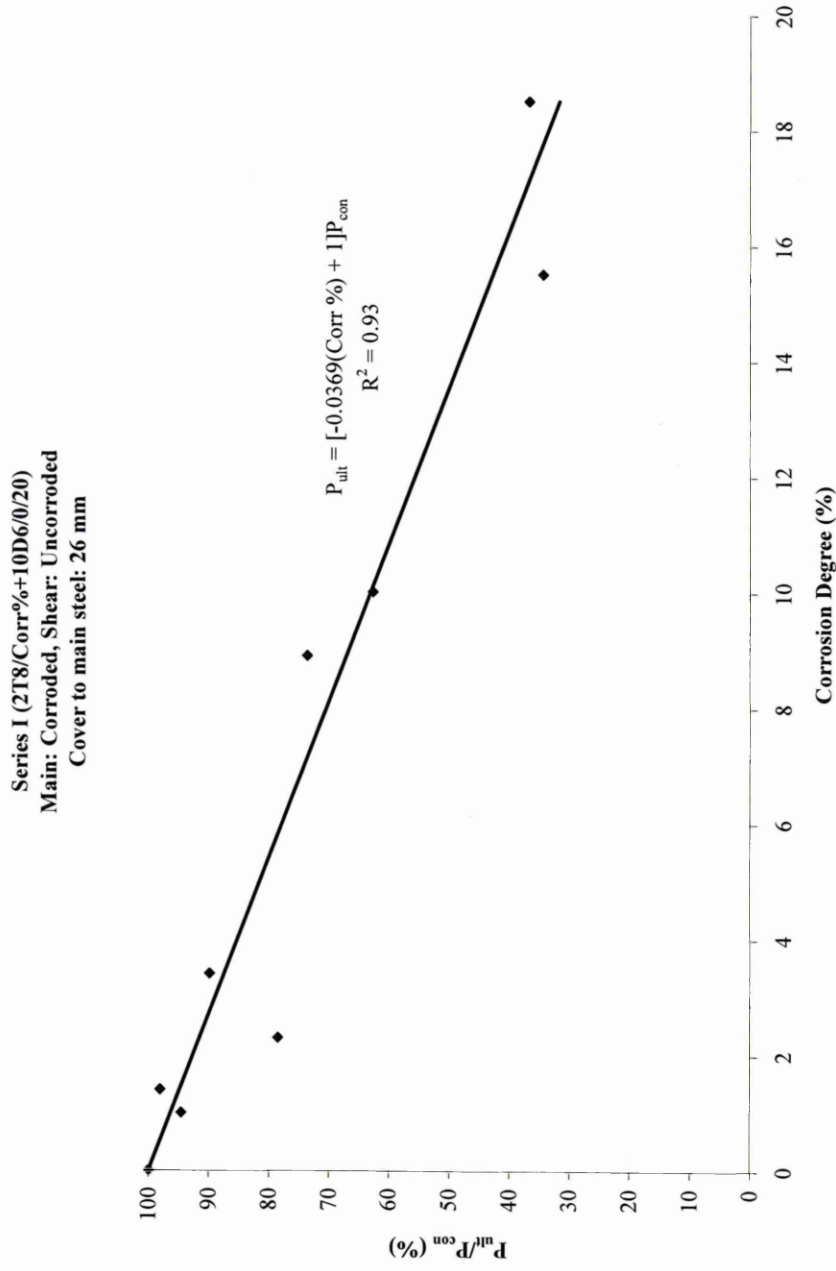


Figure 8.5 Relationship between  $P_{ult} / P_{con}$  and degree of corrosion for beam designed with 2T8 and 26 mm cover to main steel

(Main reinforcement corrosion)

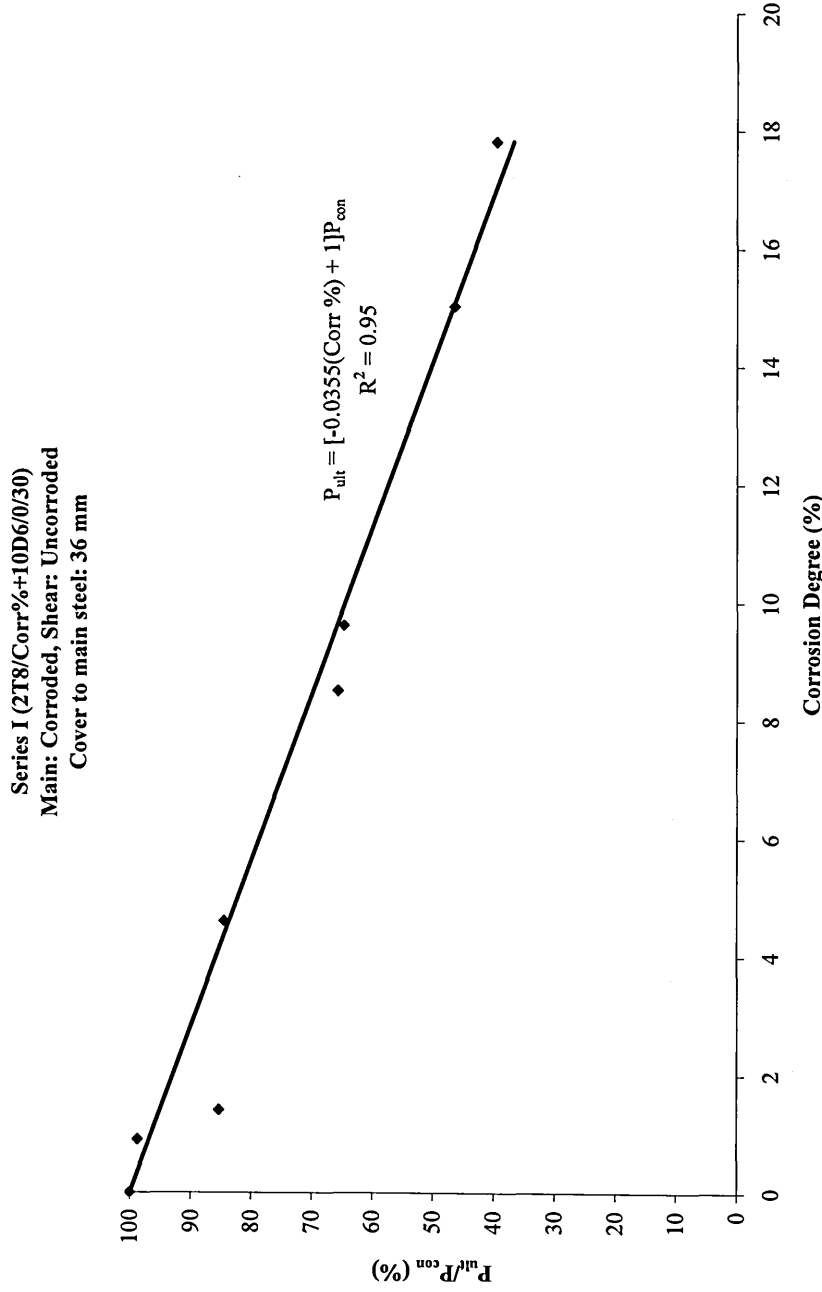


Figure 8.6 Relationship between  $P_{ult} / P_{con}$  and degree of corrosion for beam designed with 2T8 and 36 mm cover to main steel

(Main reinforcement corrosion)

Series I (2T8/Corr%+12D6/0/50)  
 Main: Corroded, Shear: Uncorroded  
 Cover to main steel: 56 mm

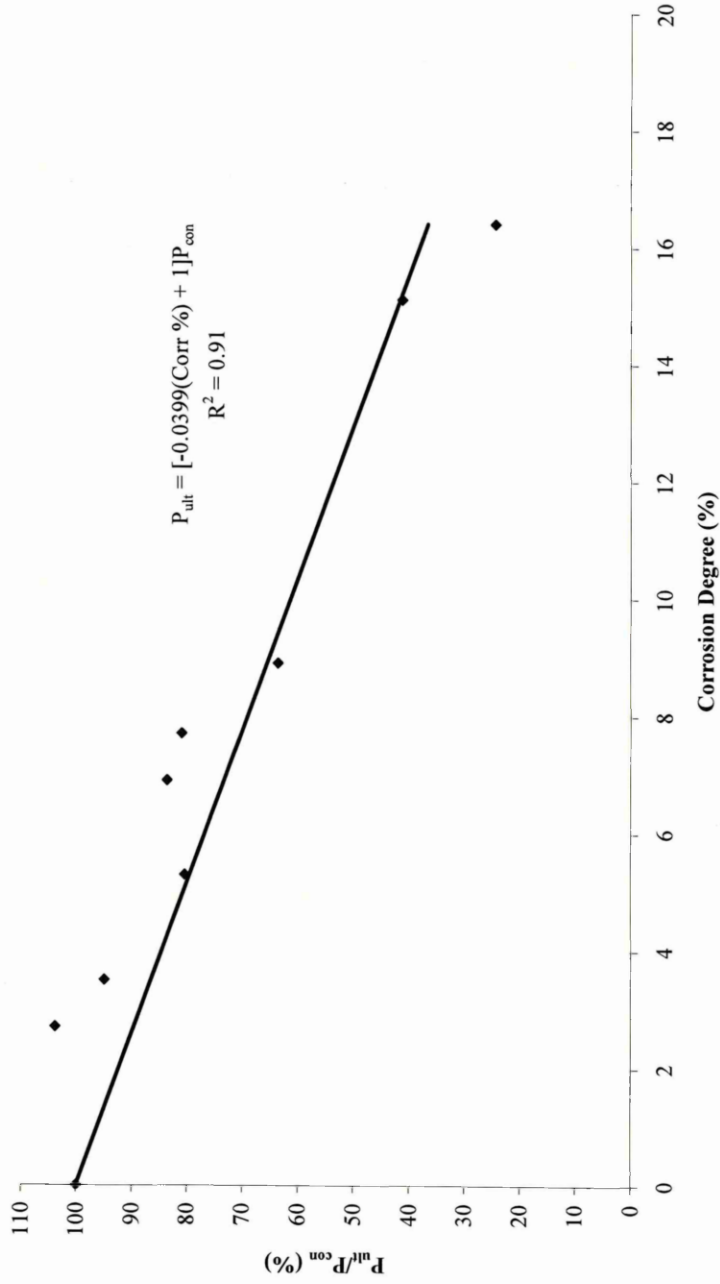


Figure 8.7 Relationship between  $P_{ult} / P_{con}$  and degree of corrosion for beam designed with 2T8 and 56 mm cover to main steel

Table 8.2 Comparison of residual strength at different covers and degrees of corrosion

Degree of Corrosion (%)	P <sub>ult</sub> / P <sub>con</sub> (%)		
	Cover to main steel		
	26 mm	36 mm	56 mm
4	84	86	90
10	63	65	62
16	41	43	33

It was also evident during testing that the time taken for the first crack to develop was dependant on cover. For example, the beams with 26 mm cover cracked at 5% corrosion whereas the beams designed with 56 mm cover cracked at a higher degree of corrosion (10%). However, cracking was more severe for beams with 56 mm cover than for beams with 26 mm cover at similar degrees of corrosion, thereby leading to a lower residual strength (see Figures 8.8 (a) to (d)).

Figures 8.5 to 8.7 clearly show that reinforcement corrosion tends to reduce the average flexural load capacity of the beam significantly. This behaviour may be attributed to reduced cross sectional area of reinforcement due to corrosion, and also to inadequate transmission of stresses between concrete and reinforcement resulting from reduced bond strength at concrete–reinforcement interface due to the accumulation of corrosion products at the interface. However, at corrosion degrees of 5% and beyond, it is clear from Table 8.1 and Figures 8.5 to 8.7 that the average flexural load capacity decreased with increasing corrosion rate, which may be explained in terms of the cracks initiated in concrete matrix due to the formation of

(Main reinforcement corrosion)



Figure 8.8 (a) Control beam crack pattern at ultimate load

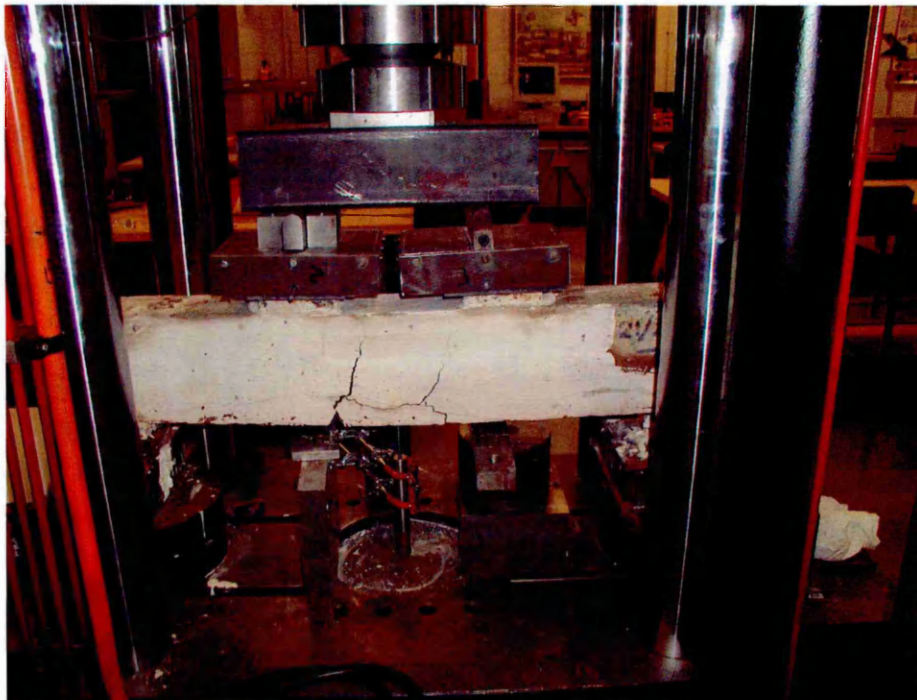


Figure 8.8 (b) Beam 2T8/18.45+10D6/0/20 crack pattern at ultimate load level

(Main reinforcement corrosion)



Figure 8.8 (c) Beam 2T8/17.76+10D6/0/30 crack pattern at ultimate load level



Figure 8.8 (d) Beam 2T8/16.35+12D6/0/50 crack pattern at ultimate load level

## (Main reinforcement corrosion)

corrosion products becoming wider and increased in number with higher corrosion rates, resulting in more deterioration in bond strength.

The relation between  $P_{ult}$  and  $2RT/D$  % was fitted by a linear relationship given as follows:

$$P_{ult} = [\beta \times (\text{Corr \%}) + 1] P_{con}$$

where

$P_{ult}$  is the failure load of the corroded beams

$\beta$  is the slope

Corr % is degree of corrosion of the main reinforcement

$P_{con}$  is the failure load of the control beams

Regression analysis of the test data gave the correlation coefficient ranging from 0.93, 0.95 and 0.91 for covers 26 mm, 36 mm and 56 mm respectively. These good correlation coefficient indicate that there is a strong positive relationship between the ratio of flexural load of corroded beam to that of non-corroded control beam and the amount of corrosion.

The main conclusions from the results reported in this section are as follows:

- reinforced concrete beams show a loss in residual strength with increasing corrosion of the main steel reinforcement;
- the cracking in the cover concrete was more severe at 56 mm cover compared to 26 mm cover at similar levels of main steel reinforcement corrosion;
- deteriorated reinforced concrete beams in this test appear to suffer the most reduction in flexural strength when designed with high reinforcement cover

*(Main reinforcement corrosion)*

and are subjected to high levels of main steel corrosion, but more data is required.

**8.4.2 Beam Series I reinforced with 2T10 main steel reinforcement****8.4.2.1 Load / Deflection**

Similarly as in Section 8.4.1, load – deflection curves for beam Series I which were reinforced with 2T10 main steel in the tensile zone are plotted in Figures 8.9 to 8.11.

These beams were subjected to different degrees of main steel corrosion and were tested under four point bending. Each degree of corrosion was selected to provide a predefined percentage reduction in the rebar diameter within a short time scale. Each curve in regards to the control specimens represents at least the average of two beam specimens.

The load – deflection relationships for the beam specimens of Series I (2T10/Corr%) were obtained and the results are given Table 8.3. Table 8.3 showed the results from testing 36 beams in flexure in the laboratory. The cover to the main steel used in this test series was varied as reported in the previous section, from 26, 36 and 56 mm (column 1). Each beam is identified by the amount of main steel, target corrosion and cover, e.g 2T10/5+12D6/0/50 indicates that the main steel is 2T10 with 5% target corrosion whereas the shear reinforcement is 12D6, remained uncorroded and the cover is 50 mm, column 2. The actual corrosion (calculated as described in Chapter 3) is also given in column 3 along with the ultimate load at failure, column

(Main reinforcement corrosion)

Series I (2T10/Corr%+10D6/0/20)  
 Main: Corroded, Shear: Uncorroded  
 Cover to main steel: 26 mm

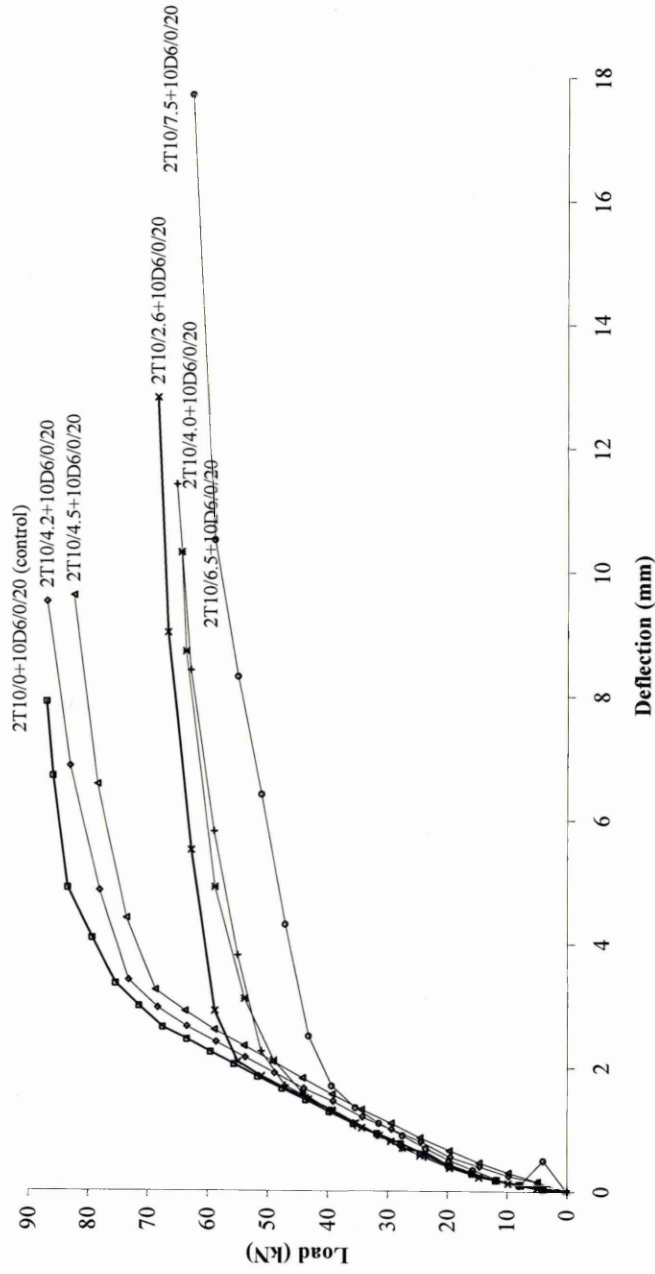


Figure 8.9 Average load – deflection curves of corroded reinforced concrete beams of Series I under four point bending test

(Main reinforcement corrosion)

Series I (2T10/Corr%+10D6/0/30)  
Main: Corroded, Shear: Uncorroded  
Cover to main steel: 36 mm

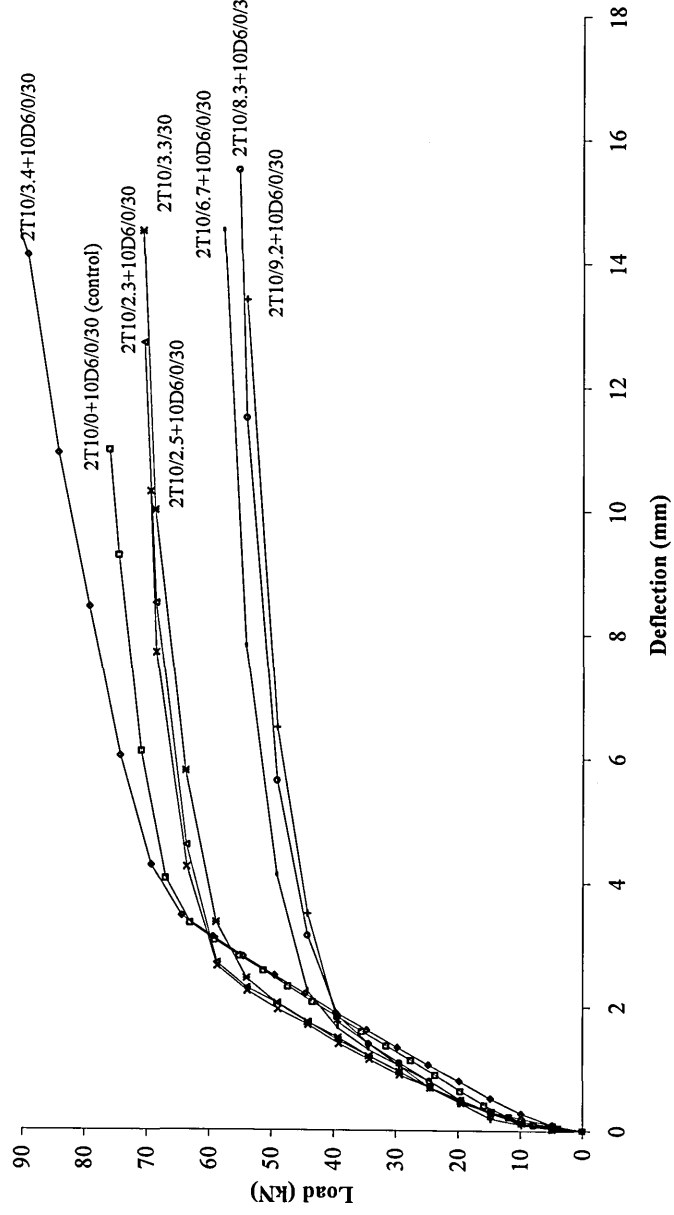


Figure 8.10 Average load – deflection curves of corroded reinforced concrete beams of Series I under four point bending test

(Main reinforcement corrosion)

Series I (2T10/Corr%+12D6/0/50)  
Main: Corroded, Shear: Uncorroded  
Cover to main steel: 56 mm

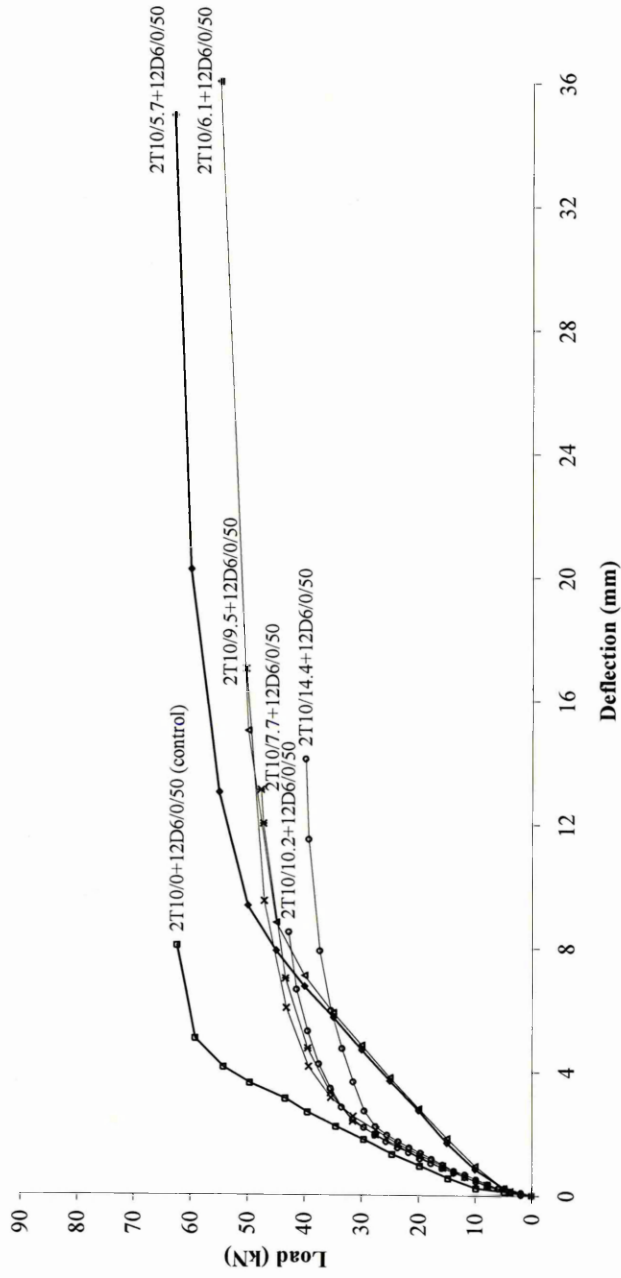


Figure 8.11 Average load – deflection curves of corroded reinforced concrete beams of Series I under four point bending test

(Main reinforcement corrosion)

Table 8.3 Beam Series I (2T10/Corr%) test results

Cover	Beam Identification	Actual Corrosion	Stiffness	Ultimate Load	Failure Mode
mm		%	kN/mm	kN	
(1)	(2)	(3)	(4)	(5)	(6)
26 mm cover to main steel	2T10/0+10D6/0/20	0	22.1	84.63	Flexure
	2T10/0+10D6/0/20	0		89.40	Flexure
	2T10/0+10D6/0/20	0		87.45	Flexure
	2T10/0+10D6/0/20	0		88.80	Flexure
	2T10/0+10D6/0/20	0		96.50	Flexure
	2T10/0+10D6/0/20	0		86.50	Flexure
	2T10/0+10D6/0/20	0		85.02	Flexure
	2T10/0+10D6/0/20	0		78.40	Flexure
	2T10/2.6+10D6/0/20	2.6	21.8	68.50	Flexure
	2T10/4.0+10D6/0/20	4.0	18.0	65.30	Flexure
	2T10/4.2+10D6/0/20	4.2	20.4	86.98	Flexure
	2T10/4.5+10D6/0/20	4.5	19.0	82.50	Flexure
	2T10/6.5+10D6/0/20	6.5	17.1	64.48	Flexure
	2T10/7.5+10D6/0/20	7.5	11.8	62.70	Flexure
36 mm cover to main steel	2T10/0+10D6/0/30	0	16.5	75.65	Flexure
	2T10/0+10D6/0/30	0		73.30	Flexure
	2T10/0+10D6/0/30	0		76.30	Flexure
	2T10/0+10D6/0/30	0		74.30	Flexure
	2T10/0+10D6/0/30	0		79.70	Flexure
	2T10/0+10D6/0/30	0		77.90	Flexure
	2T10/0+10D6/0/30	0		74.80	Flexure
	2T10/2.3+10D6/0/30	2.3	18.4	70.49	Flexure
	2T10/2.5+10D6/0/30	2.5	18.7	69.42	Flexure
	2T10/3.3+10D6/0/30	3.3	17.4	70.66	Flexure
	2T10/3.4+10D6/0/30	3.4	17.1	90.35	Flexure
	2T10/6.7+10D6/0/30	6.7	15.5	57.66	Flexure
	2T10/8.3+10D6/0/30	8.3	15.8	55.24	Flexure
	2T10/9.2+10D6/0/30	9.2	16.2	53.99	Flexure

(Main reinforcement corrosion)

Table 8.3 Beam Series I (2T10) test results (Continued...)

Cover mm	Beam Identification	Actual	Stiffness	Ultimate	Failure
		Corrosion		Load	
(1)	(2)	%	kN/mm	kN	(6)
56 mm cover to main steel	2T10/0+12D6/0/50	0	9.6	61.42	Flexure
	2T10/0+12D6/0/50	0		63.30	Flexure
	2T10/5.7+12D6/0/50	5.7	5.0	63.00	Flexure
	2T10/6.1+12D6/0/50	6.1	5.1	55.00	Flexure
	2T10/7.7+12D6/0/50	7.7	9.4	47.70	Flexure
	2T10/9.5+12D6/0/50	9.5	9.3	50.30	Flexure
	2T10/10.2+12D6/0/50	10.2	7.9	42.80	Flexure
	2T10/14.4+12D6/0/50	14.4	7.3	39.90	Flexure

5. The stiffness calculated from the slopes of the load – deflection curves (Figures 8.9 to 8.11) is shown in column 4. Column 6 in Table 8.3 shows that the failure of each beam was flexural.

The load – deflection curves of the corroded beams show that the reinforcement corrosion tends to reduce the stiffness of the concrete beam and this trend is more pronounced at higher degrees of reinforcement corrosion. For example, referring to Figure 8.9 and Table 8.3, beam 2T10/7.5+10D6/0/20 exhibits the lowest stiffness of 11.8 kN/mm, whereas the controls 2T10/0+10D6/0/20 has a stiffness of 22.1 kN/mm.

The effect of corrosion degree on the overall stiffness of corroded flexural member is illustrate in Figure 8.12, which presents stiffness of corroded beams damaged by different degrees of corrosion, induced to 2T10 at different covers to the main

(Main reinforcement corrosion)

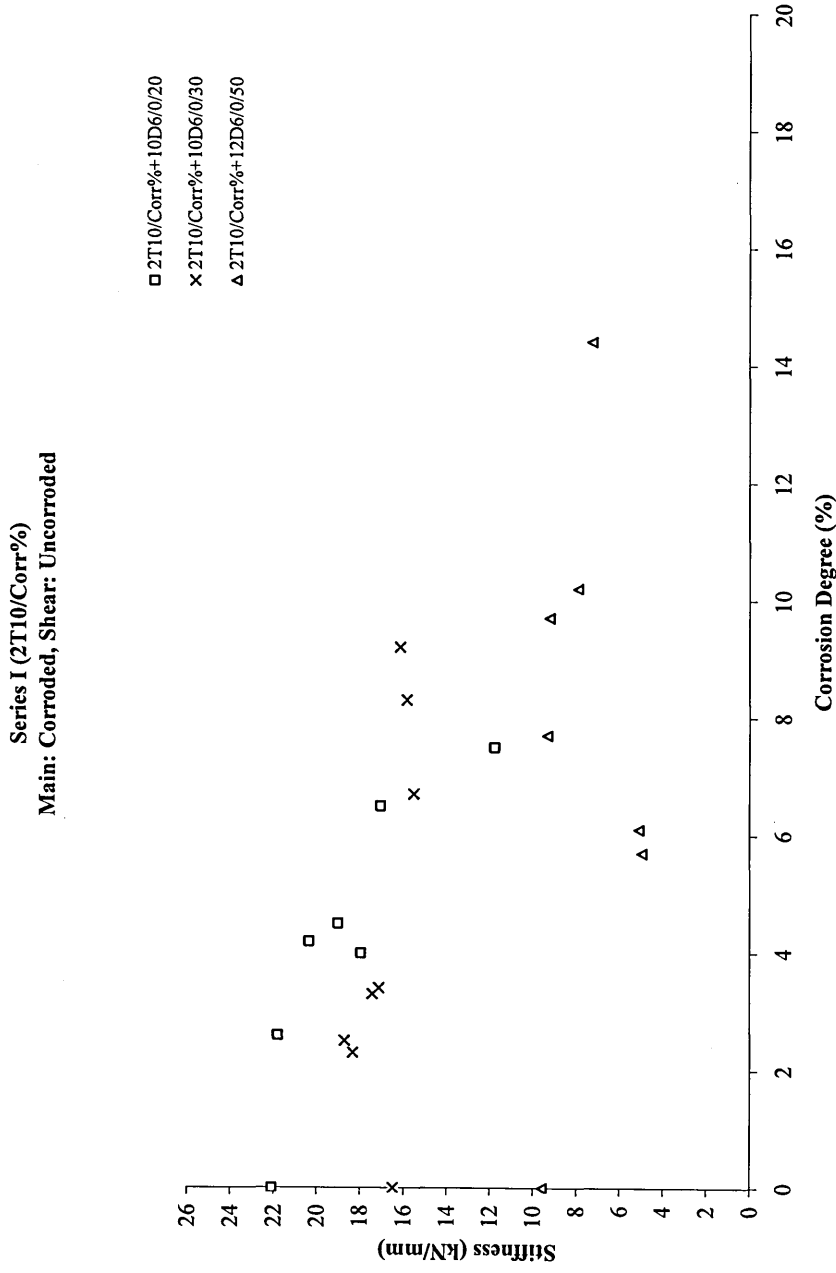


Figure 8.12 Relationship between stiffness and degree of corrosion for beam designed with 2T10

*(Main reinforcement corrosion)*

reinforcement. Figure 8.12 does not clearly indicate a relationship in support of the findings reported in Section 8.4.1.1. Further analysis, therefore, will be carried out in Chapter 11.

The experimental arrangements are shown in Figures 8.13 (a) to (c) where beams are under test. The beams are loaded according to a four point bending test to get uniform bending at the central part of the beam and uniform shear in the outer parts.

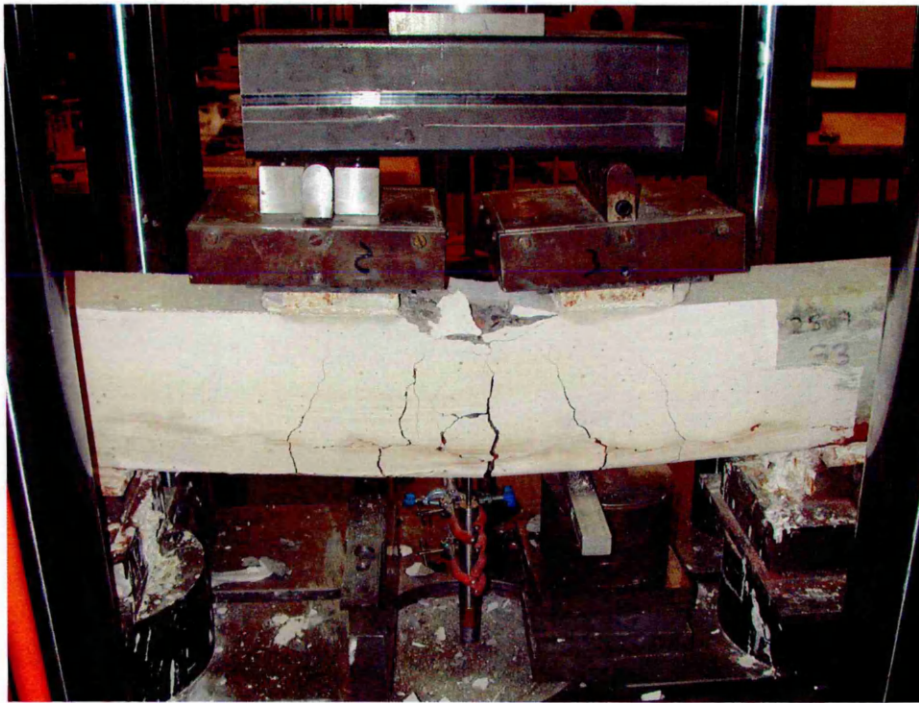


Figure 8.13 (a) Beam 2T10/7.5+10D6/0/20 crack pattern at ultimate load level

(Main reinforcement corrosion)



Figure 8.13 (b) Beam 2T10/6.7+10D6/0/30 crack pattern at ultimate load level



Figure 8.13 (c) Beam 2T10/6.1+12D6/0/50 crack pattern at ultimate load level

#### 8.4.2.2 Residual strength

It is clear from the ultimate loads given in Table 8.3 that the strength of the beams decrease with increasing main steel corrosion (compare the control load of beam 2T10/0+10D6/0/20 with that of 2T10/7.5+10D6/0/20, the ultimate load decreases from 85.00 kN to 62.70 kN). This is also applicable to the other two categories (36 and 56 mm cover to main steel, Table 8.3) which also show significant reductions in ultimate strength due to corrosion.

Figures 8.14 to 8.16 show the relationship between  $P_{ult}/P_{con}$  and the degree of corrosion to the main steel reinforcement.  $P_{ult}$  is the ultimate load obtained from testing the beams in the laboratory (those exhibiting main steel corrosion) and  $P_{con}$  is the average failure load of the control specimens (0% corrosion to the main steel reinforcement). In all cases, the actual percentage of corrosion was used in the analysis of data as opposed to the target corrosion. Referring to Table 8.4, comparisons are made between  $P_{ult}/P_{con}$  and the degree of corrosion at arbitrary values of 5, 7.5 and 10% corrosion (calculated from the best fit equations in Figures 8.14 to 8.16). It is evident from Table 8.4 that the variation of in cover results in only a small difference in residual strength at 4 and 10% for beam categories 26, 36 and 56 mm cover to the main steel (83, 86 and 88% at 5% corrosion and 74, 79 and 82% at 7.5% corrosion respectively). At 10% corrosion, the beams with 26, 36 and 56 mm cover exhibit a residual strength of 65, 72 and 76% respectively. Therefore, based on these results, it appears that beams designed with low reinforcement cover suffer a higher reduction in flexural strength when exposed to significant reinforcement corrosion (up to 10% loss of cross section).

(Main reinforcement corrosion)

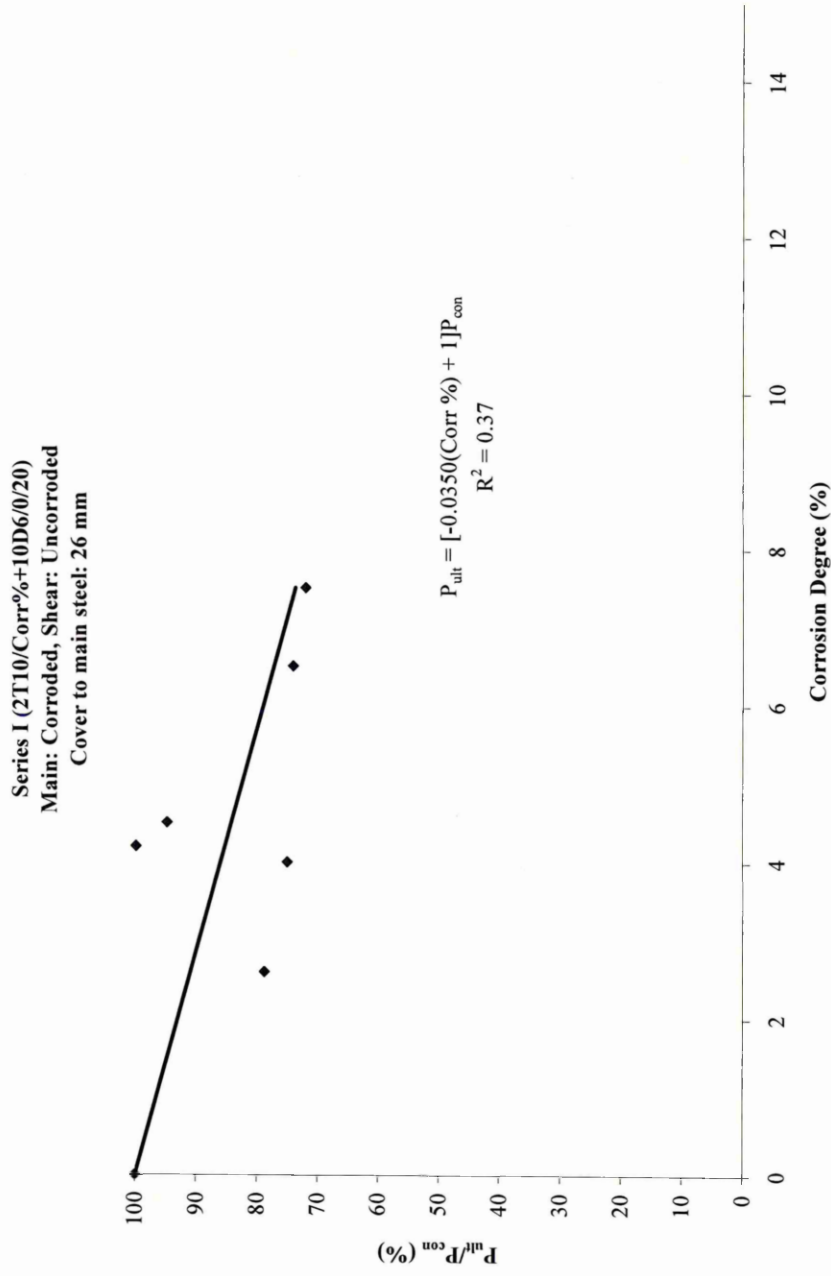


Figure 8.14 Relationship between  $P_{ult} / P_{con}$  and degree of corrosion for beam designed with 2T10 and 26 mm cover to main steel

(Main reinforcement corrosion)

Series I (2T10/Corr%+10D6/0/30)  
Main: Corroded, Shear: Uncorroded  
Cover to main steel: 36 mm

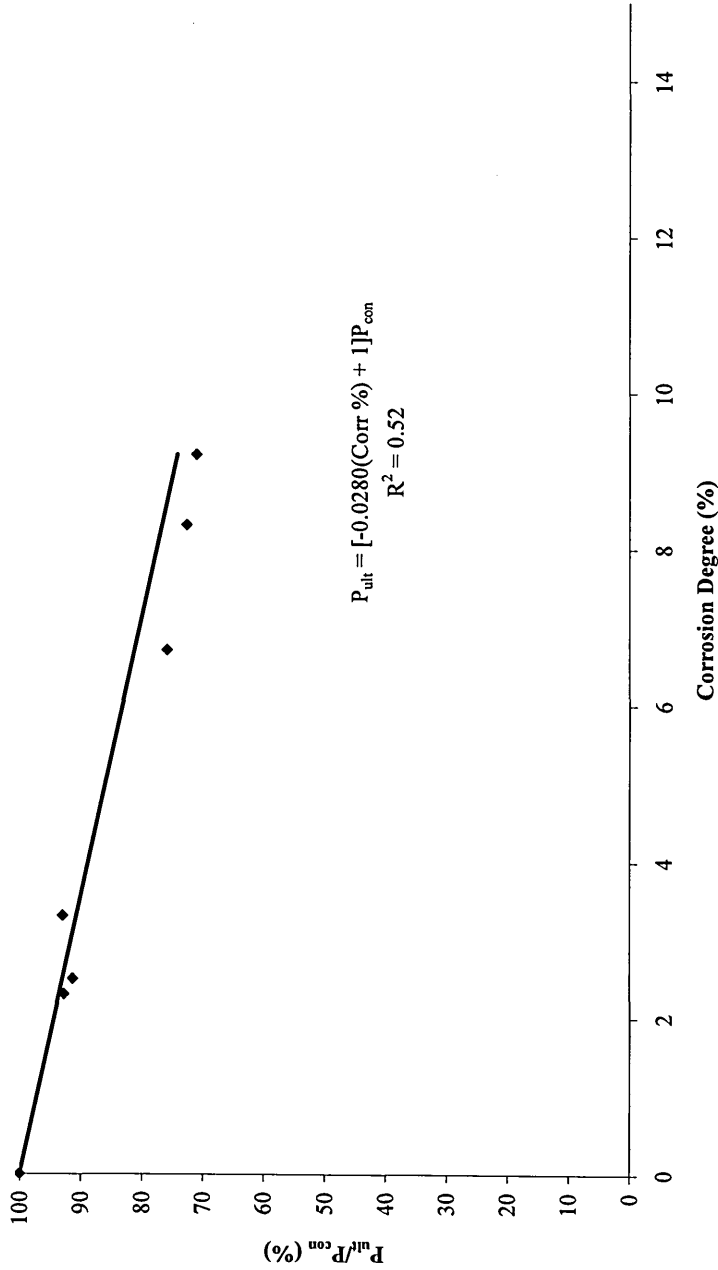


Figure 8.15 Relationship between  $P_{ult} / P_{con}$  and degree of corrosion for beam designed with 2T10 and 36 mm cover to main steel

(Main reinforcement corrosion)

Series I (2T10/Corr%+12D6/0/50)  
Main: Corroded, Shear: Uncorroded  
Cover to main steel: 56 mm

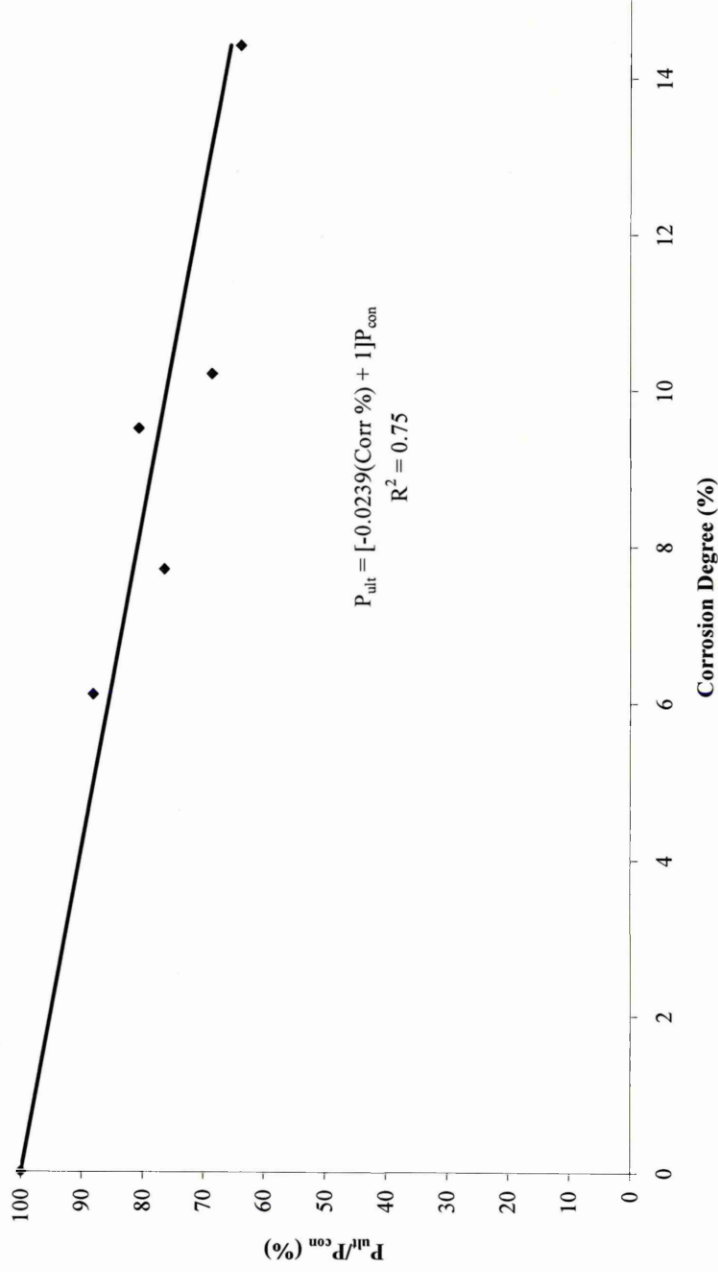


Figure 8.16 Relationship between  $P_{ult} / P_{con}$  and degree of corrosion for beam designed with 2T10 and 56 mm cover to main steel

## (Main reinforcement corrosion)

Table 8.4 Comparison of residual strength at different covers and degrees of corrosion

Degree of Corrosion (%)	$P_{ult} / P_{con}$ (%)		
	Cover to main steel		
	26 mm	36 mm	56 mm
5	83	86	88
7.5	74	79	82
10	65	72	76

The relation between  $P_{ult}$  and  $2RT/D$  % was fitted by a linear relationship given as follows:

$$P_{ult} = [\beta \times (\text{Corr \%}) + 1] P_{con}$$

where

$P_{ult}$  is the failure load on the corroded beams

$\beta$  is the slope

Corr % is degree of corrosion of the main reinforcement

$P_{con}$  is the failure load of the control beams

Regression analysis of the test data gave the correlation coefficient ranging from 0.37, 0.52 and 0.75 for covers 26 mm, 36 mm and 56 mm respectively. These correlation coefficients do not give as strong and positive relationship as it was previously found for beams reinforced with 2T8. However, this part of the results will be further analysed in Chapter 11.

The main conclusions from the results reported in this section:

*(Main reinforcement corrosion)*

- reinforced concrete beams show a loss in residual strength with increasing corrosion of the main steel reinforcement;
- the cracking in the cover concrete was more severe at 50 mm cover compared to 20 mm cover at similar levels of main steel reinforcement corrosion.

**8.4.3 Beam Series I reinforced with 2T12 main steel reinforcement**

Concrete beams reinforced with 2T12 main reinforcement were corroded to determine the residual capacity in a similar manner to those described in Sections 8.4.1 and 8.4.2. To ensure that the beams failed in flexure, double stirrups were provided to prevent shear failure.

The experimental arrangements are shown in Figure 8.17 where beam is under test.

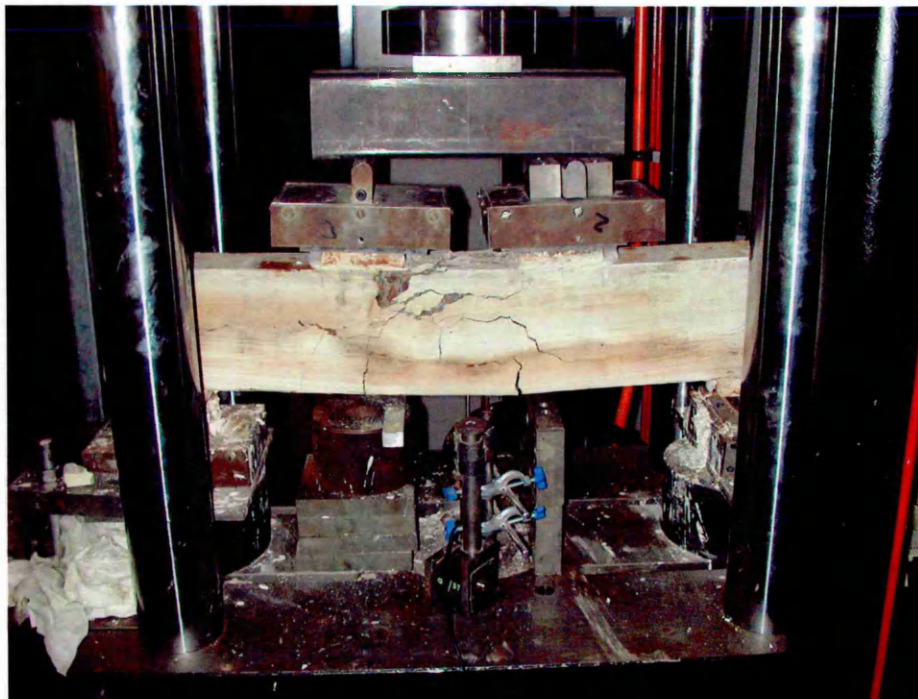


Figure 8.17 Beam 2T12/5.9/50 crack pattern at ultimate load level

#### 8.4.3.1 Load / Deflection

Figure 8.18 shows the applied load – central deflection relationships for beams reinforced with two 12 mm tensile reinforcement subjected to different degrees of corrosion at 50 mm cover to shear reinforcement (only one depth of cover was tested in this batch of beams).

It was also observed that owing to the fact that double stirrups were used in the manufacturing of the beam specimens, less severe cracking patterns of the concrete cover zone was evident. Also beam specimens of Series I were associated with nearly the same deflection compared to the controls of the same series.

The effect of corrosion rate on the overall stiffness of corroded flexural member is illustrated in Figure 8.19, which presents stiffness of corroded beams damaged by different degrees of main steel corrosion. Figures 8.19 clearly indicate that, for the whole range of corrosion levels employed in the investigation, the reduction in the beam stiffness due to reinforcement corrosion decreased with increasing degree of corrosion as expected.

#### 8.4.3.2 Flexural strength

Table 8.5 shows the results from the testing 8 beams reinforced with 2T12 in flexure in the laboratory. Each beam is identified by the amount of main steel, actual corrosion and cover (e.g. 2T12/5.9+24D6/0/50). The actual corrosion (calculated as described in Chapter 3) is also given along with the ultimate load at failure. Table 8.5 also shows that the failure of each beam was flexural.

(Main reinforcement corrosion)

Series I (2T12/Corr%+24D6/0/50)  
 Main: Corroded, Shear: Uncorroded  
 Cover to main steel: 56 mm

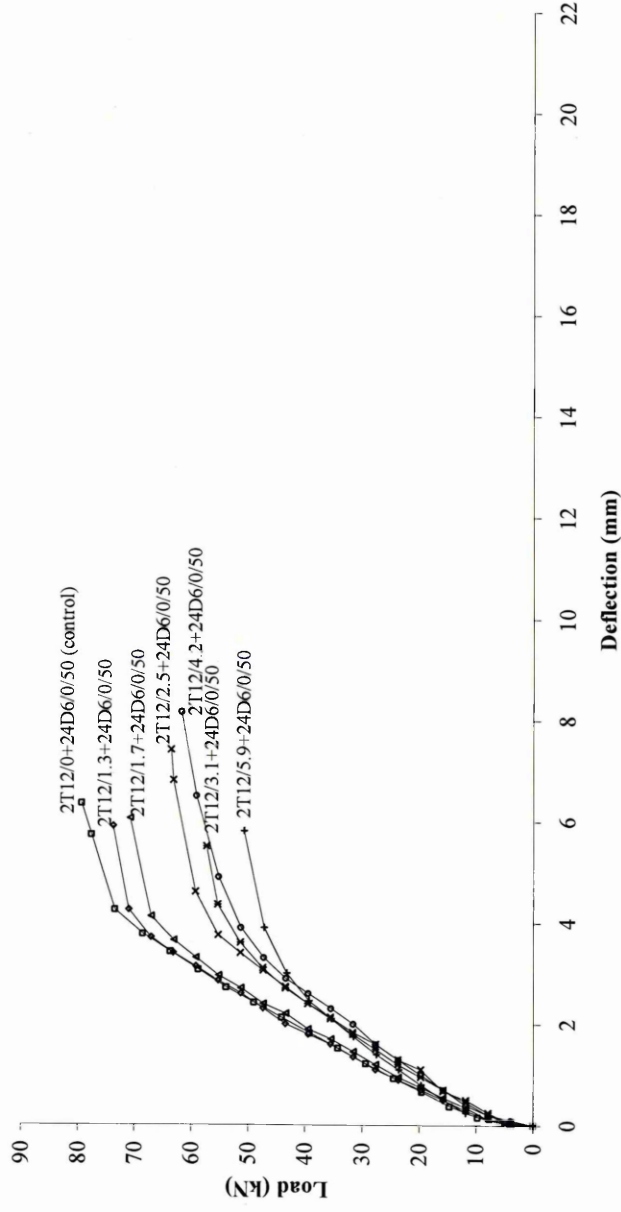


Figure 8.18 Average load – deflection curves of corroded reinforced concrete beams of Series I under four point bending test

(Main reinforcement corrosion)

Series I (2T12/Corr%+24D6/0/50)  
Main: Corroded, Shear: Uncorroded  
Cover to main bars = 56 mm

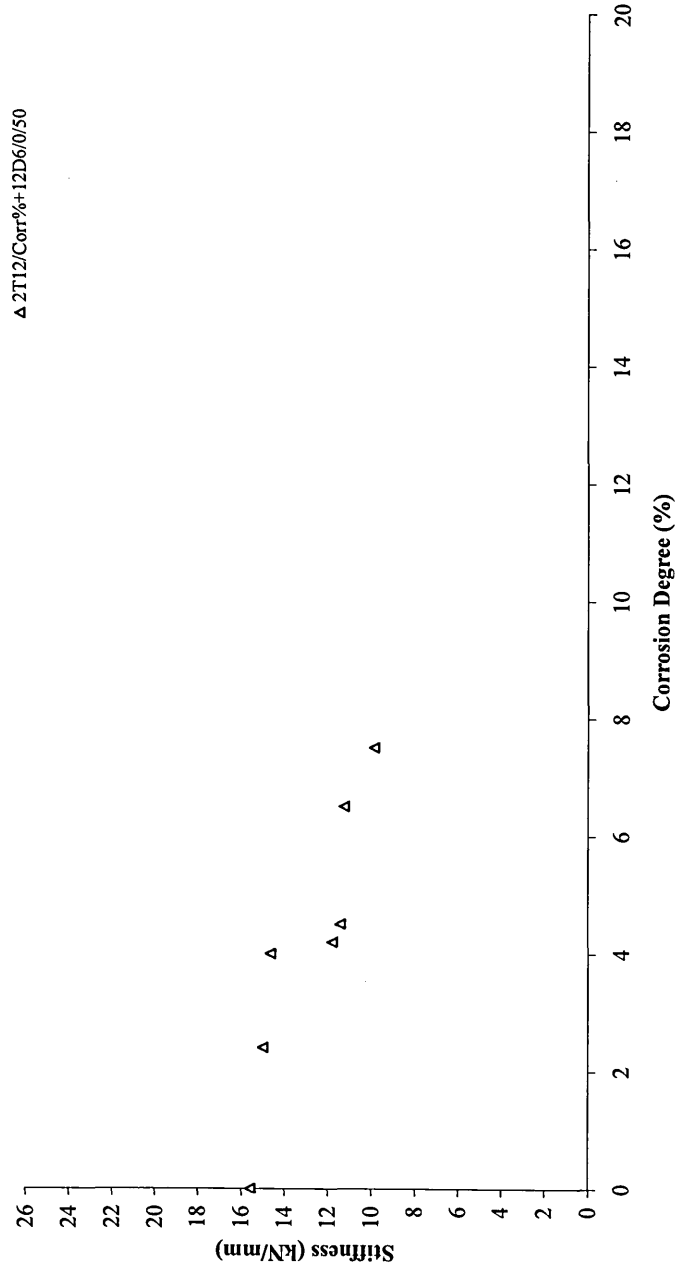


Figure 8.19 Relationship between stiffness and degree of corrosion for beam designed with 2T12

## (Main reinforcement corrosion)

It is clear from the ultimate loads given in Table 8.5 that the strength of the beams decrease with increasing main steel corrosion (compare the control load of beam 2T12/0+24D6/0/50 with that of 2T12/5.9+24D6/0/50, the ultimate load decreases from average an 81.68 kN to 50.70 kN).

Table 8.5 Beam Series I (2T12/Corr%) test results

Cover	Beam Identification	Actual Corrosion	Stiffness	Ultimate Load	Failure Mode
mm		%	kN/mm	kN	
(1)	(2)	(3)	(4)	(5)	(6)
56 mm cover to main steel	2T12/0+24D6/0/50	0	15.6	76.98	Flexure
	2T12/0+24D6/0/50	0		81.68	Flexure
	2T12/1.3+24D6/0/50	1.3	15.0	73.80	Flexure
	2T12/1.7+24D6/0/50	1.7	14.7	70.80	Flexure
	2T12/2.5+24D6/0/50	2.5	11.8	63.60	Flexure
	2T12/3.1+24D6/0/50	3.1	11.4	57.30	Flexure
	2T12/4.2+24D6/0/50	4.2	11.3	61.70	Flexure
	2T12/5.9+24D6/0/50	5.9	9.9	50.70	Flexure

To gain a better understanding of the influence of corrosion on the flexural strength of the deteriorated beams, Figure 8.20 show the relationship between  $P_{ult} / P_{con}$  and the degree of corrosion to the main steel reinforcement.  $P_{ult}$  is the ultimate load obtained from testing the beams in the laboratory (those exhibiting main steel corrosion) and  $P_{con}$  is the average failure load of the control specimens (0% corrosion to the main steel reinforcement). In all cases, the actual percentage of corrosion was used in the analysis of data as opposed to the target corrosion. This led to a better correlation between

(Main reinforcement corrosion)

Series I (2T12/Corr%+24D6/0/50)  
Main: Corroded, Shear: Uncorroded  
Cover to main steel: 56 mm

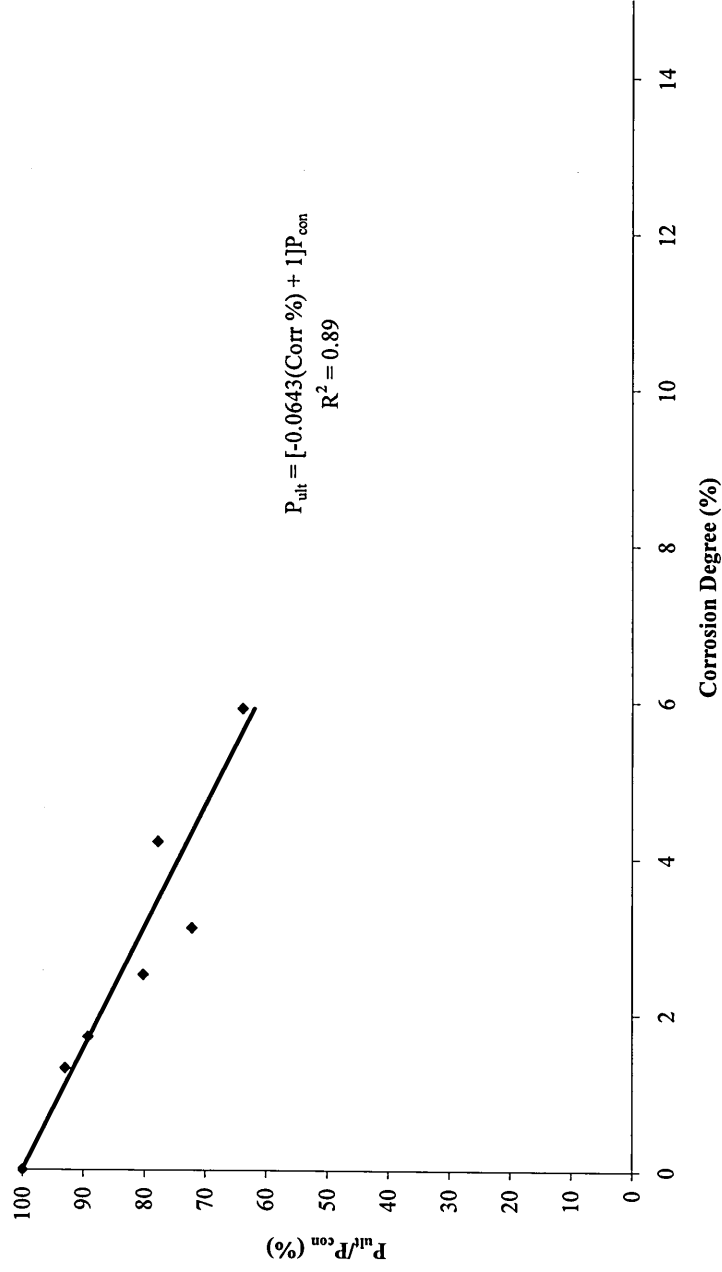


Figure 8.20 Relationship between  $P_{ult} / P_{con}$  and degree of corrosion for beam designed with 2T12 and 56 mm cover to main steel

(Main reinforcement corrosion)

flexural performance and degree of corrosion as there was some variation between target and actual values.

A strong linear relationship was also found between the degree of corrosion and  $P_{ult} / P_{con}$  (correlation coefficient 0.89). However, the results will be further analysed in Chapter 11.

## 8.5 Conclusions

The results of this series will be analysed further in order to develop analytical model in Chapter 11.

### 8.5.1 General

The following conclusions were drawn from the experimental results of Series I reported in this chapter:

- For main reinforcement corrosion, the first sign of corrosion was rust staining on the concrete surface, followed by longitudinal cracking in the concrete cover;
- The time to first cracking depended, as expected, on cover and main reinforcement diameter. The beams with larger diameters deformed bars corrosion tended to crack earlier than those with smaller diameters, possible because of the greater surface area. There is no evidence in the literature to suggest that deformed bars are more susceptible to corrosion;

*(Main reinforcement corrosion)*

- The presence of longitudinal cracking resulting from the corrosion of reinforcement up to 5% did not necessarily mean significant loss of flexural strength;
- The series of beams with the heaviest corrosion suffered significant strength loss. In most of the cases of serious strength loss, failure was precipitated as a result of local section loss.

**8.5.2 Flexure**

- For the flexure tests, the loss of strength increased as the degree of corrosion increased;
- The beams with target corrosion of 5% suffered negligible strength loss, even where longitudinal cracking was present over the length of the beam. Failure was ductile and in flexure;
- The bars with the least cover were more susceptible to loss of bond due to corrosion. The possibility of bond failure can be identified by the presence of serious corrosion cracking;
- First evidence of bond failure occurred in the beams with a target corrosion of 12%. This evidence consisted of horizontal cracking of the beam along the line of the reinforcement as the load test proceeded, suggesting local bond failure. In all beams, failure was ductile and in flexure;
- The capacity of beams with main steel corrosion only was actually enhanced by the presence of shear reinforcement, even more where the corrosion was

*(Main reinforcement corrosion)*

heavy (15%). This strength enhancement did not occur for beams without shear reinforcement as reported elsewhere in the literature;

- The presence of shear reinforcement helped maintain integrity of the beam.

**8.5.3 Load – Deflection**

- Flexural deflection at service load increased with increasing corrosion degree. That may be explained in terms of the pressure build up at the reinforcement–concrete interface, due to the accumulation of corrosion products, being increased with increasing corrosion degree, resulting in wider cracks in the concrete cover zone, hence reduced stiffness;
- Owing to the fact that four leg steel stirrups were used in the manufacturing of the beam specimens reinforced with 2T12 main reinforcement, led to less severe cracking patterns in the concrete cover zone, the beams specimens were associated with the lowest deflections compared to the beams of the other groups;
- The effect of area of reinforcement on the stiffness of the concrete beam is clearly manifested when comparing the performance of the beam specimens reinforced with 2T12 with those reinforced with 2T8 and 2T10 main reinforcement. The beams reinforced with 2T8 are associated with higher deflections compared to the beams reinforced with 2T12 main reinforcement.

**8.5.4 Further discussion**

A simplified model for predicting the residual strength of corroded reinforced concrete beams will be presented in Chapter 11.

*(Main reinforcement corrosion)*

The residual flexural capacity of beams was determined following induced accelerated corrosion in the reinforcement within between 336 and 840 hours. Such corrosion periods are gross reduction of actual corrosion periods of many years which may occur in real practice to produce the same degree of corrosion. These differences in accelerated and normal corrosion periods can have significant influence on residual strength. Longer corrosion periods allow the corrosion products to be dissipated gradually in the pore structure of the concrete matrix, thereby reducing the radial stresses exerted at the rebar–concrete interface. In the case of accelerated corrosion, however, the rapid production of corrosion products allows little time for their dissipation in the pore structure. This will result in greater residual stresses at the interface resulting in more extensive cracking and debonding than may occur in real practice. The predictive models delivered from the laboratory tests, therefore, should result in conservative values of residual strength.

### ***Experimental Results and Discussion – Series II***

#### ***(Shear reinforcement corrosion)***

##### **9.1 Introduction**

Most of the papers published so far deal with the mechanism of the corrosion process<sup>133, 134</sup>, protection of structures and field survey of deteriorated concrete structures. The literature on the structural implications of corrosion on parameters like the load carrying capacity when only shear reinforcement is corroded, is not available. The results presented in this chapter will contribute to determining the influence of shear steel corrosion on the structural performance of reinforced concrete beams.

##### **9.2 Aim**

The main objectives of the laboratory work were to evaluate the influence of different degrees of corrosion on the shear strength of reinforced concrete beams. This chapter includes experimental results and analysis of different parameters such as the effect of uniform shear reinforcement corrosion in beams with different main steel diameters.

##### **9.3 Structural performance of beams exhibiting shear reinforcement corrosion**

Reinforced concrete beams were designed and constructed as described in Chapter 6 (see Tables A.2.1 and A.2.2 in Appendix A). Beams were reinforced longitudinally

*(Shear reinforcement corrosion)*

with two deformed 8 mm and 12 mm bars respectively and reinforced for shear with 6 mm plain steel links. Cover to the shear reinforcement was 50 mm. Covers of 20 mm and 30 mm were not used as this was considered inappropriate due to the time scale of the project.

The test results reported here for sixteen reinforced concrete beams in order to examine the influence of shear reinforcement corrosion on behaviour and ultimate load capacity. The variables included in this test series were percentage of main reinforcement, effective depth of the beam and degree of shear reinforcement corrosion.

Tables 9.1 and 9.2 summarise the capacity and failure mode. Column 1 of Tables 9.1 and 9.2 shows that the cover to the shear reinforcement used in this test series was 50 mm (column 1). Column 2 of Tables 9.1 and 9.2 give the beam identification according the target corrosion e.g. beam 2T8/0+12D6/15/50 indicates that the main steel is 2T8 with 0% corrosion whereas the shear reinforcement is 12D6, target corrosion is 15% and cover is 50 mm. Column 3 gives the actual shear reinforcement corrosion measured as described in Section 3.3. The stiffness calculated from the slopes of the load – deflection curves (Figure 9.1) is shown in column 4. The ultimate load capacity at failure is given in column 5. Column 6 in Tables 9.1 and 9.2 shows that the failure of each beam was flexural, except for the two beams which were heavily corroded to around 25% (of the shear reinforcement) exhibited shear failure.

Referring to Tables 9.1 and 9.2, the actual corrosion (column 2) varied from the target corrosion, especially for beams designed with 2T12. This was due to the accelerated corrosion set up which can vary from test to test (see Figure 5.6).

(Shear reinforcement corrosion)

Table 9.1 Beam Series II (2T8/0+12D6/Corr%/50) test results

Cover mm	Beam Identification	Actual	Stiffness	Ultimate	Failure Mode
		Links Corrosion		Test Load	
(1)	(2)	%	kN/mm	kN	(6)
50 mm cover to links	2T8/0+12D6/0/50	0	10.3	40.00	Flexure
	2T8/0+12D6/0/50	0	10.0	42.70	Flexure
	2T8/0+12D6/5/50	4.9	10.1	41.11	Flexure
	2T8/0+12D6/5/50	9.2	5.5	40.59	Flexure
	2T8/0+12D6/10/50	9.4	5.2	39.09	Flexure
	2T8/0+12D6/10/50	9.8	8.3	39.71	Flexure
	2T8/0+12D6/15/50	18.7	6.8	35.07	Shear
	2T8/0+12D6/15/50	23.2	5.3	34.44	Shear

Table 9.2 Beam Series II (2T12/0+12D6/Corr%/50) test results

Cover mm	Beam Identification	Actual	Stiffness	Ultimate	Failure Mode
		Links Corrosion		Test Load	
(1)	(2)	%	kN/mm	kN	(6)
50 mm cover to links	2T12/0+12D6/0/20	0	16.6	78.30	Flexure
	2T12/0+12D6/0/50	0	16.0	84.14	Flexure
	2T12/0+12D6/5/50	0	16.4	82.70	Flexure
	2T12/0+12D6/5/50	0.7	15.8	79.7	Flexure
	2T12/0+12D6/10/50	1.1	15.3	81.5	Flexure
	2T12/0+12D6/10/50	1.8	13.3	76.5	Flexure
	2T12/0+12D6/15/50	2.6	12.7	69.4	Flexure
	2T12/0+12D6/15/50	6.1	12.2	55.8	Flexure

*(Shear reinforcement corrosion)*

As for the previous beams, the cracking due to corrosion was marked on each beam. In general, the cover concrete was cracked at all reinforcement positions. This consisted of vertical cracking at all link positions.

For this design, the beams were expected to fail in flexure, although there was not much margin between flexural and shear capacity. Corroded beams failed in flexure and only in very high degrees of corrosion in shear e.g. 2T8/0+12D6/18.7/50 and 2T8/0+12D6/23.2/50. Figures 9.1 and 9.2 show the types of failure. In all cases calculated flexural load capacity was achieved during various load tests.



Figure 9.1 Beam 2T8/0+12D6/23.2/50 crack pattern at ultimate load level

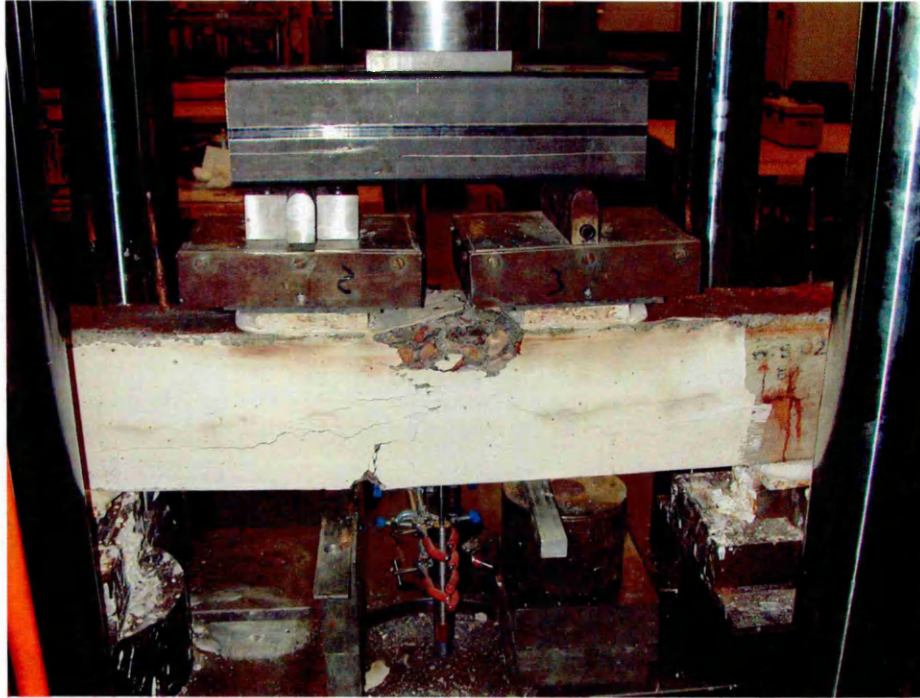


Figure 9.2 Beam 2T12/0+12D6/6.1/50 crack pattern at ultimate load level

The following sections describe the behaviour under load of the 910 mm beam specimens and the effect of the induced corrosion to the shear reinforcement only. Strengths are related to the ultimate capacity of control (uncorroded) beams for flexure and shear. For direct comparison with the test results, mean values of strength as obtained from cube and tensile tests were used in this analysis (see Appendix A, Table A.2). For corroded beams, account was taken only of the section loss in steel cross section and for the purposes of this analysis the nominal actual section loss was used.

### 9.3.1 Beam Series II reinforced with 2T8 main steel reinforcement

#### 9.3.1.1 Load – central deflection relationships

Typical load – deflection curves are shown in Figure 9.3. Figure 9.3 shows that the degree of corrosion ( $2RT/D$  %) induced in the shear reinforcement at a constant rate  $1 \text{ mA/cm}^2$  has negligible influence on the load – deflection curves. For example beam 2T8/0+12D6/9.8/50 suffered on average 95% ultimate load reduction compared to the control. The same corrosion rate when used to induce a higher degree of corrosion of 23.2% (Figure 9.3) lead to load – deflection curves being not much more corrosion degree dependent. This is evident in beam 2T8/0+12D6/23.2/50 where the load reduction is around 83%.

To gain a better understanding of the performance of the beams when shear reinforcement is subjected to corrosion, Figure 9.4 shows the impact of shear reinforcement corrosion on the stiffness. Referring to Figure 9.4, the beam stiffness, obtained from the slope of the load deflection curves in Figure 9.3, is plotted against the degree of shear reinforcement corrosion. Generally, for percentages of corrosion, up to about 15%, there is some variation in stiffness (for example,  $10.0 \text{ kN/mm}$  at 4.9% shear reinforcement corrosion to  $5.5 \text{ kN/mm}$  at 9.2% shear reinforcement corrosion). However, the stiffness decreases rapidly thereafter and the mode of failure changes from flexure to shear at high ( $>18\%$ ) degrees of shear reinforcement corrosion.

#### 9.3.1.2 Residual flexural strength

In general under four point bending, the control beams exhibited a classical bending failure of an under reinforced beam whereas the failure mode of the corroded beams

(Shear reinforcement corrosion)

Series II (2T8/0+12D6/Corr%/50)  
Main: Uncorroded, Shear: Corroded  
Cover to links : 50 mm

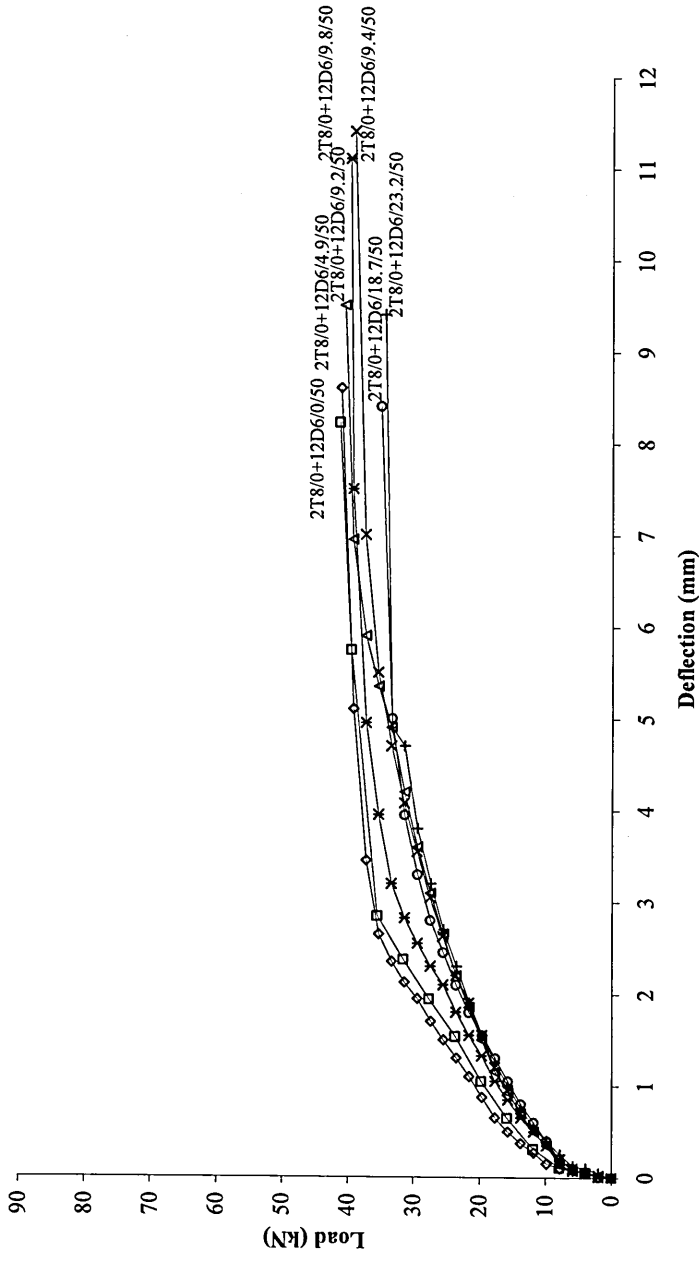


Figure 9.3 Load – deflection curves of corroded concrete beams of Series II under four point bending test

Series II (2T8/0+12D6/Corr%/50)  
Main: Uncorroded, Shear: Corroded  
Cover to links: 50 mm

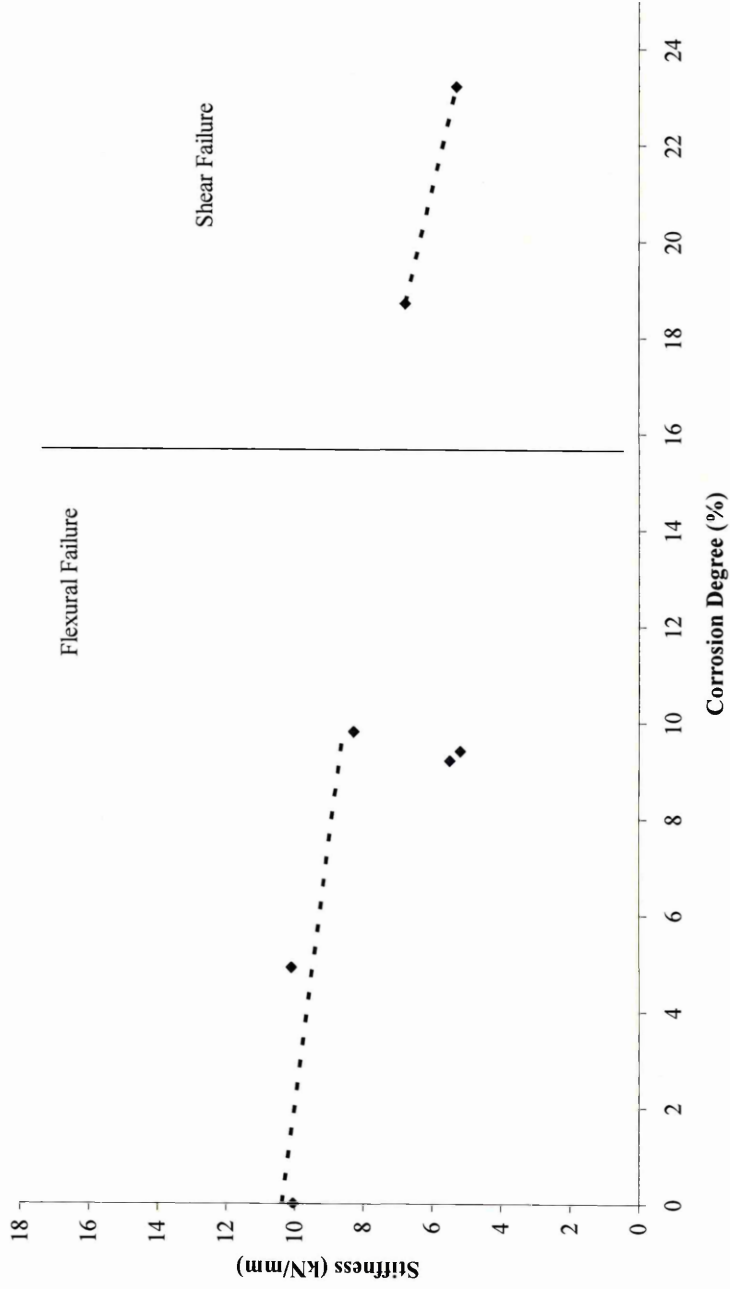


Figure 9.4 Relationship between stiffness and shear reinforcement corrosion

was controlled by bond failure. At a high degree of shear reinforcement corrosion (20%), the failure mode changed from flexure to shear as shown in Figure 9.1 as discussed in Section 9.3.1.1.

It can be seen from Figure 9.5 that with the increase of degree of corrosion, the load capacity reduces. As reported in the literature <sup>78</sup>, plain steel improves the bond when corrosion is up to 5% and this could explain the slight increase in the stiffness. At a corrosion degree of about 10% and higher, the stiffness begins to decrease.

It can be seen from Figure 9.5, that even when links were corroded at 23.2% the reduction in load capacity was negligible. Failure of these beams (high shear reinforcement corrosion) was by shear. This type of failure as reported <sup>123</sup>, occurred in beams with high spacing of the shear reinforcement, close to the effective depth. Two main reasons could explain this type of failure, which was produced before the crushing of the concrete by bending:

- The significant reduction of shear reinforcement section;
- The reduction of the effective depth of the concrete section at shear span, due to the spalling of the top concrete cover (20 mm). This spalling was produced by the shear stress, due to the loading of the beam.

### **9.3.2 Beam Series II reinforced with 2T12 main steel reinforcement**

#### **9.3.2.1 Load – central deflection relationships**

Average load – deflection relationships for the beam specimens of Series II reinforced with 2T12 tensile reinforcement and 12D6 shear reinforcement subjected to different

(Shear reinforcement corrosion)

Series II (2T8/0+12D6/Corr%/50)  
Main: Uncorroded, Shear: Corroded  
Cover to links: 50 mm

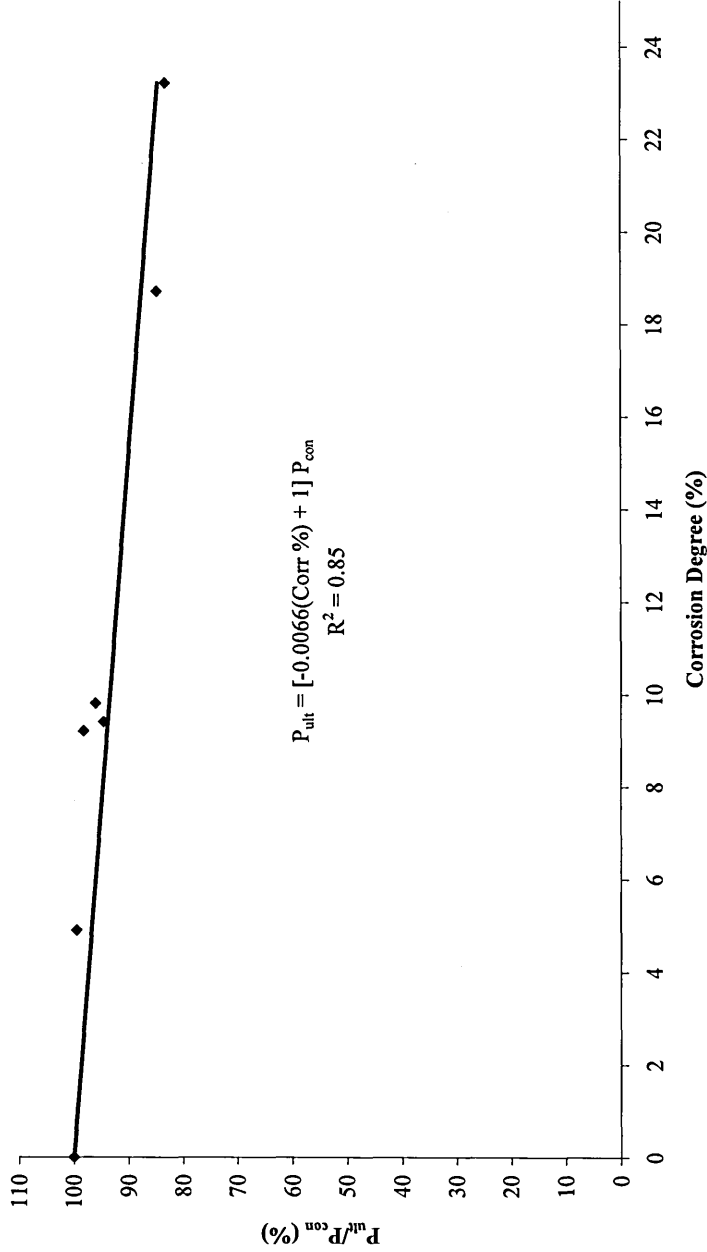


Figure 9.5 Relationship between  $P_{ult} / P_{con}$  and degree of corrosion

degrees of corrosion and 50 mm cover to the shear reinforcement, under four point bending tests are shown in Figure 9.6.

To gain a better understanding of the performance of the beams when shear reinforcement is subjected to corrosion, Figure 9.7 shows the impact of shear reinforcement corrosion on the stiffness. Referring to Figure 9.7, the beam stiffness, obtained from the slope of the load deflection curves in Figure 9.6, is plotted against the degree of shear reinforcement corrosion. Generally, increasing the percentages of corrosion, lead to decrease in stiffness (for example, 16.0 kN/mm at 0% shear reinforcement corrosion to 12.2 kN/mm at 6.1% shear reinforcement corrosion). However, due to the limited data it was not possible to establish where the mode of failure will change from flexure to shear and how the failure mode will relate to the stiffness.

### 9.3.2.2 Residual flexural strength

Figure 9.8 show the relationship between the degree of corrosion to the shear reinforcement and the flexural load capacity of corroded beams as a percentage of the average load capacity of the corresponding control beams,  $(P_{ult} / P_{con})$ .  $P_{ult}$  is the ultimate load obtained from testing the beams in the laboratory (those exhibiting shear reinforcement corrosion) and  $P_{con}$  is the average failure load of the control specimens (0% corrosion to the shear reinforcement and main steel), (see Table 9.2).

Figure 9.8 show a clear relationship between the degree of corrosion and the reduction in flexural strength. The results show that higher values of flexural load capacity are associated with degree of shear reinforcement corrosion to up to 2.6%, where the

(Shear reinforcement corrosion)

**Series II (2T12/0+12D6/Corr%/50)**  
**Main: Uncorroded, Shear: Corroded**  
**Cover to links: 50 mm**

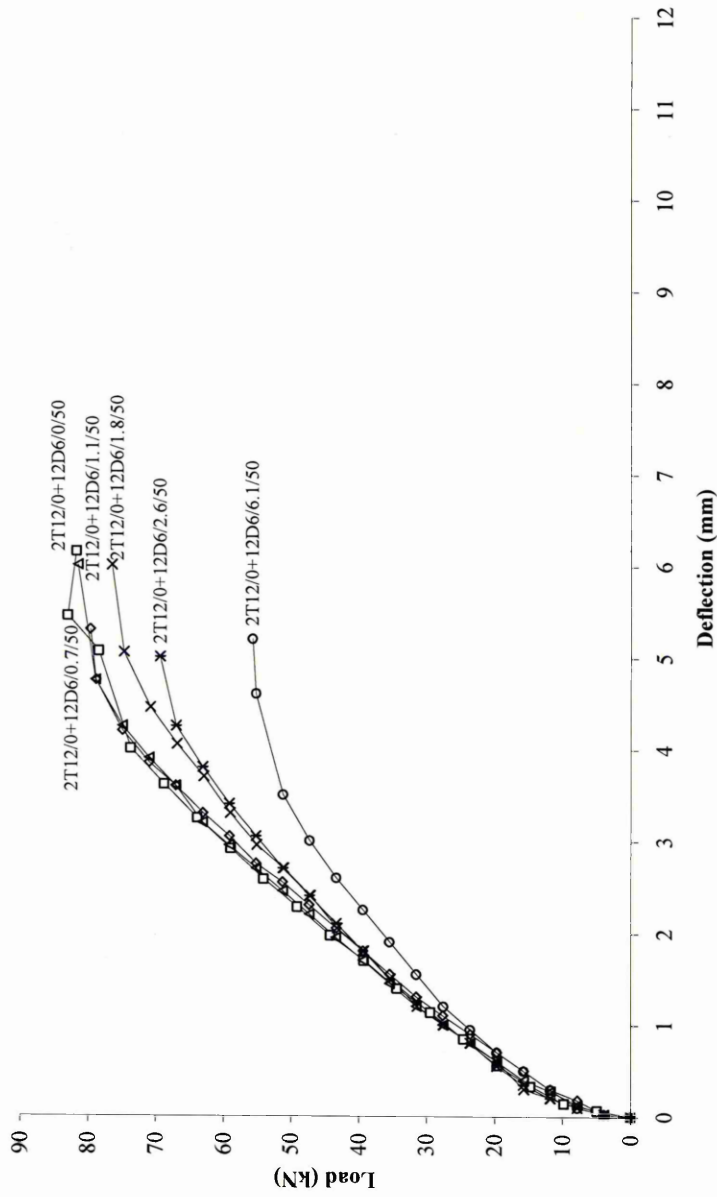


Figure 9.6 Load – deflection curves of corroded concrete beams of Series II under four point bending test

(Shear reinforcement corrosion)

Series II (2T8/0+12D6/Corr%/50)  
Main: Uncorroded, Shear: Corroded  
Cover to links: 50 mm

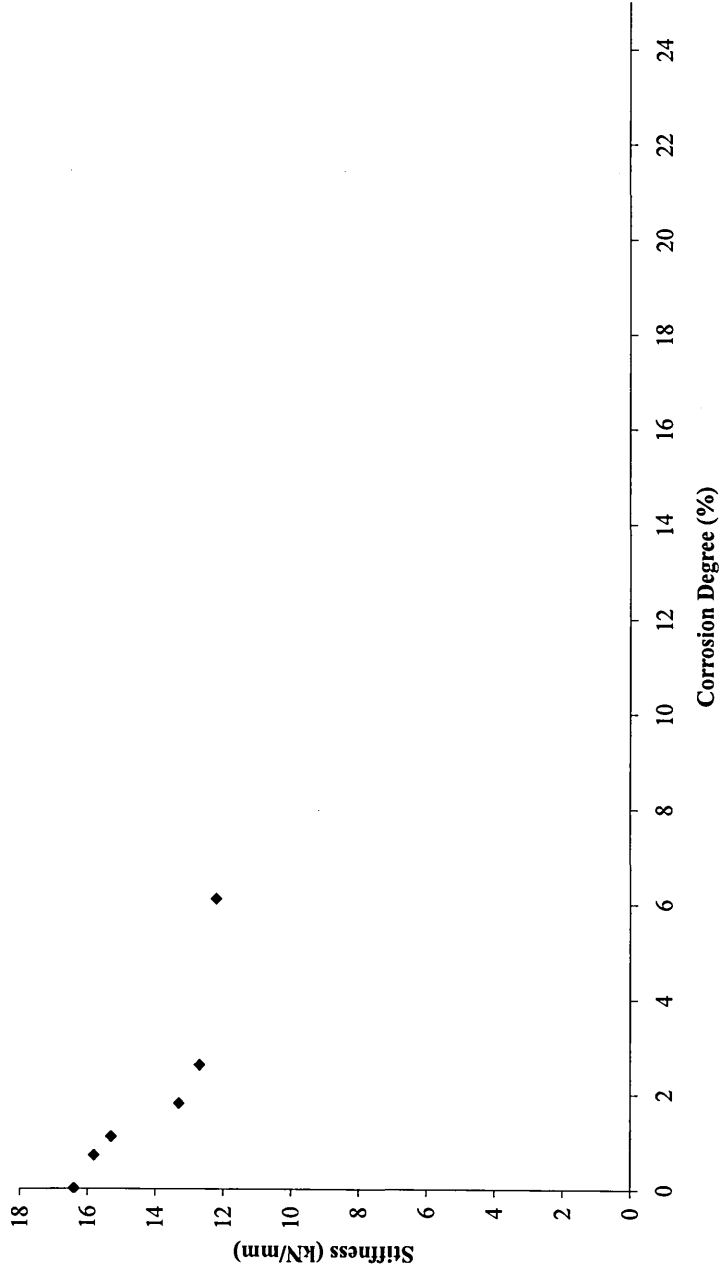


Figure 9.7 Relationship between stiffness and shear reinforcement corrosion

(Shear reinforcement corrosion)

Series II (2T12/0+12D6/Corr%/50)  
Main: Uncorroded, Shear: Corroded  
Cover to links: 50 mm

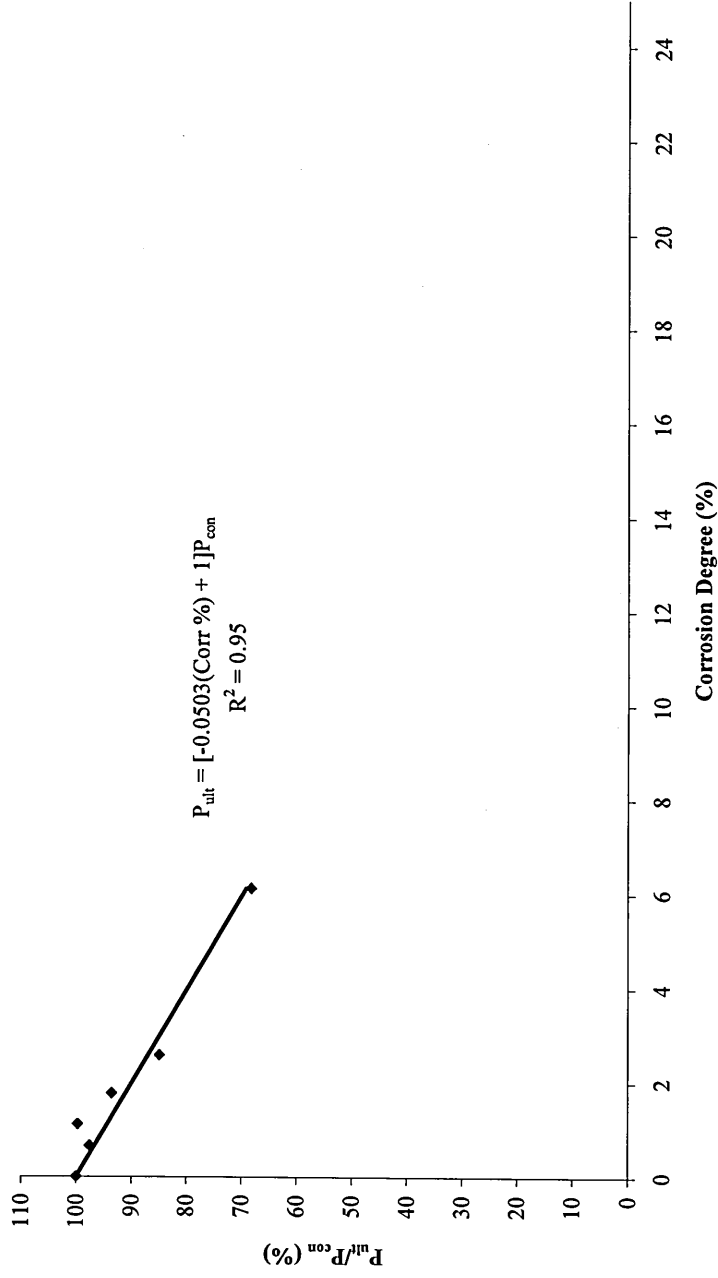


Figure 9.8 Relationship between  $P_{ult} / P_{con}$  and degree of corrosion for beam designed with 2T12 and 50 mm cover

*(Shear reinforcement corrosion)*

reduction in the load capacity was to around 85%. This is due the fact that the shear reinforcement was made of plain steel and the corrosion helped maintain the integrity of the concrete through increased bond <sup>78</sup>.

However due to the limited data further analysis was not carried out on these series for the scope of this thesis.

The following conclusions were drawn from the experimental results of Series II reported in this chapter:

- Corrosion of the shear reinforcement modifies the type of failure in concrete beams with usual ratios of reinforcement. Whereas non corroded beams failed by bending, heavily deteriorated beams (23.2% corrosion to shear reinforcement) failed by shear;
- The presence of shear reinforcement helped maintain integrity of the beam even where they were heavily corroded;
- There was little influence of shear reinforcement corrosion on the load carrying capacity for corrosion of around 5%;
- The reduction in the load carrying capacity was higher for beams reinforced with bigger diameter, e.g. 2T12 in comparison with 2T8 (Figures 9.8 and 9.5).

#### **9.4 Final remarks**

More research is needed due to insufficient data to deal with different aspects related to the performance of concrete beams with corroded shear reinforcement. Further analysis on the effect of shear reinforcement corrosion on the shear strength and the effect of

*(Shear reinforcement corrosion)*

reduced tensile properties of the shear reinforcement on the structural performance, are considered in the recommendations presented in Chapter 12.

### *Experimental Results and Discussion – Series III*

#### *(Main and shear reinforcement corrosion)*

##### **10.1 Introduction**

Concrete structures which have suffered from corrosion to the steel require maintenance to increase their service life. However, it is difficult to make a decision as when repair is required without knowing how much the capacity has been reduced due to deterioration. Shear reinforcement normally corrodes first as it is nearer to the concrete surface but main steel, too can be affected simultaneously if the corrosion products penetrate deep into the concrete. This chapter discusses the results of test beams where accelerated corrosion was induced to both main and shear reinforcement in the laboratory.

##### **10.2 Aim**

The main objectives of the laboratory work were to evaluate the influence of corrosion to the main and shear reinforcement on the residual strength of simply supported beams. This chapter includes experimental results of beams tested with parameters such as varying degrees of uniform corrosion to both the main and shear reinforcement.

### 10.3 Flexural testing

Reinforced concrete beams were design and constructed as described in Chapter 7 and the results of the design are attached at the end of this thesis (see Appendix A, Table A.3).

After accelerating the predetermined amount of corrosion to the main and shear reinforcement, the beams were tested under four point bending to determine their load – deflection curves and their ultimate flexural strength. The outputs from the testing machine and the transducer were connected to a chart recorder to plot the load – deflection curves. The load – deflection relationships for the beam specimens of Series III were obtained and the results are given Table 10.1. Table 10.1 shows that the cover to the shear reinforcement used in this test series was 50 mm (column 1). Covers of 20 mm and 30 mm were not used as this was considered inappropriate due to the time scale of the project. The beam identification according the target corrosion is given in column 2, e.g 2T8/5+12D6/10/50 indicates that the main steel is 2T8 with 5% target corrosion whereas the shear reinforcement is 12D6, target corrosion is 10% and cover is 50 mm. The actual corrosion calculated as described in Chapter 3 is given, for main bars in column 3 and for the shear reinforcement, column 4. The stiffness calculated from the slopes of the load – deflection curves (Figure 10.1) is shown in column 5. The ultimate load capacity at failure is given in column 6. Column 7 in Table 10.1 shows that the failure of each beam was flexural, except for the two beams which were heavily corroded to around 25% (of the main and shear reinforcement) exhibited shear failure.

(Main and shear reinforcement corrosion)

Table 10.1 Beam Series III (2T8/Corr %+12D6/Corr %/50) test results

Cover	Beam Identification	Actual Main bars Corrosion	Actual Shear links Corrosion	Stiffness	Ultimate Load	Failure Mode
mm		%	%	kN/mm	kN	
(1)	(2)	(3)	(4)	(5)	(6)	(7)
50 mm cover to links	2T8/5+12D6/5/50	6.5	4.3	9.5	33.64	Flexure
	2T8/5+12D6/5/50	2.9	3.0	8.5	40.27	Flexure
	2T8/10+12D6/5/50	4.8	5.6	10.0	33.69	Flexure
	2T8/10+12D6/5/50	5.3	6.5	9.1	31.86	Flexure
	2T8/15+12D6/5/50	25.7	24.7	4.5	11.07	Shear
	2T8/15+12D6/5/50	25.7	27.6	4.3	8.96	Shear
	2T8/5+12D6/10/50	8.3	6.3	6.1	33.32	Flexure
	2T8/5+12D6/10/50	3.1	3.8	7.7	36.29	Flexure
	2T8/10+12D6/10/50	4.1	3.9	8.9	33.44	Flexure
	2T8/10+12D6/10/50	4.7	8.2	8.1	32.65	Flexure
	2T8/15+12D6/10/50	7.8	4.5	6.8	26.69	Flexure
	2T8/15+12D6/10/50	8.8	9.1	6.8	27.25	Flexure
	2T8/5+12D6/15/50	10.7	12.0	5.3	25.32	Flexure
	2T8/5+12D6/15/50	11.8	14.2	6.8	26.56	Flexure
	2T8/10+12D6/15/50	6.7	9.4	11.4	44.04	Flexure
	2T8/10+12D6/15/50	7.9	8.2	6.9	27.54	Flexure
	2T8/15+12D6/15/50	6.9	7.4	9.0	30.54	Flexure
	2T8/15+12D6/15/50	6.9	4.0	8.1	32.11	Flexure

### 10.3.1 Load – deflection curves

Typical load – deflection curves are shown in Figure 10.1. Figure 10.1 shows that the degree of corrosion ( $2RT/D$  %) induced in the main and shear reinforcement at a constant rate  $1 \text{ mA/cm}^2$  has marked influence on the load – deflection curves. The same figure shows that the influence of degrees of corrosion of the main and shear reinforcement of up to 3.0% on the load – deflection curves is negligible. For example beam 2T8/2.9+12D6/3.0/50 and beam 2T8/3.1+12D6/3.8/50 suffered on average 95% ultimate load reduction compared to the control. The same corrosion rate when used to induce a higher degree of corrosion of 10% (Figure 10.1) lead to load – deflection curves being much more corrosion degree dependent. This is evident in beams 2T8/10.7+12D6/12.0/50 and beam 2T8/11.8+12D6/14.2/50 where the load reduction is around 50%.

To gain a better understanding of the performance of the beams when both main and shear reinforcement are subjected to corrosion, Figures 10.2 and 10.3 show the impact of simultaneous corrosion on the stiffness. Referring to Figure 10.2, the beam stiffness, obtained from the slope of the load deflection curves in Figure 10.1, is plotted against the degree of main reinforcement corrosion. Generally, for low percentages of corrosion, up to about 7%, there is some variation in stiffness (for example, 7.7 kN/mm at 3.1% main steel corrosion to 11.4 kN/mm at 6.7% main steel corrosion). However, the stiffness decreases rapidly thereafter and the mode of failure changes from flexure to shear at very high (>25%) degrees of corrosion.

Referring to Figure 10.3, the same beams (Series III) are considered but the stiffness is compared to the degree of corrosion of the shear reinforcement. In this instance, a

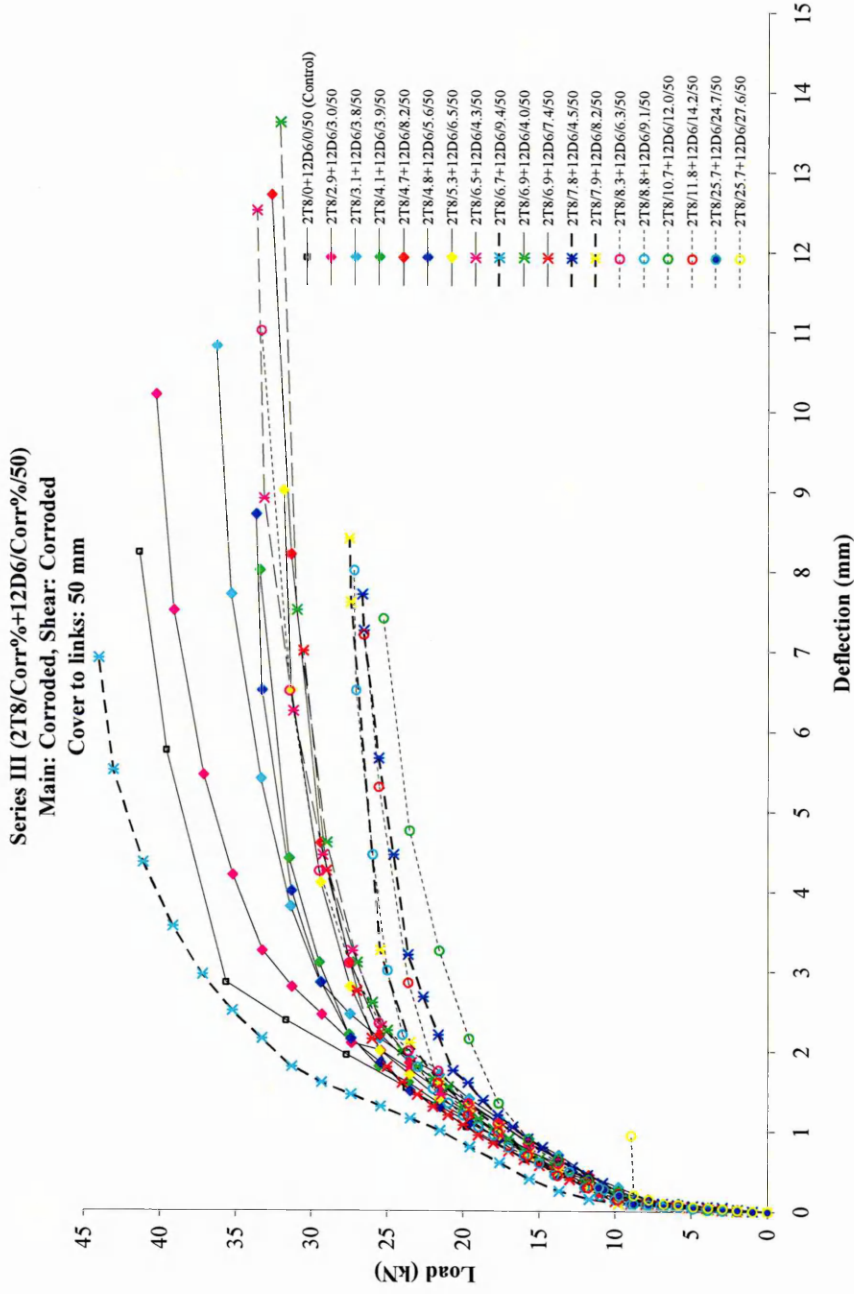


Figure 10.1 Load – deflection curves of corroded concrete beams of Series III under four point bending test

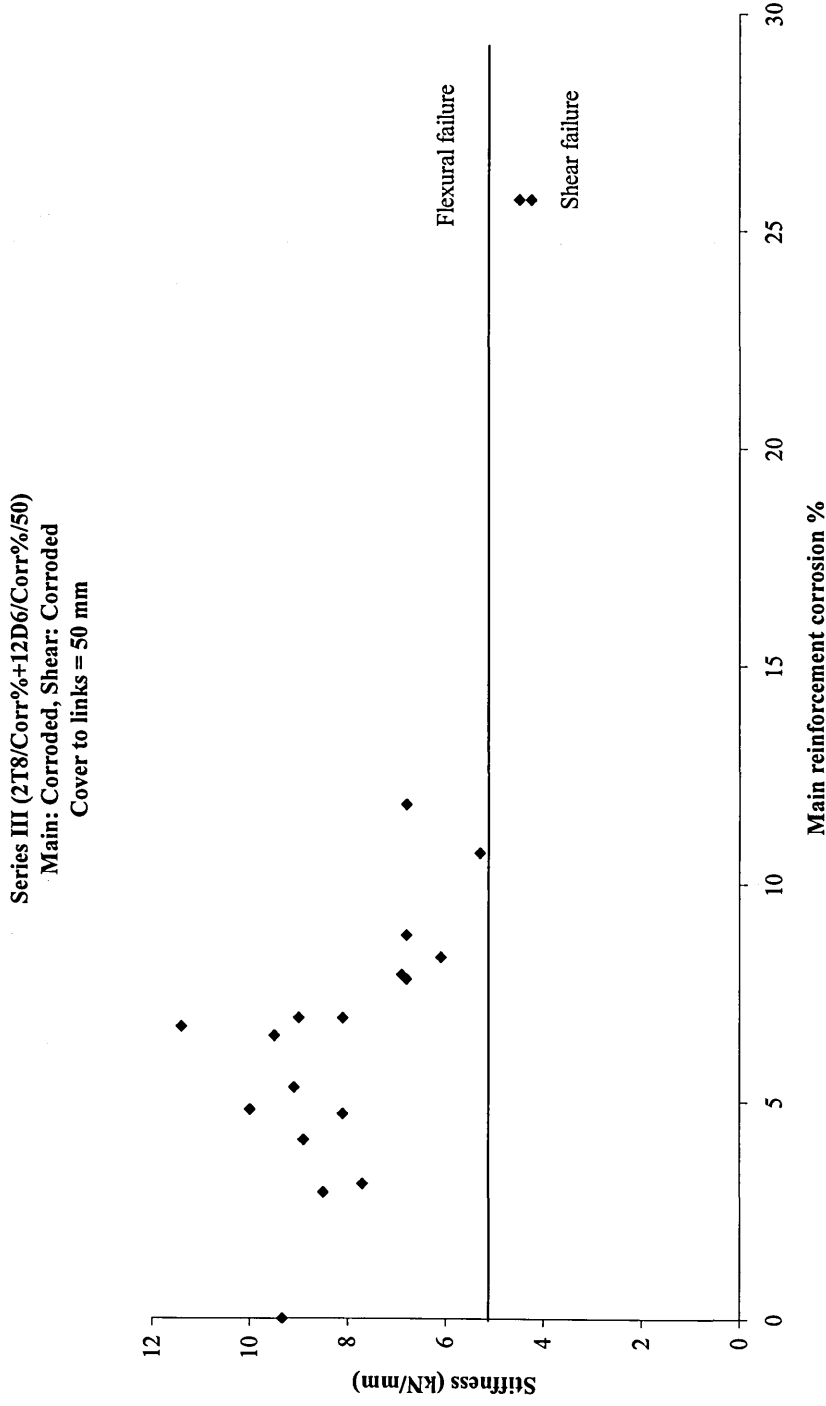


Figure 10.2 Relationship between stiffness and main reinforcement corrosion

(Main and shear reinforcement corrosion)

Series III (2T8/Corr%+12D6/Corr%/50)  
Main: Corroded, Shear: Corroded  
Cover to links = 50 mm

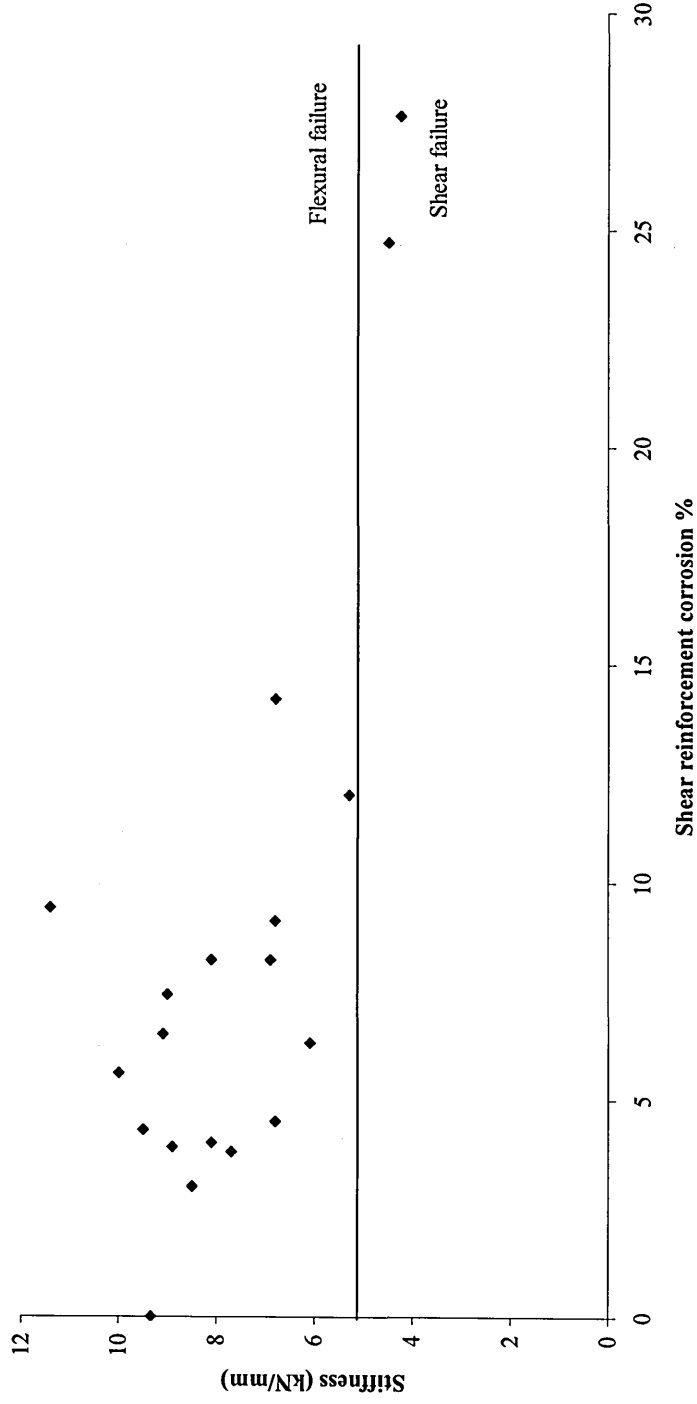


Figure 10.3 Relationship between stiffness and shear reinforcement corrosion

degree of corrosion of 14.2% on the shear reinforcement is reached and failure of the beam is nevertheless, flexural. Only at very high levels of corrosion at around >25% in both the main (Figure 10.2) and shear reinforcement (Figure 10.3) does the mode of failure change from flexure to shear.

For comparison, the stiffness – corrosion relationship is shown in Figure 10.4 for Series III when corrosion to both main and shear reinforcement is considered together. These results (and those in Figures 10.2 and 10.3) show that the stiffness of the beam is reduced to about 46% when both corrosion to the main and shear reinforcement is present.

### 10.3.2 Flexural strength

In general under four point bending, the control beams exhibited a classical bending failure of an under reinforced beam whereas the failure mode of the corroded beams was controlled by bond failure. At about 60% of the failure load for all corroding beams (between 5 and 10% corrosion), horizontal splitting of the concrete occurred along the tensile reinforcement interface. At about 90% of the ultimate load, one vertical crack appeared in the mid-span of the beam, which led to failure. At a high degree of main and shear reinforcement corrosion (25%), the failure mode changed from flexure to shear as shown in Figures 10.5 and 10.6 as discussed in Section 10.3.1.

Figure 10.7 shows the relationship between the degree of main reinforcement corrosion ( $2RT/D\%$ ) and the flexural load capacity of corroded beams as a percentage of the average load capacity of the corresponding control beams, ( $P_{ult} / P_{con}$ ). A similar graph is plotted in Figure 10.8 except that the percentage of corrosion of the shear

(Main and shear reinforcement corrosion)

Series III (2T8/Corr%+12D6/Corr%/50)  
 Main: Corroded, Shear: Corroded  
 Cover to links = 50 mm

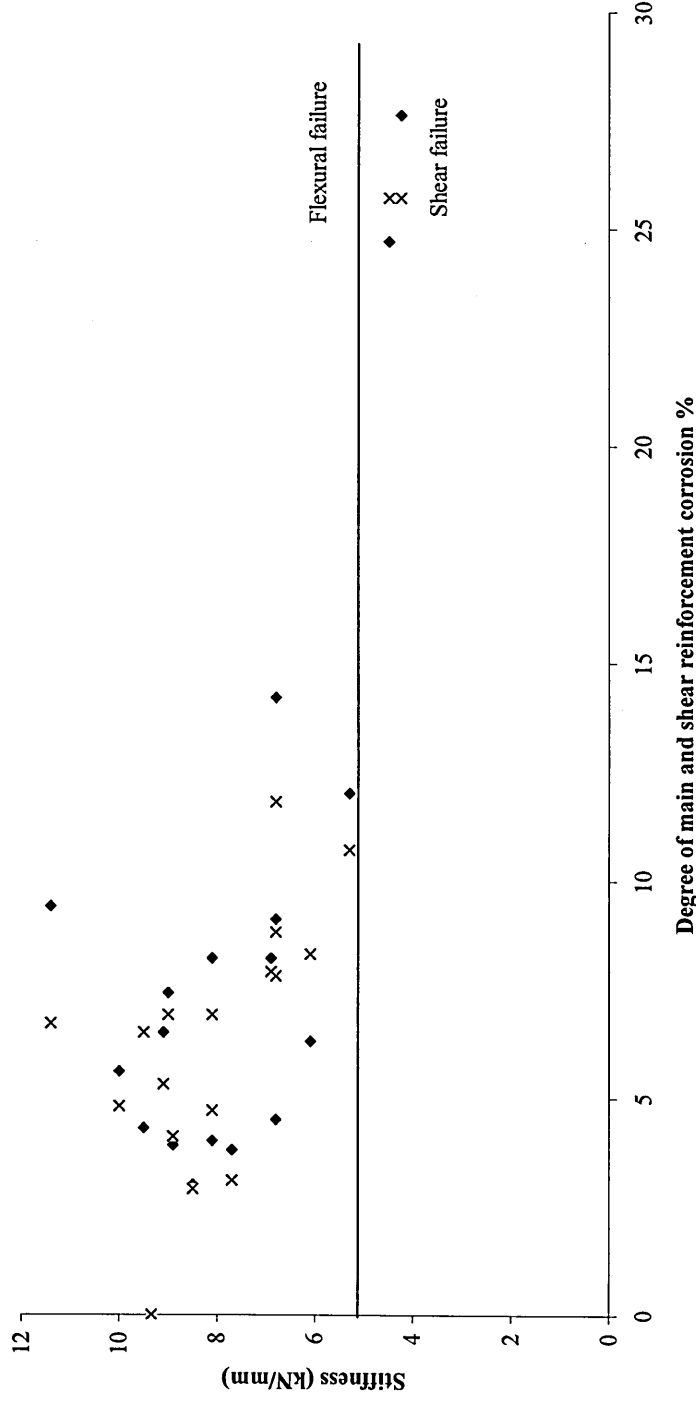


Figure 10.4 Relationship between stiffness and simultaneous main and shear reinforcement corrosion

(Main and shear reinforcement corrosion)

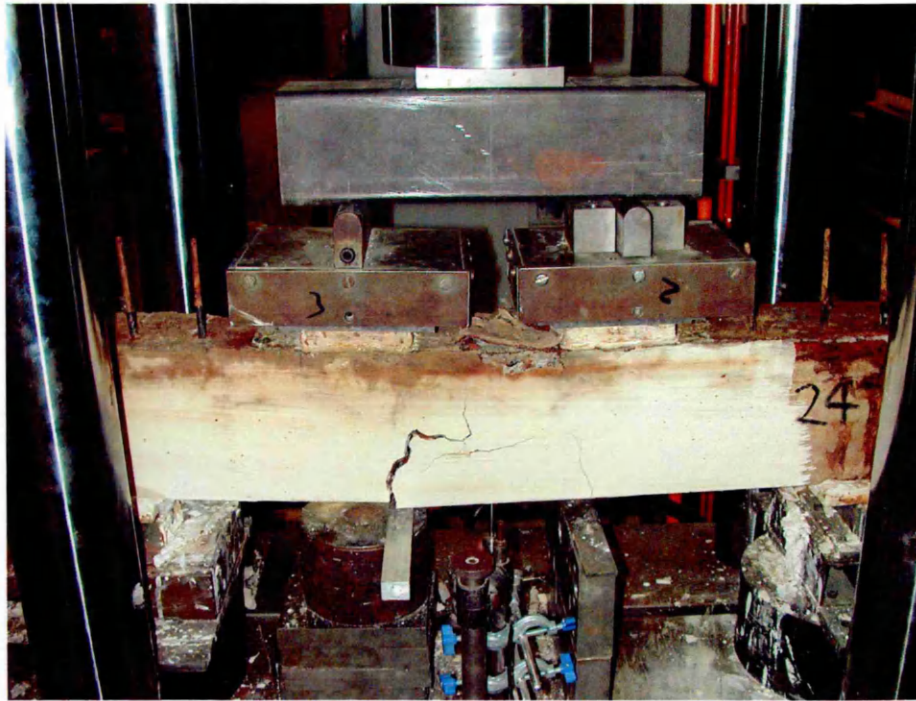


Figure 10.5 Beam 2T8/8.8/50+12D6/9.1 crack pattern at ultimate load level

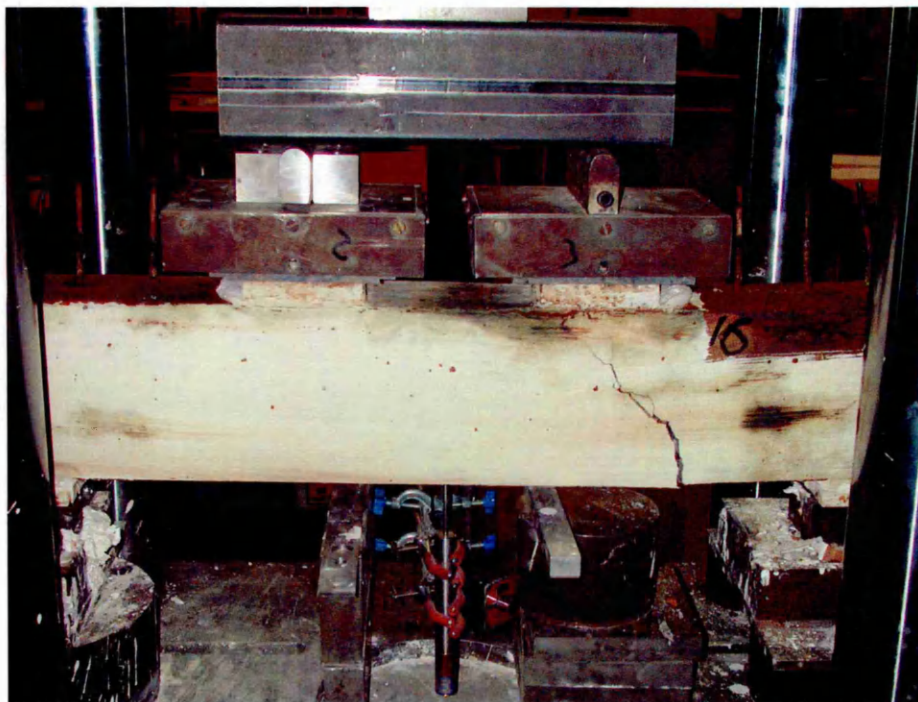


Figure 10.6 Beam 2T8/25.7/50+12D6/27.6 crack pattern at ultimate load level

(Main and shear reinforcement corrosion)

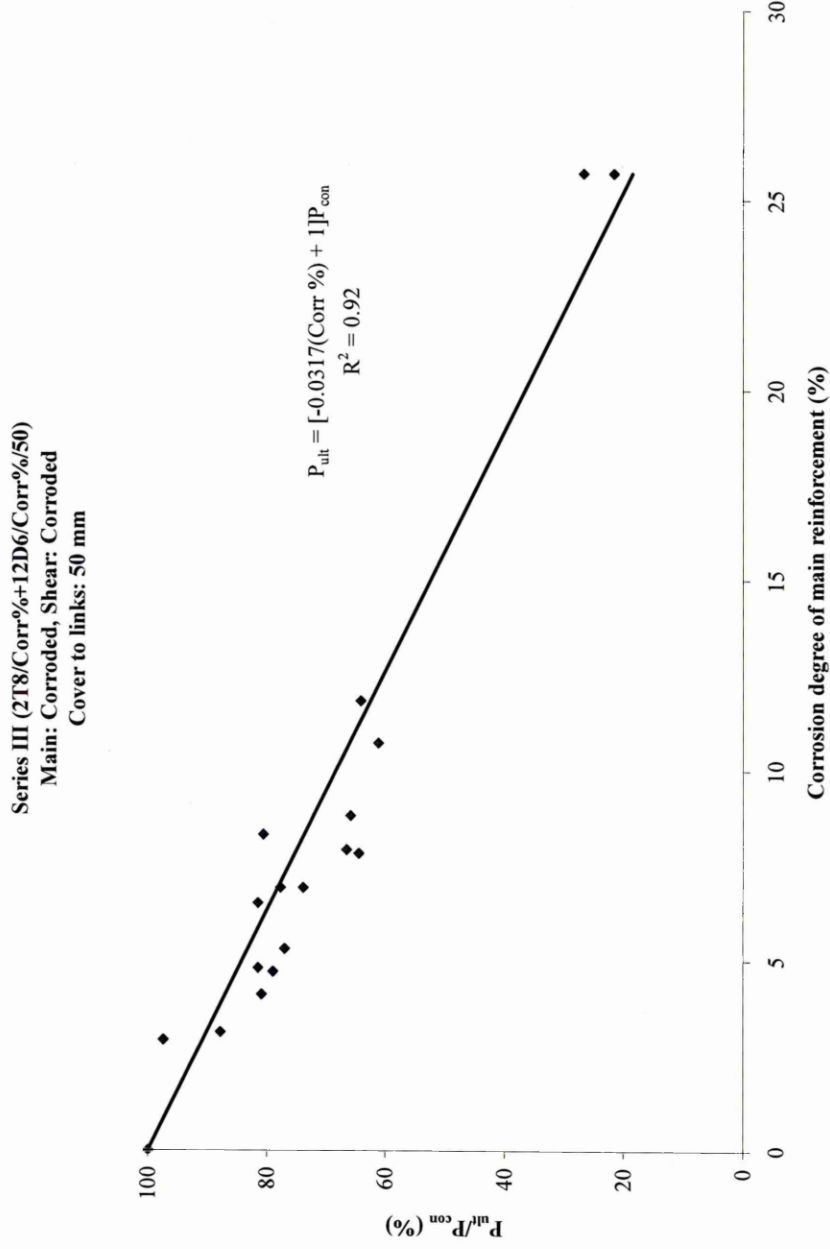


Figure 10.7 The effect of corrosion degree on the flexural load capacity of corrosion damaged reinforced concrete beams

(Main and shear reinforcement corrosion)

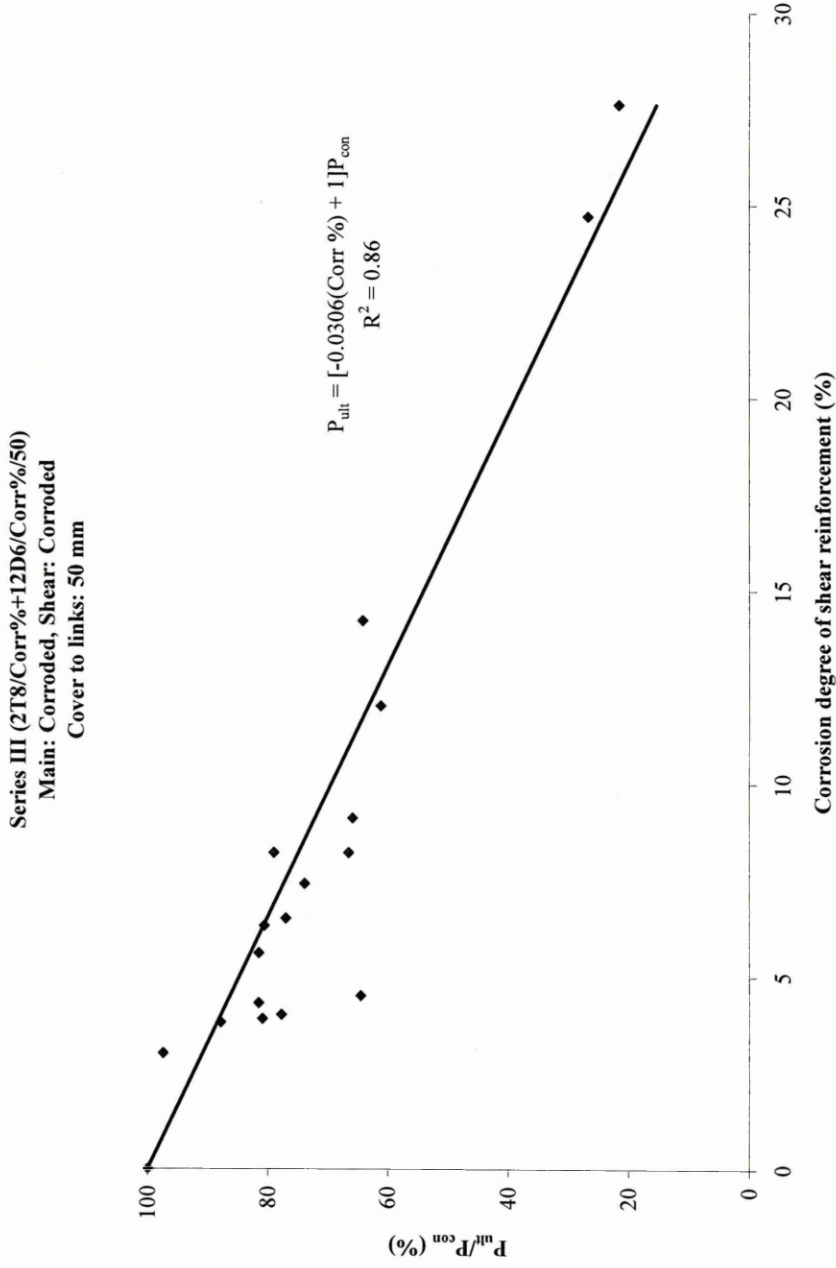


Figure 10.8 The effect of corrosion degree on the flexural load capacity of corrosion damaged reinforced concrete beams

reinforcement is plotted against ( $P_{ult} / P_{con}$ ). These graphs show a clear relationship between the degree of corrosion and the reduction in flexural strength. The results show that higher values of flexural load capacity are associated with degree of shear reinforcement corrosion to up to 5%. This is due the fact that the shear reinforcement was made of plain steel and the corrosion helped maintain the integrity of the concrete through increased bond.

Figures 10.7 and 10.8 show the relationship between the degree of main and reinforcement corrosion and the flexural load capacity, as a percentage of the control beam, of beam Series III which were corroded at a rate  $1 \text{ mA/cm}^2$ . Linear scatter between the results of individual beams is evident (coefficients of correlation 0.92, Figure 10.7 and 0.86, Figure 10.8).

This good correlation coefficient indicate that there is a strong positive relationship between the ratio of flexural load of failure of corroded beam to that of control beam and the amount of corrosion.

The following conclusions were drawn from the experimental results of Series III reported in this chapter:

- The shear reinforcement helped maintain integrity of the beam even if they were heavily corroded;
- Beams with shear reinforcement corrosion suffered negligible strength loss as can be concluded from Figures 10.7 and 10.8. These graphs show that shear reinforcement corrosion do not lead to a significant reduction of  $P_{ult} / P_{con}$  ratio (concluded in test Series II);

*(Main and shear reinforcement corrosion)*

- As it was previously reported (Chapter 9), corrosion of the shear reinforcement modifies the type of failure. Whereas control beams failed by bending, heavily deteriorated beams (both main and shear reinforcement of about 25%) failed by shear.

**10.4 Final remarks**

All data reported in this chapter support previously reported data in Chapter 9. Test data was insufficient to make conclusions in regards of the failure mode. Therefore more test data is required before more rigorous analysis is to be undertaken for these test series. Due to time limitation this analysis was not carried further for the purpose of this thesis. However, the compatible data will be used to support the analysis carried out on test Series I in Chapter 11.

### *Analytical Modelling of Experimental Data*

#### **11.1 Introduction**

The ability to predict the residual strength of concrete structures is becoming increasingly important as the nation's infrastructure ages. The problems with steel reinforcement corrosion highlights the need for the service life (the period of time over which it is assumed that a structure will be used for its intended purpose with anticipated maintenance but without major repair being necessary) to be addressed at the design stage. The environment to which the concrete will be exposed is a key factor in designing for a given service life.

Decisions on whether to repair or to demolish structures may depend on the estimated service life. The estimation of the remaining service life of corroding structures is mainly based on empirical or qualitative models and on the subjective experience and expertise of the engineer. These methods primarily involve the use of mathematical models and life time extrapolations based on corrosion current measurements. In the assessment of an existing concrete structure, engineers may have to evaluate the capacity of a beam with reinforcement corrosion. A quantitative model could not be found in the literature to assist the engineer in conducting this assessment.

The methodology presented here relates the loss in steel cross section to the loss in load carrying capacity of reinforced concrete beams. It is a simplified method of predicting

the residual flexural strength of simply supported reinforced concrete beams with steel reinforcement corrosion.

## 11.2 Current method of residual life prediction

The increasing age of the bridge stock throughout Europe has highlighted the problems associated with deterioration in existing structures. Surveys have indicated that the main reasons for deterioration, besides normal wear and tear, are the increasing weights and volume of traffic using the road network, and adverse environment conditions such as exposure to chlorides and freeze thaw attack. The magnitude of the capital investment in European bridge stock requires that effective maintenance is required to ensure that the bridges are kept in safe service at minimum cost. The assessment methods currently being used do not normally include reliable techniques for the evaluation of the structural consequences of deterioration<sup>135, 136</sup>.

It is clear from previous published work<sup>137, 138</sup> that the corrosion of steel due to chloride contamination and the carbonation of concrete is a serious problem in bridges. Other forms of deterioration such as alkali silica reaction, freeze thaw action and sulphate attack are also common. In this thesis, simplified models for taking account of corrosion deterioration are developed for use in general assessments of deteriorated reinforced concrete beams.

The general practice of accounting for deterioration is by using actual section dimensions as measured on site or obtained from design data, and modifying the material properties based on material tests or NDT methods. Taking account of deterioration, in general, depends on the knowledge and experience of the assessing engineer. In the case of the UK, there are assessment documents<sup>139, 140, 141</sup> relating to

deterioration arising from chloride induced corrosion. These documents tend to be general in nature and contain little quantitative guidelines.

Due to the lack of quantitative information on the structural behaviour of beams suffering reinforcement corrosion, a quantitative model based on structural analysis does not exist but is urgently needed.

The general steps currently involved in the detailed assessment of any deteriorated structure are:

A decision to appraise a structure in detail is usually triggered by observations taken during routine inspection. The purpose of the appraisal must be established at the onset, since it dictates the scope of the investigation and the measurements to be taken.

Normally, it breaks down to the following component parts:

- A general appraisal of the structure, covering geometry, material properties and any physical deterioration. Usually this includes crack pattern analysis as an aid to establishing the causes of deterioration. There may be a number of causes and clear identification is important;
- Measurements to establish the general environment. For corrosion, local micro-climate is crucial, including the concrete cover;
- A progressive diagnostic approach to establish the current state (and likely future extent) of damage due to the dominant deterioration mechanism.

Situations may be encountered in which the remaining strength of concrete can only be estimated by predicting its original life using a service life model. Such a situation could arise where the concrete can not be inspected or samples taken due to inaccessibility or to potential hazard involved with its inspection. This would

necessitate obtaining or estimating the values of the material properties required to solve the model.

In general, this work is carried out by specialists but guidance<sup>142, 143, 144</sup> is available and procedures well established.

For corrosion in particular, measurement of the concrete cover is important together with moisture conditions. Progressive diagnosis may then follow involving a mix of site measurement and detailed laboratory analysis:

- Define current levels of safety and serviceability;
- Estimate rate of future deterioration;
- Estimate time to minimum technical performance (calculate critical section, i.e. establish minimum technical performance). Currently in use is BD 21/01<sup>145</sup>;
- Decision of remedial action and future management;
- Discussion with client and owners.

The key to this is the assembly of representative data and the interpretation of that data, in moving towards a realistic structural assessment. This process requires judgement to be made against limiting criteria. This is not straightforward, and the model developed in this thesis puts forward a suggestion on how it may be done.

### **11.3 British code BS 8110 and design of concrete structures EC2**

The current British Standard BS 8110<sup>146</sup> for design of reinforced concrete structures is due to be withdrawn by 2010 and will be replaced BS EN 1992-2:2005 Eurocode 2 Design of Concrete Structures<sup>147</sup>. The design of flexural elements to EC2 is very similar to that of BS 8110<sup>148</sup> as shown in Figures 11.1 (a) and (b) and the reinforcement

provision dictates the mode of failure of a concrete beam in bending. The section fails due to yielding of the steel reinforcement (under reinforced) and the failure mode is far more ductile resulting in large deformations, cracking and spalling of concrete on the tension face.

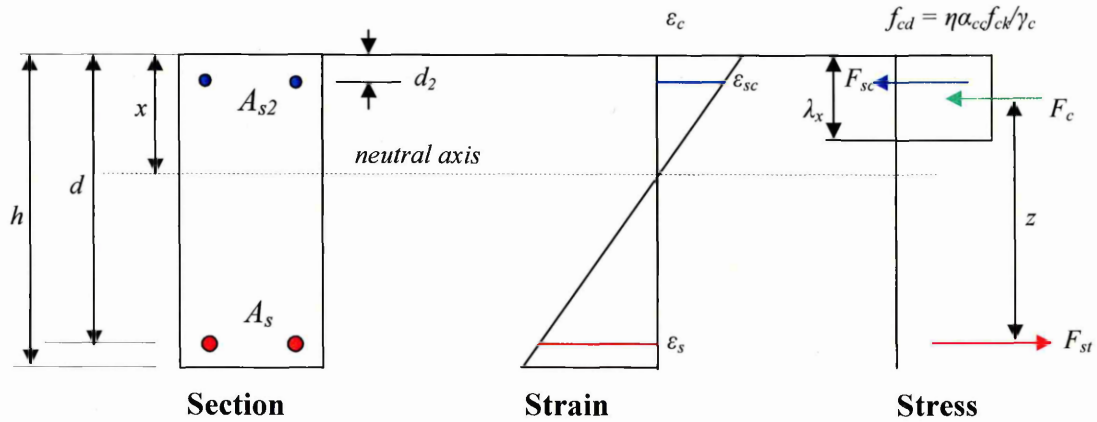


Figure 11.1 (a) EC2 stress block <sup>148</sup>

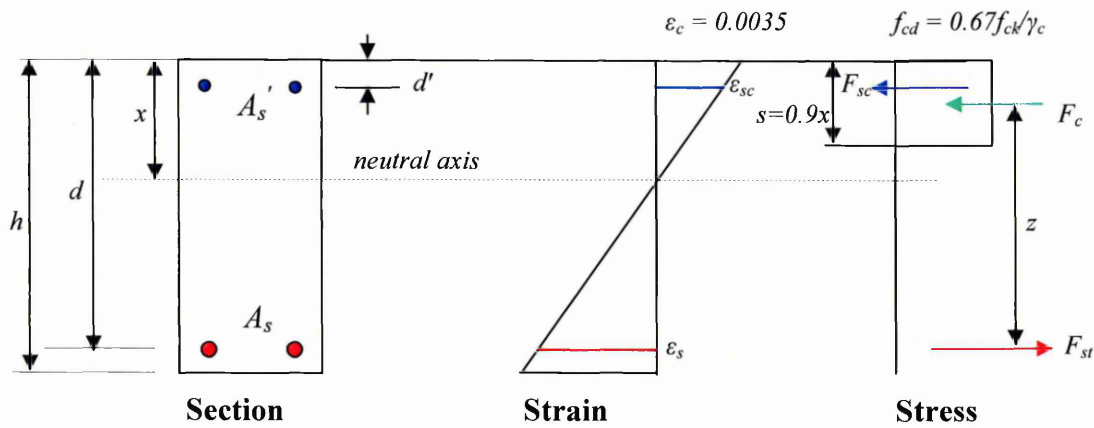


Figure 11.1 (b) BS 8110 stress block <sup>148, 149</sup>

## 11.4 Analysis of a doubly reinforced rectangular section

The analysis presented in this chapter is based upon the current design standard, BS 8110, since beams which are currently showing signs of distress in the field would have been designed in accordance with one of its predecessors. The ultimate moment of resistance of the cross section is calculated from the following data and factors of safety are excluded for research purposes.

### 11.4.1 Design for moment of resistance

For equilibrium of the tensile and compressive forces on the section, see Figure 11.1 (b)

$$F_{st} = F_{cc} + F_{sc} \quad \text{Equation 11.1}$$

where

$F_{st}$  is the ultimate force in tensile reinforcement taken as:  $F_{st} = f_y \times A_s$ , where  $f_y$  is the yield stress of the tensile reinforcement and  $A_s$  is the area of tensile steel

$F_{cc}$  is the ultimate concrete compression force taken as:  $0.67 \times f_{cu} \times b \times s$ , where  $f_{cu}$  is a characteristic strength of the concrete,  $b$  is the width of the beam and  $s$  is the stress block depth

$F_{sc}$  is the ultimate force in compression reinforcement taken as:  $F_{sc} = f_y' \times A_s'$ , where  $f_y'$  is the yield stress of the compression reinforcement and  $A_s'$  is the area of compression steel (hanger bars)

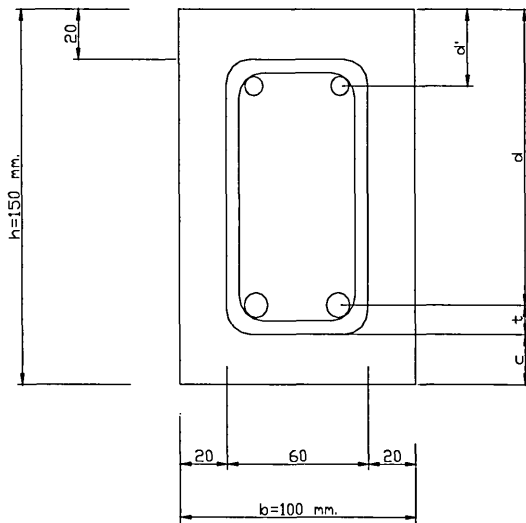
Therefore, Equation 11.1 can be re-written

$$f_y \times A_s = 0.67 \times f_{cu} \times b \times s + f_y' \times A_s' \quad \text{Equation 11.2}$$

Therefore, Equation 11.2 can be re-written

$$s = \frac{f_y \times A_s - f'_y \times A'_s}{0.67 \times f_{cu} \times b} \text{ [mm]} \quad \text{Equation 11.3}$$

As shown in Figure 11.2:



$$d = 150 - c - t \text{ [mm]}$$

$$t = \phi' + D/2 \text{ [mm]}$$

$$z = d - s/2 \text{ [mm]}$$

$$d' = 20 + \phi' + \phi'/2 \text{ [mm]}$$

Figure 11.2 Cross sectional area of reinforced concrete beams used in the analysis

Taking the moments about the tension steel  $A_s$ , the ultimate design moment is given by the following equation

$$M_c = F_{sc} \times (d - d') + F_{cc} \times z \quad \text{Equation 11.4}$$

The maximum value for  $z$  is  $0.775 \times d$  as given in BS 8110<sup>146</sup>.

The ultimate concrete design stress is  $0.67 \times f_{cu} / \gamma_c$  where the factor 0.67 relates the cube crushing strength to the flexural strength of concrete<sup>150</sup> and  $\gamma_c$  is the partial safety factor

for the strength of concrete for designing members cast in situ (normally 1.5).

$$F_{sc} = \gamma_s \times f_y' \times A_s' \quad \text{Equation 11.5}$$

$$F_{cc} = (0.67 \times f_{cu} / \gamma_c) \times b \times s \quad \text{Equation 11.6}$$

Substituting Equation 11.5 and Equation 11.6 into Equation 11.4 gives

$$M_c = \gamma_s \times f_y' \times A_s' \times (d-d') + [(0.67 \times f_{cu} / \gamma_c) \times b \times s] \times (0.775 \times d) \quad [\text{kNm}]$$

$$\text{Equation 11.7}$$

For the purpose of analysis, the material partial factor of safety,  $\gamma_s$  and  $\gamma_c$  are taken as unity (the actual steel stress at yielding was adopted from tests), substituting these into Equation 11.7 and taking  $s = 0.45 \times d$  gives

$$M_c = [0.234 \times f_{cu} \times b \times d^2 + f_y' \times A_s' \times (d-d')] \times 10^{-6} \quad [\text{kNm}]$$

$$\text{Equation 11.8}$$

Equation 11.8 was used to calculate the maximum compressive moment of resistance of the beams,  $M_c$ .

#### 11.4.2 Design for shear resistance

The design shear stress,  $v$ , at cross section should be calculated from

$$v = \frac{1000 \times V}{b_w \times d} \quad [\text{N/mm}^2] \quad \text{Equation 11.9}$$

where

$V$  is the ultimate shear force in kN

$b_w$  is the width of the beam web in mm

$d$  is the effective depth in mm

Large shearing forces are also liable to cause crushing of the concrete along the direction of the principal compression stresses, and therefore at the face of support the average shear stress should never exceed  $0.8 \times \sqrt{f_{cu}}$  or  $5 \text{ N/mm}^2$  whichever is lesser.

The shear stress,  $v_c$ , which the concrete on its own can resist, is derived from the expression

$$v_c = 0.79 \times (100 \times A_s / (b_w \times d))^{1/3} \times (400/d)^{1/4} \times \gamma_m \quad \text{Equation 11.10}$$

where

the term  $A_s$  is the area of longitudinal tension reinforcement

$\gamma_m$  is factor of safety equal to 1.0, not 1.25

Shear reinforcement in the form of vertical links was provided in accordance with the minimum areas as given by BS 8110.

$$(v_c + 0.40) < v < 5 \text{ N/mm}^2$$

The area of shear reinforcement in was calculated from:

$$A_{sv} = b_w \times s_v \times (v - v_c) / f_{yv} \text{ [mm}^2\text{]} \quad \text{Equation 11.11}$$

where

$A_{sv}$  is the cross sectional are of the two legs of the stirrup in  $\text{mm}^2$

$s_v$  is the spacing of the stirrups in mm

$f_{yv}$  is the characteristic strength of the stirrups in  $\text{N/mm}^2$

The spacing of the shear reinforcement in the direction of the span should not exceed  $0.75 \times d \text{ [mm]}$ .

Figure 11.3 shows the schematic representation of stress due to external loading.

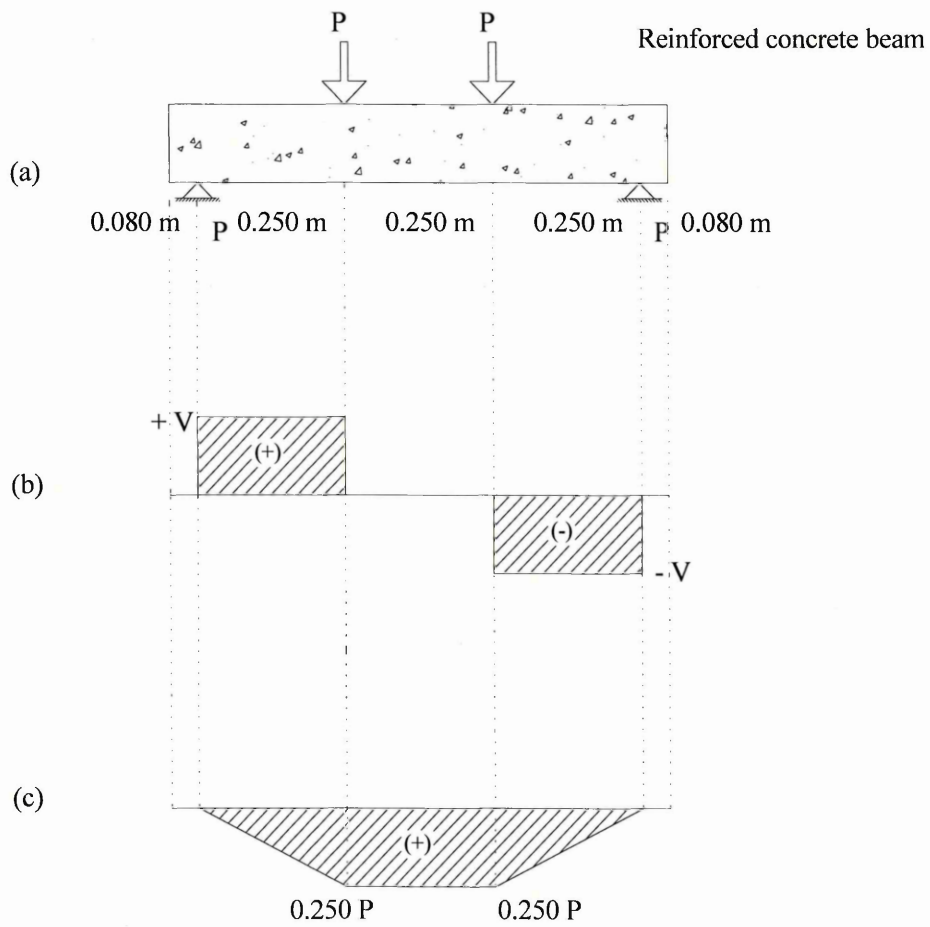


Figure 11.3 Schematic representation of stress due to external loading

(a) loading configuration

(b) shear force diagram,  $Q$  [kN]

(c) bending moment diagram,  $M$  [kNm]

## 11.5 Characteristics of reinforced concrete beams

In reinforced concrete beam design<sup>99</sup>, the moment of resistance in the tensile zone,  $M_{t(0)}$  is designed to be less than the moment of resistance in the compressive zone,  $M_c$ . Designing beams in this manner ensures a ductile failure at yielding. The level of under reinforcement can depend upon the preferences of the designer in complying with design and construction constraints, codes and availability of materials such as steel diameters and bar lengths. The quantity of tensile steel in a rectangular section can vary between a minimum of 0.13% to a maximum of 4% of the gross cross sectional area when designing in accordance with BS 8110. The designer will specify the number, type and diameter of steel reinforcement bars required to satisfy the area of steel required. The arrangement of the reinforcing bars is constrained by practical considerations such as construction tolerances, clearance between bars and available bar size and length. In addition, the cover to the steel can also vary from 20 mm to 70 mm depending on the exposure conditions and fire resistance requirements.

This means that beams can possess different levels of under reinforcement (or  $M_{t(0)}/M_c$  ratios). Once in service, this ratio is further influenced by corrosion of the steel reinforcement as cracking and spalling of the cover concrete will decrease the moment of resistance in the tensile zone.

Despite the majority of reinforced concrete structures meeting or exceeding their intended service life<sup>151</sup>, many undergo some maintenance and repair<sup>152, 153</sup>. Studies have been conducted which led to design procedures for enhanced design life<sup>110, 154</sup>, but nevertheless, repairs to such structures are costly.

## 11.6 Effect of corrosion on the flexural capacity of reinforced concrete beams

The ultimate aim is to develop analytical models for the deterioration process which can be used as a part of the general assessment procedure to enable a reliable estimate of load carrying capacity to be produced and used in an overall bridge management system.

The purpose of the analysis in this section, therefore, is two fold: firstly, to investigate the influence of  $M_{t(0)}/M_c$  on residual flexural strength of corroded beams and secondly, to determine which detailing parameters (e.g. size and percentage of steel reinforcement, cover) influence  $M_{t(0)}/M_c$ . Consideration of the implications of detailing on the residual strength of corroded flexural members may help reduce the enormous repair costs in Europe each year.

A successful understanding of the influence of the design parameters listed above will contribute to the development of analytical procedures for predicting the residual service life of reinforced concrete beams.

### 11.6.1 Characteristics of beam Series I

A total of 74 beams with main steel corrosion, were tested in Series I. The main variables (Table 11.1) were main steel diameter (consisted of either two diameter 8, 10 or 12 mm) and cover to main reinforcement (either 26, 36 or 56 mm). Each beam was tested independently. All beams contained non corroded shear reinforcement.

### 11.6.2 $M_{t(0)}/M_c$ relationship for various degrees of corrosion

An idealised stress block was used to analyse the section to determine the maximum compressive moment of resistance,  $M_c$ , as shown in Figure 11.1 (b).

Table 11.1 Variables in test programme.

Main Steel	Cover to main reinforcement (mm)	$c/d$	Target Corrosion (%)
2T8	26	3.3	0 – 15% in increments of 5%
	36	4.5	
	56	7.0	
2T10	26	2.6	
	36	3.6	
	56	5.6	
2T12	56	4.7	

Table 11.2 gives geometric details and material properties for the beams under consideration. In addition, similar properties from beams tested by other researchers are also presented to extend the  $M_{t(0)}/M_c$  range of beams considered<sup>4, 78, 86, 155</sup>. Some of these beams were reinforced in the tensile zone only and the shear capacity was enhanced via other means. In addition, certain details were unavailable from the publications, for example, actual yield strength for the steel reinforcement, precise cover information etc. and these were estimated by the authors from the information given. The corrosion rate applied to corrode the steel ranged from 0.1 – 2 mA/cm<sup>2</sup> as opposed to 1 mA/cm<sup>2</sup> employed in this investigation which may have an influence on the overall performance. Nevertheless, these results were included to support the data presented in this section.

Table 11.2 Beams properties

	2T8	2T8	2T8	2T8	2T10	2T10	2T10	2T10	2T10	2T12	Mangat et al 2T10 <sup>86</sup>	Mangat et al 2T8 <sup>78</sup>	Al Sulamani et al 1T12 <sup>4</sup>	Rodriguez et al 2T10 <sup>155</sup>
$C$ (mm)	26	36	56	56	26	36	56	56	56	56	20	20	29	20
$f_{cu}$ (N/mm <sup>2</sup> )	56.0*	52.5*	52.2*	52.2*	49.1*	59.8*	53.6*	57.5*	57.5*	57.5*	40.0	40.0	40.0	50.0
$b$ (mm)	100	100	100	100	100	100	100	100	100	100	100	100	150	150
$\phi'$ (mm)	6 <sup>+</sup>	6 <sup>+</sup>	6 <sup>+</sup>	6 <sup>+</sup>	6 <sup>+</sup>	6 <sup>+</sup>	–	–	–	6				
$f_y'$ (N/mm <sup>2</sup> )	328*	341*	345*	345*	326*	366*	328*	384*	384*	384*	–	–	–	626
$As'$ (mm <sup>2</sup> )	57	57	57	57	57	57	57	57	57	57	–	–	–	57
$d'$ (mm)	23	23	23	23	23	23	23	23	23	23	–	–	–	23
$h$ (mm)	150	150	150	150	150	150	150	150	150	150	150	150	150	200
$D$ (mm)	8 <sup>+</sup>	8 <sup>+</sup>	8 <sup>+</sup>	8 <sup>+</sup>	10 <sup>+</sup>	10 <sup>+</sup>	10 <sup>+</sup>	12 <sup>+</sup>	12 <sup>+</sup>	12 <sup>+</sup>	10	8	12	10
$d$ (mm)	126	116	96	96	125	115	95	94	94	94	125	126	115	175
$M_c$ (kNm)	22.7	18.3	12.7	12.7	19.8	20.4	12.6	13.4	13.4	13.4	14.6	14.9	18.6	59.1
$i$ (mA/cm <sup>2</sup> )	1	1	1	1	1	1	1	1	1	1	1	2	2	0.1

\* average values of all specimens

+ nominal values

Equation 11.8 was used to calculate the maximum compressive moment of resistance of the beams,  $M_c$ . The tensile moment at failure due to increasing levels of corrosion was obtained from  $M_{t(Corr)} = 0.250 \times (P_{ult}/2)$  (Figure 11.3) where  $P_{ult}$  is the ultimate load from laboratory beam tests. The relationship  $M_{t(Corr)}/M_c$  against the actual percentages of corrosion for the beams in Series I are shown in Figures 11.4 to 11.10. These graphs show that a higher degree of corrosion lead to a reduction in the  $M_{t(Corr)}/M_c$  ratio.

Regression analysis of the test data gave the correlation coefficient ranging from 0.95 to 0.88 for beams reinforced with 2T8 (Figures 11.4 to 11.6), 0.73 to 0.88 for beams reinforced with 2T10 (Figures 11.7 to 11.9) and 0.57 for beams reinforced with 2T12 (Figure 11.10).

Figure 11.11 shows a summary of the results from beams reinforced with 2T8, 2T10 and 2T12 main steel and three different covers to the main steel (26 mm, 36 mm and 56 mm respectively, Figures 11.4 to 11.10). The relationship is generally a linear decrease in  $M_{t(Corr)}/M_c$  with increasing percentages of corrosion. The equation for the line of best fit is tabulated along with the coefficient of correlation ( $R^2$ ). Beams 2T12/56 (Figure 11.11) exhibit the lowest correlation of the beams under consideration 0.57.

In addition, Figure 11.12 shows the relationship between  $M_{t(Corr)}/M_c$  and percentages of corrosion for beam Series III.

The summary results of the regression analysis are shown in Table 11.3. These fairly good values of correlation coefficients for beams reinforced with 2T8 and 2T10 indicate that there is a strong relationship between the ratio of bending moment of corroded beams to that of moment in compression and the amount of corrosion.

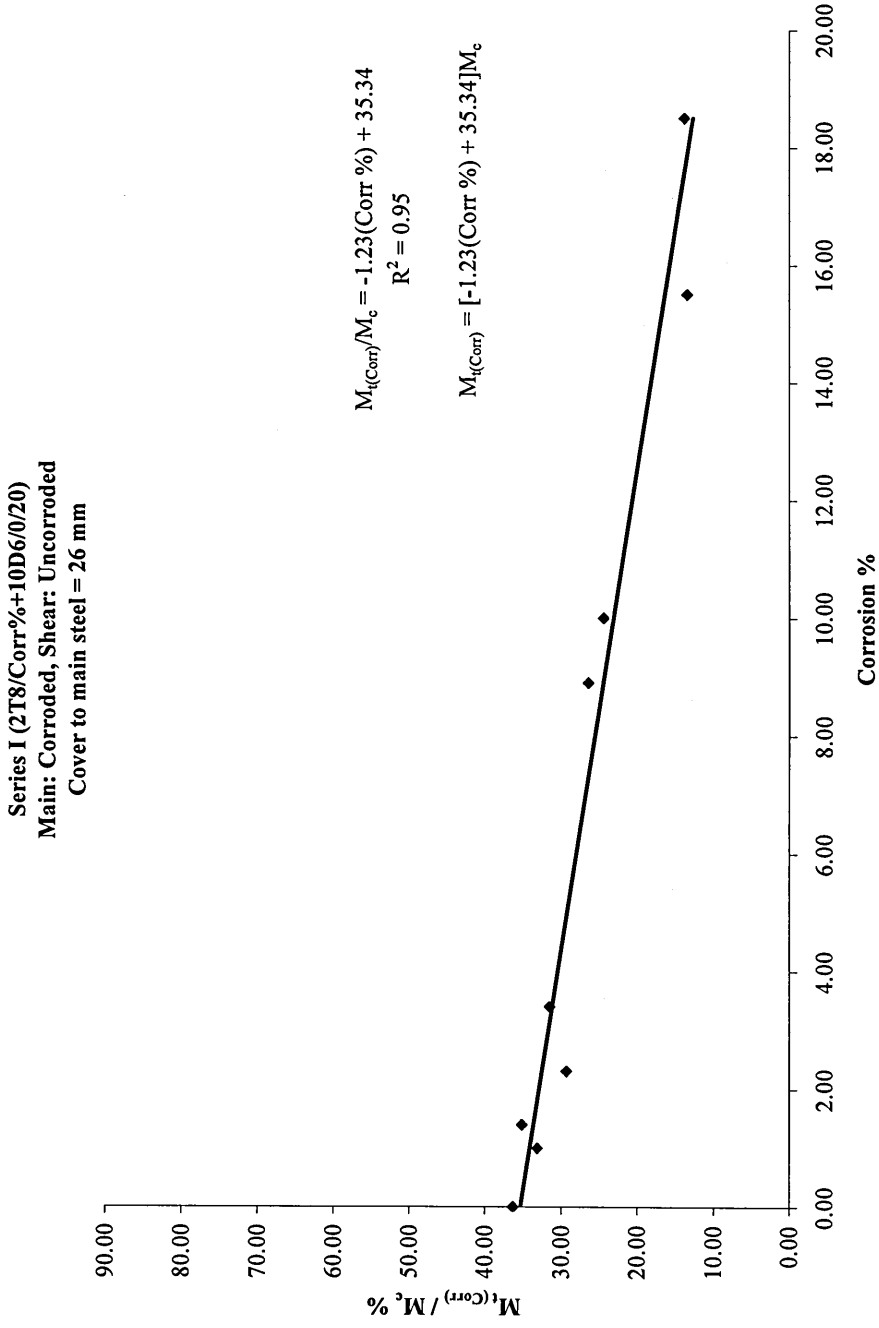


Figure 11.4 Effect of corrosion on the  $M_{t(\text{Corr})}/M_c$  ratio for 2T8/Corr%+10D6/0/20 beams

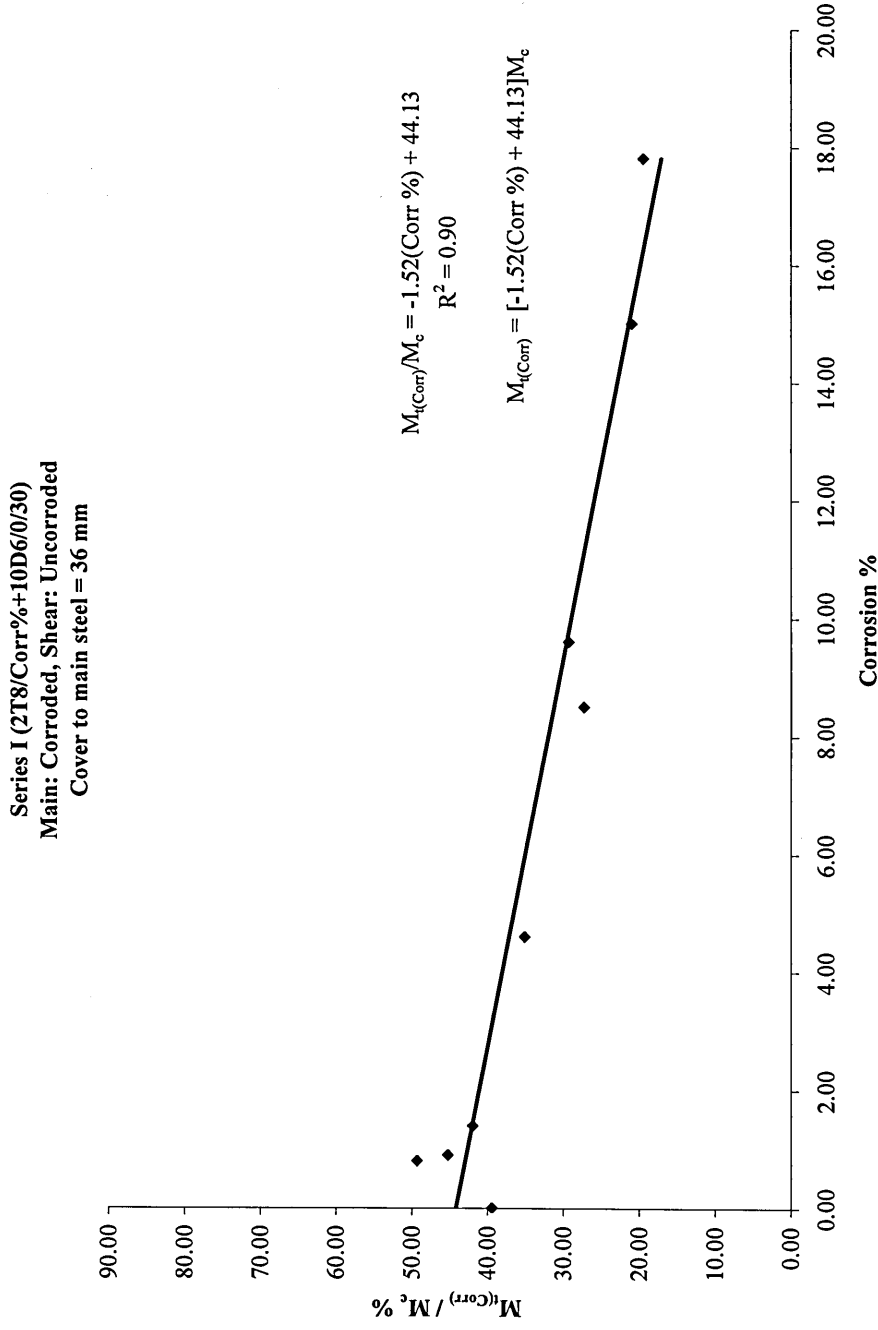


Figure 11.5 Effect of corrosion on the  $M_{r(Corr)}/M_c$  ratio for 2T8/Corr%+10D6/0/30 beams

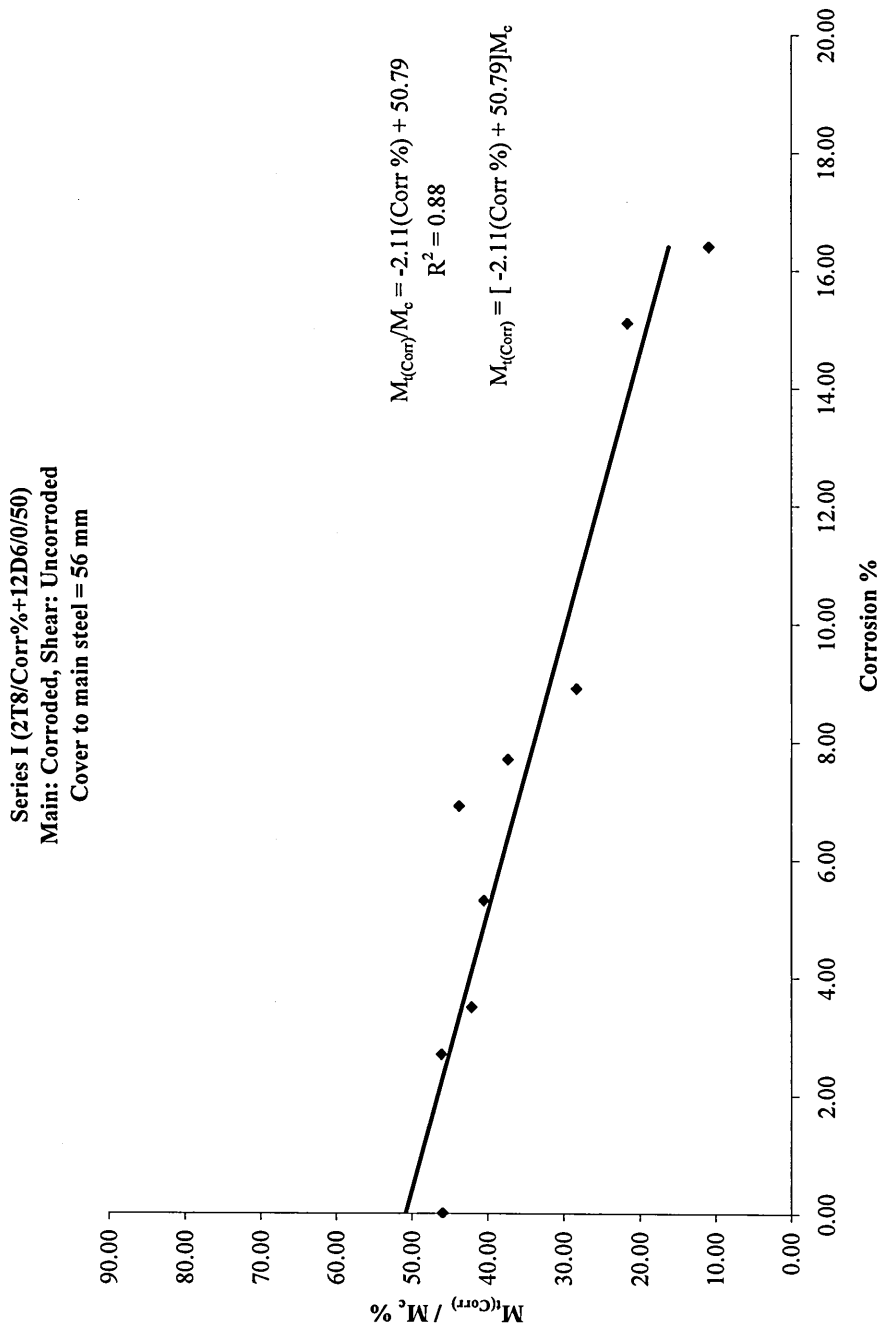


Figure 11.6 Effect of corrosion on the  $M_{t(Corr)}/M_c$  ratio for 2T8/Corr%+12D6/0/50 beams

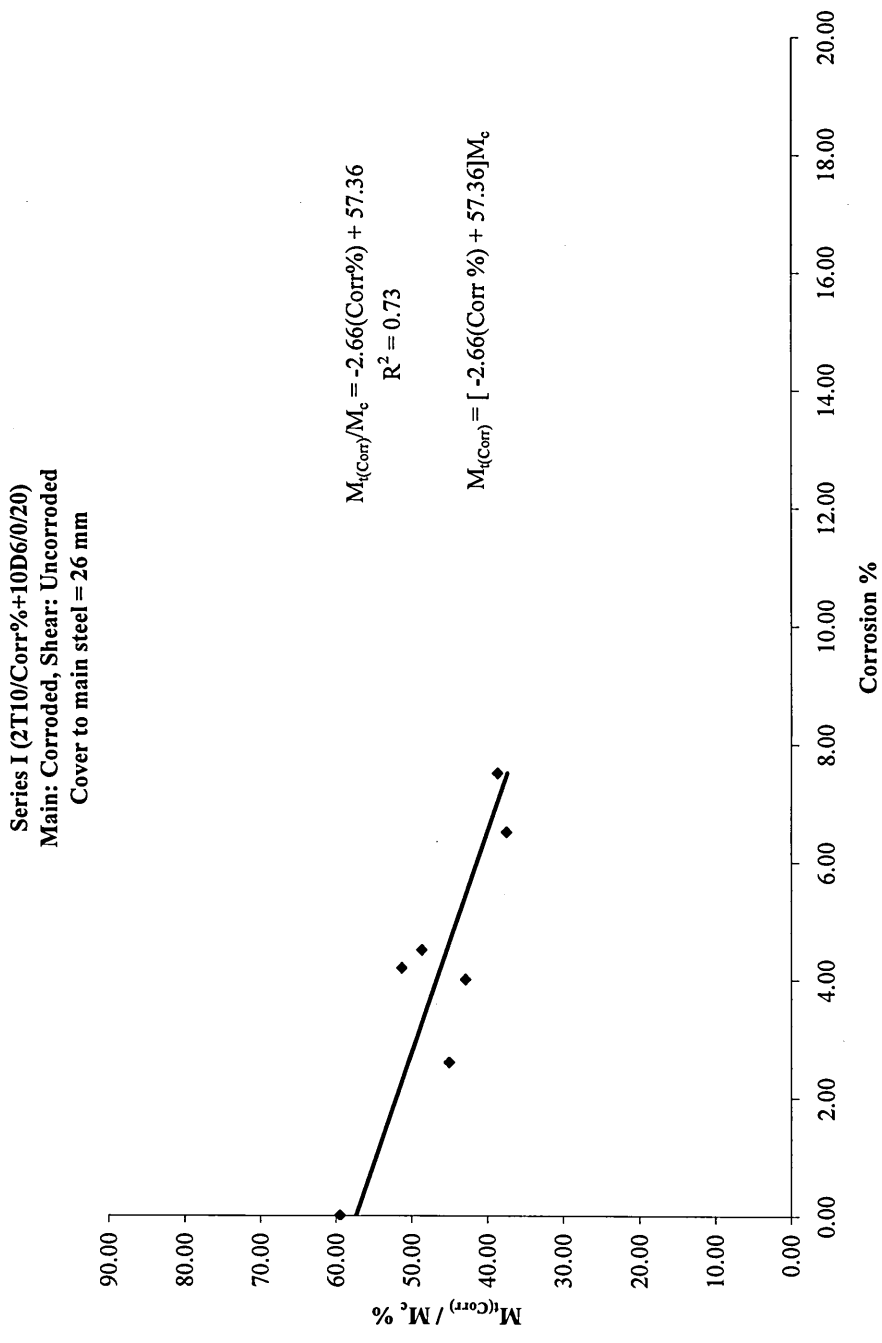


Figure 11.7 Effect of corrosion on the  $M_{t(Corr)}/M_c$  ratio for 2T10/Corr%+10D6/0/20 beams

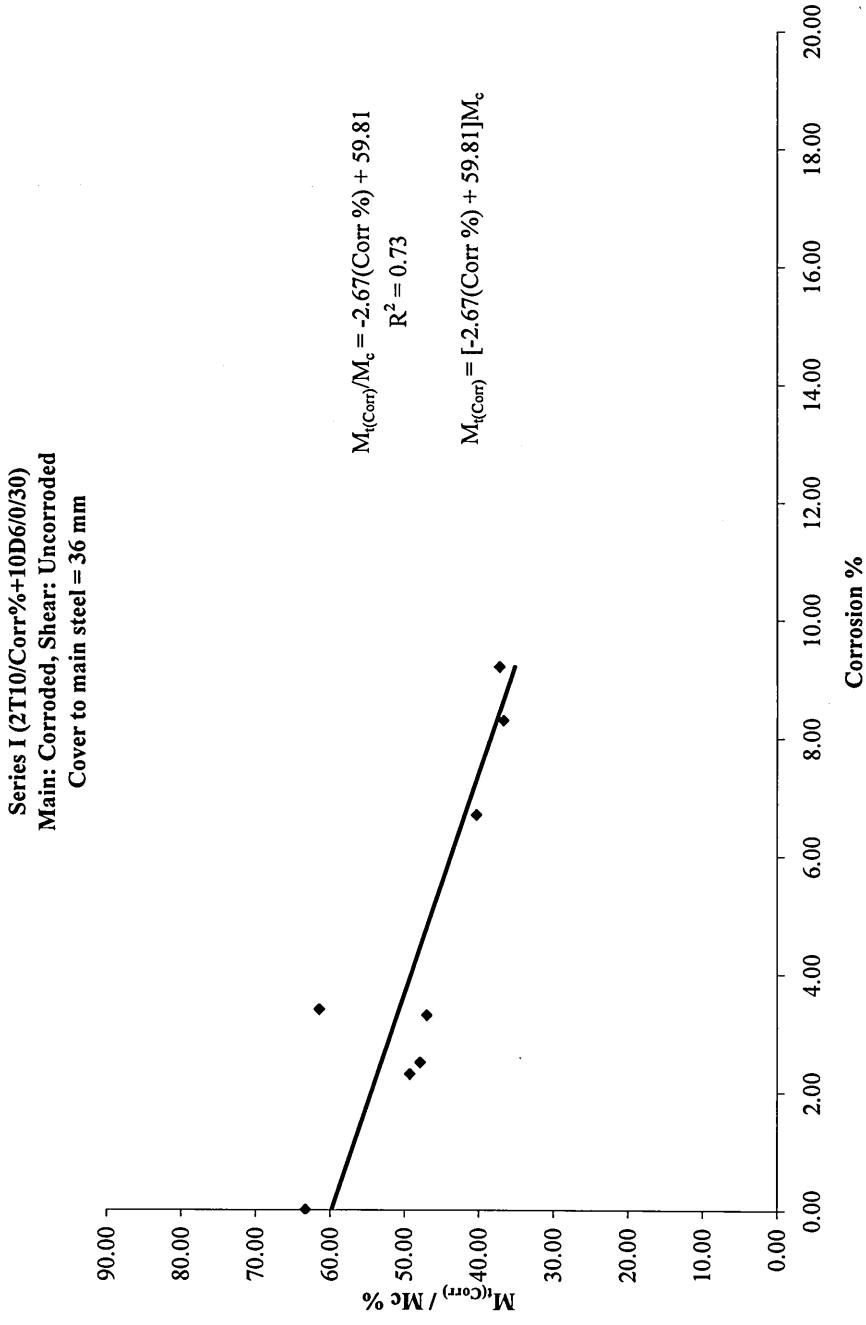


Figure 11.8 Effect of corrosion on the  $M_{t(Corr)}/M_c$  ratio for 2T10/Corr%+10D6/0/30 beams

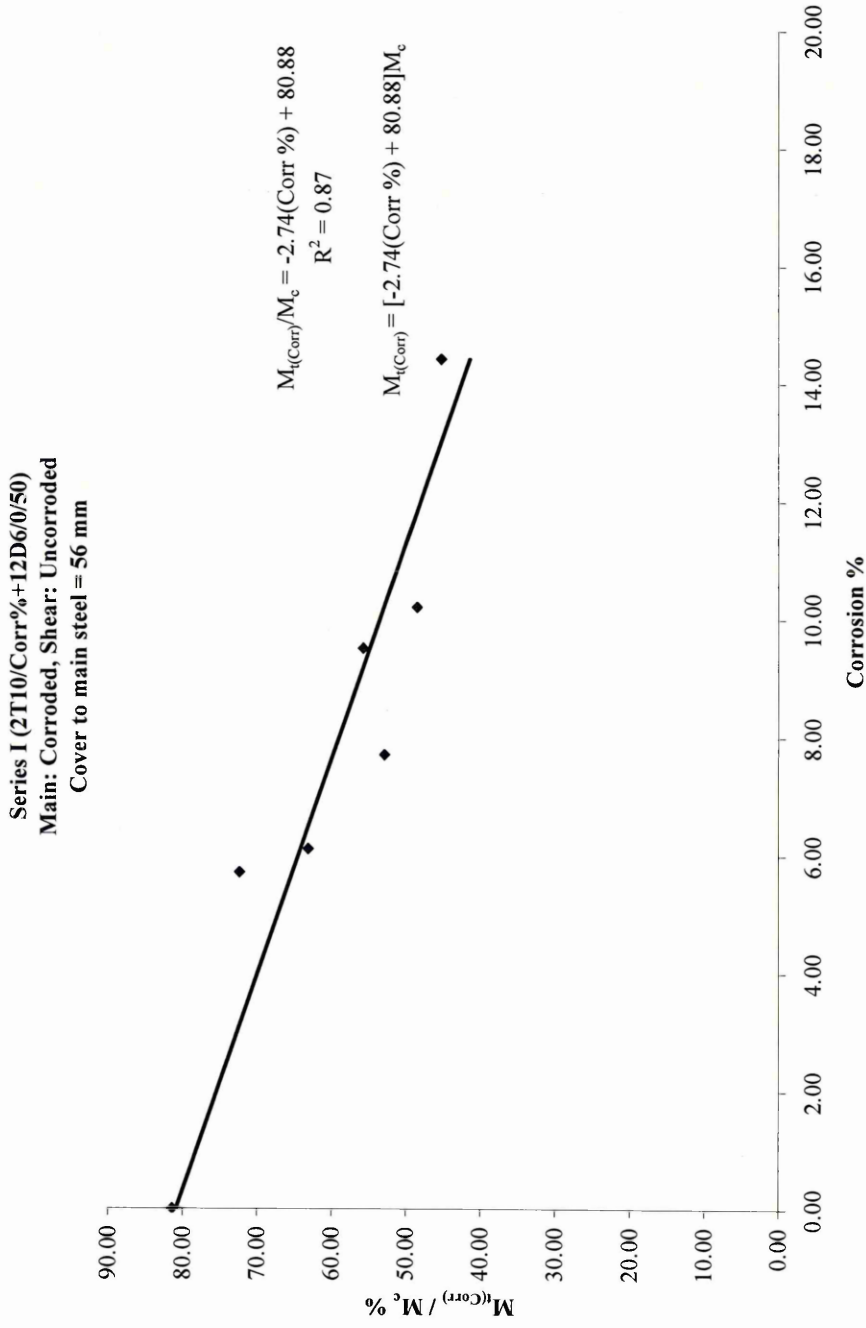


Figure 11.9 Effect of corrosion on the  $M_{t(Corr)} / M_c$  ratio for 2T10/Corr%+12D6/0/50 beams

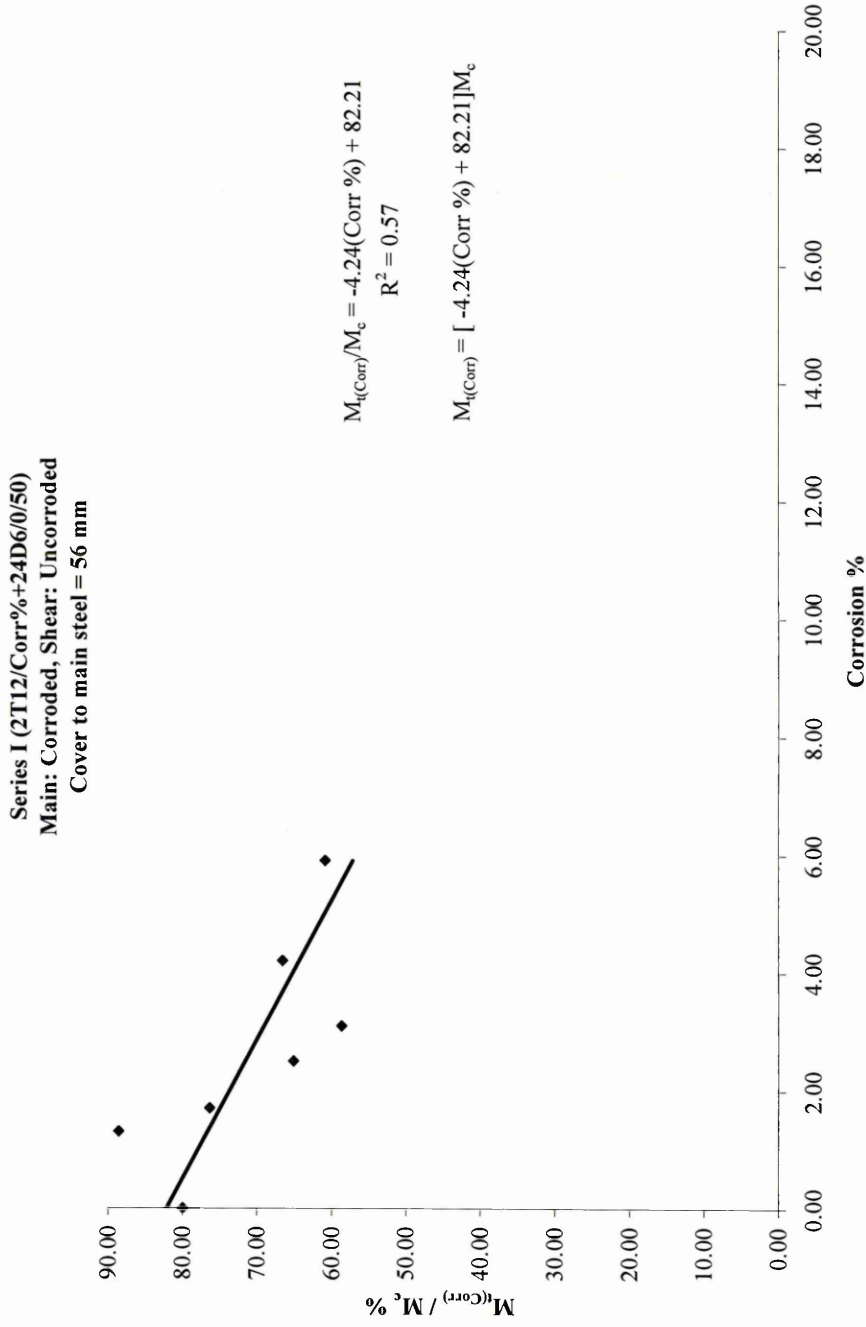


Figure 11.10 Effect of corrosion on the  $M_{t(Corr)}/M_c$  ratio for 2T12/Corr%+24D6/0/50 beams

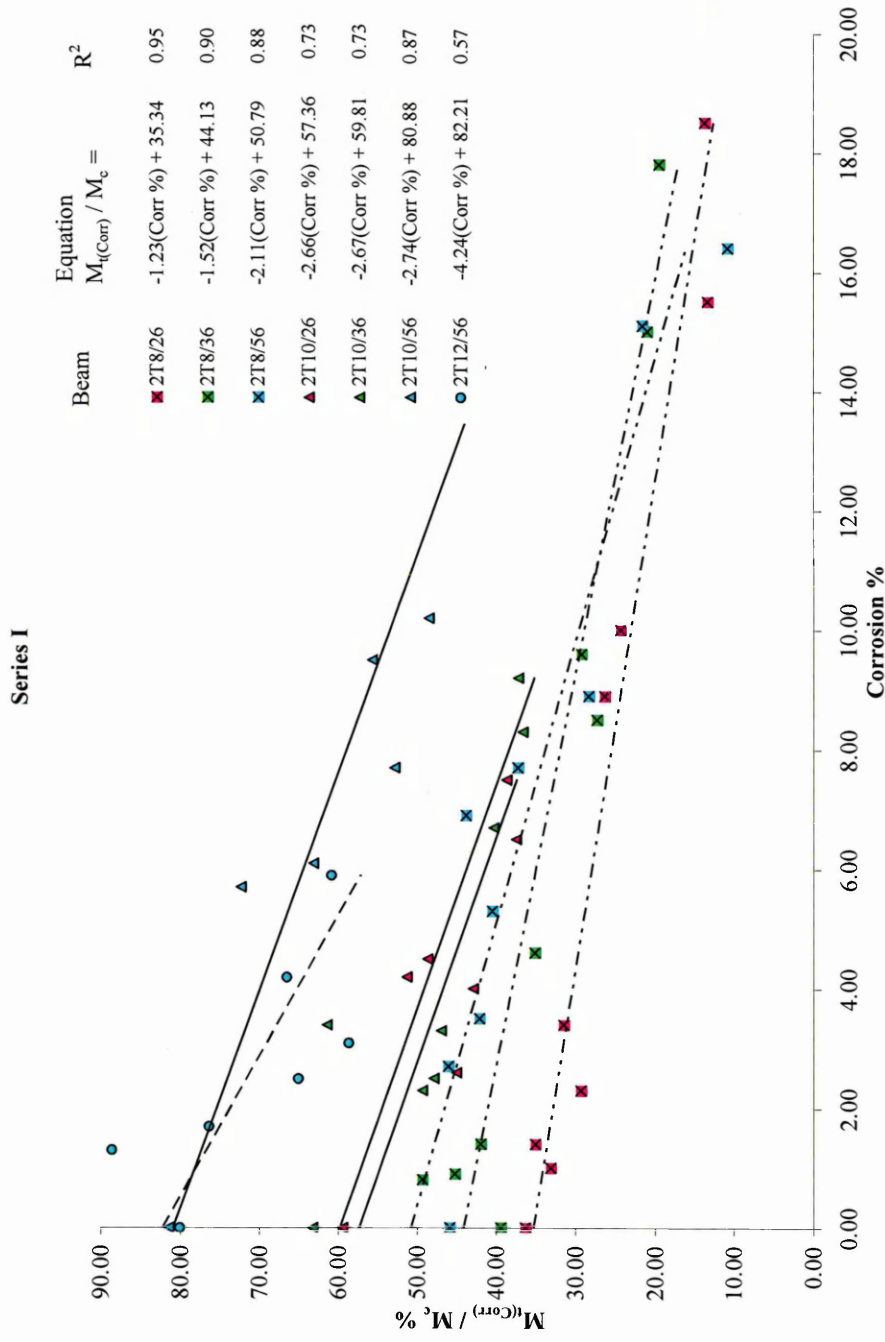


Figure 11.11 Summary of the effect of corrosion on the  $M_{t(Corr)}/M_c$  ratio for beam Series I

Series III (2T8/Corr%+12D6/Corr%/50)  
 Main: Corroded, Shear: Corroded  
 Cover to links = 50 mm

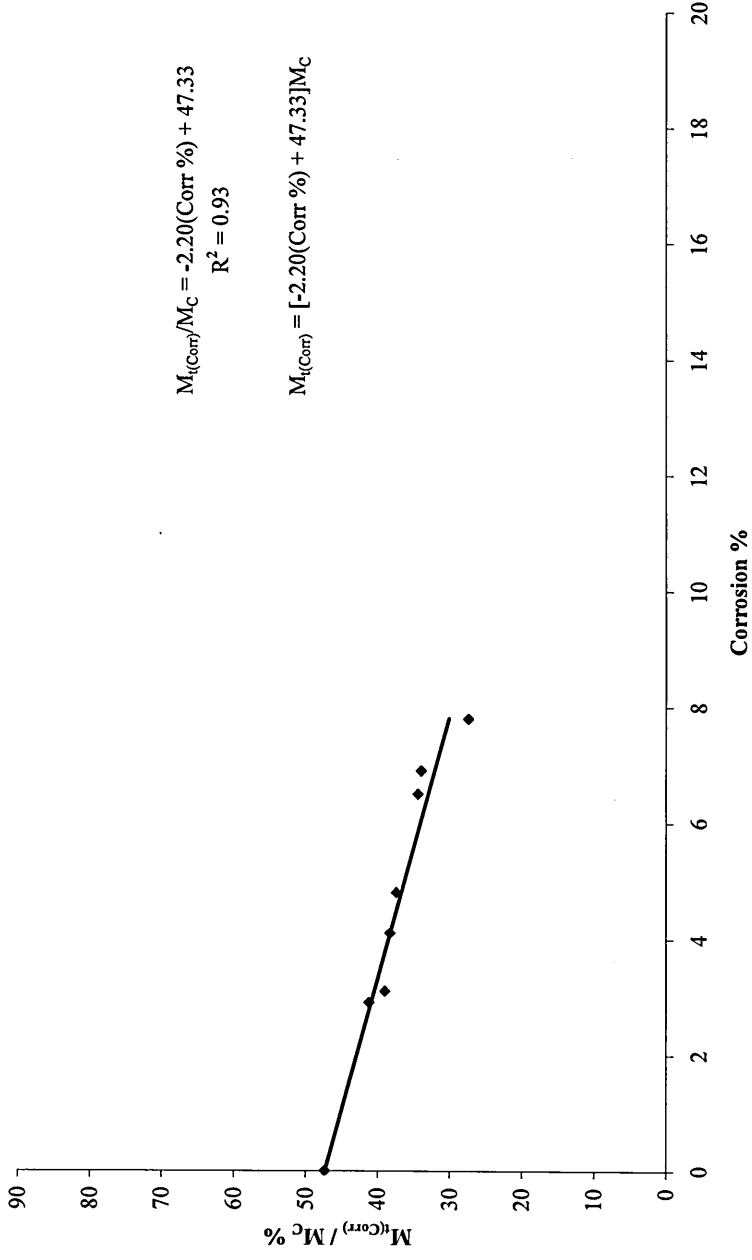


Figure 11.12 Effect of corrosion on the  $M_{f(Corr)}/M_c$  ratio for 2T8/Corr%+12D6/Corr%/50 (beam Series III shear reinforcement corrosion  $\leq 5\%$ )

Table 11.3 Results of regression analysis

Main reinforcement diameter	Cover [mm]	$\alpha$	$\beta$	Correlation coefficient $R^2$
2T8	26	-1.23	35.34	0.95
2T8	36	-1.52	44.13	0.90
2T8	56	-2.11	50.79	0.88
2T10	26	-2.66	57.36	0.73
2T10	36	-2.67	59.81	0.73
2T10	56	-2.74	80.88	0.87
2T12	56	-4.24	82.21	0.57

As reported in Chapter 9 and 10, there was little influence on the residual flexural strength when shear reinforcement were corroded to around 5%. Therefore, the data presented in Figure 11.12 is also used to support the data from beam Series I (Figures 11.4 to 11.10).

Beams are reinforced with 2T8 main steel and 12D6 exhibiting corrosion ( $\leq 5\%$ ), with cover to the main steel of 56 mm. The relationship is generally a linear decrease in  $M_{I(Corr)}/M_c$  with increasing percentages of corrosion. The equation for the line of best fit is almost identical to beam Series I, reinforced with 2T8 and cover to the main steel of 56 mm.

In addition, Figure 11.13 shows the relationship between  $M_{I(Corr)}/M_c$  and percentages of corrosion for beams tested by other researchers. In instances where full details were unavailable from the data presented to enable  $M_c$  to be estimated, for example, cover to the steel, an estimate was made for the purpose of utilising the data.

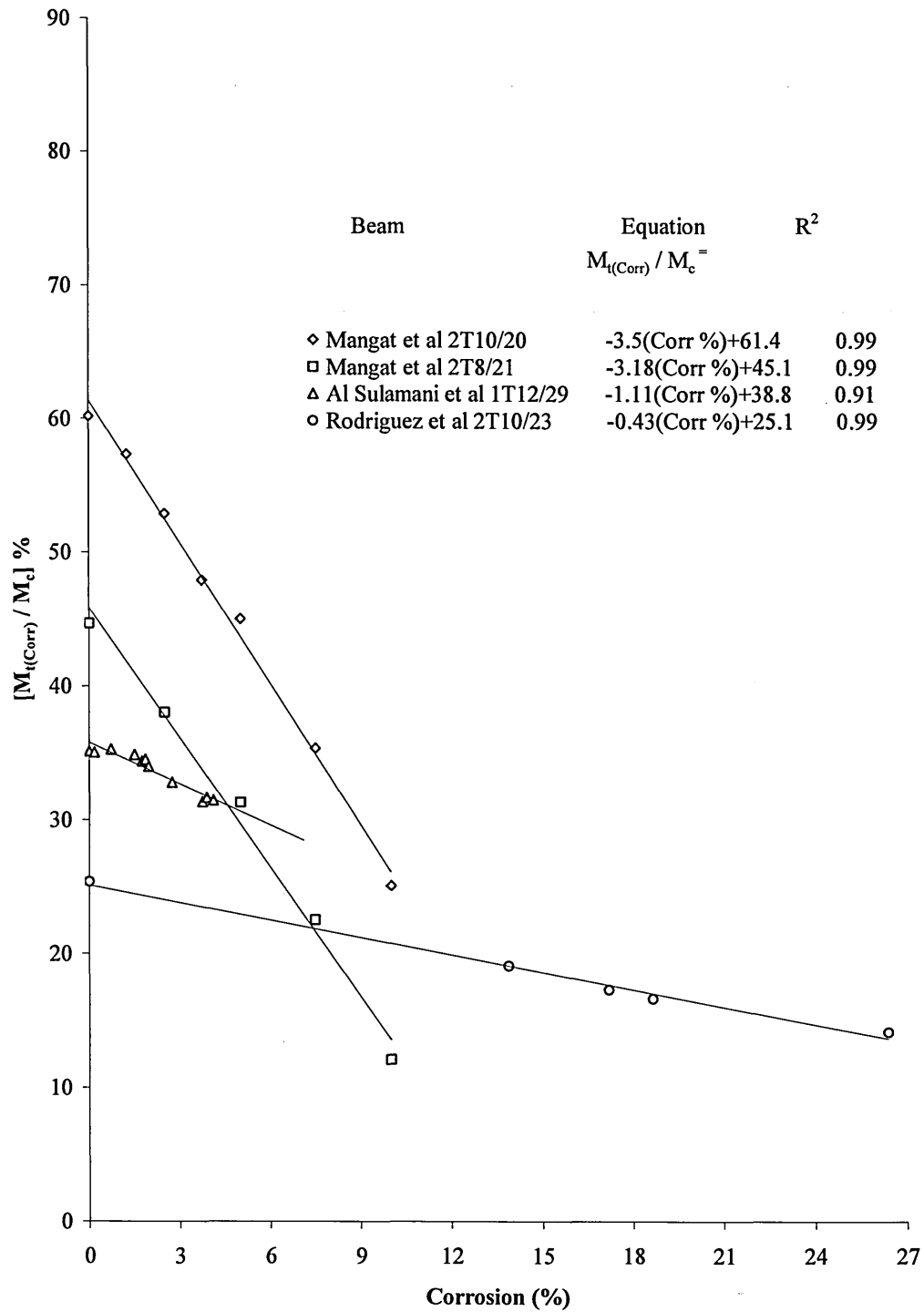


Figure 11.13 Comparison with other researchers

The best fit equation and  $R^2$  is also given for each of the four relationships and show very good agreement.

Concentrating on Figure 11.11, beams reinforced with smaller steel diameters tend to exhibit a lower  $M_{I(Corr)}/M_c$  ratios at zero percent corrosion [ $M_{I(Corr)} = M_{I(0)}$  for control beams (0% corrosion), hence  $M_{I(0)}$  will be used to identify the tensile moment of resistance at 0% corrosion]. For example, beam 2T12/56 exhibits the highest  $M_{I(0)}/M_c$  ratio at 0% corrosion (86.91%) whereas beam 2T8/26 exhibits a ratio of only 36.31%. The influence of lower  $M_{I(0)}/M_c$  ratios on the flexural strength of corroded beams will be considered in Section 11.6.3.

Referring to the tables in Figures 11.11 and 11.13, the relationship between  $M_{I(Corr)}/M_c$  and percent of corrosion is generally in the form

$$M_{I(Corr)}/M_c = \alpha \times (Corr \%) + \beta \quad \text{Equation 11.12}$$

where:

$M_{I(Corr)}$  is the flexural moment of resistance of corroded beam

$M_c$  is the maximum moment of resistance in the compression zone

$\alpha$  is the slope of the line of best fit

$(Corr \%)$  is the amount of corrosion

$\beta$  is the intercept ( $M_{I(Corr)}/M_c$ ) ratio

The slopes ( $\alpha$ ) generally tend to increase in negativity for beams with higher  $M_{I(0)}/M_c$  ratios. For example, the slope of beam 2T8/26 is  $-1.23$  whereas the slope for beam 2T12/56 is  $-4.24$ . Steeper slopes, therefore, mean that beams suffer a more rapid

decrease in flexural strength with higher corrosion. However, in order to optimise the design of beams for enhanced performance in a corrosive environment, the main parameters which influence the slopes in Figures 11.11 and 11.13 ( $M_{t(0)}/M_c$  ratios), cover to the main steel and percentages of main reinforcement are summarised in Table 11.4 and analysed in the next section.

Table 11.4 Overall comparisons

Identification	$M_{t(0)}/M_c$ (%)	Slope $\alpha^*$	Cover (mm)	Steel reinforcement $100 \times A_s/b \times h$ (%)
2T8/26	36.3	-1.23	26	0.67
2T8/36	39.4	-1.52	36	0.67
2T8/56	45.9	-2.11	56	0.67
2T10/26	59.5	-2.66	26	1.05
2T10/36	63.3	-2.67	36	1.05
2T10/56	81.5	-2.74	56	1.05
2T12/56	86.9	-4.24	56	1.51
Mangat et al 2T10/20 <sup>86</sup>	60.2	-3.52	20	1.05
Mangat et al 2T8/21 <sup>78</sup>	44.0	-3.18	21	0.67
Al Sulamani et al 1T12/29 <sup>4</sup>	38.1	-1.11	29	0.50
Rodriguez et al 2T10/20 <sup>155</sup>	25.4	-0.43	23	0.52

\* Slopes from Figures 11.11 and 11.13

### 11.6.3 Designing for durability

Figure 11.14 shows the relationship between the slopes,  $\alpha$  (Table 11.4) against  $M_{t(0)}/M_c$ .

Lower  $M_{t(0)}/M_c$  ratios generally correspond with lower slopes, meaning that these beams

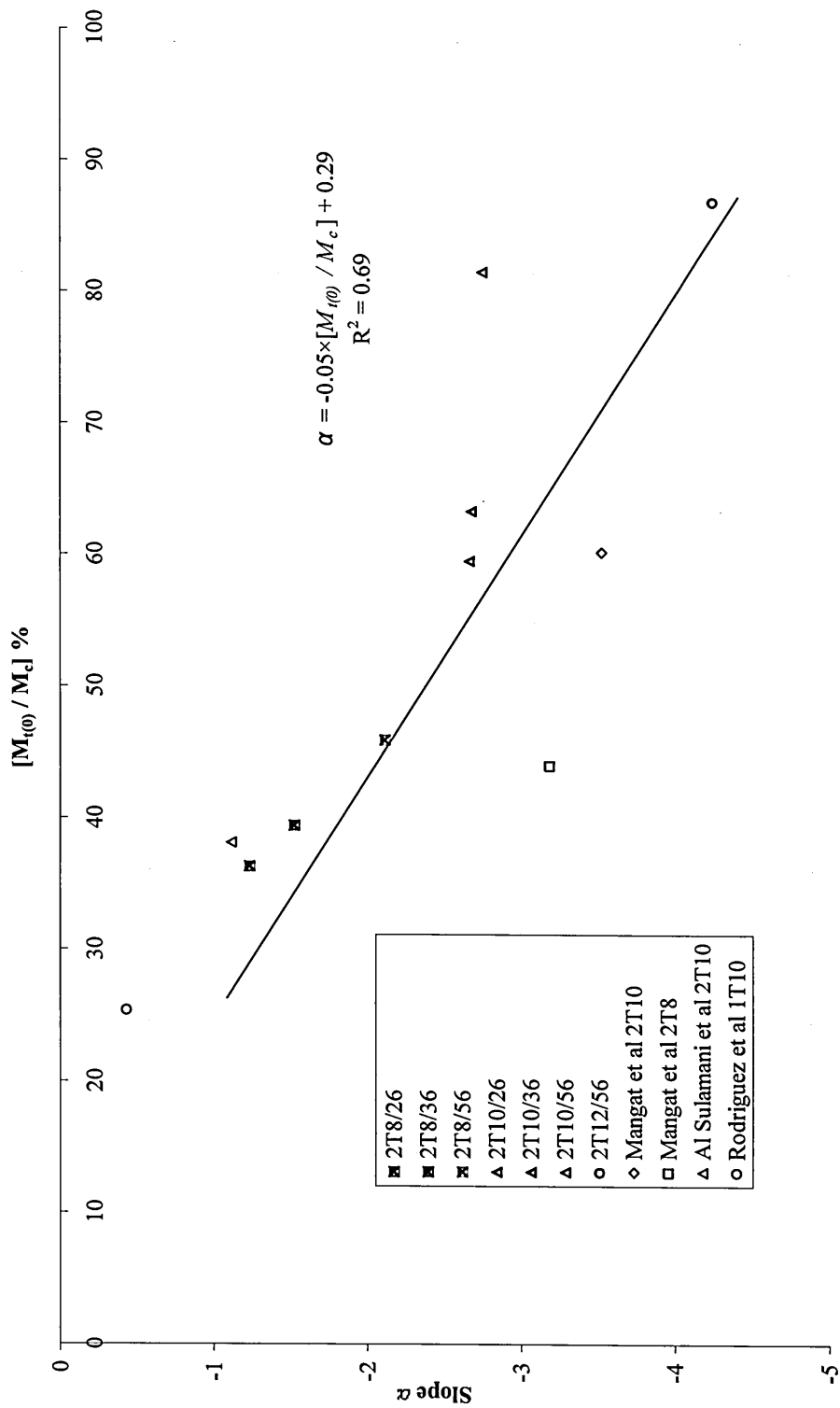


Figure 11.14 Effect of α on the M<sub>t(0)</sub>/M<sub>c</sub> ratio

will not suffer rapid deterioration when corrosion occurs. The aim of the designer, therefore, should be to specify beams with low  $M_{t(0)}/M_c$  ratios. This is achieved by considering the influence of parameters such as the quantity and diameter of main steel and cover in the design as outlined below.

Referring to Figure 11.15, the percentage of main steel reinforcement ( $100 \times A_s/b \times h$ ) is plotted against  $M_{t(0)}/M_c$  for the eleven types of beams under consideration. The linear relationship shows that lower percentages of main steel results in lower  $M_{t(0)}/M_c$ , which is beneficial in the event of corrosion to the main steel. Therefore, the designer should aim to reinforce the section with percentages as close as possible to the allowable minimum (0.13%). However, the designer should not reduce the percentage of main steel by simply increasing the cover and therefore increasing the section size ( $b \times h$ ).

Referring to Figure 11.16, the cover to the main steel is plotted against  $M_{t(0)}/M_c$ .

The scattered nature of the points indicates that an increase in cover to the main steel does not necessarily lead to lower  $M_{t(0)}/M_c$  ratios. Therefore, sufficient cover should be provided to meet the requirements of the design code for durability and fire resistance, but not unnecessarily increased simply to reduce the percentage of reinforcement.

The added benefits, therefore, of reducing the quantity of steel are that material costs will be lower due to less reinforcement in the section and smaller diameter corroding bars will exert lower rupture forces at the steel–concrete interface<sup>156</sup>. It has also been reported that bond strength decreases with increased bar diameter, so smaller diameter bars will help minimise the effect of corrosion induced bond deterioration<sup>156</sup>.

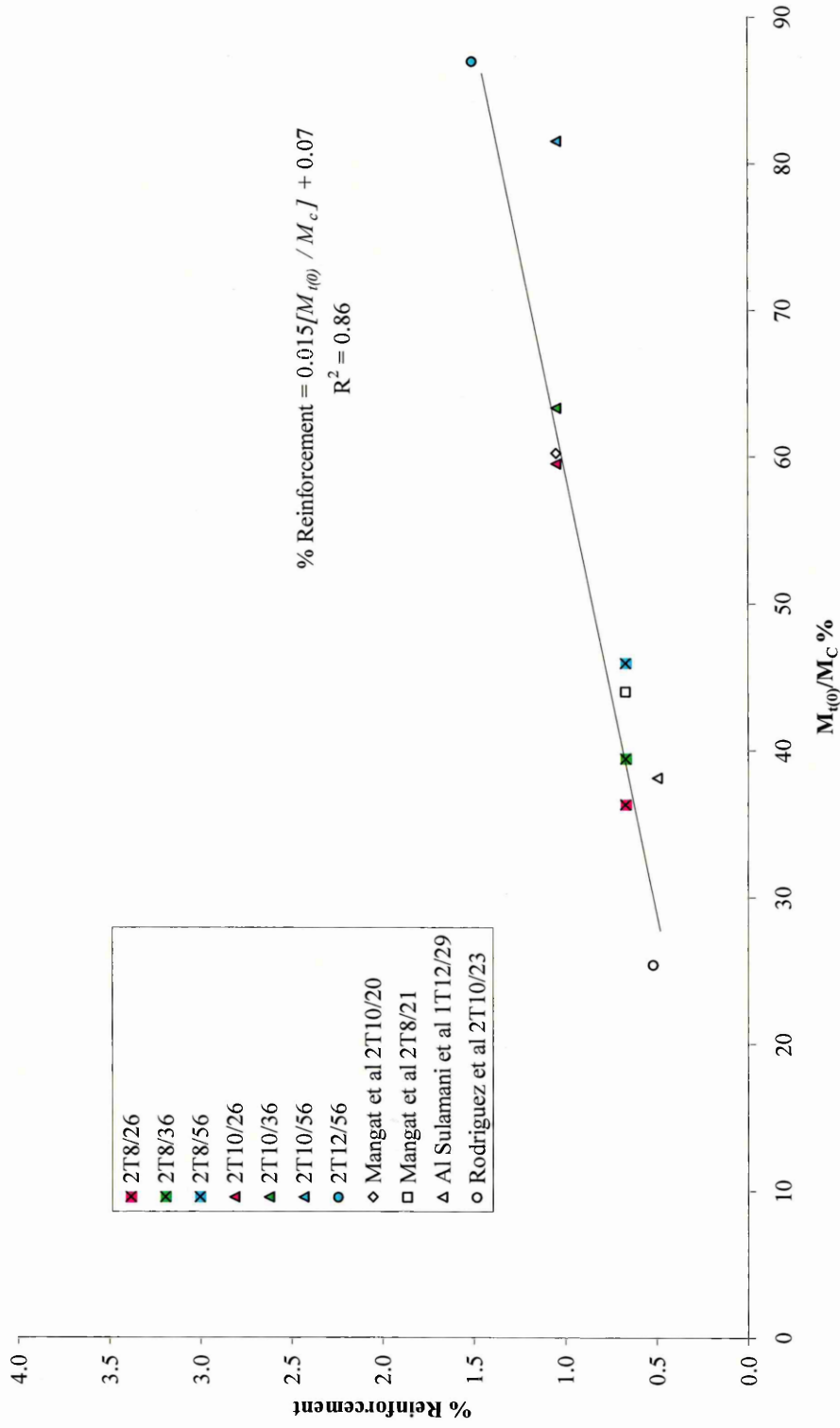


Figure 11.15 Effect of % Reinforcement on the  $M_{t(0)}/M_c$  ratio

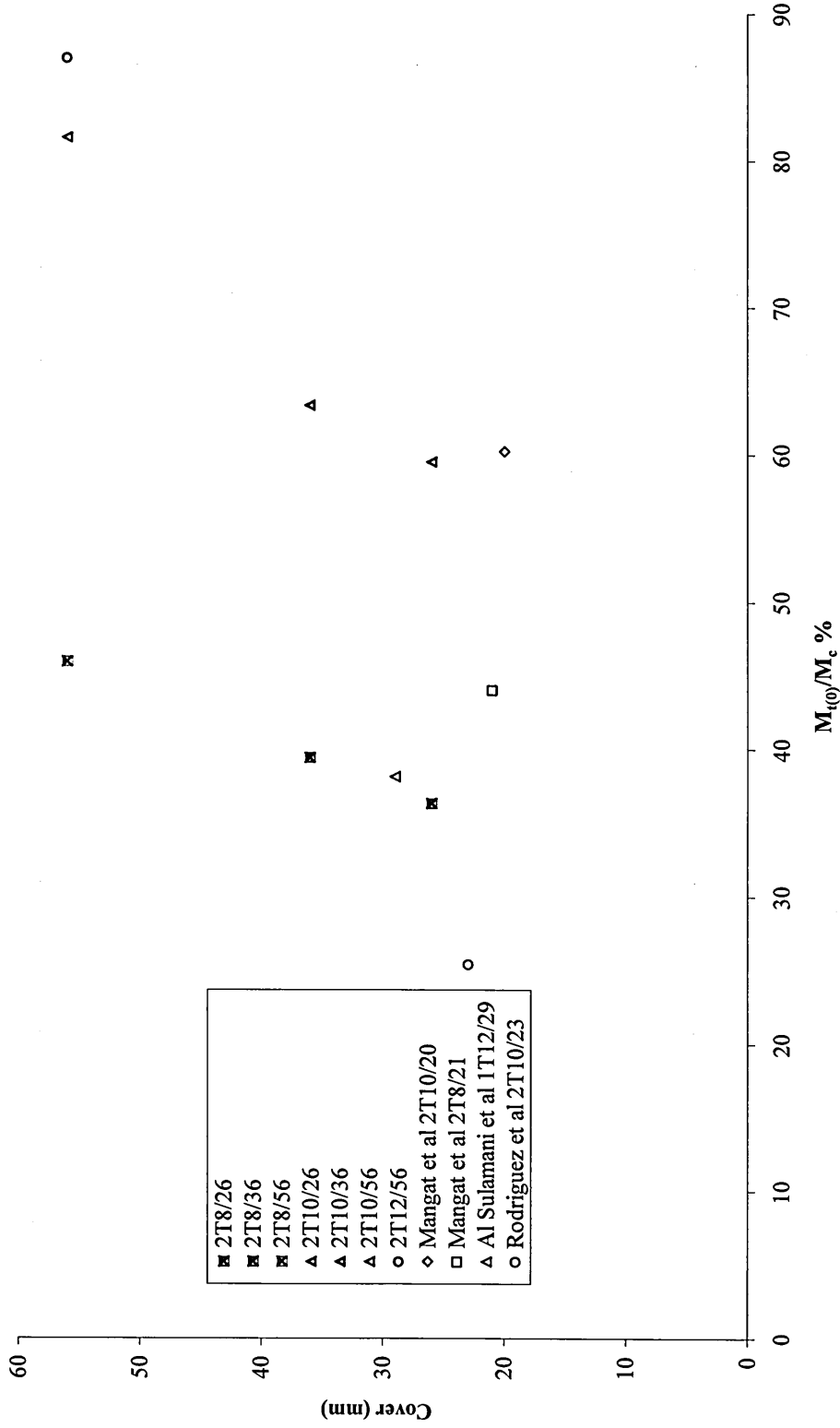


Figure 11.16 Effect of Cover on the  $M_{t(0)}/M_c$  ratio

#### 11.6.4 Residual tensile moment of resistance

The data presented in this chapter also allows an estimate of the residual tensile moment of resistance of corroded beams to be obtained. Design values such as  $M_{t(0)}$  and  $M_c$  will be available to the engineer, hence by rearranging Equation 11.12,  $M_{t(Corr)}$  can be estimated from:

$$(M_{t(Corr)} / M_c) \% = \alpha \times (Corr\%) + (M_{t(0)} / M_c) \% \quad \text{Equation 11.13}$$

where  $M_{t(0)}/M_c$  is the intercept  $\beta$ . Multiplying Equation 11.13 by  $M_c$  and dividing by 100 (since Equation 11.13 is in percentage terms) gives

$$M_{t(Corr)} = [M_c \times \alpha \times (Corr\%) / 100 + M_{t(0)}] \quad \text{Equation 11.14}$$

where  $Corr\%$  is the actual corrosion of the main steel in the beam in service and  $\alpha$  is obtained from Figure 11.14 or estimated from the line of best fit as follows:

$$\alpha = 0.06[(M_{t(0)} / M_c) \%] - 0.89 \quad \text{Equation 11.15}$$

A factor of safety should also be applied to Equation 11.14 ( $\gamma_c$ ) which, for concrete, is normally taken as 1.5. Therefore, substituting  $\gamma_c$  into Equation 11.14 gives:

$$M_{t(Corr)} = [M_c \times \alpha \times (Corr\%)/100 + M_{t(0)}] / \gamma_c \quad \text{Equation 11.16}$$

Therefore, through the application of Equation 11.16, the engineer will be able to assess the residual strength (moment of tensile resistance) of a corroded reinforced concrete beam once the level of corrosion (*Corr%*) in the main steel is obtained from a field inspection in addition to having design data such as  $M_{t(0)}$  and  $M_c$ .

Several means of measurement (*Corr%*) and testing in the field are available. They include measurement of electrical resistivity, measurement of surface water absorption, determination of ultrasonic pulse velocity and exposing reinforcement. The Half Cell technique used for measuring corrosion potentials is well known and will locate areas of high corrosion risk. The polarisation resistance technique measure the change in potential divided by the applied current is implemented in portable devices<sup>157</sup>.

## 11.7 Conclusions

The scope for study into corrosion damaged reinforced concrete elements is vast. Extensive research into concrete and steel corrosive processes, the action of corrosion products on concrete cracking, methods of surveying, identifying damaged regions, repairing techniques and materials have already been made. However, the objectives of the present study as set out in Chapter 1 were born out of the fact that very little previous work had been done to provide assistance to engineers responsible for structural integrity assessment of concrete structures impaired by reinforcement corrosion.

As the data available in Series II and III was rather limited, only Series I was fully analysed.

The main conclusions from the results reported in this chapter are as follows:

- Reinforcement corrosion in concrete has a marked effect on both the flexural load capacity and deflection of beams. At a degree of corrosion  $(2RT/D)\%$  of 15%, for example, the residual strength reduces to about 30% of the flexural capacity of control beam;
- The reduction in rebar cross section has an insignificant effect on the residual flexural strength of beams. The reduction in flexural strength is primarily due to the loss of bond or breakdown of the steel – concrete interface;
- Beams designed with lower  $M_{t(0)}/M_c$  ratios generally do not rapidly deteriorate when subjected to corrosion of the main steel reinforcement;
- Lower  $M_{t(0)}/M_c$  ratios can be achieved in beam design through:
  1. keeping the percentage of main steel reinforcement as close as possible to 0.13%
  2. specifying smaller diameter reinforcing bars;
- Cover to the main steel reinforcement generally do not have an influence on the  $M_{t(0)}/M_c$  ratio hence sufficient cover should be provided as required by the code to protect against corrosion;
- There was not found a correlation between  $M_{t(0)}/M_c$  ratios and stiffness;
- The percentage of steel reinforcement should be decreased through specifying smaller areas of steel and not unnecessarily increasing the size of the section;

- Specifying smaller diameter bars will help to enhance the interfacial bond with the concrete and minimise the effects corrosion induced deterioration;
- An estimate of the residual tensile moment of resistance of corroded beams can be obtained from:

$$M_{I(Corr)} = [M_c \times \alpha \times (Corr\%)/100 + M_{I(0)}] / \gamma_c$$

where

$M_{I(Corr)}$  is the flexural moment of resistance of corroded beam

$\alpha$  is the slope of the line of best fit

$(Corr \%)$  is the amount of corrosion

$M_c$  is the maximum moment of resistance of the concrete in the compression zone

$M_{I(0)}$  is the flexural moment of resistance of control beam

$\gamma_c$  is factor of safety for concrete (normally 1.5)

If possible, the conclusions derived and the results measured should be verified by some amount of field testing on real structures.

### ***Conclusions and Recommendations***

#### **12.1 Introduction**

The experimental results produced from this investigation have been presented and thoroughly discussed in the preceding chapters of the thesis. A summary of the main conclusions and findings developed in these previous sections is presented below. Further, through the current study, it has become apparent that there are several aspects of the work that would benefit from further investigation into the residual strength of corroded reinforced concrete members and these are also summarised in this chapter.

#### **12.2 Conclusions**

Based on the results of the experimental programme presented in this thesis, the following conclusions are summarised below.

##### **12.2.1 Conclusions from experimental design**

- As the aim of this research was to replicate as much as possible the real situations, the beams were designed for both bending and shear. The incorporation of corrosion resistant stirrups in the design of the reinforced concrete beams (Series I) increase the reliability of the experimental results.
- The use of stirrups in the manufacturing of a concrete beams leads to less severe cracking patterns in the concrete cover.

- The use of stirrups in the reinforced concrete beams has a significant influence on the residual strength obtained for high corrosion levels.
- In order to minimise the effect of corrosion induced bond deterioration it is advisable at the design stage to choose a greater number of rebars with smaller diameter rather than a smaller number of greater diameter.

### **12.2.2 Conclusions from accelerated corrosion tests**

- The use of impressed current was a practical and convenient method of producing corroded specimens for examining the structural effects of reinforcement corrosion.
- The first sign of corrosion was rust staining on the concrete surface, followed by longitudinal cracking in the concrete cover. Where cover was low, cracking occurred at weight losses of about 0.8%. Where cover was greater, cracking first appeared at corrosion values of about 2%.
- Corrosion tended to occur, between the cathodic links.
- Where the corrosion did occur, the damage was generally spread along the bottom of the bars, with variable section loss along the bar. Where serious section loss occurred, it was in the form of general corrosion rather than localised pitting corrosion. Therefore, general corrosion was assumed for the purpose of this research.
- The time to first cracking depended, as expected, on cover and type of corroded bar. The beams with main steel corrosion only tended to crack earlier than those with link reinforcement corrosion, possible because of the greater

surface area. There is no evidence to suggest that deformed bars are more susceptible to corrosion.

- For the same level of corrosion, deterioration of the concrete cover associated with the laboratory accelerated corrosion process is likely to be more severe than that found in the field. However, the structural reliability of reinforced concrete beams determined in the laboratory is an under estimate, and therefore is on the safe side.

### **12.2.3 Conclusions from load tests**

- The presence of longitudinal cracking resulting from the corrosion of reinforcement does not necessarily mean loss of strength.
- The beams with actual corrosion of the main steel of around 2.5% suffered negligible strength loss, even where longitudinal cracking was present over the length of the beam. Failure was ductile and in flexure. There was no evidence of bond failure.
- First evidence of bond failure occurred in the beams with an actual corrosion of the main steel of about 10%. This evidence consisted of horizontal cracking of the beam along the line of the main reinforcement as the load test proceeded, suggesting local bond failure. In all beams failure was ductile and in flexure.
- In the series of beams with heaviest shear reinforcement corrosion (actual corrosion of around 20%) the beams failed in shear.

#### 12.2.4 Performance of corroded reinforced concrete beams

- The average flexural load capacity of a concrete beam is reduced significantly due to main reinforcement corrosion.
- Reinforcement corrosion tends to reduce the stiffness of the reinforced concrete beam significantly at higher degrees of reinforcement corrosion.
- Generally, the deflection at ultimate load increases with increasing corrosion degree.
- The reduction in rebar cross section has an insignificant effect on the residual flexural strength of beams. The reduction in flexural strength is primarily due to the loss of bond or breakdown of the steel – concrete interface.

#### 12.2.5 Practical implications

- Reinforcement corrosion in concrete has a marked effect on both the flexural load capacity and deflection of beams. At a degree of corrosion ( $2RT/D$  %) of 15%, for example, the residual strength reduces to about 30% of the flexural capacity of control beam.
- Beams designed with lower  $M_{t(0)}/M_c$  ratios generally do not rapidly deteriorate when subjected to corrosion of the main steel reinforcement.
- Lower  $M_{t(0)}/M_c$  ratios can be achieved in beam design through:
  - keeping the percentage of main steel reinforcement as close as possible to 0.13%
  - specifying smaller diameter reinforcing bars

- Cover to the main steel reinforcement generally do not have an influence on the  $M_{t(0)}/M_c$  ratio hence sufficient cover should be provided as required by the code to protect against corrosion.
- The percentage of steel reinforcement should be decreased through specifying smaller areas of steel and not unnecessarily increasing the size of the section.
- Specifying smaller diameter bars will help to enhance the interfacial bond with the concrete and minimise the effects corrosion induced bond failure.
- An estimate of the residual tensile moment of resistance of corroded beams can be obtained from:

$$M_{t(Corr)} = [M_c \times \alpha \times (Corr\%) / 100 + M_{t(0)}] / \gamma_c$$

where

$M_{t(Corr)}$  is the flexural moment of resistance of corroded beam

$\alpha = 0.06[(M_{t(0)} / M_c) \%] - 0.89$  (is the slope of the line of best fit)

$(Corr \%)$  is the amount of corrosion (obtainable from field inspections)

$M_c$  is the maximum moment of resistance of the concrete in the compression zone (obtainable from the design data)

$M_{t(0)}$  is the flexural moment of resistance of control beam (obtainable from the design data)

$\gamma_c$  is factor of safety for concrete (normally 1.5)

### 12.3 Recommendations

There are areas of further study that have the possibility to expand the findings of this research, but which could not be pursued during the timescale and scope of this project.

These are listed below as a series of recommendations:

- Data on the influence of corrosion on the strength in existing corroded structures is very limited. It would be very useful if more data is made available on the actual corroded structures. This will help developing a correlation between laboratory results and data from existing structures.
- More data is needed to evaluate the effect of stirrups corrosion on the flexural and shear capacity.
- A laboratory investigation is required to verify the effect of reinforcement corrosion on the mechanical characteristics of the steel.
- A detailed analytical study is needed on the residual strength of reinforced concrete beams concerning the mechanical characteristics of the reinforcing steel.
- A laboratory study is required to determine the influence of corrosion on the moments of resistance of continuous beams.
- A laboratory study is also required to determine the influence of corrosion on the moments of resistance of “T” sections.

### 12.4 Final remarks

The scope for study into corrosion damaged reinforced concrete members is vast. Extensive studies into concrete and steel corrosive processes, the action of corrosion

products on concrete cracking, methods for surveying, identifying damaged regions, repairing techniques and materials have already been made. However, the objectives of the present programme of study as set in Chapter 1 were born out of the fact that very little research had been done to provide assistance to engineers responsible for structural integrity assessment of reinforced concrete structures impaired by reinforcement corrosion. One of the aims of this research, therefore, was to present the data in a simplified form which can be easily understood and employed by busy practicing engineers.

The present investigation has therefore been successful in providing substantial insight into the behaviour of corroded reinforced concrete beams, previously not available to structural assessment engineers. It is trusted that the important conclusions and recommendations for future study presented herein will be addressed and promote the much needed research required for the understanding of the behaviour of corroded reinforced concrete flexural members. It is hoped that this research will greatly enhance the expertise of engineers dedicated to the structural integrity assessment of corrosion damaged reinforced concrete members in order to prescribe the best and most efficient form of remedial treatment.

However, further analysis will be carried out and the results will be published in appropriate journals, as the scope of this thesis was bigger than anticipated.

### References

- 1 'Corrosion of steel in concrete – durability of reinforced concrete structures', BRE Centre for Concrete Construction Digest 444 Part 1 (2000).
- 2 Clayton, N., 'Tension tests for concrete', BRE Centre for Concrete Construction Digest 451 (2000).
- 3 Mangat, P. S. and Molloy, B. T., 'Factors influencing chloride – induced corrosion of reinforcement in concrete', *Materials and Structures* **25** (1992) 404–411.
- 4 Al-Sulaimani, G., Kaleemullah, M., Basunbul, I. and Rasheeduzzafar, 'Influence of corrosion and cracking on the bond behaviour and strength of reinforced concrete members', *ACI Structural Journal* **87** (2) (1990) 220–231.
- 5 Webster, M. P. and Clark, L. A., 'The structural effects of corrosion – an overview of the mechanisms', Concrete Communication Conference (29–30 June 2000) Birmingham, pp 409–421.
- 6 Mangat, P. S. and O'Flaherty, F. J., 'Long – term performance of high – stiffness repairs in highway structures', *Magazine of Concrete Research* **51** (5) (1999) 325–339.
- 7 Mangat, P. S. and O'Flaherty, F. J., 'Influence of elastic modulus on stress redistribution and cracking in repair patches', *Cement and Concrete Research* **30** (2000) 125–136.

- 8 Mangat, P. S. and O'Flaherty, F. J., 'Serviceability characteristics of flowing repairs to propped and unpropped bridge structures', *Materials and Structures* **32** (1999) 663–672.
- 9 Mangat, P. S. and O'Flaherty, F. J., 'Factors affecting the efficiency of repair to propped and unpropped bridge beams', *Magazine of Concrete Research* **52** (4) (2000) 303–319.
- 10 Borgard, B., Warren, C., Somayaji, S. and Heidersbach, R., 'Mechanisms of corrosion of steel in concrete', Corrosion Rates of Steel in Concrete ASTM STR 1065, N. S. Berke, V. Chaker, and D. Whiting, Eds., American Society for Testing Materials, Philadelphia (1990), pp 174–188.
- 11 Parker, D., 'Shock collapse sparks lift slab fears', *Magazine of the Institution of Civil Engineers* (1997) 3.
- 12 Oliver, A., 'High levels of calcium chloride found in the collapsed bridge grout', *Magazine of the Institution of Civil Engineers* (1 June 2000) 7.
- 13 Neville, A. M., 'Properties of concrete', 2<sup>nd</sup> Edition, Pitman Publisher, London, 1977.
- 14 Biczok, I., 'Concrete corrosion – concrete protection', Academia Kiado, Budapest, 1972.
- 15 Murdock, L. J., Brook, K. M. and Dewar, J. D., 'Concrete materials and practice', 6<sup>th</sup> Edition, Edward Arnold, London, 1991.
- 16 Lea, F. M., 'The chemistry of cement and concrete', E. Arnold Ltd, London, 1970.

- 17 Hencsei, P. and Jantai, A., 'Corrosion of reinforcement samples', *ACH-Models in Chemistry* **132** (4) (1995) 713–720.
- 18 Misra, S. and Uomoto T., 'Effect of corrosion of reinforcement on the load carrying capacity of RC beams', *Proceedings of JCI* **6** (2) (1987) 675–680.
- 19 Uomoto, T. and Misra, S., 'Deterioration of concrete beams and columns caused by corrosion of reinforcing steel bars', 4<sup>th</sup> International Conference on Durability of Building Materials and Components, Singapore, 1987.
- 20 Morinaga, S., 'Prediction of service lives of reinforced concrete buildings based on the corrosion rate of reinforcing steel', Special Report of Institute of Technology, Shimizu Corporation, Tokyo, Japan (23) (June 1988).
- 21 Rodriguez, J., Ortega, L. M. and Garcia, A. M., 'Assessment of structural elements with corroded reinforcement', International Congress on Corrosion and Protection of Steel in Concrete (1994) pp 171–185.
- 22 Cochrane, D. J., 'Austenitic stainless steel – the solution to rebar corrosion', *Steel Times* (January 1996) 19–20.
- 23 Page, C. L., 'Corrosion and its control in reinforced concrete', The Sixth Sir Frederick Lea Memorial Lecture, 26<sup>th</sup> Annual Convention, Bosworth Hall Hotel, (6–8 April 1998).
- 24 Swamy, R. N., 'Durability of rebars in concrete', *Durability of Concrete SP 131–3* pp 67–98.
- 25 Mangat, P. S. and Manarakis, G. S., 'Slip forming with fibre – reinforced concrete for efficient crack control', *Materials and Structures* **26** (1993) 433–440.

- 26 Andrade, C., Alonso, C. and Molina F. J., 'Cover cracking as a function of bar corrosion: Part I – Experimental test', *Materials and Structures* **26** (1993) 453–464.
- 27 Alonso, C., Andrade, C., Rodriguez, J., Casal, J. and Garcia, M., 'Rebar corrosion and time to cover cracking' Concrete Across Borders International Conference (1994) 301–313.
- 28 Andrade, C., Alonso, C., Rodriguez, J. and Garcia, M., 'Cover cracking and amount of rebar corrosion: Importance of the current applied accelerated tests' 4<sup>th</sup> International Congress on Concrete in the Service Mankind, Dundee (1996) pp 263–273.
- 29 Beeby, A. W., 'Cracking, cover and corrosion of reinforcement', *Cement and Concrete Association* (1981) 63–66.
- 30 Broomfield, J. P., Langford, P. E. and Ewins A. J., 'The use of a potential wheel to survey reinforced concrete structures', Corrosion Rates of Steel in Concrete, ASTM STP 1065, N. S. Berke, V. Chaker, and D. Whiting, Eds., American Society for Testing and Materials, Philadelphia (1990) pp 157–173.
- 31 Dhir, R. K., Jones, M. R. and McCarthy, M. J., 'Quantifying chloride induced corrosion from half – cell potential', *Cement and Concrete Research* **23** (6) (1993) 1443–1454.
- 32 Swarup, J., 'Corrosion of reinforcement in various environments' *Transactions of the Metal Finishers' Association of India* **7** (1) (1998) 73–78.

- 33 Swarup, J. and Trikha, D. N., 'Corrosion of reinforcement in concrete structures under various conditions', *Transactions of the Metal Finishers' Association of India* **5** (1) (1996) 15–22.
- 34 Swarup, J. and Sharma, P. C., 'Electrochemical techniques for the monitoring of corrosion of reinforcement in concrete structures', *Bulletin of Electrochemistry* **12** (1–2) (1996) 103–108.
- 35 ACI Committee 222, 'Corrosion of metals in concrete' *ACI Journal* **82** (1) (1985) 3–32.
- 36 Browne, R., 'Mechanisms of corrosion of steel in concrete', *American Concrete Institute SP65 – Performance of Concrete in Marine Environment*, Detroit (1980) 169–204.
- 37 Broomfield, J. P., 'Corrosion of Steel in Concrete – Understanding, investigation and repair' ISBN 0419196307.
- 38 Hausmann, D. A., 'Steel corrosion in concrete' *Materials Protection* **6** (1967) 19–23.
- 39 Broomfield, J. P., 'Electrochemical processes in the detection, assessment control and repair of reinforcement corrosion', CPD programme of *The Institution of Structural Engineers* (1996).
- 40 Kumar, V., 'Protection of steel reinforcement for concrete – a review', *Corrosion reviews* **16** (4) (1998).
- 41 Alonso, M. C., Andrade, C., Farina, J., Lopez, F., Merino, P. and Novoa, X. R., 'Galvanic corrosion of steel in concrete', *Materials Science Forum* **192–194** (1995) 899–906.

- 42 Pourbaix, M., 'Lectures on electrochemical corrosion', Plenum Press (1973).
- 43 Cornet, I., Ishikawa, T. and Bresler, B., 'The mechanism of steel corrosion in concrete structures', *Materials Protection* (March 1968) 44–47.
- 44 Page, C. L., Lambert, P. and Vassie P. R. W., 'Investigation of reinforcement corrosion. 1. The pore electrolyte phase in chloride – contaminated concrete', *Materials and Structures* **24** (1991) 243–252.
- 45 Lambert, P., Page, C. L. and Vassie P. R. W., 'Investigation of Reinforcement Corrosion. 2. Electrochemical monitoring of steel in chloride – contaminated concrete', *Materials and Structures* **24** (1991) 351–358.
- 46 Dhir R., Jones R., McCarthy M., 'Measurement of reinforcement corrosion in concrete structures' *Concrete* (January 1991) 15–19.
- 47 Locke, C., 'Corrosion of steel in Portland cement concrete: fundamental studies', Corrosion Effect of Stray Currents and the Techniques for Evaluating Corrosion of Rebars in Concrete ASTM STR 906, American Society for Testing and Materials, Philadelphia (1986), pp 5–14.
- 48 Elsener, B., 'Corrosion rate of steel in concrete – from laboratory to reinforced structures', *Materials Science Forum* **247** (1997) 127–138.
- 49 Mangat, P. S. and Molloy, B. T., 'Influence of PFA, slag and microsilica on chloride induced corrosion of reinforcement in concrete', *Cement and Concrete Research* **21** (1991) 819–834.
- 50 Mangat, P. S. and Molloy, B. T., 'Prediction of long term chloride concentration in concrete', *Materials and Structures* **27** (1994) 338–346.

- 51 Mangat, P. S. and Molloy, B. T., 'Prediction of free chloride concentration in concrete using routine inspection data', *Magazine of Concrete Research* **46** (169) (1994) 279–287.
- 52 Hobbs D. W., 'Chloride ingress and chloride – induced corrosion in reinforced concrete members', Special Publication 183, The Royal Society of Chemistry, (1996) 124–135.
- 53 Hobbs, D. W., 'Chemical attack on concrete', Proceedings of the 10<sup>th</sup> British Cement Association Annual Conference on Higher Education and the Concrete Industry (2000) pp 93–102.
- 54 Poupard, O., Ait–Mokhtar, A. and Dumargue, P., 'Corrosion by chlorides in reinforced concrete: determination of chloride concentration threshold by impedance spectroscopy', *Cement and Concrete Research* **34** (6) (2004) 991–1000.
- 55 Tuutti, K., 'The effect of individual parameters on chloride induced corrosion', Chloride penetration into concrete structures, Nordic Mini–seminar, (January 1993) ISBN 02807262, pp 18–25.
- 56 Hussain, S., Al–Gahtani, A. and Rasheeduzzafar, 'Chloride threshold for corrosion of reinforcement in concrete', *ACI Materials Journal* **93** (November–December 1996) 534–538.
- 57 Andrade, C., Alonso, C. and Gonzalez, J. A., 'Approach to the calculation of the residual life in corroding concrete reinforcements based on corrosion intensity values', 9<sup>th</sup> EURO Congress on Corrosion, (October 1989), BU–049.

- 58 Suryavanshi, A. K., Scantlebury, J. D. and Lyon, S. B., 'Corrosion of reinforcement steel embedded in high water – cement ratio concrete contaminated with chloride', *Cement and Concrete Composites* **20** (4) (1998) 263–381.
- 59 Gower, M. R. and Windsor, D. M., 'Cathodic protection and condition monitoring: residential tower block', N. Lanarkshire, Ordinary Meeting, *Institution of Structural Engineers* (11 May 2000).
- 60 Mangat, P. S. and Gurusamy, K., 'Chloride diffusion in steel fibre reinforced marine concrete', *Cement and Concrete Research* **17** (3) (1987) 385–396.
- 61 Morinaga, S., 'Remaining life of reinforced concrete structures after corrosion cracking', *Durability of Building Materials and Components* (13) (1996) 127–136.
- 62 Watkins, R. A. M. and Jones, A. P., 'Carbonation: a durability model related to site data', *Proceedings Institution Civil Engineers Structures and Buildings* **99** (5) (1993) 155–166.
- 63 Cleland, D. J., Yeoh, K. M. and Long, A. E., 'Corrosion of reinforcement in concrete repair', *Construction and Building Materials* **11** (4) (1997) 233–238.
- 64 Bennett, J. E., 'Stop corrosion of reinforced concrete structures', *Chemical Engineering Progress* **94** (1998) 77–81.
- 65 Cabrera, J. G., 'Deterioration of concrete due to reinforcement steel corrosion', *Cement and Concrete Composites* **18** (1) (1996) 47–59.
- 66 Saifullah, M. and Clark, L. A., 'Effect of corrosion on reinforcement bond strength', Proceeding of an International Conference, University of Sheffield, (July 1994), pp 591–602.

- 67 Clark, L. A. and Saifullah, M., 'Effect of corrosion rate on the bond strength of corroded reinforcement', Proceeding of 5<sup>th</sup> International Conference on Structural Faults and Repair, (1993), pp 113–119.
- 68 Auyeung, Y., Balaguru, P. and Chung, L., 'Bond behavior of corroded reinforcement bars', *ACI Materials Journal* **97** (2) (2000) 214–220.
- 69 Lee, H., Noguchi, T. and Tomosawa, F., 'Evaluation of the bond properties between concrete and reinforcement as a function of the degree of reinforcement corrosion', *Cement and Concrete Research* **32** (2002) 1313–1318.
- 70 Chana, P. S., 'A test method to establish realistic bond stresses', *Magazine of Concrete Research* **42** (151) (1990) 83–90.
- 71 Cabrera, J. G. and Ghoddoussi, P., 'The effect of reinforcement corrosion on the strength of the steel / concrete bond', Proceedings of the International Conference on Bond in Concrete, CEB, Riga, Latvia, (1992), pp 10/11–10/24.
- 72 Uomoto, T., Tsuji, K. and Kakizawa, T., 'Deterioration mechanism of concrete structures caused by corrosion of reinforcing bars', *Transaction of the Concrete Institute* **6** (1984) 163.
- 73 Lin, C. Y., 'Bond deterioration due to corrosion of reinforcing steel', *American Concrete Institute SP65 – Performance of Concrete in Marine Environment*, Detroit, (1980), pp 255–269.
- 74 Andrade, C., Alonso, J. A., Gonzalez, J. A. and Rodriguez, J., 'Remaining service life of corroding structures', International Association for Bridge and Structural Engineering Publication 57/I, (1986), pp. 359.

- 75 Baker, K. N. and McLeish, A., Evaluating the strength of concrete structures, Symposium on revaluation of concrete structures, Danish Concrete Institute, Copenhagen, (June 1988).
- 76 Mangat, P. S. and Elgarf, M. S., 'Bond characteristics of corroding reinforcement in concrete beams', *Materials and Structures* **32** (March 1999) 89–97.
- 77 Almusallam, A., Al-Gahtani, A., Aziz, A. and Rasheeduzzafart, 'Effect of reinforcement corrosion on bond strength', *Construction and Building Materials* **10** (2) (1996) 123–129.
- 78 Mangat, P. S. and Elgarf, M. S., 'Strength and serviceability of repaired reinforced concrete beams undergoing reinforcement corrosion', *Magazine of Concrete Research* **51** (2) (1999) 97–112.
- 79 Castel, A., François, R. and Arliguie, G., 'Mechanical behaviour of corroded reinforced concrete beams – Part 1: Experimental study of corroded beams', *Materials and Structures* **33** (November 2000) 539–544.
- 80 Castel, A., François, R. and Arliguie, G., 'Mechanical behaviour of corroded reinforced concrete beams – Part 2: Bond and notch effects', *Materials and Structures* **33** (November 2000) 545–551.
- 81 Okada, K., Kobayashi, K. and Miyagawa, T., 'Influence of longitudinal cracking due to reinforcement corrosion on the characteristics of reinforced concrete members', *ACI Structural Journal* **85** (2) (1988) 134–140.
- 82 Tachibana, Y., Maeda, K. I., Kajikawa, Y. and Kawamura, M., 'Mechanical behaviour of reinforced concrete beams damaged by corrosion of reinforcement',

- Proceedings of Third International Symposium on Corrosion of Reinforcement in Concrete Construction, Wishaw, UK, (May 1990), pp 178–187.
- 83 Perno, S., Rinaldi, Z., Valente, C. and Pardi, L., 'Experimental evaluation of the load bearing capacity of corroded beams', *Bridge Management 5*, Thomas Telford, London, (2005), pp 508–516.
- 84 Uomoto, T. and Misra, S., 'Behaviour of concrete beams and columns in marine environment when corrosion of reinforcing bars take place', *American Concrete Institute SP109* (1988) 127–145.
- 85 Rodriguez, J., Ortega, L. M., Casal, J. and Diez, J. M., 'Load carrying capacity of concrete structures with corroded reinforcement', *International Conference S. F. & R*, London, (1995).
- 86 Mangat, P. S. and Elgarf, M. S., 'Flexural strength of concrete beams with corroding reinforcement', *ACI Structural Journal* **96** (1) (1999) 149–158.
- 87 Regan, P. E., Rezai-Jorabi, H. and Kyriacou, A. G., 'Structural implications of loss of cover to main steel in reinforced concrete beams', *Structural Engineering Research Group, Department of Civil Engineering, Polytechnic of Central London*, (1988).
- 88 Cleland, D. J., Cummings, S. J., Rankin, G. I. B, Taylor, S. and Scott, R. H., 'Influence of reinforcement anchorage on the bending and shear capacity of bridge decks', *The Structural Engineer* **79** (16) (2001) 24–31.

- 89 Burley, E., Rigden, S. and Abu-Tair, A., 'The performance of different repair techniques and materials under static loading', *Structural Faults and Repair*, University of London, Edited by Forde, M. C., **1** (1989) pp 79–86.
- 90 Zhang, S. and Raoof, M., 'Prediction of the behaviour of RC beams with exposed reinforcement', *Magazine of Concrete Research* **47** (173) (1995) 335–344.
- 91 Regan, P.E., 'Research on shear: a benefit to humanity or a waste of time?', *The Structural Engineer* **71** (19) (1993) 337–346.
- 92 Omar, W. and Clark, L. A., 'Shear capacity of honeycombed reinforced concrete beams', *The Structural Engineer* **79** (15) (2001) 17–22.
- 93 Kani, G. N. J., 'The riddle of shear failure and its solution', *Journal of the American Concrete Institute* **61.I** (1964) 411–467.
- 94 Mangat, P. S. and Gurusamy, K., 'Corrosion resistance of steel fibres in concrete under marine exposure', *Cement and Concrete Research* **18** (1) (1988) 44–54.
- 95 Atkinson, J. and Van-Droffelaar, H., 'Corrosion and its control: An introduction to the subject', National Association of Corrosion Engineers (1982) pp 21.
- 96 Thangavel, K. and Rengaswamy, N. S., 'Environmental influence on the electrode potential of steel in concrete', *Transactions of the Metal Finishers' Association of India* **5** (1) (1996) 23–30.
- 97 Tuutti, K., 'Service life of structures with regard to corrosion of embedded steel', *American Concrete Institute SP65-13 – Performance of Concrete in Marine Environment*, Detroit, (1980), pp 223–236.

- 98 'Stainless reinforced concrete bars', *Wire materials* **46** (4) (1996) 260–261.
- 99 Park, R. and Paulay, T. (1975) 'Reinforced concrete structures', John Wiley & Sons, London.
- 100 Gedge, G., 'Stainless steel reinforcement for concrete – a solution chloride induced corrosion of reinforced concrete structures', *Bridge Management* 4, Thomas Telford, London, (2000), pp 315–322.
- 101 European Federation of Corrosion Publications Number 18, 'Stainless steel in concrete', The Institute of Materials, (1996), ISBN 1861250088.
- 102 British Standard Institution. (1983). *Method for normal curing of test specimens (20 °C method)*, BS 1881: Part 111.
- 103 British Standard Institution. (1978). *Specification for ordinary and rapid hardening Portland cement*, BSI, 1978. BS12.
- 104 British Standard Institution. (1983). *Specification for aggregates from natural sources for concrete*, London 1983. BS 882.
- 105 BRE Publication, 'Design of normal concrete mixes', (1992), ISBN 0851252222.
- 106 Pruckner, F. and Gjorv, O. E., 'Effect of CaCl<sub>2</sub> and NaCl additions on concrete corrosivity', *Cement and Concrete Research* **34** (7) (2004) 1209–1217.
- 107 Swiss Bank Corporation (Stockbrokers) 1989. Quarterly building bulletin, 26 January 1989, London.
- 108 Department of Transport 1989. 'The Performance of concrete in bridges: A survey of 200 highway bridges'. Report by G. Maunsell and Partners, HMSO, London.

- 109 Wang, Y. and Liu, B., 'Study and application of salt-scaling resistant admixture in concrete', *Environmental and Technology of Concrete Key Engineering Materials*, 302–303, (2006) pp 105–110.
- 110 Mangat, P.S., O'Flaherty, F.J., 'Analysis of interfacial shrinkage stress in patch repairs', *Magazine of Concrete Research* **56** (7) (2004) 375–386.
- 111 Rodriguez, J., Ortega, L.M. and Casal, J., 'Corrosion of reinforcing bars and service life of reinforced concrete structures: corrosion and bond deterioration', *International Conference on Concrete Across Borders*, Odense, Denmark, (1994) pp 315–326.
- 112 Cairns, J., 'Consequences of bond loss for behaviour of reinforced concrete beams', *Proceedings of 5<sup>th</sup> International Conference on Structural Faults and Repairs*, (July 1993) pp 149–154.
- 113 Lundgren, K. and Gylltoft, K., 'A model for bond between concrete and reinforcement', *Magazine of Concrete Research* **52** (1) (2000) 53–63.
- 114 Lundgren, K. 'Modelling the effect of corrosion on bond in reinforced concrete', *Magazine of Concrete Research* **54** (3) (2002) 165–173.
- 115 Wang, X. and Liu, X., 'Modelling bond strength of corroded reinforcement without stirrups', *Cement and Concrete Research* **34** (8) (2004) 1331–1339.
- 116 Cairns, J. and Zhao, Z., 'Behaviour of concrete beams with exposed reinforcement', *Proceedings of the Institution of Civil Engineers Structures and Buildings* **99** (1993) 141–154.

- 117 Cairns, J. and Rafeeqi, S. F. A., 'Analysis of reinforced concrete beams strengthened by external unbonded bars', *Magazine of Concrete Research* **54** (2) (2002) 141–153.
- 118 Rodriguez, J., Ortega, L.M. and Garcia, A. M., 'Assessment of structural elements with corroded reinforcement', International Congress on Corrosion and Protection of Steel in Concrete, Sheffield, (1994) pp 171–185.
- 119 Andrade, C., Alonso, C., Gonzalez, J. A. and Rodriguez, J., 'Remaining service life of corroding structures', IABSE Symposium on Durability, Lisbon, (1989) pp 359–364.
- 120 Andrade, C., Alonso, C., Garcia, D. and Rodriguez, J., 'Remaining lifetime of reinforced concrete structures: effect of corrosion on the mechanical properties of the steel', Lifetime Prediction of Corrodible Structures, Volume I, R. N. Parkins, Editor (1994) pp 546–557. ISBN 187791466.
- 121 Clifton, J., 'Methods for predicting remaining life of concrete in structures', Report NISTIR 4954 NIST–US Department of Commerce, (1992).
- 122 Cairns, J., 'Assessment of effects of reinforcement corrosion on residual strength of deteriorated concrete structures', Proceedings of the 1<sup>st</sup> International Conference on behaviour of damaged structures, Rio de Janeiro, 1998.
- 123 Fagerlund, G., Somerville, G. and Tuutti, K., 'The residual service life of concrete exposed to the combined effect of frost attack and reinforcement corrosion', Concrete across borders International Congress, Odense, Denmark, (1994) pp 351–365.

- 124 Pullar–Strecker, P., 'Corrosion damage concrete: Assessment and repair', CIRIA (1987) ISBN 0408025565.
- 125 Maruyama, K. and Shimomura, T., 'Effect of rebar corrosion on the structural capacity of concrete structures', Conference on Concrete in Severe Environments, Norway, (1998) pp 364–371.
- 126 Kawamura, A., Maruyama, K., Yoshida, S. and Masuda, T., 'Residual capacity of concrete beams damaged by salt attack', Concrete Under Severe Conditions: Environment and Loading, (1995) pp1448–1457.
- 127 Uomoto, T., Kobayashi, K. and Tsuji, K., 'Deterioration of concrete beams and columns caused by corrosion of reinforcing steel bars', 4<sup>th</sup> Asian Pacific Corrosion Control Conference, Tokyo, (1985) pp 700–707.
- 128 Rodriguez, J., Ortega, L. M., Casal, J. and Diez, J. M., 'Assessing structural conditions of concrete structures with corroded reinforcement', 4<sup>th</sup> International Congress in the Service of Mankind, Dundee, 1996, pp 65–78.
- 129 Rodriguez, J., Ortega, L. M., Casal, J. and Diez, J. M., 'Corrosion of reinforcement and service life of concrete structures', *Durability of Building Materials and Components* 7 (1) (1996) 117–126.
- 130 Bard, E., 'Encyclopaedia of electrochemistry of the elements', Vol. 1–10, Inorganic series, Marcel Dekker, New York, 1973.
- 131 Thomson, A.W. and Bermiston, I. M. B., 'Advance in corrosion science and technology', Vol. 7, Eds. R. W. Staehle and N. G. Fountana, Plenum Press, New York, 1980.

- 132 Dhir, R. K. and Byars, E. A., 'PFA Concrete: Chloride diffusion rates', *Magazine of Concrete Research* **45** (162) (1993) 1–9.
- 133 Cairns, J., 'Strength in shear of concrete beams with exposed reinforcement', *Proceedings Institution of Civil Engineers Structures and Buildings* **110** (1995) 176–185.
- 134 Toongoenthong, K. and Maekawa, K., 'Multi-mechanical approach to structural performance assessment of corroded RC members in shear', *Journal of Advanced Concrete Technology* **3** (1) (2005) 107–122.
- 135 Daly, A. F., 'Bridge management in Europe (BRIME): modelling of deteriorated structures', *Bridge Management 4*, Thomas Telford, London, 2000.
- 136 Allison, B. and Woodward, R. J., 'Inspection, testing and monitoring of trunk road bridges in England', *Bridge Management 5*, Thomas Telford, London, 2005.
- 137 Eyre, J. R. and Nokhasteh, M. A., 'Strength assessment of corrosion damaged reinforced concrete slabs and beams', *Proceedings Institution of Civil Engineers Structures and Buildings* **94** (1992) 197–203.
- 138 Hookham, C. J., 'A life prediction methodology for reinforced concrete structures', *Life Prediction of Corrodible Structures Volume I*, R. N. Parkins Editor, 1994, ISBN 1877914606, pp 558–572.
- 139 Institution of Structural Engineers, 'Appraisal of existing structures', *Institution of Structural Engineers* (1996) pp 60.

- 140 Construction Industry Research and Information Association (CIRIA), 'Testing concrete in structures. A guide to equipment for testing concrete in structures', CIRIA Technical Note 143 (1992) pp 87.
- 141 British Cement Association (BCA), 'The diagnosis of alkali-silica reaction', Report of a Working Party 45.042 (1992) pp 44.
- 142 Andrade, C. and Alonso, C., 'Progress on design and residual life calculation with regard to rebar corrosion of reinforced concrete', Techniques to Assess the Corrosion Activity of Steel Reinforced Concrete Structures, ASTM STP 1276, (1996) pp 23-40.
- 143 Andrade, C. and Alonso, C., Corrosion rate monitoring in the laboratory and on-site', *Construction and Building Materials* **10** (5) (1996) 315-328.
- 144 Andrade, C., 'The practical assessment of damage due to corrosion', Concrete Across Borders, International Congress, Odense, Denmark, (1994) pp 337-350.
- 145 Design Manual for Roads and Bridges. Volume 3 Highway Structures: Inspection and Maintenance. Section 4: Assessment. Part 3. BD21/01. 'The Assessment of Highway Bridges and Structures'. (2001).
- 146 British Standard Institution 1997. Structural use of concrete: Code of practice for design and construction. BS 8110-1.
- 147 BS EN 1992-2:2005 Eurocode 2 Design of Concrete Structures. Concrete Bridges. Design and detailing rules.
- 148 Moss, R. M. and Webster, R, 'EC2 and BS8110 compared', *The Structural Engineer* **82** (2004) 33-38.

- 149 Hognestad, E., Hanson, N. W. and McHenry, D., 'Concrete stress distribution in ultimate strength design', *Proceedings of the American Concrete Institute* **52–28** (1955–1956) 455–479.
- 150 Mosley, W.H., Bungey, J.H., 'Reinforced concrete design', 4<sup>th</sup> Edition, MacMillan Press Ltd., 1990. ISBN 0333537181.
- 151 Walker, M., 'An overview of rehabilitation methods and selection of an appropriate system', Proceedings of the international seminar on controlling concrete degradation, University of Dundee, Scotland, UK, (7 September 1999) pp 169–180.
- 152 Mangat, P. S. and Limbachiya M. C., 'Repair material properties for effective structural application', *Cement and Concrete Research* **27** (4) (1997) 601–617.
- 153 Mangat, P. S. and Limbachiya M. C., 'Repair material properties which influence long-term performance of concrete structures', *Construction and Building Materials* **9** (2) (1995) 81–90.
- 154 O'Flaherty, F.J. and Mangat, P.S., 'A simplified design approach to prevent shrinkage cracking in patch repairs', *Magazine of Concrete Research* **58** (1) (2006) 31–42.
- 155 Rodriguez, J., Ortega, L. M. and Casal, J., 'Load carrying capacity of concrete structures with corroded reinforcement', *Construction and Building Materials* **11** (4) (1997) 239–248.
- 156 Elgarf, M. S., 'The effect of reinforcement corrosion on the structural performance of concrete flexural members', PhD Thesis, University of Aberdeen, 1994.

- 157 Rodriguez, J., Ortega, L. M., Garcia, A. M., Johansson, L. and Petterson, K., 'On site corrosion rate measurements in concrete structures using a device developed under the EUREKA project EU-401', International Conference on Concrete Across Borders, Odense, Denmark, 1 (1994) pp 215-226.

**Test Beam Series Design Data**

**A.1 Design data for beam Series I**

Table A.1.1 Moment and shear resistance for beam Series I (2T8/Corr %+10D6/0/20)

Beam identification	$f_{cu}$ (28 <sup>th</sup> day) [N/mm <sup>2</sup> ]	$f_{cu}$ (day of test) [N/mm <sup>2</sup> ]	$f_y$ [N/mm <sup>2</sup> ]	$f'_y$ [N/mm <sup>2</sup> ]	$A_s$ [mm <sup>2</sup> ]	$A'_s$ [mm <sup>2</sup> ]	s [mm]	d [mm]	z [mm]	$d'$ [mm]
(1)	(2)	(3)	(4)	(5)	(6)	(7)	(8)	(9)	(10)	(11)
2T8/0+10D6/0/20	56.40	56.40	496.91	324.34	99.86	46.48	9.14	120.58	116.01	28.16
2T8/0+10D6/0/20	56.40	56.40	496.91	324.34	99.86	46.48	9.14	120.58	116.01	28.16
2T8/1.0+10D6/0/20	50.53	58.53	496.91	344.99	99.86	47.18	8.50	120.54	116.29	28.22
2T8/1.4+10D6/0/20	53.03	57.25	496.91	324.34	99.86	46.48	9.01	120.58	116.08	28.16
2T8/2.3+10D6/0/20	52.42	54.87	496.91	324.34	99.86	46.48	9.40	120.58	115.88	28.16
2T8/3.4+10D6/0/20	50.53	58.53	496.91	344.99	99.86	47.18	8.50	120.54	116.29	28.22
2T8/8.9+10D6/0/20	53.03	57.25	496.91	324.34	99.86	46.48	9.01	120.58	116.08	28.16
2T8/10.0+10D6/0/20	49.75	52.70	496.91	324.34	99.86	46.48	9.78	120.58	115.69	28.16
2T8/15.5+10D6/0/20	49.75	52.70	496.91	324.34	99.86	46.48	9.78	120.58	115.69	28.16
2T8/18.5+10D6/0/20	52.42	54.87	496.91	324.34	99.86	46.48	9.40	120.58	115.88	28.16

Table A.1.1 Moment and shear resistance for beam Series I (2T8/Corr %+10D6/0/20) (Continued....)

Beam identification	$M_t$ [kNm]	$M_c$ [kNm]	V [kN]	$b_v \times d$ [mm <sup>2</sup> ]	v [N/mm <sup>2</sup> ]	$v_c$ [N/mm <sup>2</sup> ]	$s_v$ [mm]	s [mm]	Actual s [mm]
(1)	(12)	(13)	(14)	(15)	(16)	(17)	(18)	(19)	(20)
2T8/0+10D6/0/20	5.40	19.19	21.60	12058	1.79	1.00	190.83	90.44	85
2T8/0+10D6/0/20	5.40	19.19	21.60	12058	1.79	1.00	190.83	90.44	85
2T8/1.0+10D6/0/20	5.38	19.90	21.52	12054	1.79	1.00	206.03	90.41	85
2T8/1.4+10D6/0/20	5.40	19.48	21.60	12058	1.79	1.00	190.83	90.44	85
2T8/2.3+10D6/0/20	5.40	18.67	21.60	12058	1.79	1.00	190.83	90.44	85
2T8/3.4+10D6/0/20	5.38	19.90	21.52	12054	1.79	1.00	206.03	90.41	85
2T8/8.9+10D6/0/20	5.40	19.48	21.60	12058	1.79	1.00	190.83	90.44	85
2T8/10.0+10D6/0/20	5.39	17.93	21.56	12058	1.79	1.00	190.83	90.44	85
2T8/15.5+10D6/0/20	5.39	17.93	21.56	12058	1.79	1.00	190.83	90.44	85
2T8/18.5+10D6/0/20	5.40	18.67	21.60	12058	1.79	1.00	190.83	90.44	85

Table A.1.1 Moment and shear resistance for beam Series I (2T8/Corr %+10D6/0/30) (Continued...)

Beam identification	$f_{cu}$ (28 <sup>th</sup> day) [N/mm <sup>2</sup> ]	$f_{cu}$ (day of test) [N/mm <sup>2</sup> ]	$f_y$ [N/mm <sup>2</sup> ]	$f'_y$ [N/mm <sup>2</sup> ]	$A_s$ [mm <sup>2</sup> ]	$A'_s$ [mm <sup>2</sup> ]	s [mm]	d [mm]	z [mm]	$d'$ [mm]
(1)	(2)	(3)	(4)	(5)	(6)	(7)	(8)	(9)	(10)	(11)
2T8/0+10D6/0/30	47.16	58.55	496.91	344.99	99.86	47.18	8.50	110.54	106.29	28.22
2T8/0+10D6/0/30	47.16	58.55	496.91	344.99	99.86	47.18	8.50	110.54	106.29	28.22
2T8/0.8+10D6/0/30	49.40	50.37	496.91	344.99	99.86	47.18	9.88	110.54	105.60	28.22
2T8/0.9+10D6/0/30	49.40	50.37	496.91	344.99	99.86	47.18	9.88	110.54	105.60	28.22
2T8/1.4+10D6/0/30	46.69	46.86	496.91	324.34	99.86	46.48	11.00	110.58	105.08	28.16
2T8/4.6+10D6/0/30	49.86	55.54	496.91	344.99	99.86	47.18	8.96	110.54	106.06	28.22
2T8/8.5+10D6/0/30	49.86	55.54	496.91	344.99	99.86	47.18	8.96	110.54	106.06	28.22
2T8/9.6+10D6/0/30	54.40	51.05	496.91	344.99	99.86	47.18	9.75	110.54	105.67	28.22
2T8/15.0+10D6/0/30	54.40	51.05	496.91	344.99	99.86	47.18	9.75	110.54	105.67	28.22
2T8/17.8+10D6/0/30	46.69	46.86	496.91	324.34	99.86	46.48	11.00	110.58	105.08	28.16

Table A.1.1 Moment and shear resistance for beam Series I (2T8/Corr %+10D6/0/30) (Continued...)

Beam identification	$M_t$ [kNm]	$M_c$ [kNm]	V [kN]	$b_v \times d$ [mm <sup>2</sup> ]	v [N/mm <sup>2</sup> ]	$v_c$ [N/mm <sup>2</sup> ]	$s_v$ [mm]	s 0.75d [mm]	Actual s [mm]
(1)	(12)	(13)	(14)	(15)	(16)	(17)	(18)	(19)	(20)
2T8/0+10D6/0/30	4.88	16.74	19.52	11054	1.77	1.05	226.06	82.91	80
2T8/0+10D6/0/30	4.88	16.74	19.52	11054	1.77	1.05	226.06	82.91	80
2T8/0.8+10D6/0/30	4.86	14.40	19.44	11054	1.76	1.05	229.25	82.91	80
2T8/0.9+10D6/0/30	4.86	14.40	19.44	11054	1.76	1.05	229.25	82.91	80
2T8/1.4+10D6/0/30	4.87	13.41	19.48	11058	1.76	1.05	212.33	82.94	80
2T8/4.6+10D6/0/30	4.88	15.88	19.52	11054	1.77	1.05	226.06	82.91	80
2T8/8.5+10D6/0/30	4.88	15.88	19.52	11054	1.77	1.05	226.06	82.91	80
2T8/9.6+10D6/0/30	4.86	14.60	19.44	11054	1.76	1.05	229.25	82.91	80
2T8/15.0+10D6/0/30	4.86	14.60	19.44	11054	1.76	1.05	229.25	82.91	80
2T8/17.8+10D6/0/30	4.87	13.41	19.48	11058	1.76	1.05	212.33	82.94	80

Table A.1.1 Moment and shear resistance for beam Series I (2T8/Corr %+10D6/0/50) (Continued...)

Beam identification	$f_{cu}$ (28 <sup>th</sup> day) [N/mm <sup>2</sup> ]	$f_{cu}$ (day of test) [N/mm <sup>2</sup> ]	$f_y$ [N/mm <sup>2</sup> ]	$f'_y$ [N/mm <sup>2</sup> ]	$A_s$ [mm <sup>2</sup> ]	$A'_s$ [mm <sup>2</sup> ]	s [mm]	d [mm]	z [mm]	$d'$ [mm]
(1)	(2)	(3)	(4)	(5)	(6)	(7)	(8)	(9)	(10)	(11)
2T8/0+12D6/0/50	53.68	53.44	496.91	344.99	99.86	47.18	9.31	90.54	85.88	28.22
2T8/0+12D6/0/50	53.68	53.44	496.91	344.99	99.86	47.18	9.31	90.54	85.88	28.22
2T8/2.7+12D6/0/50	49.95	55.39	496.91	344.99	99.86	47.18	8.99	90.54	86.04	28.22
2T8/3.5+12D6/0/50	49.95	55.39	496.91	344.99	99.86	47.18	8.99	90.54	86.04	28.22
2T8/5.3+12D6/0/50	54.03	48.28	496.91	344.99	99.86	47.18	10.31	90.54	85.38	28.22
2T8/6.9+12D6/0/50	51.07	46.18	496.91	344.99	99.86	47.18	10.78	90.54	85.15	28.22
2T8/7.7+12D6/0/50	54.03	53.16	496.91	344.99	99.86	47.18	9.36	90.54	85.85	28.22
2T8/8.9+12D6/0/50	46.60	55.26	496.91	344.99	99.86	47.18	9.01	90.54	86.03	28.22
2T8/15.1+12D6/0/50	51.07	46.18	496.91	344.99	99.86	47.18	10.78	90.54	85.15	28.22
2T8/16.4+12D6/0/50	46.60	55.26	496.91	344.99	99.86	47.18	9.01	90.54	86.03	28.22

Table A.1.1 Moment and shear resistance for beam Series I (2T8/Corr %+10D6/0/50) (Continued...)

Beam identification	$M_t$ [kNm]	$M_c$ [kNm]	V [kN]	$b_v \times d$ [mm <sup>2</sup> ]	v [N/mm <sup>2</sup> ]	$v_c$ [N/mm <sup>2</sup> ]	$s_v$ [mm]	s 0.75d [mm]	Actual s [mm]
(1)	(12)	(13)	(14)	(15)	(16)	(17)	(18)	(19)	(20)
2T8/0+12D6/0/50	3.88	11.26	15.51	9054	1.71	1.18	307.15	67.90	65
2T8/0+12D6/0/50	3.88	11.26	15.51	9054	1.71	1.18	307.15	67.90	65
2T8/2.7+12D6/0/50	3.88	11.64	15.53	9054	1.72	1.18	305.76	67.90	65
2T8/3.5+12D6/0/50	3.88	11.64	15.53	9054	1.72	1.18	305.76	67.90	65
2T8/5.3+12D6/0/50	3.86	10.27	15.45	9054	1.71	1.18	311.46	67.90	65
2T8/6.9+12D6/0/50	3.85	9.87	15.41	9054	1.70	1.18	313.53	67.90	65
2T8/7.7+12D6/0/50	3.88	11.21	15.51	9054	1.71	1.18	307.36	67.90	65
2T8/8.9+12D6/0/50	3.88	11.61	15.53	9054	1.72	1.18	305.85	67.90	65
2T8/15.1+12D6/0/50	3.85	9.87	15.41	9054	1.70	1.18	313.53	67.90	65
2T8/16.4+12D6/0/50	3.88	11.61	15.53	9054	1.72	1.18	305.85	67.90	65

Table A.1.2 Moment and shear resistance for beam Series I (2T10/Corr %+10D6/0/20)

Beam identification	$f_{cu}$ (28 <sup>th</sup> day) [N/mm <sup>2</sup> ]	$f_{cu}$ (day of test) [N/mm <sup>2</sup> ]	$f_y$ [N/mm <sup>2</sup> ]	$f'_y$ [N/mm <sup>2</sup> ]	$A_s$ [mm <sup>2</sup> ]	$A'_s$ [mm <sup>2</sup> ]	s [mm]	d [mm]	z [mm]	$d'$ [mm]
(1)	(2)	(3)	(4)	(5)	(6)	(7)	(8)	(9)	(10)	(11)
2T10/0+10D6/0/20	42.80	42.80	545.46	324.34	159.38	46.48	25.06	119.53	107.00	28.16
2T10/0+10D6/0/20	42.80	42.80	545.46	324.34	159.38	46.48	25.06	119.53	107.00	28.16
2T10/0+10D6/0/20	47.13	47.13	545.46	324.34	159.38	46.48	22.76	119.53	108.15	28.16
2T10/0+10D6/0/20	51.85	51.85	545.46	324.34	159.38	46.48	20.69	119.53	109.18	28.16
2T10/0+10D6/0/20	51.85	51.85	545.46	324.34	159.38	46.48	20.69	119.53	109.18	28.16
2T10/0+10D6/0/20	50.08	50.08	545.46	324.34	159.38	46.48	21.42	119.53	108.82	28.16
2T10/0+10D6/0/20	60.39	61.77	533.82	344.99	154.30	47.22	15.97	119.57	111.58	28.22
2T10/0+10D6/0/20	49.78	55.05	524.46	422.79	154.48	47.74	16.49	119.53	111.28	28.27
2T10/2.6+10D6/0/20	45.02	51.39	524.46	422.79	154.48	47.74	17.67	119.53	110.70	28.27
2T10/4.0+10D6/0/20	45.02	51.39	524.46	422.79	154.48	47.74	17.67	119.53	110.70	28.27

Table A.1.2 Moment and shear resistance for beam Series I (2T10/Corr %+10D6/0/20) (Continued...)

Beam identification	$M_t$ [kNm]	$M_c$ [kNm]	V [kN]	$b_v \times d$ [mm <sup>2</sup> ]	v [N/mm <sup>2</sup> ]	$v_c$ [N/mm <sup>2</sup> ]	$s_v$ [mm]	s 0.75d [mm]	Actual s [mm]
(1)	(12)	(13)	(14)	(15)	(16)	(17)	(18)	(19)	(20)
2T10/0+10D6/0/20	9.07	15.69	36.26	11953	3.03	1.18	81.14	89.64	85
2T10/0+10D6/0/20	9.07	15.69	36.26	11953	3.03	1.18	81.14	89.64	85
2T10/0+10D6/0/20	9.15	17.13	36.60	11953	3.06	1.18	79.95	89.64	85
2T10/0+10D6/0/20	9.22	18.71	36.89	11953	3.09	1.18	78.91	89.64	85
2T10/0+10D6/0/20	9.22	18.71	36.89	11953	3.09	1.18	78.91	89.64	85
2T10/0+10D6/0/20	9.20	18.12	36.79	11953	3.08	1.18	79.27	89.64	85
2T10/0+10D6/0/20	8.86	22.15	35.44	11957	2.96	1.16	90.44	89.67	85
2T10/0+10D6/0/20	8.61	20.25	34.45	11953	2.88	1.16	117.48	89.65	85
2T10/2.6+10D6/0/20	8.58	19.02	34.30	11953	2.87	1.16	118.31	89.65	85
2T10/4.0+10D6/0/20	8.58	19.02	34.30	11953	2.87	1.16	118.31	89.65	85

Table A.1.2 Moment and shear resistance for beam Series I (2T10/Corr %+10D6/0/20) (Continued...)

Beam identification	$f_{cu}$ (28 <sup>th</sup> day) [N/mm <sup>2</sup> ]	$f_{cu}$ (day of test) [N/mm <sup>2</sup> ]	$f_y$ [N/mm <sup>2</sup> ]	$f'_y$ [N/mm <sup>2</sup> ]	$A_s$ [mm <sup>2</sup> ]	$A'_s$ [mm <sup>2</sup> ]	s [mm]	d [mm]	z [mm]	$d'$ [mm]
(1)	(2)	(3)	(4)	(5)	(6)	(7)	(8)	(9)	(10)	(11)
2T10/4.2+10D6/0/20	53.58	59.25	545.46	324.34	159.38	46.48	18.10	119.53	110.47	28.16
2T10/4.5+10D6/0/20	53.58	59.25	545.46	324.34	159.38	46.48	18.10	119.53	110.47	28.16
2T10/6.5+10D6/0/20	48.60	59.79	533.82	344.99	154.30	47.22	16.50	119.57	111.32	28.22
2T10/7.5+10D6/0/20	49.78	55.05	524.46	422.79	154.48	47.74	16.49	119.53	111.28	28.27

Table A.1.2 Moment and shear resistance for beam Series I (2T10/Corr %+10D6/0/20) (Continued...)

Beam identification	$M_t$ [kNm]	$M_c$ [kNm]	V [kN]	$b_v \times d$ [mm <sup>2</sup> ]	v [N/mm <sup>2</sup> ]	$v_c$ [N/mm <sup>2</sup> ]	$s_v$ [mm]	s [mm]	Actual s [mm]
(1)	(12)	(13)	(14)	(15)	(16)	(17)	(18)	(19)	(20)
2T10/4.2+10D6/0/20	9.32	21.18	37.26	11953	3.12	1.18	77.64	89.64	85
2T10/4.5+10D6/0/20	9.32	21.18	37.26	11953	3.12	1.18	77.64	89.64	85
2T10/6.5+10D6/0/20	8.84	21.49	35.37	11957	2.96	1.16	90.73	89.67	85
2T10/7.5+10D6/0/20	8.61	20.25	34.45	11953	2.88	1.16	117.48	89.65	85

Table A.1.2 Moment and shear resistance for beam Series I (2T10/Corr %+10D6/0/30) (Continued...)

Beam identification	$f_{cu}$ (28 <sup>th</sup> day) [N/mm <sup>2</sup> ]	$f_{cu}$ (day of test) [N/mm <sup>2</sup> ]	$f_y$ [N/mm <sup>2</sup> ]	$f'_y$ [N/mm <sup>2</sup> ]	$A_s$ [mm <sup>2</sup> ]	$A'_s$ [mm <sup>2</sup> ]	s [mm]	d [mm]	z [mm]	$d'$ [mm]
(1)	(2)	(3)	(4)	(5)	(6)	(7)	(8)	(9)	(10)	(11)
2T10/0+10D6/0/30	49.57	49.57	545.46	324.34	159.38	46.48	21.64	109.53	98.71	28.16
2T10/0+10D6/0/30	46.67	46.67	545.46	324.34	159.38	46.48	22.98	109.53	98.03	28.16
2T10/0+10D6/0/30	46.67	46.67	545.46	324.34	159.38	46.48	22.98	109.53	98.03	28.16
2T10/0+10D6/0/30	51.18	51.18	545.46	324.34	159.38	46.48	20.96	109.53	99.05	28.16
2T10/0+10D6/0/30	51.18	51.18	545.46	324.34	159.38	46.48	20.96	109.53	99.05	28.16
2T10/0+10D6/0/30	49.24	49.24	545.46	324.34	159.38	46.48	21.78	109.53	98.63	28.16
2T10/0+10D6/0/30	49.24	49.24	545.46	324.34	159.38	46.48	21.78	109.53	98.63	28.16
2T10/2.3+10D6/0/30	53.22	58.91	533.82	344.99	154.30	47.22	16.74	109.57	101.19	28.22
2T10/2.5+10D6/0/30	53.25	59.81	533.82	344.99	154.30	47.22	16.49	109.57	101.32	28.22
2T10/3.3+10D6/0/30	57.44	62.21	533.82	344.99	154.30	47.22	15.85	109.57	101.64	28.22
2T10/3.4+10D6/0/30	56.43	61.12	545.46	324.34	159.38	46.48	17.55	109.53	100.75	28.16
2T10/6.7+10D6/0/30	53.22	58.91	533.82	344.99	154.30	47.22	16.74	109.57	101.19	28.22
2T10/8.3+10D6/0/30	57.44	62.21	533.82	344.99	154.30	47.22	15.85	109.57	101.64	28.22
2T10/9.2+10D6/0/30	53.25	59.81	533.82	344.99	154.30	47.22	16.49	109.57	101.32	28.22

Table A.1.2 Moment and shear resistance for beam Series I (2T10/Corr %+10D6/0/30) (Continued...)

Beam identification	$M_t$ [kNm]	$M_c$ [kNm]	V [kN]	$b_v \times d$ [mm <sup>2</sup> ]	v [N/mm <sup>2</sup> ]	$v_c$ [N/mm <sup>2</sup> ]	$s_v$ [mm]	s 0.75d [mm]	Actual s [mm]
(1)	(12)	(13)	(14)	(15)	(16)	(17)	(18)	(19)	(20)
2T10/0+10D6/0/30	8.32	15.14	33.28	10953	3.04	1.24	83.71	82.14	80
2T10/0+10D6/0/30	8.27	14.33	33.09	10953	3.02	1.24	84.54	82.14	80
2T10/0+10D6/0/30	8.27	14.33	33.09	10953	3.02	1.24	84.54	82.14	80
2T10/0+10D6/0/30	8.34	15.59	33.38	10953	3.05	1.24	83.30	82.14	80
2T10/0+10D6/0/30	8.34	15.59	33.38	10953	3.05	1.24	83.30	82.14	80
2T10/0+10D6/0/30	8.31	15.05	33.26	10953	3.04	1.24	83.80	82.14	80
2T10/0+10D6/0/30	8.31	15.05	33.26	10953	3.04	1.24	83.80	82.14	80
2T10/2.3+10D6/0/30	8.01	17.87	32.05	10957	2.92	1.22	95.77	82.17	80
2T10/2.5+10D6/0/30	8.02	18.13	32.08	10957	2.93	1.22	95.60	82.17	80
2T10/3.3+10D6/0/30	8.04	18.80	32.16	10957	2.94	1.22	95.17	82.17	80
2T10/3.4+10D6/0/30	8.47	18.38	33.87	10953	3.09	1.24	81.29	82.14	80
2T10/6.7+10D6/0/30	8.01	17.87	32.05	10957	2.92	1.22	95.77	82.17	80
2T10/8.3+10D6/0/30	8.04	18.80	32.16	10957	2.94	1.22	95.17	82.17	80
2T10/9.2+10D6/0/30	8.02	18.13	32.08	10957	2.93	1.22	95.60	82.17	80

Table A.1.2 Moment and shear resistance for beam Series I (2T10/Corr %+12D6/0/50) (Continued...)

Beam identification	$f_{cu}$ (28 <sup>th</sup> day) [N/mm <sup>2</sup> ]	$f_{cu}$ (day of test) [N/mm <sup>2</sup> ]	$f_y$ [N/mm <sup>2</sup> ]	$f'_y$ [N/mm <sup>2</sup> ]	$A_s$ [mm <sup>2</sup> ]	$A'_s$ [mm <sup>2</sup> ]	s [mm]	d [mm]	z [mm]	$d'$ [mm]
(1)	(2)	(3)	(4)	(5)	(6)	(7)	(8)	(9)	(10)	(11)
2T10/ <b>0</b> +12D6/0/50	46.12	46.12	545.46	324.34	159.38	46.48	23.26	89.53	77.90	28.16
2T10/ <b>0</b> +12D6/0/50	46.12	46.12	545.46	324.34	159.38	46.48	23.26	89.53	77.90	28.16
2T10/ <b>5.7</b> +12D6/0/50	49.05	53.13	545.46	324.34	159.38	46.48	20.19	89.53	79.43	28.16
2T10/ <b>6.1</b> +12D6/0/50	49.05	53.13	545.46	324.34	159.38	46.48	20.19	89.53	79.43	28.16
2T10/ <b>7.7</b> +12D6/0/50	50.97	55.21	545.46	324.34	159.38	46.48	19.43	89.53	79.81	28.16
2T10/ <b>9.5</b> +12D6/0/50	50.97	55.21	545.46	324.34	159.38	46.48	19.43	89.53	79.81	28.16
2T10/ <b>10.2</b> +12D6/0/50	47.93	53.83	545.46	324.34	159.38	46.48	19.92	89.53	79.56	28.16
2T10/ <b>14.4</b> +12D6/0/50	47.93	53.83	545.46	324.34	159.38	46.48	19.92	89.53	79.56	28.16

Table A.1.2 Moment and shear resistance for beam Series I (2T10/Corr %+12D6/0/50) (Continued...)

Beam identification	$M_t$ [kNm]	$M_c$ [kNm]	V [kN]	$b_v \times d$ [mm <sup>2</sup> ]	v [N/mm <sup>2</sup> ]	$v_c$ [N/mm <sup>2</sup> ]	$s_v$ [mm]	s 0.75d [mm]	Actual s [mm]
(1)	(12)	(13)	(14)	(15)	(16)	(17)	(18)	(19)	(20)
2T10/ <b>0</b> +12D6/0/50	6.52	9.57	26.09	8953	2.91	1.39	99.03	67.14	65
2T10/ <b>0</b> +12D6/0/50	6.52	9.57	26.09	8953	2.91	1.39	99.03	67.14	65
2T10/ <b>5.7</b> +12D6/0/50	6.63	10.89	26.53	8953	2.96	1.39	95.92	67.14	65
2T10/ <b>6.1</b> +12D6/0/50	6.63	10.89	26.53	8953	2.96	1.39	95.92	67.14	65
2T10/ <b>7.7</b> +12D6/0/50	6.66	11.28	26.64	8953	2.98	1.39	95.18	67.14	65
2T10/ <b>9.5</b> +12D6/0/50	6.66	11.28	26.64	8953	2.98	1.39	95.18	67.14	65
2T10/ <b>10.2</b> +12D6/0/50	6.64	11.02	26.57	8953	2.97	1.39	95.67	67.14	65
2T10/ <b>14.4</b> +12D6/0/50	6.64	11.02	26.57	8953	2.97	1.39	95.67	67.14	65

Table A.1.3 Moment and shear resistance for beam Series I (2T12/Corr %+24D6/0/50)

Beam identification	$f_{cu}$ (28 <sup>th</sup> day) [N/mm <sup>2</sup> ]	$f_{cu}$ (day of test) [N/mm <sup>2</sup> ]	$f_y$ [N/mm <sup>2</sup> ]	$f'_y$ [N/mm <sup>2</sup> ]	$A_s$ [mm <sup>2</sup> ]	$A'_s$ [mm <sup>2</sup> ]	s [mm]	d [mm]	z [mm]	$d'$ [mm]
(1)	(2)	(3)	(4)	(5)	(6)	(7)	(8)	(9)	(10)	(11)
2T12/0+24D6/0/50	54.59	62.09	525.55	344.99	220.50	47.22	23.94	88.60	76.63	28.22
2T12/0+24D6/0/50	54.59	62.09	525.55	344.99	220.50	47.22	23.94	88.60	76.63	28.22
2T12/1.3+24D6/0/50	48.63	50.10	525.55	422.79	220.50	47.74	28.51	88.57	74.32	28.27
2T12/1.7+24D6/0/50	53.48	56.51	525.55	422.79	220.50	47.74	25.28	88.57	75.93	28.27
2T12/2.5+24D6/0/50	55.13	61.13	525.55	344.99	220.50	47.22	24.32	88.60	76.44	28.22
2T12/3.1+2D6/0/50	55.13	61.13	525.55	344.99	220.50	47.22	24.32	88.60	76.44	28.22
2T12/4.2+24D6/0/50	53.48	56.51	525.55	422.79	220.50	47.74	25.28	88.57	75.93	28.27
2T12/5.9+24D6/0/50	48.63	50.10	525.55	422.79	220.50	47.74	28.51	88.57	74.32	28.27

Table A.1.3 Moment and shear resistance for beam Series I (2T12/Corr %+24D6/0/50) (Continued...)

Beam identification	$M_t$ [kNm]	$M_c$ [kNm]	V [kN]	$b_v \times d$ [mm <sup>2</sup> ]	v [N/mm <sup>2</sup> ]	$v_c$ [N/mm <sup>2</sup> ]	$s_v$ [mm]	s [mm]	Actual s [mm]
(1)	(12)	(13)	(14)	(15)	(16)	(17)	(18)	(19)	(20)
2T12/0+24D6/0/50	8.62	11.41	34.48	8860	3.89	1.56	139.83	66.45	65
2T12/0+24D6/0/50	8.62	11.41	34.48	8860	3.89	1.56	139.83	66.45	65
2T12/1.3+24D6/0/50	8.33	9.20	33.32	8857	3.76	1.56	183.49	66.43	65
2T12/1.7+24D6/0/50	8.48	10.37	33.92	8857	3.83	1.56	177.83	66.43	65
2T12/2.5+24D6/0/50	8.60	11.23	34.40	8860	3.88	1.56	140.43	66.45	65
2T12/3.1+24D6/0/50	8.60	11.23	34.40	8860	3.88	1.56	140.43	66.45	65
2T12/4.2+24D6/0/50	8.48	10.37	33.92	8857	3.83	1.56	177.83	66.43	65
2T12/5.9+24D6/0/50	8.33	9.20	33.32	8857	3.76	1.56	183.49	66.43	65

## A.2 Design data for beam Series II

Table A.2.1 Moment and shear resistance for beam Series II (2T8/0+12D6/Corr %/50)

Beam identification	$f_{cu}$ (28 <sup>th</sup> day) [N/mm <sup>2</sup> ]	$f_{cu}$ (day of test) [N/mm <sup>2</sup> ]	$f_y$ [N/mm <sup>2</sup> ]	$f'_y$ [N/mm <sup>2</sup> ]	$A_s$ [mm <sup>2</sup> ]	$A'_s$ [mm <sup>2</sup> ]	s [mm]	d [mm]	z [mm]	$d'$ [mm]
(1)	(2)	(3)	(4)	(5)	(6)	(7)	(8)	(9)	(10)	(11)
2T8/0+12D6/0/50	53.68	53.44	496.91	344.99	99.86	47.18	9.31	90.54	85.88	28.22
2T8/0+12D6/0/50	53.68	53.44	496.91	344.99	99.86	47.18	9.31	90.54	85.88	28.22
2T8/0+12D6/4.9/50	54.07	66.63	507.72	422.79	95.72	47.74	6.37	90.59	87.40	28.27
2T8/0+12D6/9.2/50	49.37	51.72	496.91	422.79	99.86	47.74	8.50	90.51	86.26	28.27
2T8/0+12D6/9.4/50	49.37	51.72	496.91	422.79	99.86	47.74	8.50	90.51	86.26	28.27
2T8/0+12D6/9.8/50	54.07	66.63	507.72	422.79	95.72	47.74	6.37	90.59	87.40	28.27
2T8/0+12D6/18.7/50	48.65	58.03	507.72	422.79	95.72	47.74	7.31	90.59	86.93	28.27
2T8/0+12D6/23.2/50	48.65	58.03	507.72	422.79	95.72	47.74	7.31	90.59	86.93	28.27

Table A.2.1 Moment and shear resistance for beam Series II (2T8/0+12D6/Corr%/50) (Continued...)

Beam identification	$M_t$ [kNm]	$M_c$ [kNm]	$V$ [kN]	$b_v \times d$ [mm <sup>2</sup> ]	$v$ [N/mm <sup>2</sup> ]	$v_c$ [N/mm <sup>2</sup> ]	$s_v$ [mm]	$s$ [mm]	Actual $s$ [mm]
(1)	(12)	(13)	(14)	(15)	(16)	(17)	(18)	(19)	(20)
2T8/0+12D6/0/50	3.88	11.26	15.51	9054	1.71	1.18	307.15	67.90	65
2T8/0+12D6/0/50	3.88	11.26	15.51	9054	1.71	1.18	307.15	67.90	65
2T8/0+12D6/4.9/50	3.74	14.05	14.97	9059	1.65	1.17	415.63	67.94	65
2T8/0+12D6/9.2/50	3.80	11.17	15.18	9051	1.68	1.18	408.76	67.88	65
2T8/0+12D6/9.4/50	3.80	11.17	15.18	9051	1.68	1.18	408.76	67.88	65
2T8/0+12D6/9.8/50	3.74	14.05	14.97	9059	1.65	1.17	415.63	67.94	65
2T8/0+12D6/18.7/50	3.73	12.40	14.91	9059	1.65	1.17	420.75	67.94	65
2T8/0+12D6/23.2/50	3.73	12.40	14.91	9059	1.65	1.17	420.75	67.94	65

Table A.2.2 Moment and shear resistance for beam Series II (2T12/0+12D6/Corr %/50)

Beam identification	$f_{cu}$ (28 <sup>th</sup> day) [N/mm <sup>2</sup> ]	$f_{cu}$ (day of test) [N/mm <sup>2</sup> ]	$f_y$ [N/mm <sup>2</sup> ]	$f'_y$ [N/mm <sup>2</sup> ]	$A_s$ [mm <sup>2</sup> ]	$A'_s$ [mm <sup>2</sup> ]	s [mm]	d [mm]	z [mm]	$d'$ [mm]
(1)	(2)	(3)	(4)	(5)	(6)	(7)	(8)	(9)	(10)	(11)
2T12/0+12D6/0/50	58.70	66.19	525.55	344.99	220.50	47.22	22.46	88.60	77.37	28.22
2T12/0+12D6/0/50	58.70	66.19	525.55	344.99	220.50	47.22	22.46	88.60	77.37	28.22
2T12/0+12D6/0/50	54.44	60.21	525.55	344.99	220.50	47.22	24.69	88.60	76.25	28.22
2T12/0+12D6/0.7/50	62.91	62.80	525.55	344.99	220.50	47.22	23.67	88.60	76.76	28.22
2T12/0+12D6/1.1/50	62.91	62.80	525.55	344.99	220.50	47.22	23.67	88.60	76.76	28.22
2T12/0+12D6/1.8/50	56.34	61.71	525.55	344.99	220.50	47.22	24.09	88.60	76.55	28.22
2T12/0+12D6/2.6/50	54.44	60.21	525.55	344.99	220.50	47.22	24.69	88.60	76.25	28.22
2T12/0+12D6/6.1/50	56.34	61.71	525.55	344.99	220.50	47.22	24.09	88.60	76.55	28.22

Table A.2.2 Moment and shear resistance for beam Series II (2T12/0+12D6/Corr %/50) (Continued...)

Beam identification	$M_t$ [kNm]	$M_c$ [kNm]	V [kN]	$b_v \times d$ [mm <sup>2</sup> ]	v [N/mm <sup>2</sup> ]	$v_c$ [N/mm <sup>2</sup> ]	$s_v$ [mm]	s [mm]	Actual s [mm]
(1)	(12)	(13)	(14)	(15)	(16)	(17)	(18)	(19)	(20)
2T12/0+12D6/0/50	8.69	13.14	34.75	8860	3.92	1.56	68.96	66.45	65
2T12/0+12D6/0/50	8.69	13.14	34.75	8860	3.92	1.56	68.96	66.45	65
2T12/0+12D6/0/50	8.58	12.04	34.31	8860	3.87	1.56	70.46	66.45	65
2T12/0+12D6/0.7/50	8.63	12.52	34.51	8860	3.90	1.56	69.77	66.45	65
2T12/0+12D6/1.1/50	8.63	12.52	34.51	8860	3.90	1.56	69.77	66.45	65
2T12/0+12D6/1.8/50	8.61	12.32	34.43	8860	3.89	1.56	70.05	66.45	65
2T12/0+12D6/2.6/50	8.58	12.04	34.31	8860	3.87	1.56	70.46	66.45	65
2T12/0+12D6/6.1/50	8.61	12.32	34.43	8860	3.89	1.56	70.05	66.45	65

## A.3 Design data for beam Series III

Table A.3 Moment and shear resistance for beam Series III (2T8/Corr % + 12D6/Corr % / 50)

Beam identification	$f_{cu}$ (28 <sup>th</sup> day) [N/mm <sup>2</sup> ]	$f_{cu}$ (day of test) [N/mm <sup>2</sup> ]	$f_y$ [N/mm <sup>2</sup> ]	$f'_y$ [N/mm <sup>2</sup> ]	$A_s$ [mm <sup>2</sup> ]	$A'_s$ [mm <sup>2</sup> ]	s [mm]	d [mm]	z [mm]	$d'$ [mm]
(1)	(2)	(3)	(4)	(5)	(6)	(7)	(8)	(9)	(10)	(11)
2T8/2.9+12D6/3.0/50	53.35	57.20	496.91	422.79	99.86	47.74	7.68	90.51	86.66	28.27
2T8/3.1+12D6/3.8/50	53.93	54.05	507.72	422.79	95.72	47.74	7.85	90.59	86.66	28.27
2T8/4.1+12D6/3.9/50	52.30	50.31	507.72	422.79	95.72	47.74	8.43	90.59	86.37	28.27
2T8/4.7+12D6/8.2/50	52.30	50.31	507.72	422.79	95.72	47.74	8.43	90.59	86.37	28.27
2T8/4.8+12D6/5.6/50	51.57	52.14	496.91	422.79	99.86	47.74	8.43	90.51	86.29	28.27
2T8/5.3+12D6/6.5/50	51.57	52.14	496.91	422.79	99.86	47.74	8.43	90.51	86.29	28.27
2T8/6.5+12D6/4.3/50	53.35	57.20	496.91	422.79	99.86	47.74	7.68	90.51	86.66	28.27
2T8/6.7+12D6/9.4/50	61.07	63.17	507.72	422.79	95.72	47.74	6.71	90.59	87.23	28.27
2T8/6.9+12D6/4.0/50	51.53	54.94	507.72	422.79	95.72	47.74	7.72	90.59	86.73	28.27

Table A.3 Moment and shear resistance for beam Series III (2T8/Corr % + 12D6/Corr %/50) (Continued...)

Beam identification	$M_t$ [kNm]	$M_c$ [kNm]	V [kN]	$b_v \times d$ [mm <sup>2</sup> ]	v [N/mm <sup>2</sup> ]	$v_c$ [N/mm <sup>2</sup> ]	$s_v$ [mm]	s 0.75d [mm]	Actual s [mm]
(1)	(12)	(13)	(14)	(15)	(16)	(17)	(18)	(19)	(20)
2T8/2.9+12D6/3.0/50	3.81	12.22	15.23	9051	1.68	1.18	404.42	67.88	65
2T8/3.1+12D6/3.8/50	3.72	11.64	14.88	9059	1.64	1.17	423.74	67.94	65
2T8/4.1+12D6/3.9/50	3.71	10.92	14.85	9059	1.64	1.17	427.02	67.94	65
2T8/4.7+12D6/8.2/50	3.71	10.92	14.85	9059	1.64	1.17	427.02	67.94	65
2T8/4.8+12D6/5.6/50	3.80	11.25	15.19	9051	1.68	1.18	408.39	67.88	65
2T8/5.3+12D6/6.5/50	3.80	11.25	15.19	9051	1.68	1.18	408.39	67.88	65
2T8/6.5+12D6/4.3/50	3.81	12.22	15.23	9051	1.68	1.18	404.42	67.88	65
2T8/6.7+12D6/9.4/50	3.74	13.39	14.95	9059	1.65	1.17	417.51	67.94	65
2T8/6.9+12D6/4.0/50	3.72	11.81	14.89	9059	1.64	1.17	423.03	67.94	65

Table A.3 Moment and shear resistance for beam Series III (2T8/Corr %+12D6/Corr %/50) (Continued...)

Beam identification	$f_{cu}$ (28 <sup>th</sup> day) [N/mm <sup>2</sup> ]	$f_{cu}$ (day of test) [N/mm <sup>2</sup> ]	$f_y$ [N/mm <sup>2</sup> ]	$f'_y$ [N/mm <sup>2</sup> ]	$A_s$ [mm <sup>2</sup> ]	$A'_s$ [mm <sup>2</sup> ]	s [mm]	d [mm]	z [mm]	d' [mm]
(1)	(2)	(3)	(4)	(5)	(6)	(7)	(8)	(9)	(10)	(11)
2T8/6.9+12D6/7.4/50	51.53	54.94	507.72	422.79	95.72	47.74	7.72	90.59	86.73	28.27
2T8/7.8+12D6/4.5/50	48.62	56.80	507.72	422.79	95.72	47.74	7.47	90.59	86.85	28.27
2T8/7.9+12D6/8.2/50	61.07	63.17	507.72	422.79	95.72	47.74	6.71	90.59	87.23	28.27
2T8/8.3+12D6/6.3/50	53.93	54.05	507.72	422.79	95.72	47.74	7.85	90.59	86.66	28.27
2T8/8.8+12D6/9.1/50	48.62	56.80	507.72	422.79	95.72	47.74	7.47	90.59	86.85	28.27
2T8/10.7+12D6/12.0/50	52.23	49.46	507.72	422.79	95.72	47.74	8.57	90.59	86.30	28.27
2T8/11.8+12D6/14.2/50	52.23	49.46	507.72	422.79	95.72	47.74	8.57	90.59	86.30	28.27
2T8/25.7+12D6/24.7/50	48.15	43.30	496.91	422.79	99.86	47.74	10.15	90.51	85.43	28.27
2T8/25.7+12D6/27.6/50	48.15	43.30	496.91	422.79	99.86	47.74	10.15	90.51	85.43	28.27

Table A.3 Moment and shear resistance for beam Series III (2T8/Corr %+12D6/Corr %/50) (Continued...)

Beam identification	$M_t$ [kNm]	$M_c$ [kNm]	$V$ [kN]	$b_v \times d$ [mm <sup>2</sup> ]	$v$ [N/mm <sup>2</sup> ]	$v_c$ [N/mm <sup>2</sup> ]	$s_v$ [mm]	$s$ [mm]	Actual $s$ [mm]
(1)	(12)	(13)	(14)	(15)	(16)	(17)	(18)	(19)	(20)
2T8/6.9+12D6/7.4/50	3.72	11.81	14.89	9059	1.64	1.17	423.03	67.94	65
2T8/7.8+12D6/4.5/50	3.73	12.16	14.90	9059	1.65	1.17	421.63	67.94	65
2T8/7.9+12D6/8.2/50	3.74	13.39	14.95	9059	1.65	1.17	417.51	67.94	65
2T8/8.3+12D6/6.3/50	3.72	11.64	14.88	9059	1.64	1.17	423.74	67.94	65
2T8/8.8+12D6/9.1/50	3.73	12.16	14.90	9059	1.65	1.17	421.63	67.94	65
2T8/10.7+12D6/12.0/50	3.71	10.75	14.84	9059	1.64	1.17	427.84	67.94	65
2T8/11.8+12D6/14.2/50	3.71	10.75	14.84	9059	1.64	1.17	427.84	67.94	65
2T8/25.7+12D6/24.7/50	3.77	9.56	15.08	9051	1.67	1.18	417.85	67.88	65
2T8/25.7+12D6/27.6/50	3.77	9.56	15.08	9051	1.67	1.18	417.85	67.88	65

### ***List of Publications***

#### **B.1 Publications**

Hristova E. H., O'Flaherty F. J., Mangat P. S. and Lambert P., 'Influence of Cover on the Flexural Performance of Deteriorated Reinforced Concrete Beams', Proceedings of the Second International Conference on Structural and Construction Engineering, 23-26 September 2003, Rome, Italy.

Hristova E. H., O'Flaherty F. J., Mangat P. S. and Lambert P., 'Impact of Main Steel Diameter on the Flexural Capacity of Deteriorated Reinforced Concrete Beams', Proceedings of the Second International Conference on Bridge Maintenance, Safety and Management, 19-22 October 2004, Kyoto, Japan.

#### **B.2 Short papers and posters**

Hristova E. H., 'Determination of the Residual Strength of Corroded Reinforced Concrete Beams', Young Researchers' Conference, Institution of Structural Engineers, March 2002.

Hristova E. H. & O'Flaherty F. J., 'Residual Strength of Corroded Reinforced Concrete Beams', Poster Presentation, Britain's Younger Engineers, House of Commons, December 2001.